

Open Research Online

The Open University's repository of research publications and other research outputs

Genetic and Acquired Abnormalities in C3 Glomerulopathy and Primary Immune Complex-Mediated MPGN

Thesis

How to cite:

Piras, Rossella Alberta (2018). Genetic and Acquired Abnormalities in C3 Glomerulopathy and Primary Immune Complex-Mediated MPGN. PhD thesis The Open University.

For guidance on citations see [FAQs](#).

© 2018 The Author

Version: Submitted Version

Copyright and Moral Rights for the articles on this site are retained by the individual authors and/or other copyright owners. For more information on Open Research Online's data [policy](#) on reuse of materials please consult the policies page.

oro.open.ac.uk

**GENETIC AND ACQUIRED ABNORMALITIES
IN C3 GLOMERULOPATHY AND PRIMARY
IMMUNE COMPLEX-MEDIATED MPGN**

Thesis submitted by

Rossella Alberta Piras, Chem.Pharm D.

for the degree of

Doctor of Philosophy

Discipline of Life and Biomolecular Sciences

The Open University, United Kingdom

IRCCS Istituto di Ricerche Farmacologiche Mario Negri, Italy

Director of Studies

Dr. Marina Noris, PhD

Supervisor

Prof. Matthew Pickering, PhD

February, 2018

ABSTRACT

Membranoproliferative glomerulonephritis (MPGN) is an uncommon cause of glomerular injury that mainly occurs in children and young adults.

MPGN is currently classified in immune complex-mediated MPGN (IC-MPGN), characterized by activation of the complement classic pathway, and C3 Glomerulopathy (C3G), with predominant complement alternative pathway (AP) activation. C3G is further classified in Dense Deposit Disease (DDD) and C3 glomerulonephritis (C3GN).

The first part of the thesis describes a large cohort of patients with IC-MPGN ($n=96$), DDD ($n=26$) and C3GN ($n=77$). Data obtained from genetic and biochemical analysis were correlated with histological and clinical parameters. We found that the majority of patients across the three histology groups (from 70 to 85 %) showed low C3 and normal C4. About 18% of patients carried likely pathogenic variants (LPVs) in complement genes, mainly in *CFH* regulatory gene and in *C3* and *CFB*, encoding the two convertase components. Interestingly, two LPVs in *THBD* gene, were identified in two patients with C3G. C3NeF, an autoantibody stabilizing AP convertase, resulted abundant in DDD patients (79%) but was also present in patients with IC-MPGN (40%) or C3GN (39%).

To classify IC-MPGN and C3G patients based on the underlying pathogenesis, a three-step algorithm based on histological, genetic and biochemical data was used to classify patients in 4 clusters identifying 4 different pathogenetic patterns.

In the second part of the thesis, copy number variation (CNV) studies, disclosed abnormal CNVs both in IC-MPGN and C3G. Interestingly, we describe, for the first time, genomic rearrangements involving the *CFHR4* gene. Finally, Western Blot studies

in DDD patients showed the presence of abnormal FHR molecular pattern in patients with normal CNVs and without *CFHR* LPVs.

In conclusion, the present study increased our understanding in IC-MPGN and C3G and provided new insights in the pathogenetic mechanisms underlying these complex glomerular diseases.

To my family

ACKNOWLEDGEMENTS

I am grateful to Prof. Silvio Garattini and to Prof. Giuseppe Remuzzi, Director and Research Coordinator of the IRCCS Istituto di Ricerche Farmacologiche “Mario Negri”, respectively, for giving me the opportunity to attend the PhD course.

My sincere thanks go to Dr. Marina Noris, my Director of Studies, for her continuous suggestions that enriched my research and for her immense knowledge; to Dr. Matthew Pickering, my Supervisor, for all the time he kindly dedicated to supervise my research.

Especially thanks to all my colleagues of the “Laboratory of Immunology and Genetic of Rare Diseases”, and of the “Laboratory of Rare Diseases Documentation and Research”, in particular Paraskevas Iatropoulos, Elisabetta Valoti, Caterina Mele, Marta Alberti, Serena Bettoni, Roberta Donadelli, Matteo Breno , Paola Cuccarolo, Manuela Curreri and Elena Bresin for their precious and helpful contribution to my research.

A very special gratitude goes to Fabrizio Spoleti, president of the “Progetto DDD Onlus - Associazione per la lotta alla DDD” for supporting my research and for his enthusiasm for the Research. I express my gratitude to Prof. Richard Smith who gave me the possibility to spend time in his laboratory, an experience that helped me to grow professionally and personally.

This thesis would not have been possible without the incessant encouragement of my parents, the understanding and love of Massy and the magical energies transmitted from my little Filippo.

Contribution to the Thesis by other Researchers

Part of the thesis project was carried on with the collaboration of other researchers that contributed to the research as follows:

Internal collaborations in the IRCCS Istituto di Ricerche Farmacologiche Mario Negri

- All kidney reports were centrally reviewed by pathologists at Mario Negri Institute.
- Clinical data and biological samples were collected through the MPGN registry by Dr. Paraskevas Iatropoulos, Dr. Manuela Curreri, Dr. Bresin, Dr. Daina, and Ms. Sara Gamba.
- Regarding to the six gene NGS panel for IC-MPGN/C3G cohort, Dr Paraskevas Iatropoulos and Dr. Caterina Mele participated in the "wet-lab" and the bioinformatic set-up. The screening of the 6 complement genes was performed by the candidate together with Dr. Elisabetta Valoti, Dr. Caterina Mele, Dr. Paraskevas Iatropoulos and Ms Marta Alberti. Analysis of the NGS sequencing was performed by Dr. Matteo Breno.
- SC5b-9 assays were performed by Dr. Serena Bettoni and Dr Paola Cuccarolo.
- FH quantification by ELISA in DDD patients was performed by Dr Paola Cuccarolo.
- The presence of anti-FH autoantibodies was evaluated by Dr Elisabetta Valoti.
- C3 and C4 assays were performed by Dr. Flavio Gaspari and the Antonio Nicola Cannata.

External collaborations

- Marina Vivarelli, Francesco Emma Division (both at the Nephrology and Dialysis, Bambin Gesù Pediatric Hospital, Roma, Italy) and Luisa Murer (at the Unit of Pediatric Nephrology, Dialysis and Transplantation, Azienda Ospedaliera of Padova, Italy) participated in the recruitment of IC-MPGN/C3G patients.
- C3NeF assays were performed by Dr. Veronique Fremaux-Bacchi's group at the Department of Immunology, Assistance Publique-Hopitaux de Paris, Hopital Europeen George-Pompidou and INSERM UMRS 1138, Cordelier Research Center, Complement and Diseases Team, Paris, France.
- Library preparation using CasCADE panel was performed by the candidate at the Molecular Otolaryngology and Renal Research Laboratories of University of Iowa while NGS sequencing was performed by the University staff.

All other experiments and analyzes described in this thesis were performed by the PhD candidate, Dr Rossella Alberta Piras.

Research Funding

This work was supported by:

- Progetto DDD Onlus-Associazione per la lotta alla DDD, Milan, Italy;
- Fondazione ART per la Ricerca sui Trapianti ART ONLUS (Milano, Italy);
- Fondazione Aiuti per la Ricerca sulle Malattie Rare ARMR ONLUS (Bergamo, Italy);
- Telethon grant GGP09075;
- European Union Seventh Framework Programme FP7-EURenOmics project number 305608;
- Kidneeds grant 2016.

TABLE OF CONTENTS

TABLE OF CONTENTS.....	I
INTRODUCTION	1
1. THE ROLE OF COMPLEMENT IN DENSE DEPOSIT DISEASE, C3 GLOMERULONEPHRITIS AND IMMUNE COMPLEX-MEDIATED.....	1
1.1 The complement system.....	1
1.2 The renal glomerulus	5
1.2.1 Glomerular Endothelial Cells.....	6
1.2.2 Glomerular basement membrane.....	7
1.2.3 Podocytes	9
1.2.4 The Mesangium.....	11
1.3 Diagnosis and pathogenesis of C3 glomerulopathy and IC-MPGN	13
1.4 Genetic drivers of C3G and IC-MPGN.....	17
1.4.1 Complement gene variants.....	17
1.4.2 Genomic rearrangements in RCA cluster	21
1.5 Acquired drivers of C3G and IC-MPGN	25
1.6 Association of C3G/IC-MPGN with other diseases.....	27
1.6.1 Acquired partial lipodystrophy	27
1.6.2 Ocular Drusen.....	27
1.6.3 Secondary forms of C3G and IC-MPGN.....	28
1.6.4 The spectrum of complement rare genetic variants among C3G, IC-MPGN and atypical HUS.....	30
1.7 Therapy	34
1.8 Summary	36
2. COMPLEMENT ABNORMALITIES IN AN ITALIAN COHORT OF PATIENTS WITH C3 GLOMERULOPATHY AND IMMUNE COMPLEX-MEDIATED MPGN.....	39
2.1 Introduction.....	39
2.2 Patients.....	41
2.3 Diagnosis.....	42
2.4 Methods.....	44
2.4.1 Complement component assays.....	44
2.4.2 DNA samples.....	44
2.4.3 Complement Minipanel and Genetic data analysis.....	44
2.4.4 Cluster analysis.....	46
2.4.5 Statistics	47
2.5 Results.....	48

2.5.1 Complement abnormalities in patients with IC-MPGN, DDD and C3GN.....	49
2.5.1.1 Patients and clinical parameters	49
2.5.1.2 Complement serum profile.....	51
2.5.1.3 Genetic screening	52
2.5.1.4 Effect of complement genetic and acquired abnormalities on complement profile	56
2.5.1.5 Renal survivals.....	65
2.5.1.6 Effect of complement genetic and acquired abnormalities on clinical parameters	66
2.5.1.7 Susceptibility genetic variants	70
2.5.2 Complement abnormalities and clinical outcome in patients with kidney injury classified by a three-step algorithm.	75
2.5.2.1 Classification of recently recruited patients.....	75
2.5.2.2 Algorithm-based cluster classification on the updated Italian cohort of patients with complement-mediated kidney injury.	77
2.5.2.3 Renal survival	82
2.5.2.4 Susceptibility genetic variants	83
2.5.3 Discussion.....	89
3. COMPLEMENT AND COAGULATION GENETIC SCREENING IN PATIENTS WITH DENSE DEPOSIT DISEASE	97
3.1 Introduction	97
3.2 Patients	100
3.3 Methods	100
3.3.1 DNA samples	100
3.3.2 CasCADE panel.....	100
3.4 Results	102
3.5 Discussion.....	110
4. ABNORMALITIES IN FH-FHR FAMILY	115
4.1 Introduction	115
4.2 Methods	117
4.2.1 Patients	117
4.2.2 Complement Minipanel and Genetic data analysis	117
4.2.3 Anti-FH Autoantibodies Assessment.....	118
4.2.4 FH quantification	119
4.2.5 Copy Number Variations (CNVs).....	119
4.2.6 Breakpoint Analyses	121
4.2.7 Western-Blot	123
4.2.8 FHR quantitative Western Blot analysis.....	123

4.2.9	<i>AP convertase formation and C3 convertase decay</i>	124
4.2.10	<i>Statistics</i>	125
4.3	Results.....	126
4.3.1	Copy number variations (CNVs)	126
4.3.1.1	<i>Common CNVs</i>	126
4.3.1.2	<i>Uncommon CNVs in IC-MPGN and DDD</i>	128
4.3.1.3	<i>CFHR abnormalities in a DDD patient</i>	132
4.3.2	The FHR ₃₁₋₄ -FHR ₄₉ hybrid protein	140
4.3.2.1	<i>Protein studies on a DDD patient with multiple FHR abnormalities</i>	140
4.3.2.2	<i>Effect of DDD_{CFHR31-5-CFHR410} patient serum on C3 and C5 convertase formation and C3 convertase decay</i>	143
4.3.2.3	<i>Future studies</i>	145
4.3.3	Likely pathogenic variants across CFH-CFHR gene cluster in DDD patients.	146
4.3.4	Circulating levels and molecular pattern of FH/FHR proteins in a cohort of DDD patients.	147
4.3.4.1	<i>Quantitative WB analysis confirmed FHR deficiency in DDD patients</i>	163
4.3.5	Prospective Studies	165
4.3.6	Discussion	167
5.	CONCLUSIONS.....	171
	BIBLIOGRAPHY	178

INDEX OF FIGURES

Figure 1.....	4
Figure 2.....	5
Figure 3.....	6
Figure 4.....	12
Figure 5.....	14
Figure 6.....	15
Figure 7.....	16
Figure 8.....	21
Figure 9.....	22
Figure 10.....	28
Figure 11.....	43
Figure 12.....	46
Figure 13.....	49
Figure 14.....	51
Figure 15.....	53
Figure 16.....	54
Figure 17.....	56
Figure 18.....	57
Figure 19.....	57
Figure 20.....	58
Figure 21.....	58
Figure 22.....	59
Figure 23.....	59
Figure 24.....	61
Figure 25.....	61
Figure 26.....	63
Figure 27.....	63
Figure 28.....	65

Figure 29	65
Figure 30	66
Figure 31	67
Figure 32	68
Figure 33	69
Figure 34	81
Figure 35	82
Figure 36	82
Figure 37	102
Figure 38	103
Figure 39	107
Figure 40	109
Figure 41	126
Figure 42	128
Figure 43	130
Figure 44	131
Figure 45	132
Figure 46	133
Figure 47	134
Figure 48	135
Figure 49	135
Figure 50	136
Figure 51	137
Figure 52	138
Figure 53	140
Figure 54	141
Figure 55	142
Figure 56	142
Figure 57	144
Figure 58	148

Figure 59.....	149
Figure 60.....	150
Figure 61.....	151
Figure 62.....	152
Figure 63.....	155
Figure 64.....	156
Figure 65.....	157
Figure 66.....	158
Figure 67.....	159
Figure 68.....	160
Figure 69.....	161
Figure 70.....	162
Figure 71.....	164
Figure 72.....	165

INDEX OF TABLES

Table 1	20
Table 2	24
Table 3	50-51
Table 4	55
Table 5	71-72
Table 6	73
Table 7	74
Table 8	76
Table 9	76
Table 10	79
Table 11	80-81
Table 12	83-86
Table 13	87
Table 14	88
Table 15	104
Table 16	118
Table 17	121
Table 18	122
Table 19	123
Table 20	127
Table 21	139
Table 22	153
Table 23	163
Table 24	164

**MATERIAL PUBLISHED CONTAINING WORK DESCRIBED
IN THE THESIS**

~ Iatropoulos P, Noris M, Mele C, **Piras R**, Valoti E, Bresin E, Curreri M, Mondo E, Zito A, Gamba S, Bettoni S, Murer L, Fremeaux-Bacchi V, Vivarelli M, Emma F, Daina E, Remuzzi G. *“Complement gene variants determine the risk of immunoglobulin-associated MPGN and C3 glomerulopathy and predict long-term renal outcome.”* Mol Immunol. 2016;71:131-42.

~ Iatropoulos P, Daina E, Curreri M, **Piras R**, Valoti E, Mele C, Bresin E, Gamba S, Alberti M, Breno M, Perna A, Bettoni S, Sabadini E, Murer L, Vivarelli M, Noris M, Remuzzi G *“Cluster Analysis Identifies Distinct Pathogenetic Patterns in C3 Glomerulopathies/Immune Complex-Mediated Membranoproliferative GN”.* J Am Soc Nephrol. 2018; 29:283-294.

INTRODUCTION

1. THE ROLE OF COMPLEMENT IN DENSE DEPOSIT DISEASE, C3 GLOMERULONEPHRITIS AND IMMUNE COMPLEX-MEDIATED.

1.1 The complement system

The complement cascade is an immune-surveillance system that protects from pathogen invasion and participates in physiological processes to maintain tissue homeostasis. It consists of a series of proteins that are mostly synthesized in the liver, and exist in the plasma and on cell surfaces as inactive precursors then activated in a cascading manner. Complement system normally operates at a low steady state level of activation and is tightly controlled at each level by multiple complement regulators and inhibitors that discriminate between self and non-self surfaces. However, an inadequate balance between complement regulators and inhibitors have a pathologic role in several glomerular diseases^{15,16}.

Complement cascade can be initiated by three major activation pathways, the alternative (AP), the classical (CP), or the lectin (LP) pathway (Fig.1). The AP is spontaneously and continuously activated¹⁷. The CP is initiated by generation of antigen/antibodies complexes or by virus and Gram-negative bacteria¹⁸. The LP is triggered by carbohydrates on microbial or altered host surfaces¹⁹⁻²¹. The resulting activation from each pathway generates the C3 convertases, the first proteolytic complexes of the cascade (AP convertase, C3bBb, and CP and LP convertase, C4bC2a) that can cleave the component 3 (C3) into C3a and C3b. C3a acts as an anaphylatoxin. C3b covalently binds to surface membranes, e.g. intact host cells, microbial membranes and modified host surfaces (apoptotic cells or damaged tissues). On healthy host cells C3b can be

inactivated to generate iC3b by the protease Factor I (FI), in presence of complement regulators with factor I cofactor activity which include Factor H (FH), membrane cofactor protein (MCP/CD46), and Complement receptor 1 (CR1/CD35). Thrombomodulin (THBD), an ubiquitous transmembrane endothelial-cell glycoprotein, binds C3b and, in presence of FH, facilitates FI-mediated C3b inactivation²².

In contrast, on microbial or apoptotic cells, complement regulators are not present and therefore complement activation is not controlled. C3b can generate, in presence of Factor B (FB) and Factor D (FD), additional C3 convertase, thereby amplifying the deposition of C3b through “the amplification loop”. The AP C3 convertase is stabilized by properdin (FP). Accumulation of C3b favors the generation of C5 convertases (AP convertase, C3bBbC3b, and CP and LP convertase, C4bC2aC3b), the second proteolytic complexes of complement cascade, that process the C5 into the potent anaphylatoxin C5a and C5b. C5b recruits complement components C6, C7, C8 and multiple molecules of C9 to the surface to assemble the terminal complex C5b-9 (TCC) which can be soluble (sC5b-9) when formed in the fluid-phase or inserted into a membrane (membrane attack complex; MAC) leading to pore formation and cell lysis²³⁻²⁵.

On healthy host cells each step of complement system is also controlled by soluble or membrane regulators. Among soluble proteins C1 inhibitor (C1-INH) and C4b-binding protein (C4BP) regulate the CP and LP, while FH and FI control AP. Factor H, besides its cofactor activity for FI-mediated cleavage of C3b to iC3b, accelerates the decay of the AP C3 convertase, C3bBb. Vitronectin (VN; also known as S Protein) and Clusterin (Cl) bind soluble nascent C5b-7/8/9 complexes, blocking their incorporation into cell membranes and forming soluble complexes commonly indicated as "sC5b-9"²⁶. Membrane proteins include the convertase regulators represented by CR1, MCP and

decay accelerating factor (DAF) and the terminal pathway regulator CD59 (or protectin) that binds C5b-8 complexes, inhibiting the recruitment of C9, thus preventing MAC formation.

Furthermore, interactions between complement and coagulation systems have been proposed although the molecular pathway of this interplay is still unclear. Some coagulation factors have effects on complement system. Factor (F) Xa, FXIa and plasmin may cleave both C3 and C5 causing subsequent generation of C3a and C5a. Kallikrein cleaves selectively the C5. Factor XIIa activates C1q and thereby the complement CP while C1-INH inhibits the endogenous coagulation pathway (Kallikrein, Factor XIIa) and also classical and lectin complement pathways (CP:C1qrs; LP: MBL)²⁷⁻²⁹.

The anaphylatoxins, C3a and C5a, are chemoattractants for neutrophils and other leukocytes in the site of inflammation and exhibit potent proinflammatory properties. These include smooth muscle contraction, increased capillary permeability and release of histamine from basophils and mast cells³⁰. These effects are mediated by binding to their specific receptors, C3aR and C5aR. The activity of anaphylatoxins is abolished by carboxypeptidase N, which cleaves the carboxy-terminal arginine residue of C3a and C5a, generating desarginated forms termed C3a(desArg) and C5a (desArg). The biological activity of these forms is significantly reduced in comparison that of their full-length forms³¹. C3a and C5a are also inactivated by thrombin activatable fibrinolysis inhibitor (TAFI), a plasma procarboxypeptidase B activated both by thrombin and thrombomodulin^{22, 32, 33}.

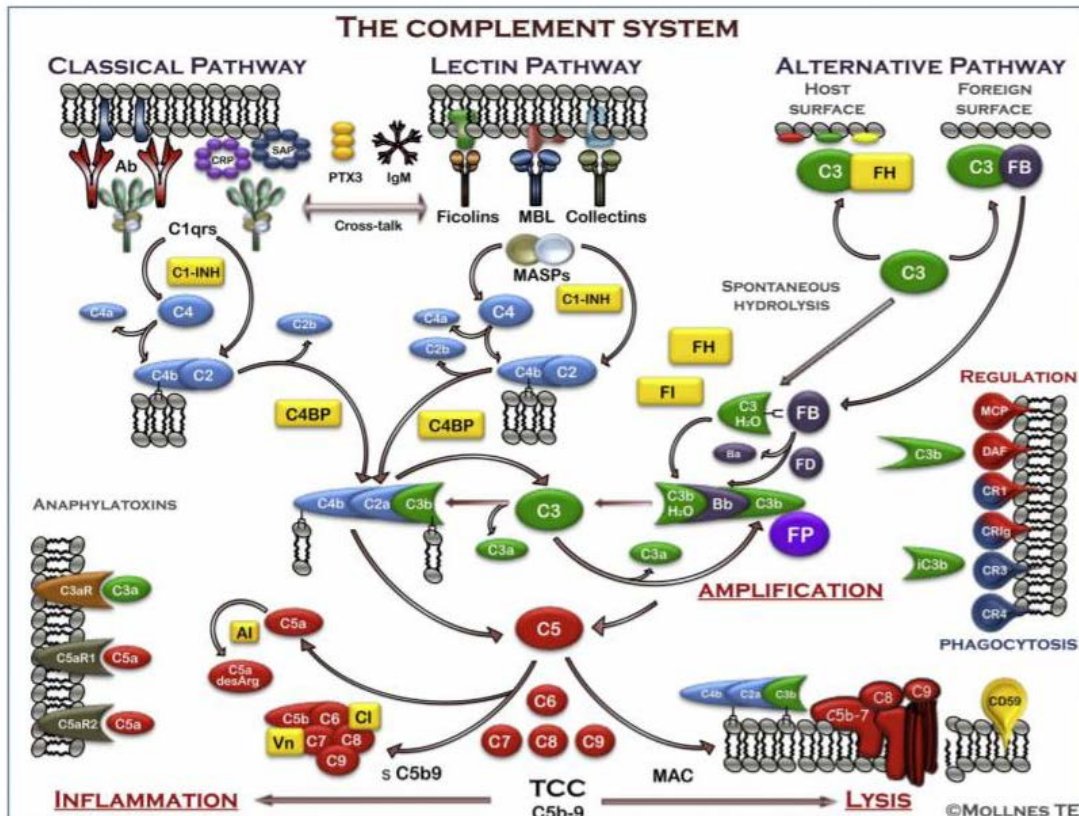


Figure1. Schematic representation of Complement System activation taken from Ricklin et al. (2017)⁷.

Complement system can be initiated by three pathways. The classical pathway (CP) is activated when C1q (part of the penta-molecular complex C1q₂S₂ of the first complement component C1) recognizes antibodies bound to their corresponding antigens with consequent activation of the proteases C1r and C1s. The latter cleaves C4 into C4a and C4b that covalently binds to surfaces close to site of activation. C1s also cleaves C2 in C2a and C2b. C4b on surfaces binds C2a, generating the C3 convertase of classical pathway (C4bC2a). The lectin pathway (LP) begins after the interaction between Mannan-Binding Lectin (MBL) and mannose residues of bacterial surfaces acting serine proteases (MASP1 and MASP2) that, similarly to C1s, cleaves C4 and C2 producing C3 convertase, C4bC2a. LP can be also activated by ficolins and collectins. The alternative pathway (AP) is spontaneously and continuously activated by C3 hydrolysis to form C3_{H₂O} that binds the Factor B protease (FB). Bound FB is cleaved by Factor D (FD) producing the AP convertase C3_{H₂O} convertase, C3_{H₂O}Bb. C3_{H₂O}Bb cleaves the C3 into the anaphylatoxin C3a and in the opsonin C3b. Surface-bound C3b can generate, in presence of FB and FD, additional C3 convertase, amplifying the deposition of C3b through “the amplification loop”. AP C3 convertase is stabilized by properdin, FP. Increased deposited C3b produced by the amplification loop, is bound by C3 convertases C4b2b and C3bBb to form larger complexes called C5 convertases, C4b2bC3b and C3bBbC3b. These proteolytic complexes process the C5 into C5a (a strong anaphylatoxin) and C5b. The latter recruits other complement component (C6, C7, C8 and C9) to the surface to assembly the terminal C5b-9 complex or the membrane attack complex (MAC). MAC forms pores causing cell lysis.

1.2 The renal glomerulus

The main function of the kidney is to filter the blood and concentrate metabolic waste to produce the urine. Production of urine is made in the nephron, the functional unit of the kidney. An average of 1 million up to 2.5 million of nephrons are contained in an adult human kidney³⁴ and contribute to filter about 140 liters of primary urine to produce about 1 liter of urine per day. Each nephron extends through the kidney cortex and medulla areas and is composed of the renal corpuscle, glomerular tubule and collecting tubules (Fig.2).

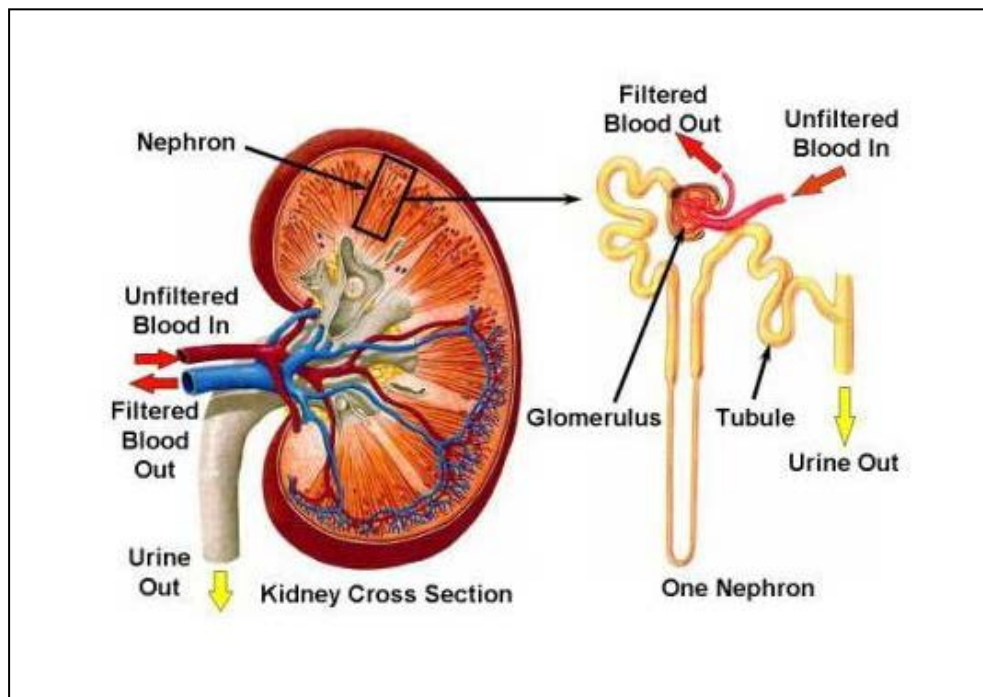


Figure 2. Image representing the nephron, the functional unit of kidney. Image taken from UNC kidney Center website.

The glomerulus is an intertwined group of capillaries surrounded by a cup-like sac called Bowman's capsule. Together the glomerulus and Bowman's capsule are known as the renal corpuscle. The area between glomerular capillaries and Bowman's capsule is

called Bowman's space and has the role to collect the primary urinary filtrate produced by the glomerular filtration barrier (GFB).

The GFB is composed by Glomerular Endothelial Cells (GECs), the glomerular basement membrane (GBM) and podocytes (Fig.3).

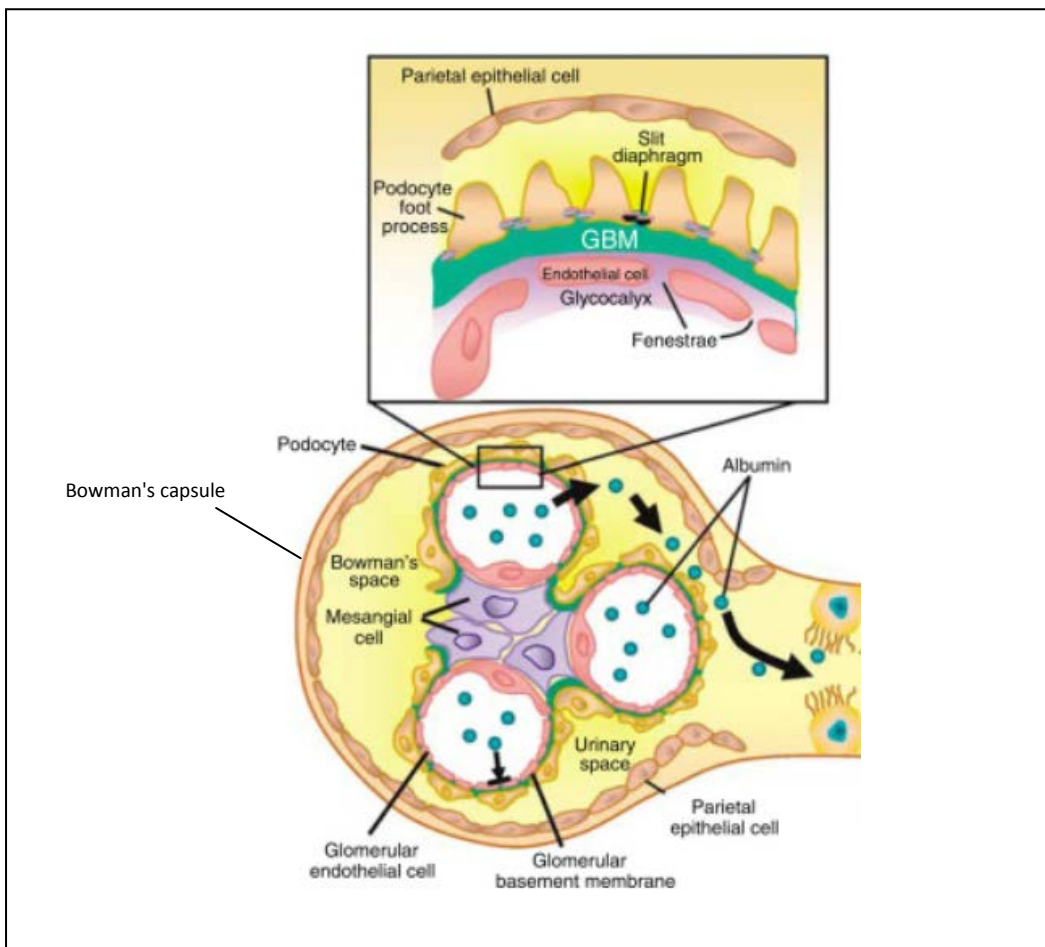


Figure 3. Image modified from Jefferson et al. (2008)¹² representing the glomerular structure.

1.2.1 Glomerular Endothelial Cells

During filtration, blood enters the afferent arteriole and flows into the glomerular capillaries characterized by transcellular pores, known as fenestrae, that are in the order of 60-100nm of diameter. These pores comprise 20-50% of the endothelial surface and

allow water and small solutes to pass into the Bowman's space, retaining large proteins as albumin^{35,36}. Numerous studies demonstrated that the filtration capability of glomerular endothelium is due to its negatively charged surface. Indeed, the luminal side of glomerular capillaries and fenestrated surfaces are covered by a layer of negatively charged glycoproteins, called glycocalyx^{37,38}. In addition, the absorption of plasma components in the glycocalyx, creates a larger coat called endothelial surface layer (ESL)³⁹. Reduced ESL depth and loss of negative charges on endothelial cells caused by enzymatic destruction of ESL components, results in increased albumin excretion. This demonstrates the important role of ESL in glomerular filtration^{40, 41}, and is confirmed in animal models^{42,43}.

1.2.2 Glomerular basement membrane

Glomerular basement membrane (GBM) is the extracellular matrix, situated between the fenestrated endothelial cells and podocytes. Although proteomic studies revealed the presence of 144 proteins in human glomerular extracellular matrix (GBM included)^{44,45} the most abundant macromolecules are type IV collagen $\alpha3\alpha4\alpha5$, laminin- $\beta2$, nidogen and the heparan sulfate proteoglycan agrin. Together, these produce a lattice with size- and charge-selective properties. In addition, GBM may contain pro-angiogenic ligands and secreted factors that play a role in the communication between GECs and podocytes. Adhesive interactions of GECs and GBM favor the adhesion of podocytes to GBM giving a stabilization of filtration barrier.

The GBM proteins are important in glomerular development, morphology and function so that mutations in genes that encode these proteins cause human kidney diseases.

Alport syndrome (AS) is a genetic disorder, characterized by hematuria, proteinuria and progression to end-stage renal disease (ESRD) determined by an incomplete maturation of GBM. These patients have mutations in the genes of *COL4A3*, *COL4A4* and *COL4A5* encoding the type IV collagen subunits $\alpha 3$, $\alpha 4$, $\alpha 5$, respectively. During the development of GBM, the $\alpha 1\alpha 1\alpha 2$ type IV collagen is substituted by $\alpha 3\alpha 4\alpha 5$ type IV collagen complex that gives long-term stability to the GBM^{46,47,48}. In the GBM of AS patients, all three $\alpha 3$, $\alpha 4$, $\alpha 5$ subunits of collagen IV are absent although only one of these chains result mutated, while the $\alpha 1$ and $\alpha 2$ chains are strongly expressed across the entire GBM. Abnormalities in the GBM are also responsible for Goodpasture's disease, an autoimmune condition characterized by pulmonary alveolar hemorrhage and anti-GBM antibodies that target the $\alpha 3$ subunit of type IV collagen located in the renal glomerulus and causing progressing glomerulonephritis⁴⁹.

Mutations in the gene *LAMB2*, encoding the laminin- $\beta 2$, a protein expressed in the GBM to anchor and differentiate podocyte foot processes, causes Pierson syndrome⁵⁰. Loss of membrane integrity causes proteinuria leading to ESRD often with an early-onset. Since laminin $\beta 2$ is also present in nervous system and in the ocular connective tissue, mutations in *LAMB2* cause also blindness and neurodevelopment problems⁵¹.

Nidogens, (also known as entactins), are two glycoproteins found in the GBM and are encoded by two different genes. Since Nidogen-1 binds to both laminin- $\gamma 1$ and type IV collagen, it has been hypothesized that it acts as a bridge to connect the laminin to type IV collagen. However, mutant nidogen-1 and nidogen-2 mice showed normal basement membranes^{52, 53} though double nidogen knockout mice resulted in perinatal lethality⁵⁴. These findings indicate that nidogens confer extra stability to GBM under unusual stress, but they are not essential for their initial formation⁵⁵.

Heparan sulfate proteoglycans (HSPGs) are characterized by a sulfated glycosaminoglycan side chains bound to a protein core. Agrin is the most abundant HSPG in the GBM⁵⁶ and through its glycosaminoglycan chains gives a negative charge to GBM suggesting a role in the charge selectivity of GFB and interactions with adjacent cells. In addition, heparan sulfate side chains may bind and sequester growth factors, as the VEGF produced by podocytes. However, in *Agrn* knockout mice, a reduction of GBM anionic charge was detected but with normal function of the GBM. In addition, the in-vivo treatment with heparanase to destroy heparan sulfate side chains did not cause proteinuria⁵⁷. These findings indicate that agrin and the negative charge of the GBM are not so crucial in the charge selectivity of GFB⁵⁸.

1.2.3 Podocytes

Podocytes (or visceral epithelial cells) are the most abundant glomerular cells and express an elaborate octopus-like cytoarchitecture, specialized in the blood ultrafiltration. On the basis of structure and function characteristics, podocytes are composed of a main body, major processes and foot processes (FPs). The main body contain the nucleus and other organelles such as Golgi apparatus, rough endoplasmic reticulum, mitochondria and lysosomes. Podocyte cell bodies with their FPs cover the outer side of GBM, facing the Bowman's capsule and the primary urine⁵⁹. The cell body is separated from the GBM by a subpodocyte space that confer dynamic properties which modulate capillary permeability and influence the response to inflammation⁶⁰. FPs of adjacent podocytes interdigitate, leaving between them the filtration fissures that are bridged by intercellular junctions that constitute a structure called slit diaphragm (SD; Fig.3). Foot processes are characterized by an highly regulated actin cytoskeletal network while SD is composed by several molecules, including nephrin, CD2

associated protein (CD2AP), protocadherin Fat 1 (FAT1), tight junction protein 1 (also known as ZO-1), P-cadherin, Podocin and Kin of IRRE-like protein 1-2 (also known as Neph 1-3, respectively), some of them are important for SD integrity⁶¹. Nephrin is a transmembrane protein that by its extracellular domain forms homodimers with nephrin from an adjacent podocyte or heterodimers with neph-1. These interactions are important to maintain the permeability characteristics of the SD^{62,63}. In addition, nephrin, through its intracellular domain, interacts with podocin and other regulatory proteins to promote actin polymerization⁶⁴. Inactivating mutations in the genes encoding for nephrin and podocin (*NPHS1* and *NPHS2*) cause congenital nephropathy characterized by collapse of FPs and the absence of SDs, an hallmark of podocyte injury correlated with proteinuria^{65,66}.

Podocytes with glomerular basement membrane and endothelial fenestrated cells form the glomerular filtration barrier promoting the filtration of small solutes, electrolytes and cationic molecules and limiting the passage of macromolecules and cationic molecules^{64, 67}.

Podocytes have also the important role to promote the proliferation, survival and the development of endothelial cells through the production of pro-angiogenic factors as VEGF, Angpt 1 and SDF1⁶⁸.

The majority of cases of glomerular proteinuria are accompanied by a shape change of podocytes, called foot processes effacement (FPE). This consists of the retraction of foot processes into the cell bodies. Proposed mechanisms causing FPE involve slit diaphragm loss⁶⁹, podocyte cytoskeleton disruption^{70,71} or abnormal podocyte-GBM interactions^{72,73}. Since experimental models with proteinuria in absence of FPE and vice versa have been reported^{63,74-78} it has been hypothesized that foot processes effacement alone do not cause proteinuria but may represent a consequence of podocyte injury¹².

1.2.4 The Mesangium

The mesangium, an important component of glomerular structure, has the main role to provide structural and functional support to the GBM. On the capillary lumen side the mesangium is in direct contact with glomerular endothelial cells and is composed by mesangial cells (MCs) and extracellular matrix. Mesangial cells are separated from podocytes by GBM and, like smooth muscle cells, have a contractile activity that may be responsible for glomerular distensibility in response to pressure^{79, 80}.

Mesangial cells generate their own extracellular matrix, which is hypothesized to give support for glomerular capillaries. The mesangial extracellular matrix is composed by collagens type I, III, IV and V, laminin, fibronectin, heparan sulfate proteoglycans and chondroitin sulfate proteoglycans. Mesangial cells have been reported to synthesize growth factors (like interleukin IL-1, platelet-derived growth factor PDGF, insulin-like growth factor IGF), cytokines (including transforming growth factor- β , TGF- β), adhesion molecules, chemokines, and vasoactive factors (as angiotensin-II). Experimental data showed that the survival of MCs depends precisely on PDGF^{81,82} while mesangial matrix expansion, typical of diabetic glomerulosclerosis, appeared to be under TGF- β control⁸³.

Mesangial cell proliferation and matrix expansion are typically associated with several diseases such as IgA nephropathy, diabetic nephropathy, mesangioproliferative glomerulonephritis, and systemic diseases such as lupus nephritis. Indeed, mesangial matrix expansion, cause a reduced glomerular capillaries area, and may eventually obstruct the lumen capillary (Fig.4)^{84,36,85}.

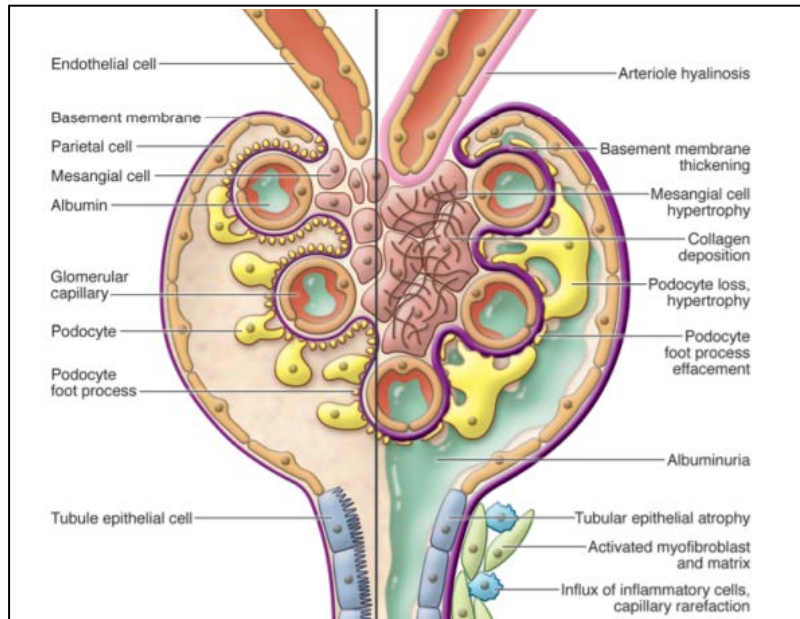


Figure 4. Images modified from Reidy et al. (2014)¹¹. Comparison of glomerulus organization between the healthy glomerulus (on the left) and glomerulus with Diabetic kidney Disease (DKD; on right). The latter is characterized by mesangial expansion, collagen deposition, GBM thickening, podocyte loss and hypertrophy, podocyte foot processes effacement and albuminuria.

1.3 Diagnosis and pathogenesis of C3 glomerulopathy and IC-MPGN

Membranoproliferative glomerulonephritis (MPGN) is a kidney disorder that mainly affects children and young adults but can occur at any age. The clinical presentation and course are variable with patients presenting with asymptomatic hematuria and proteinuria, hypertension, nephritic or nephrotic syndrome, chronic kidney disease or a rapid progressive glomerulonephritis. Primary idiopathic MPGN is rare with a prevalence of 6 cases per 100,000 European people. The pathogenesis of primary MPGN is ill defined. Hypocomplementemia is a very common finding. Secondary MPGN is most often due to autoimmune diseases, chronic infections and malignancies⁸⁶.

MPGN diagnosis requires a kidney biopsy. The typical features of glomerular injury on light microscopy (LM) includes an increase in mesangial cellularity and matrix with thickening of the peripheral capillary walls by subendothelial immune deposits and/or intramembranous dense deposits and mesangial interposition into the capillary walls⁸⁷.

Traditionally, MPGN classification was based on Electron Microscopy studies (EM). The most common variant was the MPGN type I, characterized by the predominant presence of subendothelial deposits. MPGN type II (also known Dense Deposit Disease, DDD) indicated the presence of highly electron dense deposits within (i.e. intramembranous) the basement membrane. The term MPGN type III was used to describe cases with both subendothelial and subepithelial deposits^{1,88}.

The current MPGN classification is based on Immunofluorescence studies (IF) and distinguishes immune-complex mediated MPGN (IC-MPGN) from C3 Glomerulopathy (C3G). IC-MPGN is characterized by glomerular C3 and significant immunoglobulin deposition including IgG, IgM, IgA and C1q. Association between IC-MPGN and

complement classical pathway activation is based on the presence of chronic antigenemia, with antigen-antibody immune complexes caused by chronic viral and bacterial infections (as hepatitis C, hepatitis B and endocarditis), elevated levels of circulating immune-complexes due to autoimmune diseases (as lupus erythematosus, Sjögren's syndrome and rheumatoid arthritis) or paraproteinemias due to monoclonal gammopathies¹³, although in some IC-MPGN cases an underlying cause cannot be identified³.

In C3 Glomerulopathy, IF pattern is typically characterized by dominant C3 staining with no or scanty immunoglobulins. Dominant C3 is defined as "C3c intensity ≥ 2 orders of magnitude more than other immune-reactant on a 0 to 3 scale"⁸⁹ (Fig.5). Electron microscopy (EM) provides different appearances allowing a C3G subclassification in Dense Deposit Disease (DDD, with dense osmiophilic mesangial and intramembranous electron dense deposits) and C3 glomerulonephritis (C3GN, with light dense, amorphous mesangial, subendothelial, subepithelial electron deposits)⁹⁰ (Fig.6).

Acquired partial lipodystrophy (APL) and extracellular retinal deposits (drusen) have been reported both in DDD and C3GN⁹¹⁻⁹³.

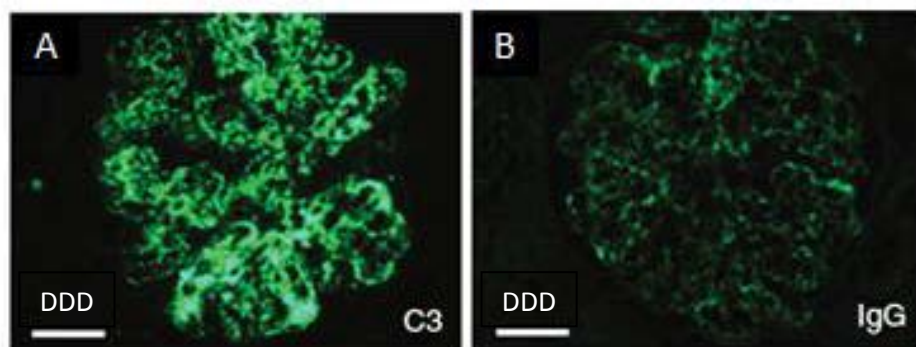


Figure 5. Immunofluorescence microscopy images modified from Houet al. (2014)⁵. Biopsy from a patient with C3 Glomerulopathy (Dense Deposit Disease) showing 3+ glomerular capillary wall and mesangial C3 staining (panel A) with 1+ of IgG (panel B).

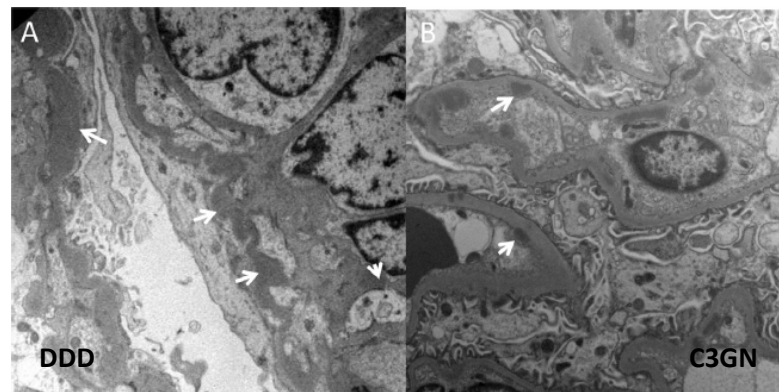


Figure 6. Electron microscopy images modified from Noris and Remuzzi, (2015)³.

The image of panel A shows the presence of osmiophilic wavy dense deposits in the GBM and also in the mesangium (arrows) of glomeruli from a patient with DDD. In panel B, the arrows indicate intramembranous and subendothelial deposits in glomeruli from a patient with C3GN.

A distinct form of C3GN is represented by CFHR5 Nephropathy, identified in two large families with reported ancestry from the Troodos mountains of Cyprus. Patients present with renal failure, C3 glomerulonephritis, synpharyngitic macroscopic hematuria, persistent microscopic hematuria and show an internal duplication in the gene of Factor H-related 5 (*CFHR5*)⁹⁴.

Hyperactivation of the complement alternative pathway (AP) appears to be a primary cause of C3G², and may be caused by both acquired and genetic factors. Indeed, the C3 nephritic factor (C3NeF), an autoantibody that stabilizes the C3 convertase, is present in around 80% and 45% of DDD and C3GN patients, respectively^{2,95}. Anti-factor B and anti-factor H autoantibodies have been also reported in a few cases⁹⁶⁻¹⁰⁰. Rare functional variants (var) in genes coding the AP complement regulators Factor H (*CFH*)

and Factor I (*CFI*) and gain of function var in the genes encoding the two components of the AP C3 convertase, complement C3 (*C3*) and Factor B (*CFB*) have been reported^{4,95,101,102} (Fig.7).

However, publications suggest that this new classification is not all-encompassing and that complement AP dysregulation may also play a role in the pathogenesis of IC-MPGN. Indeed, genetic or acquired abnormalities leading to dysregulation of the AP have been found both in C3G and IC-MPGN patients, suggesting the presence of still unknown commonalities underlying the AP dysregulation in patients with DDD, C3GN and IC-MPGN^{95, 103}.

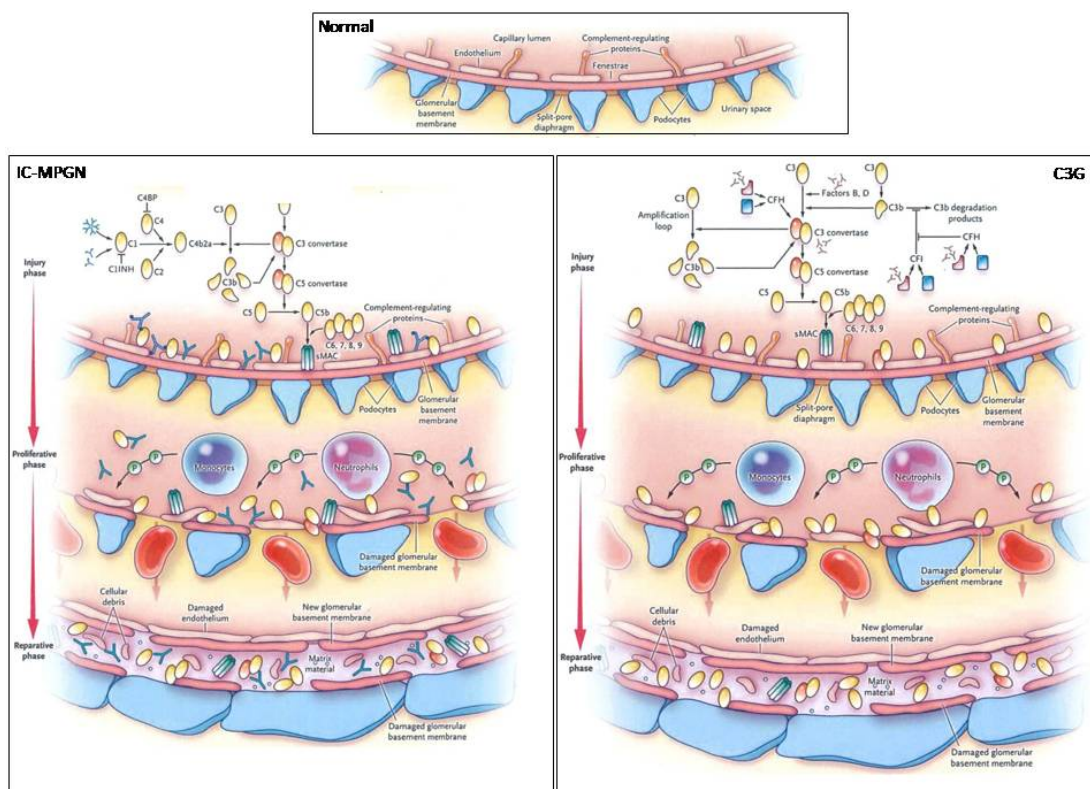


Figure 7. Images modified from Sethi et al. (2012)¹³ representing the schematic model of normal glomerular capillary wall (upper panel) and the complement activation with consequent glomerular damage in immune complex-mediated MPGN (IC-MPGN; left panel) and C3 Glomerulopathy (C3G; right panel).

1.4 Genetic drivers of C3G and IC-MPGN

1.4.1 Complement gene variants

The fact that familial forms have been reported both in C3G and IC-MPGN¹⁰⁴ indicates that genetic abnormalities may play a role in determining predisposition to these diseases. Absence of FH in plasma in association with type I and II MPGN has been reported in humans¹⁰⁵⁻¹⁰⁹, in mutant CFH deficient pigs¹¹⁰ and in *Cfh*^{-/-} mice¹¹¹.

FH is a plasma protein produced mostly by the liver that plays a central role in the regulation of the AP of complement both in fluid phase and on cellular surfaces by binding to C3b, destabilizing the AP convertase, C3bBb. In fluid phase this interaction results in dissociation of C3bBb and in irreversible inactivation of C3b to iC3b by Factor I. On cell surfaces FH competes with Factor B (FB) to bind to C3b-targeted surfaces and also favors the degradation of bound-C3b by cofactor activity. Both in patients and in pigs, FH deficiency was due to homozygous (ho) or compound heterozygous (he) *CFH* rare functional variants¹⁰⁵⁻¹⁰⁹ that determine block of protein secretion, or secreted proteins that have severely reduced cofactor and decay accelerating activity. Absence of FH in plasma causes sustained activation of the AP of complement reflected by consumption of C3 and accumulation of C3 degradation products and is associated with an early onset. However, heterozygous *CFH* var and normal FH levels have been reported in MPGN I and C3G patients^{95, 103}. Recently, rare functional variants in other complement regulatory genes *CFI*, *MCP* and gain of function var in the genes *C3* and *CFB* have been identified in a large cohort of patients with primary IC-MPGN and C3G^{4,95,101-103}. Low frequency of rare functional variants has been reported in the gene encoding thrombomodulin (*THBD*), an anticoagulant glycoprotein that also accelerates FI-mediated C3b inactivation¹⁰³. Of interest, prevalence of var was similarly distributed in IC-MPGN (16%) and C3G (20%)

underlining the common AP dysregulation implicated both in the pathogenesis of some cases of IC-MPGN and C3G.

Among C3 variants, functional studies have been reported only for two of them. Martínez-Barricarte et al. demonstrated the two aminoacid deletion of C3 ($\Delta 923-924$ AspGly), found in heterozygosity in a DDD pedigree, is a gain of function variant causing an uncontrolled C3 activation in the fluid phase. By functional studies they proved that mutant C3, the predominant circulating C3 protein in the patients, generated an active C3 convertase that cleaved wild-type C3 and that was resistant to decay by FH. Moreover, mutant C3b was resistant to proteolysis by FI in presence of FH. Altogether these abnormalities caused a continuous activation and consumption of C3 produced by the normal allele indicating that fluid-phase complement dysregulation can be caused not only by abnormalities in AP regulatory proteins, like FH, but also by components of the AP C3 convertase generating a convertase resistant to FH-inactivation¹⁰¹. In 2016, Chauvet et al, characterized a C3 missense mutation (p.I734T), present in heterozygosity in two related C3GN individuals with normal C3 levels, generating a functional C3 convertase normally regulated by FH. Assays using recombinant proteins showed a decreased binding of mutant C3 to complement receptor 1 (CR1), a regulator highly expressed on podocytes. By cellular models of complement activation the authors demonstrated that serum from patients caused an high deposition of C3 fragments on glomerular endothelial cells (GEnC) and podocytes indicating that this C3 variant causes a cell surface AP dysregulation, and evidencing podocytes as targets of complement in C3GN¹¹².

Rare variants in the gene encoding *CFB* have been described in a familial case of C3GN¹¹³ and in IC-MPGN patients¹⁰³ although their functional effects are still unknown.

Common single nucleotide polymorphisms (SNPs) have been studied in IC-MPGN and C3G. Among *CFH* SNPs, the p.Y402H (c.1204T>C; rs1061170), that has been shown to be a susceptibility factor for age-related macular degeneration¹¹⁴, is reported to be over-represented in DDD compared with controls^{95,115,116} while the p.V62I (c.184G>A; rs800292) resulted protective in patients with C3G (including DDD and C3GN)¹⁰³. Functional studies revealed that the H402 may determine lower binding of FH to glycosaminoglycans (GAGs) and, as a consequence, lower protection of cell surfaces from complement attack^{114,117,118} while the I62 increases binding affinity for C3b and enhances cofactor activity with the resulting reduction of AP activation.

Association studies revealed that the *CFH-H1* haplotype including FH-H402 (c.-331C, c.184G, c.1204C, c.2016A and c.2808G) is associated with DDD while the *CFH-H2* (331C, c.184A, c.1204T, c.2016A and c.2808G) haplotype is decreased in DDD supporting the protective effect of the FH-I62 variant (Table 1)^{14, 119}.

Servais et al. in 2012 identified one at-risk *MCP* haplotype (named *MCP*_{aagg}: c.-652A, c.-366A, c.944-78G, c.1082+638G, c.*783T) for C3GN and MPGN I. Recently, Iatropoulos et al. observed an higher frequency of *MCP* c.-366A and the c.*783T variants in patients with IC-MPGN compared with controls. Likewise, the allele c.-366A resulted significantly over expressed in DDD compared with controls.

These results highlight that common variants in *MCP*, which is expressed on endothelial and mesangial cells and participates in the generation of the C3 metabolite iC3b, influence the glomerular pattern of patients presenting fluid-phase activation of complement⁹⁵.

For the first time Iatropoulos et al., reported a significant association between C3G patients and the *THBD* A473 allele¹⁰³. *THBD* is an anticoagulant glycoprotein

expressed by glomerular endothelial cells that binds C3b and FH enhancing FI-mediated C3b inactivation²². Increased thrombomodulin expression was found in kidney biopsy of MPGN patients probably as a protective response to neutralize the complement hyperactivation occurring on MPGN glomerular cells^{120,121}.

Finally, two SNPs in *C3* (*C3*p.R102G and *C3* p.P314L), are associated with DDD¹¹⁶. Alternative complement activity assay in genotyped controls showed that the presence of the risk allele *C3* p.G102 or p.L314 increased the complement activity in comparison of *C3* p.R102 or p.P314, respectively. In addition, the *C3* p.L314 risk allele showed a synergic effect with the above described FH risk alleles p.H402 and p.V62 indicating a complotype associated with DDD¹¹⁶. These data are consistent with the functional studies reporting that FH bound C3b102G with less efficiency in comparison to C3b102R and that FI cofactor activity to inactivate C3b102G was decreased resulting in an overall increased AP activity of C3b102G¹²².

Haplotype	c. -331C>T <i>rs3753394</i>	c.184G>A (p.Val62Ile) <i>rs800292</i>	c.1204T>C (p.Tyr402His) <i>rs1061170</i>	c.2016A>G (p.Gln672Gln) <i>rs3753396</i>	c.2808G>T (p.Glu936Asp) <i>rs1065489</i>	CONTROLS Frequency <i>n</i> =317	DDD Frequency <i>n</i> = 16
H1	C	G	C	A	G	0.257	0.47
H2	C	A	T	A	G	0.203	0.12
H3	T	G	T	G	T	0.207	0.16
H4a	C	G	T	A	G	0.139	0.09
H4b	T	G	T	A	G	0.070	0.06
H5	T	G	C	A	G	0.037	-
H6	C	G	T	A	G	0.021	0.06
H7	T	G	T	A	G	0.016	-
H8	C	G	T	G	T	0.015	-

Table 1. Haplotypes of *CFH* and association with DDD. (Data from de Còrdoba and Goicoechea, 2008¹⁴). H1 haplotype (in red) is associated with DDD while H2 haplotype (green) is less present in DDD than in controls suggesting a protective effect.

1.4.2 Genomic rearrangements in RCA cluster

In the regulator of complement activation (RCA) gene cluster on chromosome 1, downstream of *CFH*, are located five factor H-related genes (*CFHRs*). This genomic segment is characterized by several large regions of sequence similarity (Fig 8).

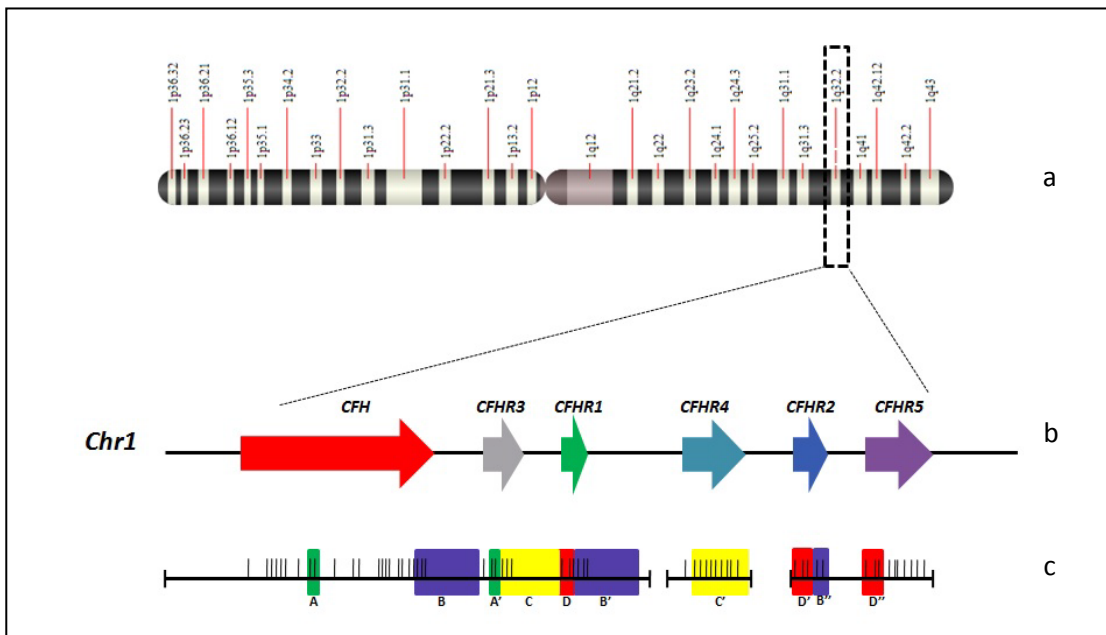


Figure 8. Regulator of complement activation (RCA) gene cluster. Images modified from de Cordoba, Immunobiology, 2012⁸. The RCA gene cluster is located on chromosome 1 (panel a) and the five *CFHR* genes are downstream of *CFH* (panel b). The coloured boxes in panel c indicate the sequence repeats, labelled with the same letter (i.e., B, B', B''). The vertical lines represent the exon position of *CFH* and *CFHRs* genes.

CFHR genes derive from *CFH* gene by tandem duplication events and encode the five Factor H-related proteins (FHRs)¹²³. These proteins, organized in short consensus repeats (SCRs), are mainly produced in the liver and, with the exception of FHR4, circulate in plasma in glycosylated isoforms. The two N-terminal domains of all five FHRs proteins share an high degree of sequence (36-94%) while the C-terminal domains show an high sequence homology with the C-terminal of FH (36-100%)¹²⁴ (Fig.9). Factor H, through its C-terminal domains (SCR 18-20) and SCR7 binds complement C3b, heparin, glomerular basement membrane (GBM), bacterial ligands

and glycosaminoglycans (GAGs) while its N-terminal region has a complement regulatory function through cofactor and decay accelerating activities.

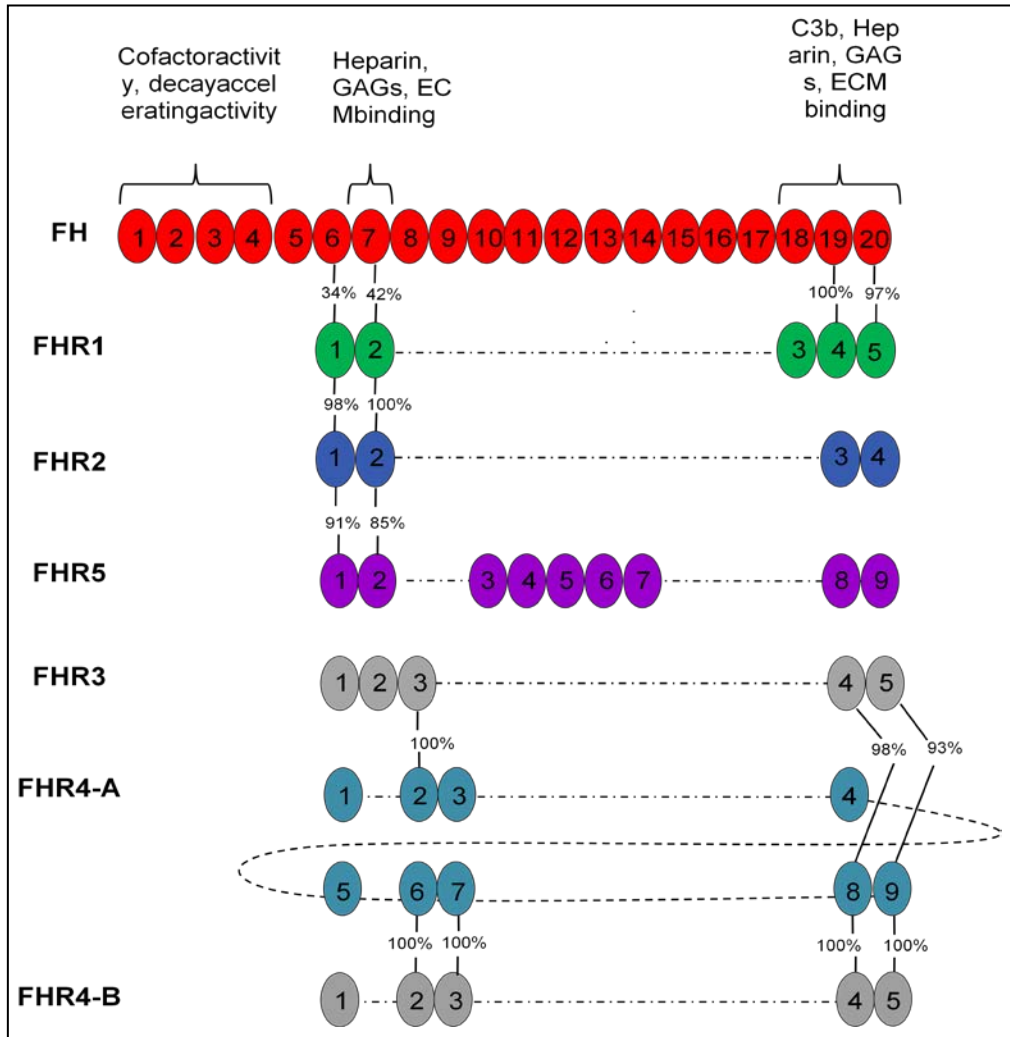


Figure 9. The Factor H (FH) and Factor H-related (FHR) proteins are aligned based on their homology. The percentage indicate the sequence similarity taken from Jozsi et al, (2015)⁹.

The homology between C-terminal domain of FH and FHR proteins suggests that FHRs can similarly bind surface ligands as FH but since they lack the N-terminal complement regulatory domains of FH do not have a similar direct complement regulatory activity.

Nevertheless some in vitro studies reported factor I cofactor activity for FHR3 and FHR4¹²⁵ and FHR5¹²⁶. FHR5 have been also reported to inhibit C3 convertase though

very high concentrations required to observe complement regulation by FHR5 interrogate about its biological relevance. Inhibition of C3 convertase and terminal complement complex assembly, but not factor I cofactor activity, have been reported for FHR2¹²⁷ while C5 convertase inhibition have been described for FHR1¹²⁸.

Native factor H-related (FHR) proteins can compete with FH for binding to C3b and other C3 activation fragments. In 2013 Goicoechea et al. showed that FHR1, FHR2 and FHR5 circulate in plasma as homo and hetero-oligomeric complexes, the formation of which is mediated by the conserved N-terminal domains^{129, 130}. This dimerization significantly enhances avidity of FHRs for their ligands that, by competing with FH, prevents the normal complement regulatory function of FH in a process termed "FH deregulation".

The presence of several large regions of sequence similarity in the RCA cluster favors genomic abnormalities including genetic rearrangements, duplications and deletions¹³¹. Indeed, genomic rearrangements in *CFHRs* have been described both in DDD and C3GN^{94,130,132-135,136} (Table 2).

In 2010 Gale et al. described an internal duplication of exons 2 and 3 of *CFHR5*, encoding the first two N-terminal domains, in Greek Cypriot patients with *CFHR5* nephropathy⁹⁴. The same duplication, with a different DNA breakpoint, has been reported in a C3G British family without Cypriot ancestry¹³⁴. A similar FHR5 protein, derived from the deletion involving exon 4 and 5 of *CFHR2* that generates a hybrid protein between the first two SCRs of FHR2 (that have 91% and 85% of sequence homology with the first two SCRs of FHR5) and the full-length FHR5 was identified in a C3G-DDD familial case¹³². Malik et al. described in a C3GN family a heterozygous deletion involving exons 4-6 of *CFHR3* and exon1 of *CFHR1* producing a hybrid protein composed of the first two SCRs of FHR3 linked to full-length FHR1¹³³. An

internal duplication of *CFHR1* resulting in the duplication of FHR1 SCR1 to SCR4 was found in a Spanish family with C3G¹³⁰. In a patient with familial C3GN, a hybrid protein containing the first two SCRs of FHR5 followed by all SCRs of FHR2 was found¹³⁵. Recently, a large deletion involving *CFHR1*, *CFHR2* and *CFHR4* leading to a FHR1-R5 hybrid protein has been described in a familial dominant form of C3G¹³⁶.

Most DDD/C3GN associated hybrid FHR proteins are characterized by duplication of the dimerization motifs, which result in the formation of large multimeric complexes leading to an increased affinity for surface bound C3b and enhanced competition with FH^{9,124,136-138}. Interestingly, in patients carrying three of these hybrids, circulating C3 levels were normal, indicating local alternative complement dysregulation within the glomeruli rather than in the circulation^{94,133,135}.

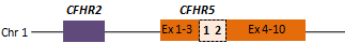

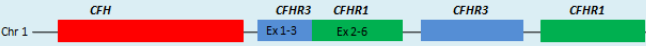

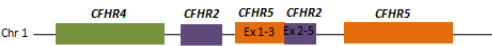


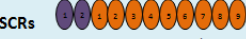
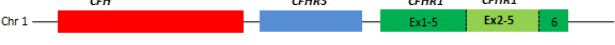

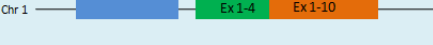
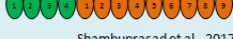
Diagnosis	Genetic abnormality	Mutant protein
C3GN	Dupl <i>CFHR5</i> ₁₂₃₂₃₋₁₀ 	FHR5 ₁₂₁₂₃₋₉ fusion protein SCRs  Gale et al, 2010; Medjeral-Thomas, 2013
C3GN	Hybrid gene <i>CFHR3</i> ₁₋₃ - <i>CFHR1</i> ₂₋₆ 	FHR3 ₁₋₂ -FHR1 ₁₋₅ fusion protein SCRs  Malik et al, 2010
C3GN	Hybrid gene <i>CFHR5</i> ₁₋₃ - <i>CFHR2</i> ₂₋₅ 	FHR5 ₁₋₂ -FHR2 ₁₋₄ fusion protein SCRs  Xiao et al, 2016
DDD	Hybrid gene <i>CFHR2</i> ₁₋₃ - <i>CFHR5</i> ₁₋₁₀ 	FHR2 ₁₋₂ -FHR5 ₁₋₉ fusion protein SCRs  Chen et al, 2014
C3GN	Dupl <i>CFHR1</i> ₁₂₃₄₅₂₃₄₅₆ 	FHR1 ₁₂₃₄₁₂₃₄₅ SCRs  Tortajada et al., 2013
Overlap C3GN/ DDD	Hybrid gene <i>CFHR1</i> ₁₋₄ - <i>CFHR5</i> ₁₋₁₀ 	FHR1 ₁₋₃ -FHR5 ₁₋₉ fusion protein SCRs  Shambuprasad et al., 2017

Table 2. List of genomic rearrangements identified in C3GN and DDD.

1.5 Acquired drivers of C3G and IC-MPGN

The commonest acquired factor associated with MPGN is C3 Nephritic factor (C3NeF), an auto-antibody directed against the AP C3 convertase (C3bBb). The binding of C3NeF to C3bBb stabilizes the complex and prolongs its half-life, preventing degradation by its normal inactivators such as FH, resulting in complement activation and chronic consumption of C3¹³⁹. C3NeF presence is equally distributed in IC-MPGN and C3GN patients although the highest prevalence (around 80%) is in DDD patients^{95, 103}. C3 nephritic factors have been also observed in APL¹⁴⁰ and in healthy individuals¹⁴¹. In around 3% of C3G patients, a C4NeF has been identified. This is an auto-antibody that stabilizes the CP and LP convertase, C4bC2a, preventing the normal convertase decay mediated by CR1 and C4BP^{142, 143}. C4NeF has been also associated with post-infectious glomerulonephritis, systemic lupus erythematosus and meningococcal infections¹⁴⁴⁻¹⁴⁶. Recently, Marinozzi et al, described auto-antibodies stabilizing the C5 convertase (C5 Nephritic Factors, C5NeFs) in around 50% of C3G patients. C5Nephritic Factors were predominantly identified in C3GN compared to DDD patients and often in concomitance with C3NeFs. Both C3NeFs and C5NeFs correlated with low C3 levels while only C5NeFs correlated with high SC5b-9 levels¹⁴⁷.

Auto-antibodies against FH have been reported in MPGN and C3G. In the French cohort, 11% of C3G patients were positive for anti-FH autoantibodies¹⁰⁰. These autoantibodies predominantly bind to the N-terminal domain^{148,149}, preserving FH binding to cell surfaces and often are associated with the presence of C3NeF in children¹⁴⁹ or with monoclonal gammopathy in adults^{100,150}.

In 2010, Strobel et al reported the presence of an autoantibody that bound FB in a DDD patient. FB antibody binds both the native FB and the Bb fragment that is part of C3 convertase, making it more stable to FH-mediated decay and increasing C3

consumption. However, the anti-FB antibody reduces *in vitro* the C5 convertase activity, possibly by preventing the binding of additional C3b molecules to C3 convertase. However, *in vivo* studies indicated that not all C5 convertases are inhibited⁹⁶. Factor B auto-antibodies have been found in additional DDD patients¹⁵¹ and also in association with auto-antibodies to C3b⁹⁹.

1.6 Association of C3G/IC-MPGN with other diseases.

1.6.1 Acquired partial lipodystrophy

Acquired partial lipodystrophy (APL) is a rare condition characterized by progressive loss of fat in the upper part of the body and in the face. It commonly affects girls and usually begins during childhood. In 2004, Misra et al described low C3 levels and the presence of C3NeF in about 83% of patients with APL. About eight years after the APL onset, 22% of patients developed DDD⁹¹. Although the pathogenesis of fat loss and DDD is not clear, the AP dysregulation on kidney and adipose tissue appears to be the basis of the association between DDD and APL¹⁵². Adipocytes express Factor D and other complement proteins and the abnormal complement AP activity, caused by C3NeF, may result in adipocyte destruction, leading to APL¹⁵².

1.6.2 Ocular Drusen

Non-renal manifestations of DDD include ocular drusen. Drusen are lipoproteinaceous deposits of complement-containing debris localized between retinal pigment epithelium and Bruch's membrane¹³⁷. The presence of ocular drusen in patients with DDD appears to be determined by structural and functional similarities between Bruch's membrane, and glomerular basement membrane (Fig.10)⁹³.

Ocular drusen are the early-age hallmark of Age-related Macular Degeneration (AMD)¹⁵³, the most common cause of acquired visual disability in the industrialized world. No correlation has been reported between disease severity in the kidney and in the retina¹. However, unlike AMD, drusen in patients with DDD occur at a young age¹³⁷, mainly in the second decade of life and initially has little impact on vision suggesting the need of ophthalmologic examination at the time of kidney diagnosis and a periodic fundoscopic examination¹.

In 2009 Han et al, reported the presence of drusen in a patient with MPGN type I who may be actually classified as C3GN¹⁵⁴. In 2012, Bomback et al, among a cohort of patients with C3G, described a C3GN patient with drusen deposition¹⁰.

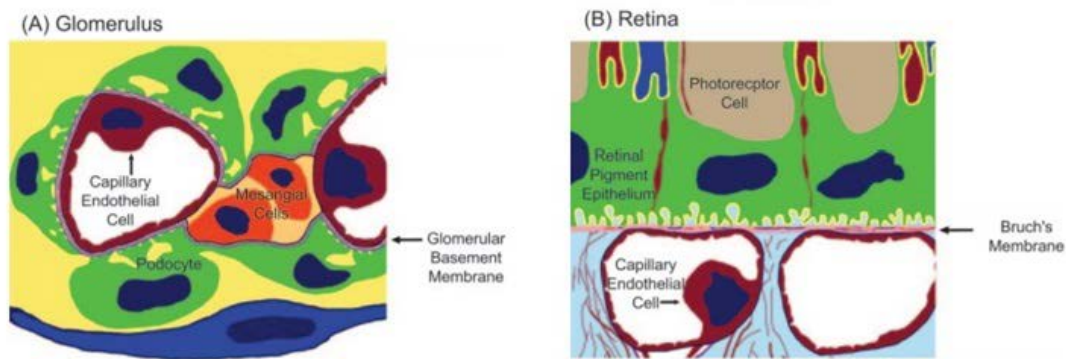


Figure 10. Figure from Appel GB et al. (2005)¹. Images representing the morphologic similarity observed in fenestrated capillaries of glomerulus (panel A) and retina (panel B). Podocytes are separated from capillary endothelial cells by GBM as well retinal pigment epithelial cells are separate from capillary endothelial cells by Bruch's membrane. In DDD have been observed electron dense deposits in both membranes¹⁰.

1.6.3 Secondary forms of C3G and IC-MPGN

Immune-complex mediated MPGN are often secondary to chronic infections, autoimmune diseases and monoclonal gammopathy³.

Among infections, hepatitis B and C are the most frequently described in association with MPGN although also bacterial (endocarditis, shunt nephritis, abscesses) and protozoal (malaria, schistosomiasis) infections have been reported¹⁵⁵⁻¹⁵⁸.

Autoimmune diseases, as systemic lupus erythematosus, scleroderma, Sjögren's syndrome and mixed cryoglobulinemia, are characterized by circulating immune

complexes that activate the complement classical pathway favoring also leukocyte accumulation, cytokine release and subsequent glomerular damage.

Monoclonal immunoglobulin deposition in mesangium and along the capillary walls, caused by monoclonal gammopathies but also by lymphomas, myelomas and leukemia can result in IC-MPGN and C3G^{97,159,160}.

1.6.4 The spectrum of complement rare genetic variants among C3G, IC-MPGN and atypical HUS

Rare genetic variants in complement genes (*CFH*, *CFI*, *CFB*, *MCP*, *C3* and *THBD*) have been reported in about 50% to 60% of patients with atypical hemolytic uremic syndrome (aHUS)¹⁶¹ and in about 18% of patients with IC-MPGN and C3G¹⁰³.

Atypical HUS is a rare disease characterized by microangiopathic hemolytic anemia, thrombocytopenia and renal impairment¹⁶¹. The histology lesion is represented by thrombotic microangiopathy (TMA) and predominantly affects the renal microvasculature, at level of glomerular capillaries and preglomerular arteries. TMA also affects brain, heart, lung, gut, pancreas and liver. The main pattern of TMA is represented by thickening of vascular walls, with prominent endothelial damage (swelling and detachment) and accumulation of proteins and cell debris in subendothelium. The hypothesis that the activation of the complement alternative pathway may have a pathogenetic role in aHUS was based on the presence of intense glomerular and arteriolar C3 and C9 staining in the biopsy of aHUS patients and on reduced serum C3 levels with normal C4 levels in 30% to 40% of them¹⁶²⁻¹⁶⁵.

The most frequent genetic abnormalities in aHUS (from 20% to 30%) are *CFH* variants. Factor H is a plasma protein that regulates the complement AP both in fluid phase and on cell surfaces. FH, through its N-terminal domains (SCR1-4) regulate AP activation by cofactor and decay accelerating activities whereas through C-terminal domains (SCR18-20) it recognizes C3b, heparin and glycosaminoglycans in host cell surfaces.

The majority of aHUS patients carry heterozygous missense changes in the C-terminus of the protein, associated with normal FH levels. Functional studies of mutant FH showed impaired binding to endothelial cells, heparin and surface-bound C3b and consequently impaired surface cofactor activity, while FH cofactor activity in fluid

phase is not affected. These events culminate with renal endothelial detachment and swelling.

IC-MPGN and C3G are glomerular diseases characterized by low C3 levels with normal C4 in about 70% of cases. Histology lesion is represented by mesangial hypercellularity, matrix expansion and thickening of peripheral capillary walls. These glomerular changes are caused by deposition of complement and /or immune complexes in the mesangium and along the capillary walls. IC-MPGN glomeruli are characterized by C3 and dominant immunoglobulin staining while C3G is mainly characterized by C3 staining.

The most frequent variants affect C3 convertase genes (*C3* and *CFB*) followed by *CFH*. Barricarte et al., showed that a two aminoacid deletion of C3 generated a C3 convertase resistant to decay by FH causing a continuous activation and consumption of C3¹⁰¹. IC-MPGN/C3G associated *CFH* rare variants are mainly located in the N-terminus of the protein and are characterized by very low serum FH levels and/or complete block of FH cofactor and decay accelerating activity in fluid phase. The effect of these abnormalities is massive C3 deposition in the GBM.

This *CFH* genotype-phenotype correlation has been confirmed by the model of *Cfh*^{-/-} mice in which a massive C3 activation caused low C3 levels and low plasmatic activities with an histological pattern of C3G. Plasma C3 levels and complement activities were recovered after the introduction into *Cfh*^{-/-} mice of a transgenic FH (FH Δ_{16-20}) shifting the phenotype from C3G to aHUS¹¹⁹.

An exception is represented by the *CFH* variant p.R1210C that is the most frequent in aHUS¹⁶⁶ and has also been reported in a patient with C3G¹⁰³. The p.R1210C variant generates complexes between FH and albumin impairing accessibility to all FH functional domains. This variant predisposes individuals to diverse pathologies but the

final phenotype is then determined by other genetic risk factors.¹⁶⁷ Indeed, beside rare genetic variants, different common SNPs have been linked to either aHUS or IC-MPGN and C3G. The *CFH*-H3 haplotype increases the risk to develop aHUS 2 to 4 fold in comparison with control group. A risk haplotype has been also identified in *MCP* (named *MCP*_{ggaac}) with a 2 fold increased risk of aHUS^{14, 168}.

On the other hand, the p.Y402H *CFH* SNP is over-represented in DDD patients compared with healthy controls while p.V62I have been reported as protective both in patients with DDD and C3GN¹¹⁶. The risk to develop DDD is associated with the presence of the *CFH*-H1 haplotype¹⁴. In 2012, one at risk-MCP haplotype (named *MCP*_{aaggt}) have been identified in IC-MPGN and C3GN⁹⁵. Finally, two *C3* SNPs (p.R102G and p.P314L) have been reported in association with DDD¹¹⁶.

The above reported SNPs are different from those identified in association with aHUS. Finally, genomic rearrangements in the RCA clusters have been described in C3G as well in aHUS. The most frequent rearrangements reported in aHUS patients result in the substitution of the last *CFH* exons (exon 23 or exon 22-23 or exon 21-23) with the last exons of *CFHR1* (hybrid *CFH*₁₋₂₂-*CFHR1*₆ gene and hybrid *CFH*₁₋₂₁-*CFHR1*₅₋₆ gene) or with *CFHR3* exons (hybrid *CFH*₁₋₂₂-*CFHR3*₂₋₆ gene and hybrid *CFH*₁₋₂₀-*CFHR3*₁₋₆ gene)^{6,169-171}. Additional CNVs have been reported in aHUS to generate reverse hybrid genes consisting of the first four or five exons of *CFHR1* and the last two or one *CFH* exons (reverse hybrid *CFHR1*₁₋₅-*CFH*₂₃ gene and reverse hybrid *CFHR1*₁₋₄-*CFH*₂₂₋₂₃ gene)^{102,172}. Overall, rearrangements related to aHUS result in gene products with a decreased complement regulation on host self-surfaces (endothelial surfaces included).

As detailed reported in section 1.4 of this chapter, genomic rearrangements described in C3G did not involve FH and are mainly characterized by the duplication of dimerization domains of FHRs. Mutant protein studies with hybrid C3G proteins showed the

generation of large multimeric complexes with an increased affinity for surface ligands and enhanced competition with FH. The hypothesis is that, differently from aHUS, FHR mutants in C3G compete with FH to bind a subset of cell surfaces but not endothelial surfaces. Of interest, the duplication of dimerization domains of FHR5 (*CFHR5₁₂₁₂*) identified in *CFHR5* nephropathy led to a mutant protein that interacted with C3 on glomerular basement membrane more than wild-type FHR5⁹⁴. While in normal conditions, C3 activation on GBM is regulated by FH, in presence of mutant FHRs C3 accumulate along GBM leading to C3 activation product deposition, typically observed in C3G^{9,136}.

Altogether these data indicate that the spectrum of kidney diseases determined by dysregulation of the AP is broad and spans from a thrombotic disorder associated with acute renal failure to chronic diseases leading to progressive renal failure.

Differences in localization and functional consequences of rare variants in complement genes and in genomic rearrangements in the *CFH-CFHR* area, may drive a fluid-phase rather than cell-surface abnormal complement regulation resulting in either IC-MPGN/C3G or aHUS, respectively.

1.7 Therapy

There is no universally effective treatment for primary MPGN and C3G. Numerous therapeutic regimens have been tried, including the use of corticosteroids and other immunosuppressants, anticoagulants and thrombolytics and plasmapheresis. In a randomized, double-blinded clinical trial, eighty children with MPGN diagnosis, were treated with alternate-day prednisone (40mg/m²) or with placebo for 41 months. An improve outcome, in terms of decreased serum creatinine and renal survival rate, was seen in patients receiving prednisone in comparison to placebo. A retrospective study reported the effectiveness of corticosteroids plus mycophenolate mofetil (MMF) in C3 glomerulonephritis¹⁷³. Case report studies described treatment with plasma exchange (PEX)¹⁷⁴, soluble CR1 (sCR1)¹⁷⁵, Cp40¹⁷⁶ and Rituximab¹⁷⁷⁻¹⁸⁰.

Eculizumab (produced by Alexion Pharmaceuticals), is a humanized monoclonal antibody against C5 that prevents C5b-9 formation and C5a production. It is licenced for the treatment of anaemia in paroxysmal nocturnal haemoglobinuria and for the treatment of atypical HUS. It has been used in C3G. For example, eculizumab reduced circulating C5b9 and reduced proteinuria in some C3G patients^{10, 177}. Eculizumab was also used in one patient with MPGN and nephrotic-range proteinuria, anemia, hypoalbuminemia, undetectable C3 and very high levels of SC5b-9. After the first dose kidney function normalized and by the sixth dose blood and urine tests normalised¹⁸¹.

There is an ongoing clinical study of Eculizumab in ten primary MPGN patients with persistent heavy proteinuria, low C3 levels and high sC5b9. This will provide more data about the effectiveness of Eculizumab in well-characterized patients¹⁸².

The recent report of KDIGO conference (“Kidney Disease: Improving Global Outcomes”⁹⁰) recommended a tiered approach to treat patients with C3G. In patients

with abnormal blood pressure, angiotensin-converting enzyme (ACE) inhibitors or angiotensin receptor blockers (ARBs) were recommended. The disease is considered moderate when proteinuria is greater than 500mg/24h despite supportive therapy, or the biopsy has a moderate inflammation or there is a disease progression defined by recent serum creatinine increase. In this condition, treatment with prednisone or MMF is recommended. Pulsed dosing of methylprednisolone and/or other anti-cellular immune suppressants were recommended when proteinuria is over 2000mg/24h despite immunosuppression and supportive therapy, renal biopsy shows severe inflammation and serum creatinine increases. Since the exact role of eculizumab in C3G is ill defined, KDIGO concluded that “Data are insufficient to recommend eculizumab as a first-line agent for the treatment of rapidly progressive disease”.

Additional anticomplement drugs including small molecules that block FD (ACH-3856, ACH-4100, ACH-4471, Achillion Pharmaceuticals), or C5aR (CCX168, ChemoCentryx) and small interfering RNA (siRNA) agents that suppress the protein production as C5 production (ALN-CC5, Alnylam Pharmaceuticals) are in development¹⁸³.

1.8 Summary

Idiopathic MPGN is a rare glomerular disease characterized by increased mesangial cellularity and structural changes in glomerular capillary walls. MPGN primarily affects children and young adults who typically present with asymptomatic hematuria and proteinuria, hypertension, nephritic or nephrotic syndrome, chronic kidney disease or a rapid progressive glomerulonephritis.

Although the pathogenesis of MPGN is not clear, hypocomplementemia is a common finding.

In the last decade, the classification of MPGN has been revised. At present, the diagnosis is based on IF data that distinguished IC-MPGN from C3G¹³. EM differentiates C3GN from DDD⁸⁹. Genetic and acquired factors have been reported as drivers for the complement hyperactivation described in patients with IC-MPGN and C3G patients. Indeed, complement gene mutations (*CFH*, *C3*, *CFI*, *CFB*, *MCP*, *THBD*, *CFHRs*) have been reported in about 20% of patients while C3NeFs, an autoantibody that stabilizes the C3 convertase, is present in around 80% of DDD patients and in 45% of C3GN patients¹⁰³. Anti-Factor B and anti-Factor H autoantibodies have been also described^{149,151}. Among genetic predisposing factors, copy number variations (CNVs) have been found both in C3GN and DDD⁹.

At present there is no universal therapy strategy to treat patients with IC-MPGN and C3G although different approach, including corticosteroids and other immunosuppressants, anticoagulants and thrombolytics are used. Some patients have been reported to benefit from the treatment with Eculizumab, a monoclonal antibody to C5 used in aHUS, but more data are necessary to confirm its effectiveness in these patients.

Further studies to identify genetic determinants in a cohort of well-characterized patients with IC-MPGN, C3GN and DDD will be instrumental to understand the mechanisms interfering with the control of the complement AP and will help to identify new therapeutic targets in these diseases.

2. COMPLEMENT ABNORMALITIES

IN AN ITALIAN COHORT OF PATIENTS WITH C3 GLOMERULOPATHY AND IMMUNE COMPLEX-MEDIATED MPGN

2.1 Introduction

Membranoproliferative glomerulonephritis (MPGN) is an uncommon kidney disorder that mainly occurs in childhood but also in late adulthood. MPGN is characterized by glomerular injury including increased mesangial cellularity, endocapillary proliferation and capillary-wall remodelling with generation of double contours¹³. Patients present with asymptomatic hematuria and proteinuria, nephritic or nephrotic syndrome, chronic kidney disease that often progress to end stage kidney disease (ESRD).

MPGN classification has been revised in the last ten years. At present, MPGN is classified on the basis of glomerular deposition detected by immunofluorescence microscopy. Cases with a glomerular C3 staining and significant immunoglobulin deposition are defined immune-complex mediated MPGN (IC-MPGN) to distinguish them from C3 Glomerulopathy (C3G) cases with a dominant C3 staining with no or scanty immunoglobulins. IC-MPGN has been associated with the activation of the complement classic pathway caused by infections (viral and bacterial), autoimmune diseases (such as systemic lupus erythematosus or rheumatoid arthritis) or paraproteinemias caused by monoclonal gammopathy. On the other hand, C3 glomerulopathy, further subclassified in Dense Deposit Disease (DDD) and C3 glomerulonephritis (C3GN) in the basis of electron microscopy findings, has been

associated with complement alternative pathway caused by genetic and acquired factors. Indeed, rare functional variants in genes encoding the complement components or regulators of the AP (*CFH*, *C3*, *MCP*, *CFI*, *CFB* and *THBD*) and autoantibodies that stabilizes the C3 convertase and C5 convertase (C3NeF and C5NeF) or anti-FH and anti-FB autoantibodies have been described in patients with C3GN and DDD^{95, 103, 184}. In addition, genomic abnormalities involving *CFHR* genes have been reported in DDD and C3GN patients and, in the majority of cases, generate hybrid FHR proteins that compete with FH to bind C3b causing an abnormal regulation of AP.

Nevertheless, genetic and acquired abnormalities affecting the AP have been also reported in patients with IC-MPGN indicating that there are commonalities that cause AP dysregulation both in C3G and IC-MPGN.

Recently, our group performed an unsupervised hierarchical cluster analysis on 173 well characterized patients from the Italian Registry of MPGN, to classify them in homogeneous groups. Using 34 variables regarding histological, biochemical, genetic and clinical features at onset, patients were divided in 4 clusters. Cluster 1 and 2 included patients with C3 and C5 activation (high prevalence of LPVs and/or C3NeF, low serum C3 and high plasma SC5b-9). Cluster 2 was composed by patients with more intense deposition of IgG and C1q. In addition in cluster 2 there was an higher prevalence of patients receiving immunosuppressive therapies, probably due to the high prevalence of nephrotic syndrome at onset. In cluster 3, patients mainly had intramembranous highly electron dense deposits with a prevalent C3 activation (high prevalence of LPVs and/or C3NeF, low serum C3 but lower levels of SC5b-9) in comparison to those in cluster 1 and 2. Finally, cluster 4 included patients with solid-phase complement activation (glomerular C3 deposits) but normal control of AP (low prevalence of LPVs and/or C3NeF, higher C3 levels and lower SC5b-9 levels in

comparison to the other clusters) in fluid phase, and with an higher risk to develop end stage renal disease (ESRD). Cluster 1 and 4 mainly included patients with C3GN and IC-MPGN. Cluster 2 was mainly composed by IC-MPGN patients while cluster 3 regrouped patients with histological diagnosis of DDD. This statistical approach allowed to identify 4 different groups of patients suggesting the presence of four different pathogenetic mechanisms underlying IC-MPGN, DDD and C3GN. It also predicted the risk of poor renal survival and may be useful to identify the most adequate anticomplement therapy. In order to easily assign patients to the different clusters, we provided a three-step algorithm (that showed a 75% of concordance with the original cluster analysis) developed on the basis of histologic, biochemical and genetic features available at onset.

This chapter was designed with the following objectives:

- 1) To evaluate the prevalence of genetic abnormalities (including rare functional variants and common variants) in known complement genes, the prevalence of C3NeF and the complement serum profile in a large cohort of patients with IC-MPGN/C3G that includes the 173 patients we reported in Iatropoulos et al² plus 26 newly recruited patients.
- 2) To apply in the enlarged cohort the three step–algorithm to classify patients into clusters.

2.2 Patients

Patients were recruited by the Italian Registry of MPGN, coordinated by the Clinical Research Center for Rare Diseases “Aldo e Cele Daccò” at Mario Negri Institute. Clinical information, demography and laboratory data from patients were collected by a case report form (Fig.11). Blood, plasma and serum were also collected for biochemical and genetic tests.

Biological samples from 48 healthy Italian donors were collected at Mario Negri Institute.

The study was approved by Ethics Committee of The Azienda Sanitaria Locale of Bergamo (Italy). All participants received detailed information on the purpose and design of the study, according to the guidelines of the Declaration of Helsinki.

2.3 Diagnosis


All kidney biopsy reports were centrally reviewed by pathologists at the Mario Negri Institute. The diagnosis of MPGN was based on light microscopy findings. On the basis of the recent classification^{89, 185}, MPGN patients were further classified as follow:

- Immune-complex MPGN: cases with complement and immunoglobulin staining at immunofluorescence (IF);
- C3 Glomerulopathy: cases with "dominant C3 staining" at IF (defined in the Consensus Report as " C3c intensity \geq 2 orders of magnitude more than any other immune reactant on a scale of 0 to 3).

On the basis of electron microscopy appearances, patients with C3 Glomerulopathy were further classified as DDD (in presence of very dense osmiophilic deposits) and C3GN.

Patients with secondary MPGN, patients with a previous diagnosis of atypical hemolytic uremic syndrome (aHUS), patients with MPGN diagnosis on allograft but without biopsy on native kidney and all patients with no IF or EM studies were excluded from this study.

MARIO NEGRI INSTITUTE FOR PHARMACOLOGICAL RESEARCH
CLINICAL RESEARCH CENTRE FOR RARE DISEASES ALDO E CELE D'ACCO*


 Villa Camozzi - 24020 Ranica (Bergamo) Italy Telephone 39-35-4535304 fax 39-35-4535373

Italian Registry of Membranoproliferative Glomerulonephritis

Registration Form

Center code	Family code	Subject code	Date of compilation
<input type="text"/>	<input type="text"/>	<input type="text"/>	<input type="text"/>

Referring Physician

Surname	Name	
<input type="text"/>	<input type="text"/>	
Hospital Address		
<input type="text"/>		
<input type="text"/>		
Telephone Number	Fax Number	Email
<input type="text"/>	<input type="text"/>	<input type="text"/>

Country

Patient Data

Surname	Name	Sex	
<input type="text"/>	<input type="text"/>	<input type="text"/>	
Birth Date	Birth Place	ISS code	
<input type="text"/>	<input type="text"/>	<input type="text"/>	
Address			
<input type="text"/>			
telephone	mobile phone	e-mail	
<input type="text"/>	<input type="text"/>	<input type="text"/>	
Codice Fiscale (for Italian resident only)		Tessera sanitaria (for Italian resident only)	
<input type="text"/>		<input type="text"/>	
Family	Affected Y/N	Cod. DNA	
<input type="text"/>	<input type="text"/>	<input type="text"/>	
Ethnicity	Race	(Please leave blank)	
<input type="text"/>	<input type="text"/>	<input type="text"/>	

Figure 11. The Italian Registry of Membranoproliferative glomerulonephritis (MPGN) used to recruit patients at Mario Negri Institute.

2.4 Methods

2.4.1 Complement component assays

Serum C3 and C4 concentrations were measured by kinetic nephelometry¹⁶⁶. Plasma levels of SC5b-9 levels were assessed using the MicroVue SC5b-9 Plus EIA commercial kit (SC5b-9 Plus, Quidel). The above evaluations were done at Mario Negri Institute.

IgGs purified from plasma were used to test C3NeF activity at the Cordelier Research Center. The assay consisted in measuring the IgG ability to stabilize the convertase of the AP, C3bBb, as previously described¹⁸⁶.

2.4.2 DNA samples

Genomic DNA (gDNA) was extracted from peripheral blood using the NucleonTM BACC2 Genomic DNA extraction kit (GE Healthcare, Little Chalfont, UK) and, more recently, the NucleoSpin Blood columns (Macherey-Nagel). DNA integrity was verified by 0.8% agarose gel electrophoresis. DNA quality was analyzed by NanoDrop Spectrometer (ND-1000; Thermo Fisher). Before library preparation, DNA was quantified by Qubit (dsDNA HS Assay kit; Invitrogen).

2.4.3 Complement Minipanel and Genetic data analysis

Genetic analysis were performed in 198 patients by a next generation sequencing (NGS) diagnostic minipanel for simultaneous sequencing of 6 complement genes (complement factor H, *CFH*, NG_007259.1; complement factor I, *CFI*, NG_007569.1; membrane cofactor protein, *CD46/MCP*, NG_007569.1; complement factor B, *CFB*,

NG_008191.1; complement C3, *C3*, NG_009557.1; and thrombomodulin, *THBD*, NG_012027.1). Amplicons were obtained by highly multiplex PCR using the Ion AmpliSeq™ Library Kit 2.0 (Life Technologies, LT). Ultra-high multiplex PCR primers have been custom designed using the online Ion AmpliSeq Designer tool (LT), creating 2 pools of primer-pairs for a total of 311 amplicons. Target were then subjected to clonal amplification on Ion PGM™ Template OT2 200 Kit and finally sequenced on Ion Torrent Personal Genome Machine Sequencer (PGM, LT).

Sequence data were analyzed using TorrentSuite Software 3.6. Targets with a depth of amplicon coverage $\geq 20X$ reads were considered appropriately analyzed. ANNOVAR software was used to functionally annotate genetic variants.

Genetic variants were considered as follows:

- Functional variants: missense variants, insertion/deletions in the coding regions and splicing variants affecting the first two nucleotides flanking the exons.
- Rare variants: variants with an allelic frequency ≤ 0.01 in ESP or 1000 Genomes Project subpopulations.
- Likely pathogenic variants (LPVs): variants with minor allele frequency (MAF) in the ExAC database < 0.001 and with Combined Annotation Dependent Depletion (CADD)¹⁸⁷ phred score ≥ 10 .

Rare variants and likely pathogenic variants were validated by Sanger sequencing on the 3730 DNA Analyzer (LT). Targets with a depth of coverage $\leq 20x$ were sequenced by Sanger sequencing, as previously described.¹⁶⁶

In the associations studies I used genotypes from 404 unphenotyped subjects of European origin from the 1000 Genomes Project (CEU, TSI, GBR and IBS subpopulations) and from 48 Italian healthy subjects.

2.4.4 Cluster analysis

As reported in Iatropoulos et al., we created a three-step algorithm to assign patients to different clusters². The algorithm (Fig.12) is based on four different features available at onset (presence of LPVs and or C3NeF, serum C3 levels, presence of intramembranous highly electron-dense deposits) and it was used to cluster all patients from our cohort.

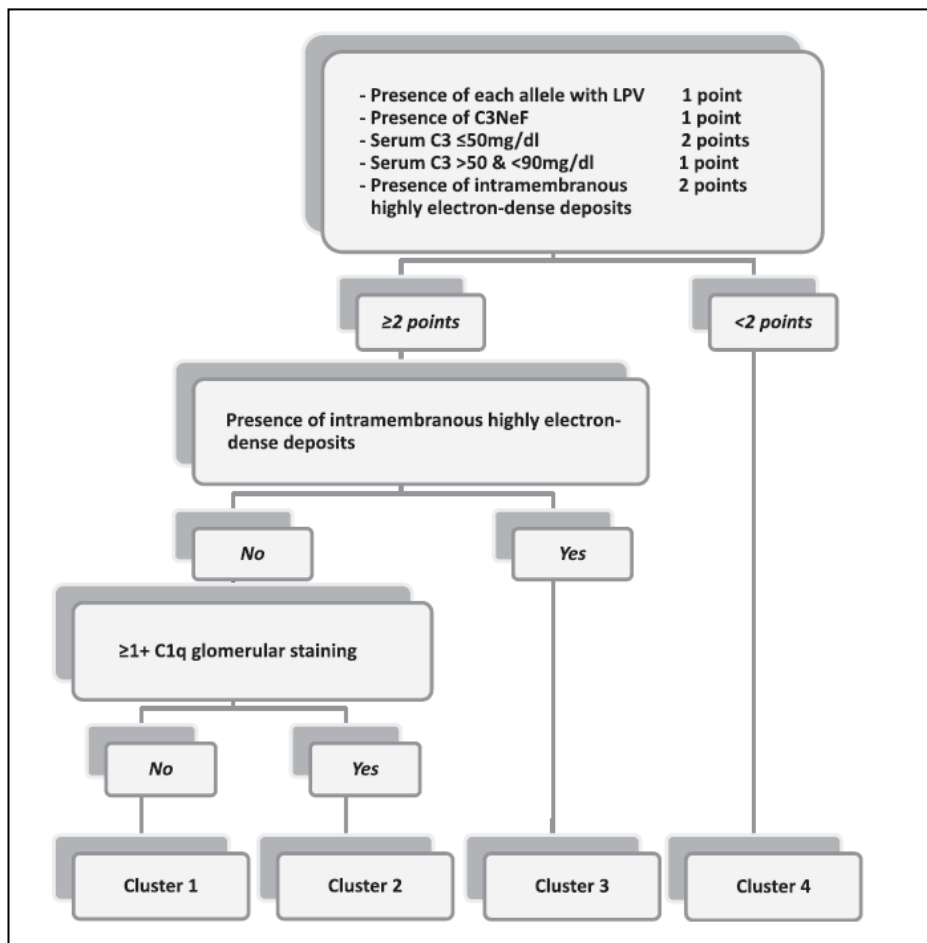


Figure 12. Image, taken from Iatropoulos et al. (2017)², representing the three-step algorithm.

2.4.5 Statistics

Clinical data in the three different groups of patients (IC-MPGN, DDD and C3GN) are reported in Table 3. To determine differences among the three histological groups, I used ANOVA test for continuous variables and the χ^2 or Fisher Exact test for categorical variables.

Candidate SNPs were selected from previous publications that associated *CFH*, *CD46*, *CFB*, *C3* and *THBD* polymorphisms with MPGN^{95, 103, 115, 116, 119}. In the association analysis was considered one patient for each family. Chi-square test was used to compare genotype and allelic frequencies between patients and controls. P-values <0.05 were considered statistically significant.

Survival analyses considered as cumulative fractions of patients free of events were estimated using Kaplan-Meier survival curves. Analyses were performed with the MedCalc software.

2.5 Results

The cohort of patients investigated in this chapter include:

- 173 patients described in the following published articles:

~"Complement gene variants determine the risk of immunoglobulin-associated MPGN and C3 glomerulopathy and predict long-term renal outcome" (Iatropoulos P. et al; Mol Immunol. 2016 Mar¹⁰³);

~"Cluster Analysis Identifies Distinct Pathogenetic Patterns in C3 Glomerulopathies/Immune Complex-Mediated Membranoproliferative GN" (Iatropoulos et al; J Am Soc Nephrol. 2018 Jan²).

- 26 unpublished patients.

2.5.1 Complement abnormalities in patients with IC-MPGN, DDD and C3GN.

2.5.1.1 Patients and clinical parameters

Kidney biopsy report review of 199 MPGN patients provided the diagnosis of IC-MPGN in 48% ($n=96$), C3GN in 39% ($n=77$) and DDD in 13% ($n=26$) of them (Fig.13).

Among the 199 patients, eight had familiarity for the disease.

As reported in table 3, age of onset and gender distribution were similar among the different histology groups.

Proteinuria and microhematuria were the main clinical features at onset in all patients. At onset, nephrotic syndrome was observed in 39%, 23% and 31% of patients with IC-MPGN, DDD and C3GN, respectively, while renal impairment was statistically more frequent in patients with IC-MPGN (24%) and C3GN (22%) than in patients with DDD (4%. IC-MPGN versus DDD: $p=0.022$; C3GN versus DDD: $p=0.038$).

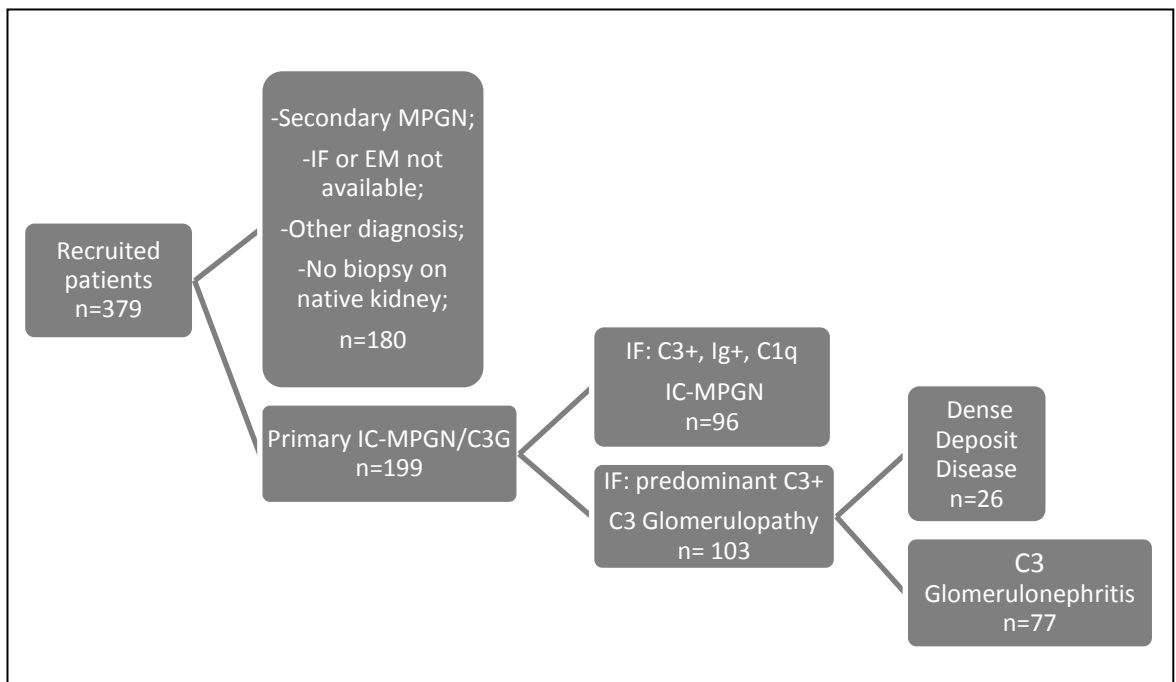


Figure 13. Histological classification of patients recruited by the Italian Registry of MPGN. IC-MPGN: Immune complex-mediated MPGN; C3G: C3 glomerulopathy; DDD: dense deposit disease; C3GN: C3 glomerulonephritis.

Variable	C3GN	DDD	IC-MPGN	Overall p-value
N	77	26	96	
Gender (% males)	58%	58%	54%	0.843
<i>Data at onset</i>				
Age (y) - Mean (SD)	17.9 (±15.4)	15.1 (±11)	19.6 (±15)	0.360
Microhematuria %	87	88	82	0.649
Gross hematuria %	34	42	29	0.455
Proteinuria %	88	88	90	0.951
Nephrotic syndrome %	31	23	39	0.281
Renal impairment %	22	4 ^{a,b}	24	0.073
Trigger event %	37	35	28	0.481
Familiarity for nephropathy %	16	12	11	0.603
Serum C3 (mg/dl)	50.7 (±42.4)	33 (±35.6) ^b	51.3 (±40.2)	0.108
Serum C4 (mg/dl)	21.8 (±9.1)	24 (±9.6)	21 (±10.3)	0.366
Plasma SC5b-9 (ng/ml)	1165 (±1274)	530 (±518) ^{a,b}	1079 (±1205)	0.061
Low serum C3 and normal serum C4 %	72	85	70	0.285
C3NeF positive %	39	79 ^{a,b}	40	0.001
LPV carriers %	24	15	15	0.284
LPV carriers and/or C3NeF%	58	83 ^{a,b}	49	0.012
<i>Data during follow-up</i>				
Nephrotic syndrome %	47 ^b	50	68	0.016
High blood pressure %	35	23 ^b	48	0.041
Chronic kidney disease %	31 ^b	27	46	0.068
ESRD %	10	4	9	0.739
Thrombotic microangiopathy %	5	0	3	0.652
<i>Histological features</i>				
Time Onset to Biopsy (yr), median (IQR)	0.4 (0.1-2.3)	1.1 (0.2-3.8)	0.4 (0.1-1.8)	0.702
<i>Light microscopy</i>				
Sclerotic glomeruli %	8 (±18)	2 (±6) ^b	9 (±14)	0.166
Crescents %	3 (±11)	7 (±20)	6 (±16)	0.485
Degree of mesangial proliferation ^d	1.6 (±1)	1.8 (±0.7)	1.9 (±0.9)	0.145
Degree of endocapillary proliferation ^d	1 (±1.1)	0.9 (±1.1)	1.2 (±1)	0.291
Degree of interstitial inflammation ^d	0.6 (±0.8) ^b	0.6 (±0.8)	0.8 (±0.8)	0.070
Degree of interstitial fibrosis ^d	0.4 (±0.7)	0.2 (±0.4) ^b	0.5 (±0.8)	0.105
Degree of arteriolar sclerosis ^d	0.3 (±0.8)	0 (±0.1) ^b	0.3 (±0.6)	0.163
<i>Immunofluorescence^d</i>				
C3	2.7 (±0.5)	2.8 (±0.3)	2.6 (±0.7)	0.045
IgA	0.1 (±0.2)	0.1 (±0.3)	0.5 (±0.8) ^{a,c}	<0.001
IgG	0.2 (±0.4)	0.2 (±0.4)	1.6 (±1.1) ^{a,c}	<0.001
IgM	0.3 (±0.4) ^b	0.7 (±0.7) ^{a,b}	1.3 (±0.9)	<0.001
C1q	0.1 (±0.3)	0.1 (±0.3)	1.1 (±1) ^{a,c}	<0.001
Fibrinogen	0.3 (±0.7)	0.3 (±0.8)	0.3 (±0.7)	0.898
<i>Electron microscopy %</i>				
Mesangial deposits	74 ^{b,c}	46	58	0.019
Subepithelial deposits	56 ^{b,c}	8 ^a	34	<0.001
Subepithelial hump-like deposits	27	9	15	0.064
Subendothelial deposits	73	12 ^{a,b}	78	<0.001
Intramembranous granular deposits	55	0 ^{a,b}	48	<0.001
Intramembranous highly electron-dense ribbon-like deposits	0	100 ^{a,b}	3	<0.001

Table 3. Clinical features, complement assesment, genetic screening and histologic features in patients classified according to the C3G/IC-MPGN classification.

Continuous variables are reported as mean (\pm SD) unless otherwise specified.

Serum C3: reference 90-180 mg/dl; serum C4: reference 10-40 mg/dl; plasma SC5b-9: reference \leq 303 ng/ml.

^a Significant different from C3GN.

^b Significant different from IC-MPGN

^c Significant different from DDD

^d Degree of mesangial proliferation, endocapillary proliferation, interstitial inflammation, interstitial fibrosis, and arteriolar sclerosis, as well as IF findings were graded using a scale of 0 to 3, including 0, trace (0.5+), 1+, 2+ and 3+.

2.5.1.2 Complement serum profile

The majority of patients from the three histology groups (IC-MPGN: 82%; DDD: 92%; C3GN:82%) showed low C3 levels (<90 mg/dl). The lowest mean C3 levels were observed in patients with DDD (DDD: 33 ± 35.6 ; IC-MPGN: 51.3 ± 40.2 ; C3GN: 50.7 ± 42.4 ; $p=0.108$). As shown in fig. 14, low C4 levels (<10 mg/dl) were present in 14%, 8% and 7% of patients with IC-MPGN, DDD and C3GN, respectively. The majority of patients from the three histology groups (IC-MPGN: 70%; DDD: 85%; C3GN:72%) showed low C3 levels and normal C4 (C3 < 90 mg/dl and C4 >10 mg/dl). High SC5b-9 levels (>303 ng/ml) were present in the three groups although patients with IC-MPGN and C3GN had statistically higher SC5b-9 levels in comparison to patients with DDD ($p=0.028$ and $p=0.018$, respectively) (Table 3).

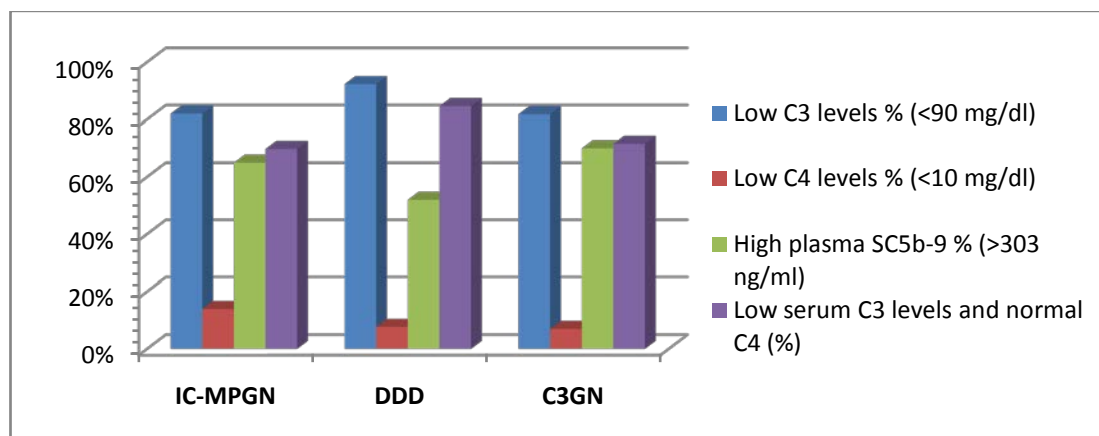


Figure 14. C3, C4, SC5b-9 levels in patients with IC-MPGN, DDD and C3GN.

The presence of C3NeF, an autoantibody that stabilizes the C3 convertase, was evaluated in all those patients whose plasma sample was available ($n=167$). Although it was found in all histology groups (IC-MPGN: 40% ; DDD: 79%; C3GN: 39%), C3NeF was statistically more frequent in DDD patients in comparison to IC-MPGN and C3GN patients ($p=0.0006$ and $p=0.0007$, respectively).

2.5.1.3 Genetic screening

Among 198 patients analyzed by NGS, likely pathogenic variants (LPVs) were identified in 36 of them (18%) (Table 3; Table 4). As reported in Table 4, LPVs were spread in the three histology groups (IC-MPGN: 15%; DDD: 15% ; C3GN: 24% ; Fig.15).

Among six complement genes included in the genetic screening, the *C3* gene was the one with the highest prevalence of LPVs, followed by *CFH* (*C3* = 42% and *CFH* = 33% of all LPVs). All *C3* LPVs were heterozygous and were found in patients with IC-MPGN and C3GN but not in patients with DDD. Their localization affected the C345C domain, important for the binding with Bb, the MG5 domain involved in the C3bBb-C3 interaction, and domains of interaction with FH and FI (MG1, TED and CUBf)^{103, 188-190} (Fig.16).

CFH likely pathogenic variants ($n=12$) were found in all histological groups and 5 of them were in homozygosity (four of five patients had parental consanguinity). The majority of LPVs in *CFH* affected N-terminal domains (SCR1-4) of the protein, which are involved in the regulation of the complement alternative pathway through cofactor and decay accelerating activities (Fig.16).

Likely pathogenic variants in the gene coding *CFB* ($n=3$) were found only in patients

with IC-MPGN and affected domains important for the binding to C3¹⁹¹ (Fig.16).

Heterozygous *CFI* LPVs were identified in two patients with C3GN and in one patient with DDD. The p.G119R, variant in FI, already found in aHUS, ARMD and MPGN, is located in the CD5 domain and was described to reduce C3b degradation^{95,192,193}. The FI G57D affected the FIMAC domain, the main binding sites important for C4b and C3b degradation by FI¹⁹⁴ (Fig.16).

Only one *CD46* LPV was found in a patient with IC-MPGN but its effect is unknown.

Two heterozygous *THBD* LPVs were identified in two patients, one with DDD and one with C3GN. Both of them reside in the serine–threonine-rich region of thrombomodulin and were previously described in aHUS (Fig.16). Functional studies showed that both mutant THBD proteins had a reduced complement regulation through FI-mediated C3b inactivation²².

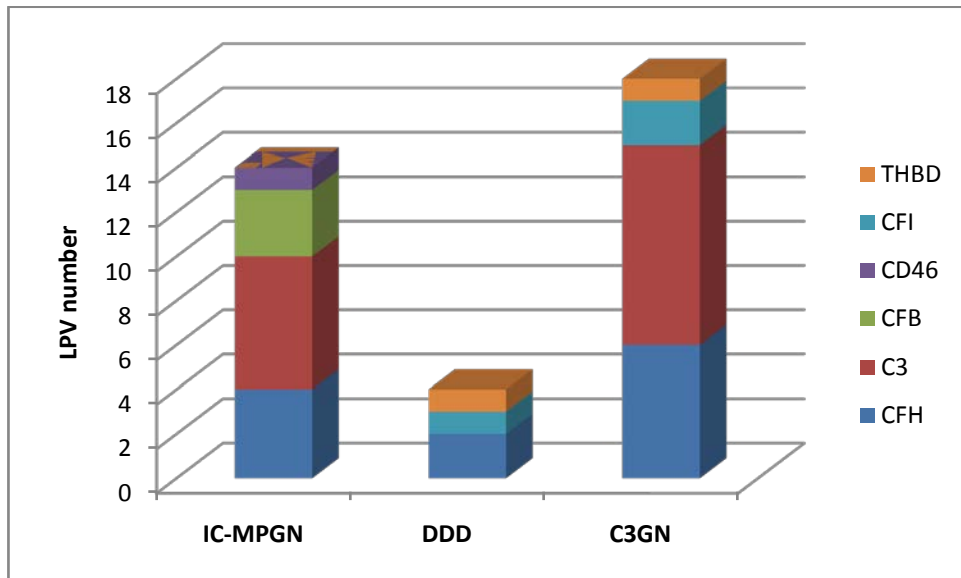


Figure 15. Complement likely pathogenic variant distribution in patients with IC-MPGN, DDD and C3GN.

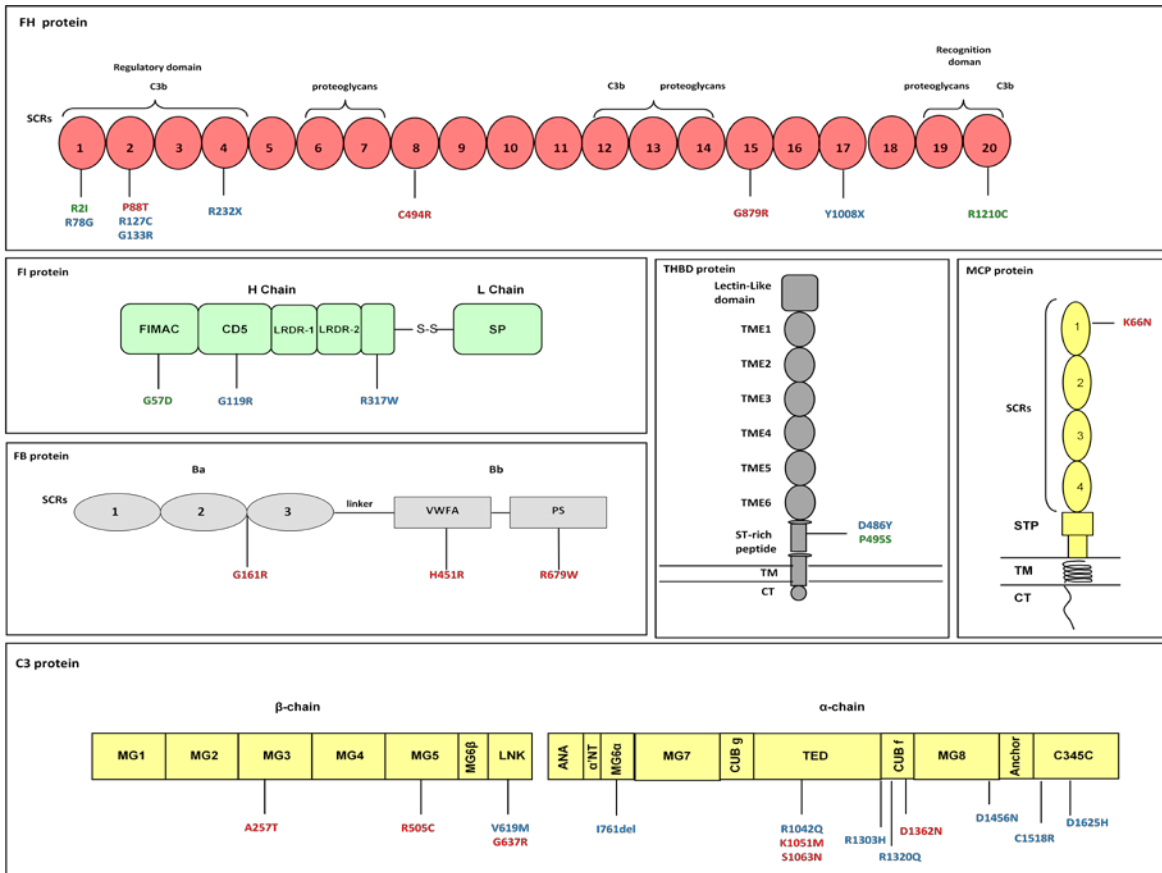


Figure 16. Localization of likely pathogenic variants in *CFH*, *CFI*, *CFB*, *THBD*, *MCP* and *C3* genes identified in patients with IC-MPGN (in red), DDD (in green) and C3GN (in blue).

Patient ID	Histologic group	Zygoty	LPV	ExAC Global Freq.	ExAC Max Subpop. Freq.	Pathogenic in functional studies	CADD
216	C3GN	Het	p.C3: R1042Q	9.9E-05	2.3E-04	No	16
419	C3GN	Hom	p.FH: Y1008X	0	0	No	32
521	IC	Het	p.C3: K1051M	1.6E-05	3.0E-05	Yes	23
1073	IC	Het	p.FH: C494R	0	0	No	24
1101	DDD	Het	p.FH: R1210C	1.7E-04	2.8E-04	Yes	12
1132	C3GN	Het	p.C3: R1320Q	0	0	No	28
1147	IC	Het	p.FB: H451R	0	0	No	25
1157	C3GN	Het	p.C3: D1625H	0	0	No	12
1264	IC	Het	p.FB: G161R	6.9E-05	3.0E-04	No	27
1284	IC	Hom	p.FH: P88T	0	0	No	29
1287	IC	Hom	p.FH: P88T	0	0	No	29
1360	C3GN	Het	p.FI: c.1-4C>T	8.4E-06	1.5E-05	No	17
1409	DDD	Het	p.FI: G57D	8.2E-06	6.1E-05	No	25
1549	DDD	Het	p.FH: R2I	0	0	No	11
1725	DDD	Het	p.THBD: P495S	5.8E-04	0.001	Yes	6
1726	IC	Hom	p.FB: R679W	0	0	No	31
1736	C3GN	Het	p.C3: R1303H	8.3E-06	1.5E-05	No	28
1741	C3GN	Het	p.THBD: D486Y	0	0	Yes	12
1828	C3GN	Het	p.C3: V619M	2.9E-04	0.001	No	22
1890	IC	Het	p.C3: G637R	2.2E-04	3.8E-04	No	24
1964	IC	Het	p.C3: R505C	8.3E-06	1.5E-05	No	25
1983	C3GN	Het	p.C3: I761del	0	0	No	14
1984	C3GN	Het	p.C3: I761del	0	0	No	14
2009	C3GN	Het	p.C3: C1518R	0	0	No	26
2011	IC	Het	p.C3: D1362N	4.9E-05	1.2E-04	No	11
2018	IC	Het	p.CD46: K66N	5.3E-04	9.0E-04	No	13
2032	C3GN	Hom	p.FH: R78G	0	0	No	16
2047*	IC	Het	p.C3: S1063N	0	0	No	10
2082	C3GN	Het	p.FH: R127C	0	0	No	33
2158	C3GN	Hom	p.FH: R78G	0	0	Yes	16
2192	C3GN	Het	p.FH: G133R	1.7E-05	3.0E-05	No	31
2508	C3GN	Het	p.C3: D1456N	0	0	No	25
SN249	C3GN	Het	p.FI: G119R	5.3E-04	9.5E-04	Yes	22
2435	C3GN	Het	p.FH: R232X	1.7E-05	6.1E-05	Yes	36
2350	IC	Het	p.C3: A257T	5.0E-05	9.1E-05	No	33
2585	IC	Het	p.FH: G879R	0	0	No	28

Table 4. List of likely pathogenic variants identified in the cohort.

2.5.1.4 Effect of complement genetic and acquired abnormalities on complement profile

A statistically higher percentage of patients with genetic and/or acquired abnormalities was found in the DDD group vs. the other two histology groups (IC-MPGN: 49%; DDD: 83%; C3GN: 58% ; p overall=0.012. DDD versus IC-MPGN, $p=0.006$; DDD versus C3GN $p=0.04$) (Fig.17).

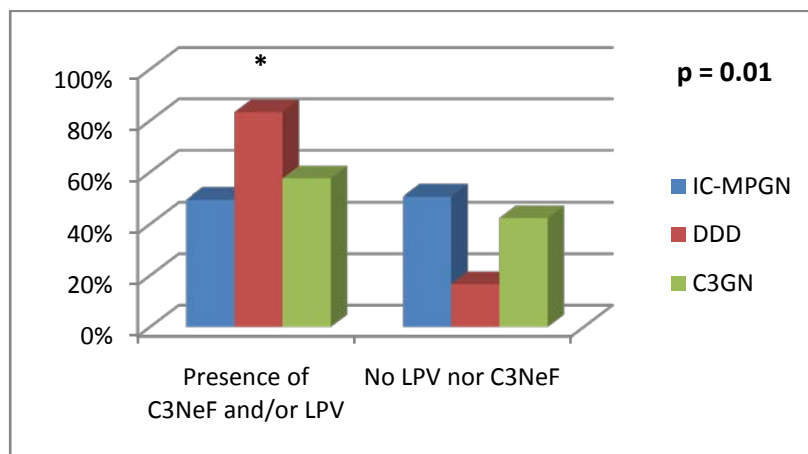


Figure 17. Representation of the presence of C3NeF and/or LPV in patients with IC-MPGN, DDD and C3GN. * Statistically different from C3GN and IC-MPGN ($p=0.04$ and $p=0.006$, respectively).

To investigate whether the LPVs reported in table 4 or the presence of C3NeF, or both, were associated with a specific complement profile in each histology group, C3 and SC5b-9 levels measured at onset in patients with LPVs or C3NeFs or both were compared with those of patients without identified genetic or acquired complement abnormalities.

Considering all patients together, low C3 levels appeared strongly associated with the presence of LPVs or C3NeF, both in single and in combination (p overall <0.001 ; Fig. 18). Complement genetic and acquired abnormalities appeared to influence also plasma SC5b-9 levels (Fig.19) since patients with LPVs and/or C3NeF had higher SC5b-9 levels than patients without genetic or acquired abnormalities. This difference is likely attributable to C3NeF since I found that SC5b-9 levels were significantly higher in

patients with only C3NeF in comparison to those in patients without complement abnormalities (Fig.19).

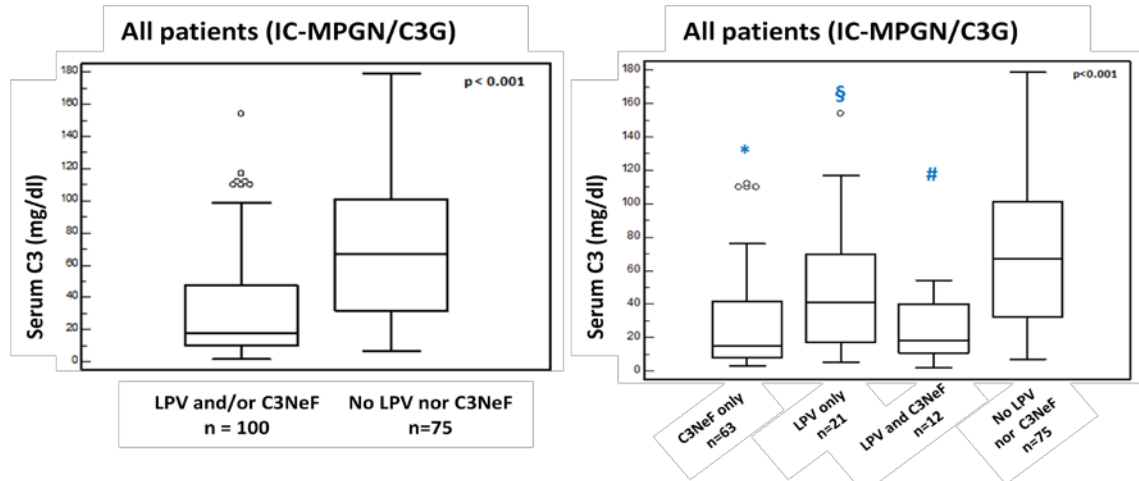


Figure 18. Box plot showing serum C3 levels in all recruited patients.
 * Significant different from the group with "No LPV nor C3NeF" ($p=2.2E^{-10}$);
 § Significant different from the group with "No LPV nor C3NeF" ($p=0.035$);
 # Significant different from the group with "No LPV and/or C3NeF" ($p=0.0005$).

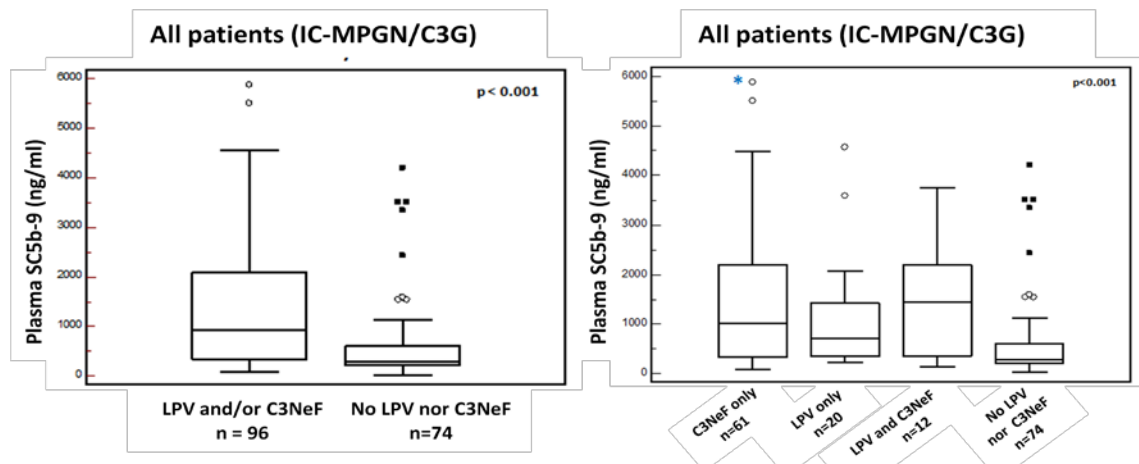


Figure 19. Box plot showing plasma SC5b-9 levels in all recruited patients.
 * Significant different from the group with "No LPV nor C3NeF" ($p=5.8E^{-5}$).

As shown in Fig. 20, C3 levels of IC-MPGN patients with LPVs and /or C3NeF were statistically lower than those of IC-MPGN patients without C3NeF or LPVs ($p<0.001$). This hypocomplementemia is mainly caused by the acquired abnormality, indeed IC-MPGN patients with only C3NeF (and no LPVs) showed lower C3 levels (median

(IQR) = 15(8-19)) in comparison to both those with only LPVs (median (IQR) = 56 (43-70)) (Fig.20) and those with no LPVs nor C3NeF (median (IQR) = 77 (48-101)).

High SC5b-9 levels (>303 ng/ml) were observed in IC-MPGN patients with LPVs and/or C3NeF (median (IQR) = 1412 (345-2408)). IC-MPGN patient groups with only acquired abnormality or in combination with LPVs showed high SC5b-9 levels ("C3NeF only" = 1643 (467-2474); "LPV and C3NeF" = 1845 (1600-1874)) although only in the former group SC5b-9 levels were statistically higher than in patients without genetic and acquired complement abnormalities (median (IQR): 307 ng/ml (232-567) $p < 0.001$) (Fig.21).

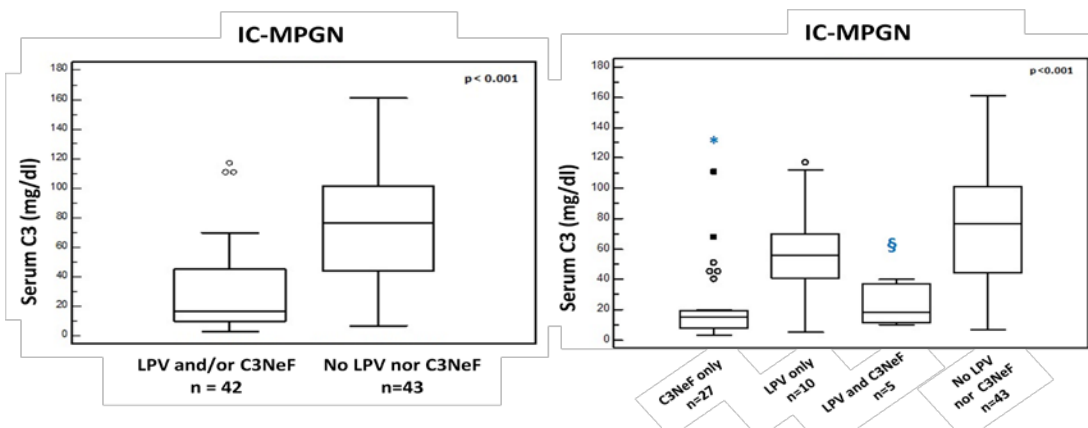


Figure 20. Box plot showing plasma C3 levels in patients with IC-MPGN.
 * Significant different from the group with "No LPV nor C3NeF" ($p = 3.1E^{-7}$).
 § Significant different from the group with "No LPV nor C3NeF" ($p = 0.008$)

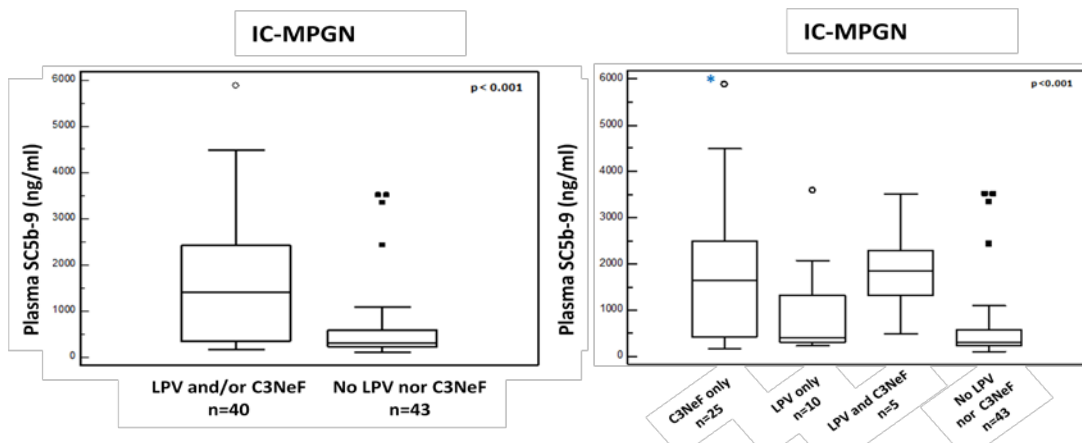


Figure 21. Box plot showing plasma SC5b-9 levels in in patients with IC-MPGN.
 * Significant different from the group with "No LPV nor C3NeF" ($p = 0.0001$).

The majority (84%) of patients with C3 glomerulopathy (C3G) had lower than normal C3 levels. Of note, patients with only C3NeF showed C3 levels statistically lower in comparison to C3G patients without genetic and acquired abnormalities (median (IQR): "C3NeF only" = 18 (9-44); "No LPV nor C3NeF" = 49 (28-101)) (Fig.22).

C3G patients with genetic and/or acquired abnormalities had higher plasma SC5b-9 levels in comparison to patients without abnormalities (Fig. 23). Among different subgroups, patients carrying only C3NeF showed SC5b-9 levels significantly higher than patients without abnormalities ("C3NeF only" = 665 (319-1894) ng/ml ; "No LPV nor C3NeF" = 273 (206-611) ng/m) (Fig.23).

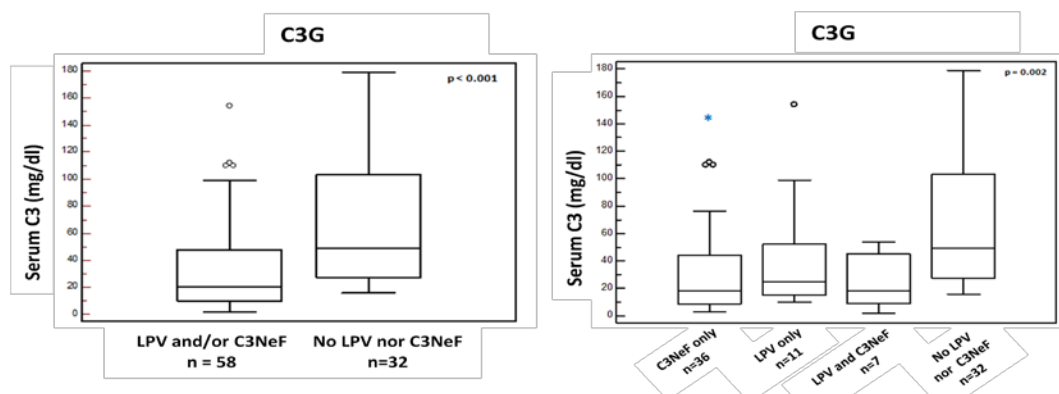


Figure 22. Box plot showing C3 levels in patients with C3 glomerulopathy (C3G).
* Significant different from the group with "No LPV nor C3NeF" ($p=0.027$)

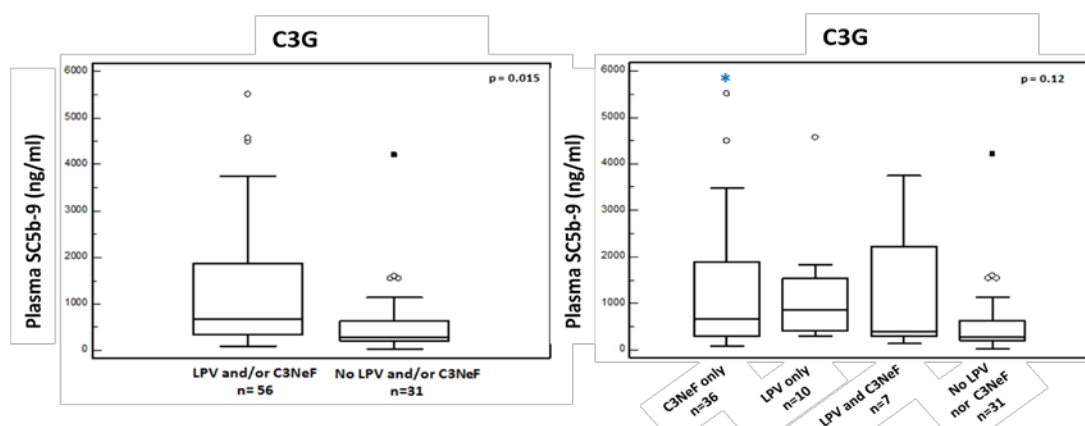


Figure 23. Box plot showing SC5b-9 levels in patients with C3 Glomerulopathy (C3G).
*Significant different from the group "No LPV nor C3NeF" ($p=0.027$).

To verify whether patients with DDD had a different complement profile from C3GN and whether it was influenced by the presence or absence of abnormalities, C3G patients were analyzed separately on the basis of electron microscopy data.

Among DDD patients tested for C3NeF, C3, SC5b-9 and genetic complement abnormalities ($n=24$), only the C3NeF negative patient carrying a LPV showed normal C3 levels (C3 = 154 mg/dl). All remaining patients, had C3 levels lower than normal (90 mg/dl), independently from the presence or absence of genetic and/or acquired abnormalities (median (IQR): “only C3NeF” = 13 (9-26); “LPV and C3NeF” = 47 (33-50); “No LPV nor C3NeF” = 41(34-46)) (Fig. 24).

50% of DDD patients had higher than normal (>303 ng/ml) SC5b-9 levels. However, no significant difference was observed in SC5b-9 levels between DDD patients with or without genetic and/or acquired abnormalities (median (IQR): “LPV and/or C3NeF” = 353 (226-583); “No LPV nor C3NeF” = 253 (234-345). Fig.25).

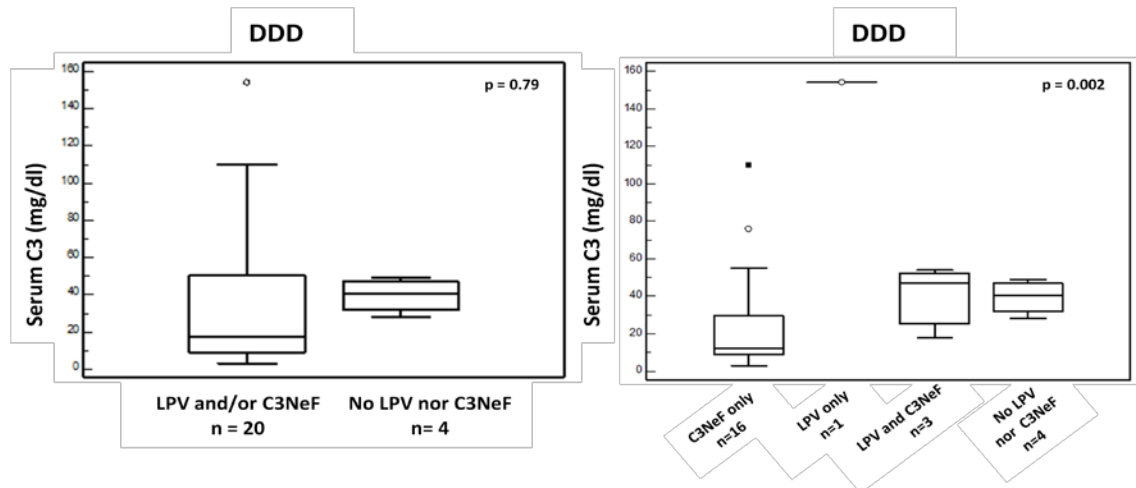


Figure 24. Box plots show that all DDD patients (including those without complement abnormalities) showed low C3 levels (<90mg/dl), with the exception of the patient carrying a LPV and negative for C3NeF.

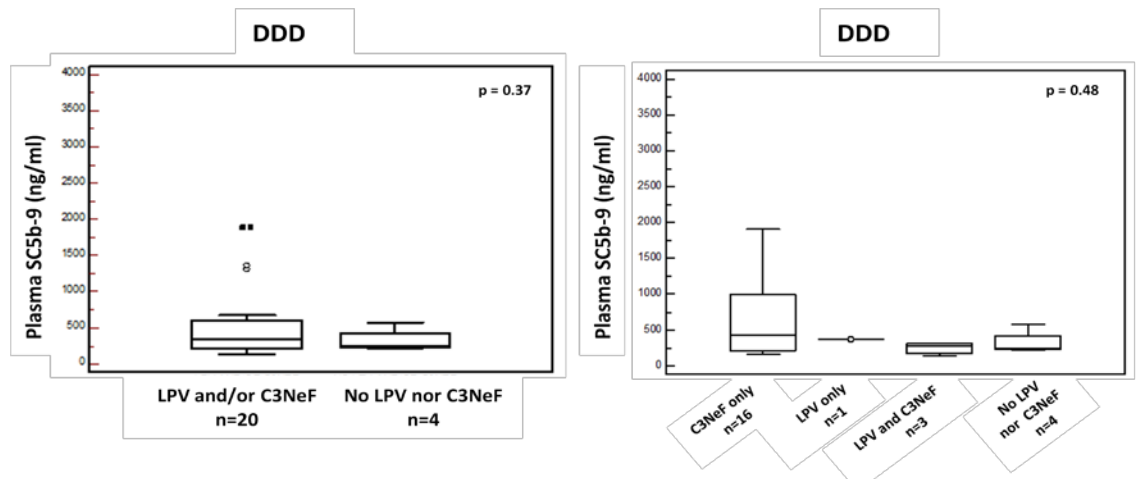


Figure 25. Box plot showing SC5b-9 levels in patients with DDD patients (Patient with " LPV only " SC5b9 levels = 368 ng/ml. Median (IQR): " C3NeF only " = 430 (226-833); "LPV and C3NeF" = 286 (211-304); "No LPV and/or C3NeF" = 253(233-345)).

C3GN patients with acquired and/or genetic abnormalities (in single or in combination) showed C3 levels lower than C3GN patients without LPV or C3NeF (median (IQR): “LPV and/or C3NeF” = 22 (10-44), “No LPV nor C3NeF” = 55 (27-108)). No difference was observed in C3 levels between patients with only C3NeF and patients with only LPV or patients with LPV and C3NeF (median (IQR): “C3NeF only” = 24 (8-46); “LPV only” = 21 (15-37); “LPV and C3NeF” = 12 (5-23)) ; (Fig.26).

Similarly to what observed in IC-MPGN patients, very high plasma SC5b-9 levels were observed only in C3GN patients with acquired and/or genetic abnormalities. Notably, patients with only C3NeF had SC5b-9 levels statistically higher than those observed in patients without abnormalities (median (IQR): “C3NeF only” = 999 (564-2380); “LPV only” = 888 (561-1530); “LPV and C3NeF” = 1909 (1073-2828) ; “No LPV nor C3NeF” = 286 (200-792)) (Fig 27).

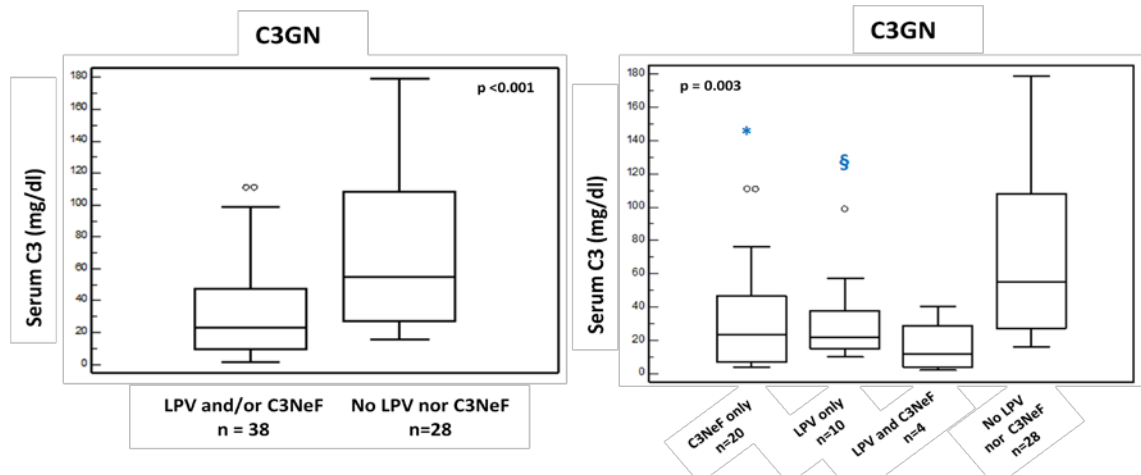


Figure 26. Box plot showing C3 levels in patients with C3GN.
 * Significant different from the group with "No LPV nor C3NeF" (p=0.003);
 § Significant different from the group "No LPV nor C3NeF" (p=0.03).

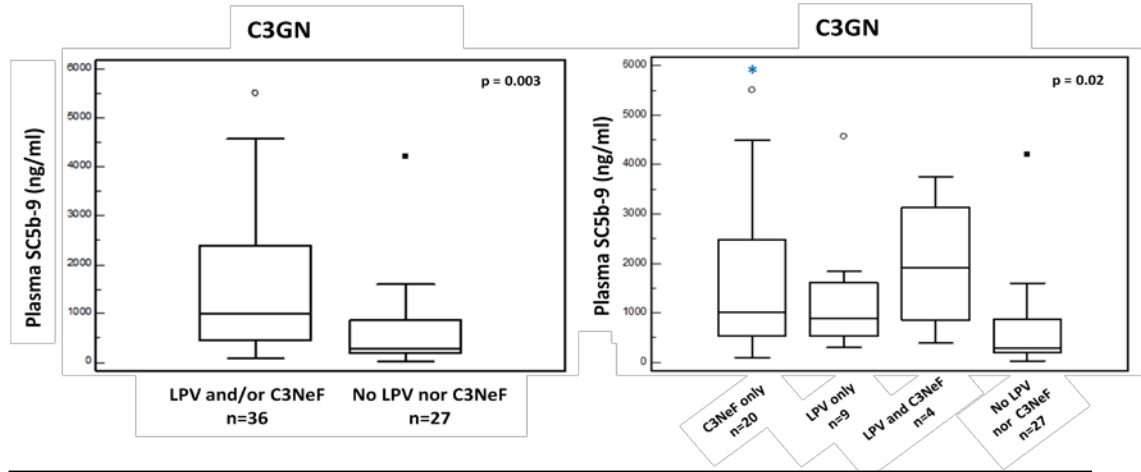


Figure 27. Box plot showing C3 levels in patients with C3GN.
 * Significant different from the group with "No LPV nor C3NeF" (p=0.014).

In summary, patients with LPVs and/or C3NeF from all the three different histology groups showed low C3 levels (median (IQR): IC-MPGN = 17 (10-45) mg/dl; DDD = 17 (9-49) mg/dl; C3GN = 24 (11-47) mg/dl; p overall = 0.888). Among patients without genetic and acquired abnormalities, DDD patients showed a trend to have lower C3 levels compared to IC-MPGN and C3GN patients, (median (IQR): IC-MPGN = 77 (47-100) mg/dl; DDD = 41 (34-46) mg/dl; C3GN = 55 (27-107) mg/dl; p overall = 0.324).

High plasma SC5b-9 clustered among patients with genetic and/or acquired abnormalities. Among them, we observed that IC-MPGN and C3GN patients had SC5b-9 levels (IC-MPGN: median (IQR): 1412 (345-2408) ng/ml; C3GN median (IQR): 999 (463-2332) ng/ml) statistically higher than those found in patients with DDD (median (IQR): 352 (226-582) ng/ml; p overall = 0.007; IC-MPGN plus C3GN vs. DDD, $p=0.002$).

2.5.1.5 Renal survivals

Eighteen patients (IC-MPGN=9; DDD=1; C3GN=8) developed end-stage renal disease (ESRD). In Kaplan-Meier plot in Fig. 28, survival curves overlapped indicating that the risk to develop ESRD is the same in IC-MPGN and C3G. Similar results were also observed among IC-MPGN, DDD and C3GN (Fig.29).

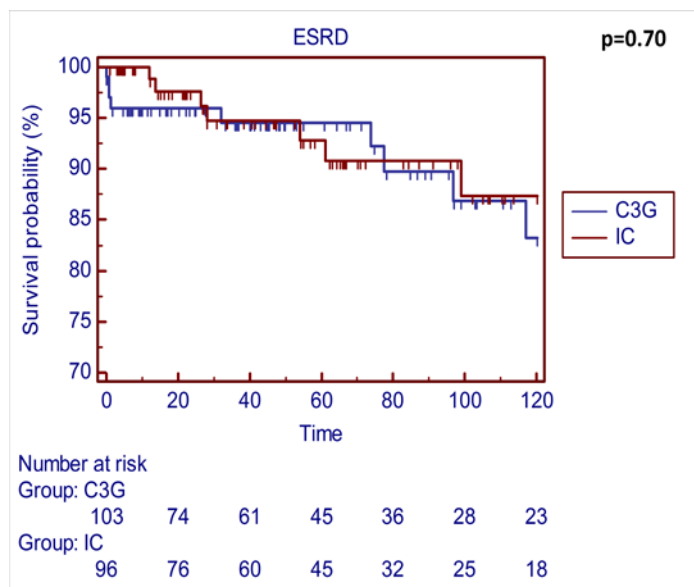


Figure 28. Kaplan-Meier representing the risk to develop ESRD in patients with IC-MPGN and C3G.

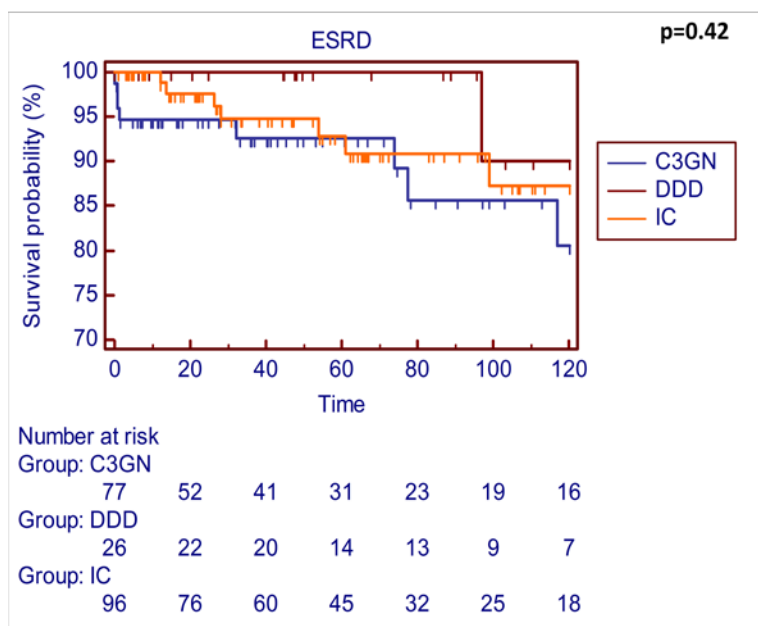


Figure 29. Kaplan-Meier representing the risk to develop ESRD in patients with IC-MPGN, DDD and C3GN.

2.5.1.6 Effect of complement genetic and acquired abnormalities on clinical parameters.

To investigate whether the outcome of patients with IC-MPGN, DDD and C3GN were influenced by the presence of LPVs and/or C3NeF, I performed survival analysis considering the nephrotic syndrome, the renal failure and end stage-renal disease during follow-up.

Kaplan Meier analysis showed that the presence of C3NeF and/or LPVs decreased the risk to develop ESRD in IC-MPGN/C3G patients ($p=0.052$; Fig.30). Although no significant difference between patients with LPVs and/or C3NeF and those without abnormalities was observed in the three different histology groups considered separately, the presence of C3NeF and/or LPVs showed a trend to decrease the risk to develop renal failure in patients with IC-MPGN ($p=0.09$; Fig.31) or C3GN ($p=0.09$, Fig.33). At variance, in DDD patients the presence of complement abnormalities showed a trend to increase the risk to develop nephrotic syndrome ($p=0.09$; Fig. 32). However, this finding may be questionable because of the low number of patients.

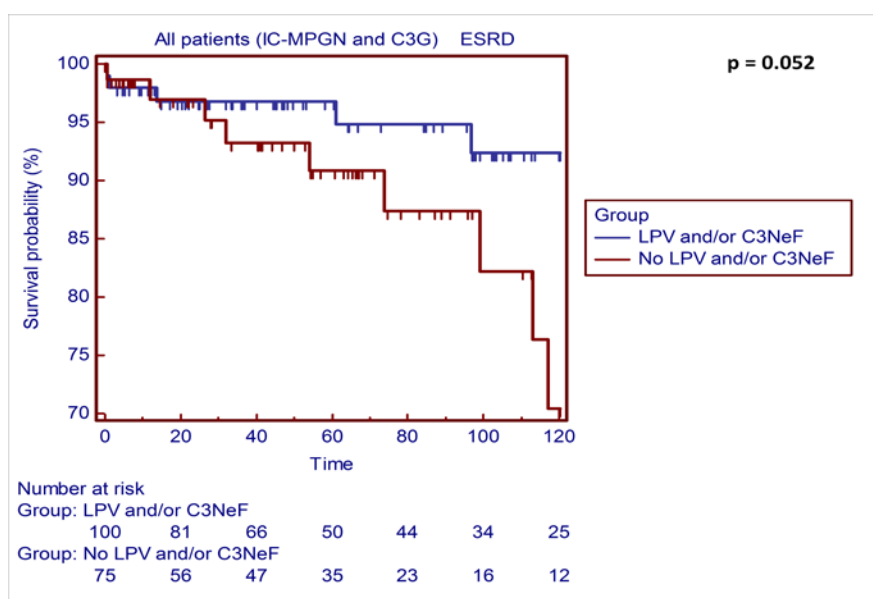


Figure 30. Kaplan-Meier representing the risk to develop end-stage renal disease (ESRD) in IC-MPGN/C3G patients with LPV or C3NeF compared to IC-MPGN/C3G patients without abnormalities.

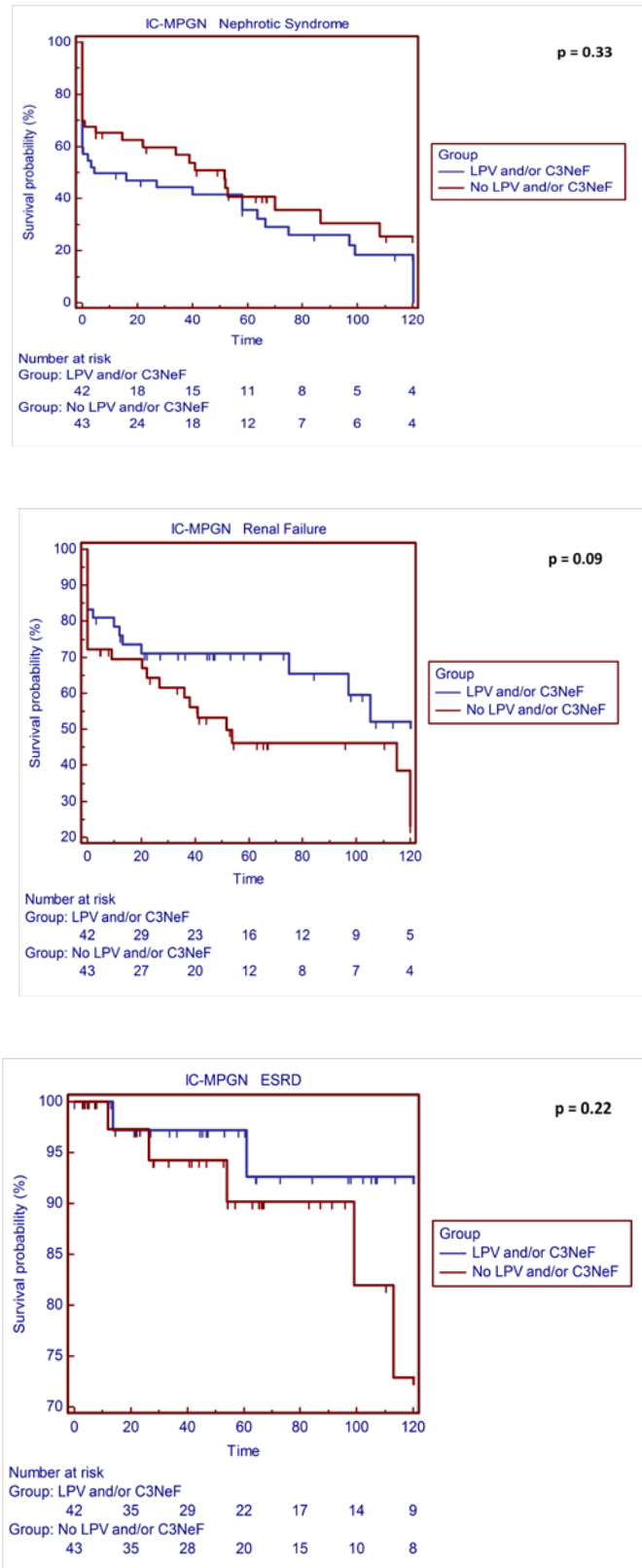


Figure 31. Kaplan-Meier representing the risk to develop nephrotic syndrome, renal failure and ESRD in IC-MPGN patients with LPV and/or C3NeF versus IC-MPGN patient without complement abnormalities.

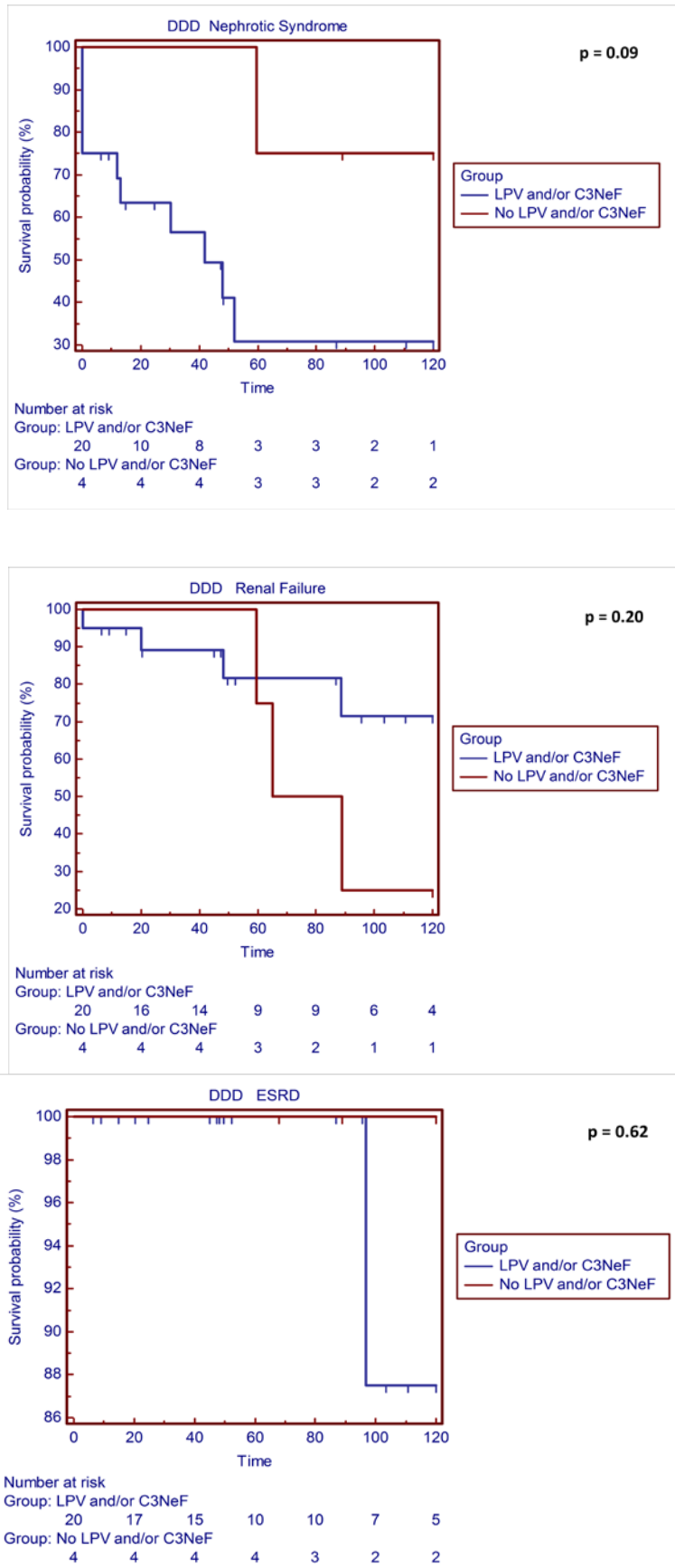


Figure 32. Kaplan-Meier representing the risk to develop nephrotic syndrome, renal failure and ESRD in DDD patients with LPV and or C3NeF versus IC-MPGN patient without complement abnormalities.

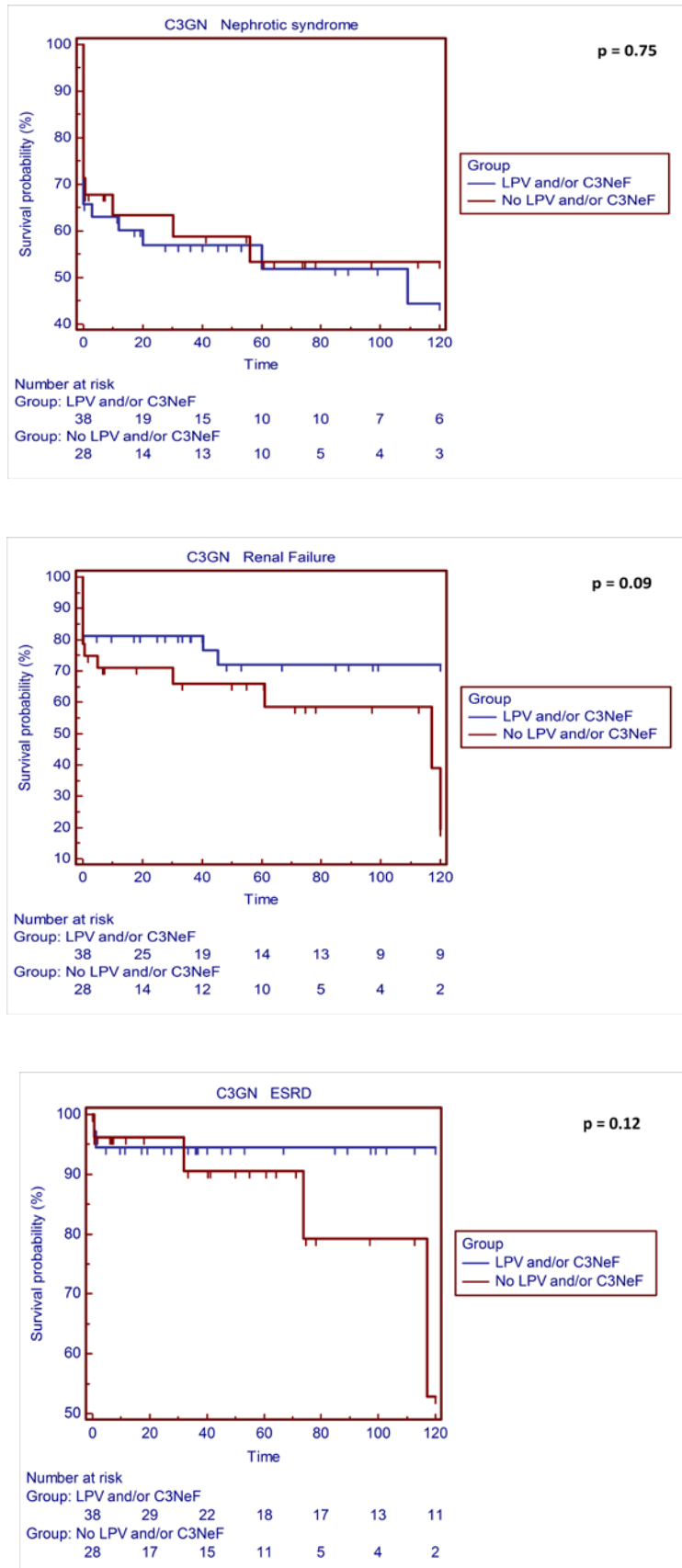


Figure 33. Kaplan-Meier representing the risk to develop nephrotic syndrome, renal failure and ESRD in C3GN patients with LPV and or C3NeF versus IC-MPGN patient without complement abnormalities.

2.5.1.7 Susceptibility genetic variants

Common single nucleotide polymorphisms (SNPs) in complement genes, previously associated with MPGN, were analyzed to determine whether they segregate preferentially with a specific histology group. As shown in table 5, I observed a trend of association for the CD46 c.*783T allele in IC-MPGN patients ($p=0.06$) and for THBD the A473 allele in DDD and C3GN patients ($p=0.09$ and $p=0.07$ respectively). Considering a recessive model, *CFH* 936D was significantly associated with IC-MPGN ($p=0.046$) while CD46 c.-366G resulted in association with DDD ($p=0.046$; Table 7).

			Genotype frequencies				Allele frequencies			
SNP	Histology Group	n	A/A	A/a	a/a	p value vs ctrs	Allele frequency allele A	Allele frequency allele a	p value vs ctrs	
<i>CFH</i>	c.-331C>T rs3753394	IC-MPGN	94	42	42	10	0.40	0.67	0.33	0.29
		DDD	26	14	10	2	0.87	0.73	0.27	0.90
		C3GN	74	31	34	9	0.21	0.65	0.35	0.14
		Ctrs	452	223	198	31		0.71	0.29	
<i>CFH</i>	p.V62I rs800292	IC-MPGN	94	57	33	4	0.68	0.78	0.22	0.52
		DDD	26	19	6	1	0.21	0.85	0.15	0.19
		C3GN	74	46	25	3	0.58	0.79	0.21	0.43
		Ctrs	452	252	180	20		0.76	0.24	
<i>CFH</i>	p.H402Y rs1061170	IC-MPGN	94	17	34	43	0.44	0.36	0.64	0.96
		DDD	26	7	8	11	0.19	0.42	0.58	0.45
		C3GN	74	13	32	29	0.76	0.39	0.61	0.52
		Ctrs	452	66	194	192		0.36	0.64	
<i>CFH</i>	p.E936D rs1065489	IC-MPGN	94	63	23	8	0.05	0.79	0.21	0.51
		DDD	26	18	8	0	0.64	0.85	0.15	0.72
		C3GN	74	43	26	5	0.20	0.76	0.24	0.11
		Ctrs	452	301	136	15		0.82	0.18	
<i>CD46</i>	c.-652G>A rs2796267	IC-MPGN	91	11	38	42	0.68	0.78	0.22	0.45
		DDD	22	4	6	12	0.42	0.32	0.68	0.66
		C3GN	68	10	27	31	0.93	0.35	0.65	0.77
		Ctrs	404	63	167	174		0.36	0.64	
<i>CD46</i>	c.-366A>G rs2796268	IC-MPGN	94	11	42	41	0.71	0.34	0.66	0.45
		DDD	26	5	5	16	0.03	0.29	0.71	0.28
		C3GN	72	14	30	28	0.48	0.40	0.60	0.55
		Ctrs	452	64	209	179		0.37	0.63	
<i>CD46</i>	p.A309V rs35366573	IC-MPGN	79	77	2	0	0.83	0.99	0.01	0.82
		DDD	22	22	0	0	0.80	1.00	0.00	0.96
		C3GN	54	54	0	0	0.58	1.00	0.00	0.56
		Ctrs	452	443	8	1		0.99	0.01	
<i>CD46</i>	c*783T>C rs7144	IC-MPGN	94	44	43	7	0.12	0.70	0.30	0.06
		DDD	26	15	6	5	0.08	0.69	0.31	0.38
		C3GN	72	34	28	10	0.45	0.67	0.33	0.34
		Ctrs	404	159	184	61		0.62	0.38	

			Genotype frequencies				Allele frequencies			
SNP	Histology Group	n	A/A	A/a	a/a	p value vs ctrs	Allele frequency allele A	Allele frequency	p value vs ctrs	
CFB	p.L9H rs4151667	IC-MPGN	93	87	6	0	0.74	0.97	0.03	0.63
		DDD	26	25	1	0	0.72	0.98	0.02	0.63
		C3GN	71	63	8	0	0.52	0.94	0.06	0.63
		Ctrs	452	415	35	2		0.96	0.04	
CFB	p.K565E rs4151659	IC-MPGN	87	84	3	0	0.87	0.98	0.02	0.87
		DDD	24	24	0	0	0.80	1.00	0.00	0.80
		C3GN	59	58	1	0	0.85	0.99	0.01	0.85
		Ctrs	452	438	14	0		0.98	0.02	
CFB	p.E566A rs45484591	IC-MPGN	88	84	4	0	0.63	0.98	0.02	0.63
		DDD	24	23	1	0	0.80	0.98	0.02	0.80
		C3GN	63	62	1	0	0.86	0.99	0.01	0.86
		Ctrs	452	439	13	0		0.99	0.01	
C3	p.R102G rs2230199	IC-MPGN	94	59	26	9	0.31	0.77	0.23	0.99
		DDD	26	17	6	3	0.36	0.77	0.23	0.87
		C3GN	73	47	24	2	0.46	0.81	0.19	0.34
		Ctrs	452	271	153	28		0.77	0.23	
C3	p.P314L rs1047286	IC-MPGN	94	62	27	5	0.79	0.80	0.20	0.70
		DDD	26	18	6	2	0.56	0.81	0.19	0.86
		C3GN	73	50	21	2	0.52	0.83	0.17	0.30
		Ctrs	452	283	146	23		0.79	0.21	
THBD	p.A473V rs1042579	IC-MPGN	94	71	20	3	0.31	0.86	0.14	0.23
		DDD	26	22	4	0	0.17	0.92	0.08	0.09
		C3GN	74	57	17	0	0.13	0.89	0.11	0.07
		Ctrs	452	306	131	15		0.82	0.18	

Table 5. Association study between common polymorphisms and patients with IC-MPGN, DDD and C3GN.

<i>CFB</i> p.R32Q/W		Genotypes						p value vs ctrs
Histology group	n	RR	RQ	QQ	RW	WW	QW	
IC-MPGN	95	59	17	0	16	2	1	0.57
DDD	26	17	5	0	1	0	3	0.08
C3GN	73	45	8	2	17	0	1	0.64
ctrs	452	274	64	5	91	5	13	

<i>CFB</i> p.R32Q/W		Allelic frequencies				
Histology group	R	p value vs ctrs	Q	p value vs ctrs	W	p value vs ctrs
IC-MPGN	0.79	0.67	0.09	0.94	0.11	0.64
DDD	0.77	0.98	0.15	0.27	0.08	0.41
C3GN	0.79	0.87	0.09	0.90	0.12	0.97
ctrs	0.78		0.10		0.13	

Table 6. Frequency of the *CFB* polymorphism p.R32Q/W in patients with IC-MPGN, DDD and C3GN compared to controls.

SNP	Risk Allele	Histology group	n	Genotype frequencies				Allele frequencies			Dominant model (homozygous or heterozygous for risk allele)			Recessive model (homozygous for risk allele)			
				A/A	A/a	a/a	p value vs ctrs	allele A	allele a	p value vs ctrs	Risk allele	Frequency	p value vs ctrs	Risk allele	Frequency	p value vs ctrs	
CFH	p.E936D rs1065489	D IC-MPGN	94	63	23	8	0.0543	0.79	0.21	0.51	31	0.33	0.97	8	0.09	0.046	
			DDD	26	18	8	0	0.64	0.85	0.15	0.72	8	0.31	0.95	0	0.00	0.71
			C3GN	74	43	26	5	0.2	0.76	0.24	0.11	31	0.42	0.20	5	0.07	0.27
			Ctrs	452	301	136	15		0.82	0.18		151	0.33		15	0.03	
CD46	c.-366A>G rs2796268	G IC-MPGN	94	11	42	41	0.71	0.34	0.66	0.45	83	0.88	0.64	41	0.44	0.54	
			DDD	26	5	5	16	0.026	0.29	0.71	0.28	21	0.81	0.67	16	0.62	0.046
			C3GN	72	14	30	28	0.48	0.40	0.60	0.55	58	0.81	0.32	28	0.39	0.99
			Ctrs	452	64	209	179		0.37	0.63		388	0.86		179	0.40	
CD46	c*783T>C rs7144	T IC-MPGN	94	44	43	7	0.11	0.70	0.30	0.063	87	0.93	0.075	44	0.47	0.23	
			DDD	26	15	6	5	0.0784	0.69	0.31	0.38	21	0.81	0.78	15	0.58	0.10
			C3GN	72	34	28	10	0.45	0.67	0.33	0.34	62	0.86	0.93	34	0.47	0.26
			Ctrs	404	159	184	61		0.62	0.38		343	0.85		159	0.39	
THBD	p.A473V rs1042579	A IC-MPGN	94	71	20	3	0.31	0.86	0.14	0.22	91	0.97	0.80	71	0.76	0.17	
			DDD	26	22	4	0	0.17	0.92	0.08	0.09	26	1.00	0.71	22	0.85	0.11
			C3GN	74	57	17	0	0.13	0.89	0.11	0.07	74	1.00	0.23	57	0.77	0.14
			Ctrs	452	306	131	15		0.82	0.18		437	0.97		306	0.68	

Table 7. Genotype and allele frequencies and models of inheritance of complement gene polymorphisms showing a trend of association to IC-MPGN, DDD and C3GN in Table 6.

2.5.2 Complement abnormalities and clinical outcome in patients with kidney injury classified by a three-step algorithm.

2.5.2.1 Classification of recently recruited patients.

173 patients from the IC-MPGN/C3G cohort described above were classified using an unsupervised hierarchical cluster analysis. Data were reported in the paper with the title "Cluster Analysis Identifies Distinct Pathogenetic Patterns in C3 Glomerulopathies/Immune Complex-Mediated Membranoproliferative GN" published in the Journal of the American Society of Nephrology (Iatropoulos P et al, Epub 2017 Oct 13²).

Newly recruited patients ($n=20$; Table 8) whose clinical, histological and laboratory data were complete, were classified using the three-step algorithm (Table 9)².

Among 20 newly recruited patients, 4 IC-MPGN and 5 C3GN patients were assigned to cluster 1. These 9 patients showed low C3 (21.1 ± 10.6 mg/dl), high SC5b-9 (1360 ± 1068 mg/dl) levels and 88% and 78% had subendothelial and mesangial deposits, respectively. Five patients were assigned to cluster 2. They were characterized by low C3 (20.8 ± 16.4 mg/dl), high SC5b-9 levels (1612 ± 1274 ng/ml) and strong C1q, IgG and IgM staining (1.6 ± 0.9 , 1.2 ± 0.8 , 0.7 ± 0.8 , respectively). Interestingly, 2 out of 5 (40%) showed low serum C4 levels suggesting a complement classical pathway activation. The single DDD patient was assigned to the cluster 3 and was characterized by low C3 (13 mg/dl) and normal SC5b-9. Finally, 3 patients with IC-MPGN and 2 patients with C3GN, went to cluster 4. They showed normal C3 (121 ± 32.4 mg/dl) and SC5b-9 (228 ± 102 ng/ml) levels, and 4 out of 5 had mesangial deposits.

Algor. Cluster	Patient ID	Histol. group	Gender	Age of onset (y)	LPV	C3NeF	Serum C3 (mg/dl)	Serum C4 (mg/dl)	Plasma SC5-9 (ng/ml)	Glomer. C1q	Intr. Dense deps
1	2287	IC	M	15.8	No	NA	20	20	386	Trace	No
1	2328	C3GN	F	7.8	No	Yes	23	17	598	Neg	No
1	2347	C3GN	F	32.2	No	No	21	NA	1588	Neg	No
1	2435	C3GN	M	23.5	Yes	No	99	37	297	Neg	No
1	2516	IC	F	6.9	No	Yes	8	17	2109	Neg	No
1	2553	C3GN	M	16.4	No	Yes	5	23	3491	Neg	No
1	2557	IC	M	4.8	No	NA	33	11	605	Neg	No
1	2685	C3GN	M	8.4	No	NA	39	43	109	Neg	No
1	2752	IC	M	6.8	No	NA	22	22	1444	Neg	No
1	2782	C3GN	F	14.4	No	NA	19	5	1914	Trace	No
2	2186	IC	F	14.3	No	Yes	14	17	2583	2+	No
2	2585	IC	M	8.8	Yes	NA	49	5	1209	3+	No
2	2742	IC	F	9.0	No	NA	11	6	966	1+	No
2	2748	IC	F	6.4	No	NA	21	17	75	1+	No
2	2760	IC	F	10.0	No	NA	9	27	3227	1+	No
3	2507	DDD	M	12.2	No	Yes	13	15	163	Neg	Yes
4	2352	IC	M	15.3	No	No	107	15	131	1+	No
4	2439	IC	F	33.3	No	No	88	26	314	1+/2+	No
4	2440	C3GN	M	10.7	No	NA	150	17	295	Neg	No
4	2453	IC	M	5.2	No	No	161	29	103	Neg	No

Table 8. Patients recently recruited by the Italian Registry of MPGN and cluster classified using a three-step algorithm.

Histologic Diagnosis	Cluster 1	Cluster 2	Cluster 3	Cluster 4
IC-MPGN (n=12)	4	5	0	3
DDD (n=1)	0	0	1	0
C3GN (n=7)	5	0	0	2

Table 9. Distribution of recently recruited IC-MPGN, DDD and C3GN patients into the four clusters.

2.5.2.2 *Algorithm-based cluster classification on the updated Italian cohort of patients with complement-mediated kidney injury.*

Then, the new patients were re-analyzed together with previously described patients². Clinical features, complement assessments, genetic screening and histologic features from all patients ($n=193$) of this cohort classified in the four algorithm-based clusters are reported in Table 11. In fig. 34 complement LPV distribution in the four clusters is reported. LPVs affecting *C3* and *CFB* were more frequent in clusters 1 (17%) and 2 (11%) vs. clusters 3 (0%) and 4 (2%) (Fig. 34).

Gender distribution was similar in the four clusters while age of onset was significantly higher in patients from cluster 4 (25.5 ± 19.3 y) in comparison to the other patients (cluster 1: 14.9 ± 11.9 y; cluster 2: 17.1 ± 12.3 y; cluster 3: 14.9 ± 10.6 y; p overall <0.001). Proteinuria and microhematuria at onset were present in all patients while nephrotic syndrome at onset was more frequent in patient from cluster 2 (cluster 1: 34%; cluster 2: 62%; cluster 3: 21%; cluster 4: 17%; p overall <0.001).

Consistent with data reported in Iatropoulos et al., cluster 1 included 65 patients with histologic diagnosis of IC-MPGN ($n=16$) and C3GN ($n=49$) who presented with microhematuria (91%), proteinuria (91%) and nephrotic syndrome. Gross hematuria at onset was similarly present in all clusters. These patients had low serum C3 (30.1 ± 20.3 mg/dl) and very high SC5b-9 levels (1307 ± 1243 ng/ml), high frequency of LPVs and/or C3NeF (75%). Electron microscopy data showed that mesangial and intramembranous granular deposits in these patients (73% and 61%, respectively) were more frequent than in patients from the other clusters.

Cluster 2 included IC-MPGN patients ($n=40$) and few C3GN patients ($n=5$). Most patients had an onset accompanied by proteinuria in the nephrotic range (62%; p overall

<0.001; cluster 2: vs. cluster 1, $p = 0.003$; vs. cluster 3, $p = 4.7E-04$; vs. cluster 4 = $3.1E-06$) that increased during follow-up (87%; $p < 0.001$). Microhematuria and gross hematuria were also present at onset (84% and 29 %, respectively). Similarly to patients in cluster 1, these patients showed high frequency of LPVs and/or C3NeF (76%), low serum C3 (21 ± 18.4 mg/dl) and high SC5b-9 levels (1958 ± 1367 ng/ml) although the latter were significantly higher in comparison to those in the other groups (cluster 2 versus cluster 1: $p = 0.014$; cluster 2 versus cluster 3: $p = 1.5E-06$; cluster 2 versus cluster 4: $p = 1.2 E-13$). Interestingly, 24% of these patients showed low serum C4 levels. Kidney biopsies from these patients were characterized by a strong IgM (1.2 ± 0.9), IgG (1.5 ± 1) and C1q (1.7 ± 0.7) deposition at immunofluorescence.

All patients with histologic diagnosis of DDD ($n = 26$) fell into cluster 3 together with 3 patients with IC-MPGN diagnosis. Among them, few patients showed renal impairment at onset (3%; $p = 0.013$); microhematuria, (90%), gross hematuria (41%) and proteinuria characterized their onset although nephrotic syndrome was present in only 21% of them. These patients, like those included in cluster 1 and 2, had high frequency of LPVs and/or C3NeF (84%), low serum C3 levels (21 ± 18.4 mg/dl) with plasma SC5b-9 significantly higher (510 ± 503 ng/ml) than those observed in patients in cluster 4 ($p = 0.007$). However in cluster 3 plasma SC5b-9 levels were significantly lower than those found in patients from cluster 1 ($p = 0.002$) and cluster 2 ($p = 1.5 E-06$). Similarly to patients in cluster 1, they had low IgA, IgG, IgM and C1q deposition but they differ from patients from the other groups for the strong predominance of intramembranous highly electron dense deposits with low subepithelial and subendothelial deposits.

Finally, cluster 4 was composed by 33 IC-MPGN and 21 C3GN patients. Microhematuria (75%), gross hematuria (31%), proteinuria (81%) (in the nephrotic range only in 17% of patients) were present at onset although renal impairment was

more frequent than in other groups (31%; $p = 0.013$). This cluster group distinguished from the others for the low prevalence of LPVs and/or C3NeF, normal serum C3 (98.1 ± 29.7 mg/dl) and plasma SC5b-9 (300 ± 151 ng/ml) and later age of onset (25.5 ± 19.3 y). This cluster had statistically higher prevalence of sclerotic glomeruli ($16\% \pm 21\%$; $p < 0.001$), interstitial fibrosis (0.7 ± 0.9 ; $p = 0.001$) and arteriolar sclerosis (0.6 ± 1 ; $p < 0.001$) in comparison to other cluster groups.

Histologic Diagnosis	Cluster 1	Cluster 2	Cluster 3	Cluster 4
IC-MPGN (n=92)	16	40	3	33
DDD (n=26)	0	0	26	0
C3GN (n=75)	49	5	0	21

Table 10. Distribution of IC-MPGN, DDD and C3GN patients from our cohort (n=193) into the four clusters.

Complement abnormalities in C3G and IC-MPGN

Variable	1	2	3	4	Overall p-value
N	65	45	29	54	.
Gender (% males)	57%	44%	59%	63%	0.308
<i>Data at onset</i>					
Age (y) - Mean (SD)	14.9 (±11.9)	17.1 (±12.3)	14.9 (±10.6)	25.5 (±19.3) ^{a,b,c}	<0.001
Microhematuria	91% ^d	84%	90%	75%	0.140
Gross hematuria	33%	29%	41%	31%	0.724
Proteinuria	91%	98% ^d	86%	81%	0.054
Nephrotic syndrome	34% ^d	62% ^{a,c,d}	21%	17%	<0.001
Renal impairment	15%	24%	3% ^b	31% ^{a,c}	0.013
Trigger event	34%	25%	35%	36%	0.681
Familiarity for nephropathy	14%	11%	10%	15%	0.928
Serum C3 (mg/dl)	30.1 (±20.3)	21 (±18.4) ^{a,c}	34.8 (±35.2)	98.1 (±29.7) ^{a,b,c}	<0.001
Serum C4 (mg/dl)	21.4 (±9.8)	19.8 (±12.3)	23.9 (±9.2)	21.7 (±7.3)	0.376
Plasma SC5b-9 (ng/ml)	1307 (±1243) ^b	1958 (±1367)	510 (±503) ^{a,b}	300 (±151) ^{a,b,c}	<0.001
Low serum C3	100% ^b	100%	93.1%	44.4% ^{a,b,c}	<0.001
Low serum C4	6%	24% ^{a,d}	7%	6%	0.007
C3NeF positive	54% ^c	61%	80%	6% ^{a,b,c}	<0.001
LPV carriers	29%	24%	14%	4% ^{a,b}	0.003
LPV carriers and/or C3NeF	75%	76%	84%	10% ^{a,b,c}	<0.001
<i>Data during follow-up</i>					
Nephrotic syndrome	49%	87% ^{a,c,d}	48%	46%	<0.001
High blood pressure	28%	44%	24%	56% ^{a,c}	0.005
Chronic kidney disease	26% ^{b,d}	44%	24% ^d	50%	0.016
ESRD	5%	7%	3%	15%	0.187
Thrombotic microangiopathy	2%	0%	0%	11% ^{a,b}	0.010
<i>Histological features</i>					
Time Onset to Biopsy (yr), median (IQR)	0.4(0.1-1.4)	0.3 (0.1-2.1)	1.1 (0.3-3.5)	0.3 (0.1-2.6)	0.859
<i>Light microscopy</i>					
Sclerotic glomeruli	3% (±7%)	5% (±11%)	2% (±6%)	16% (±21%) ^{a,b,c}	<0.001
Crescents	5% (±16%)	2% (±8%)	6% (±18%)	5% (±16%)	0.683
Degree of mesangial proliferation ^e	1.9 (±0.9)	1.8 (±1.1)	1.9 (±0.8)	1.5 (±1)	0.273
Degree of endocapillary proliferation ^e	1.3 (±1.1)	1.5 (±1) ^c	1 (±1.1)	0.6 (±0.8) ^{a,b,c}	<0.001
Degree of interstitial inflammation ^e	0.4 (±0.6) ^{b,d}	0.8 (±0.7)	0.7 (±0.8)	1 (±0.9)	0.001
Degree of interstitial fibrosis ^e	0.3 (±0.6)	0.5 (±0.7)	0.2 (±0.4)	0.7 (±0.9) ^{a,c}	0.001
Degree of arteriolar sclerosis ^e	0.1 (±0.4)	0.2 (±0.5)	0.1 (±0.2)	0.6 (±1) ^{a,b,c}	<0.001
<i>Immunofluorescence^e</i>					
C3	2.7 (±0.5)	2.8 (±0.5)	2.8 (±0.3)	2.5 (±0.7) ^{b,c}	0.016
IgA	0.1 (±0.4) ^{b,d}	0.4 (±0.6) ^c	0.1 (±0.3)	0.3 (±0.7)	0.015
IgG	0.4 (±0.9) ^{b,d}	1.5 (±1)	0.4 (±0.7) ^{b,d}	1.1 (±1.2)	<0.001
IgM	0.6 (±0.8)	1.2 (±0.9) ^{a,c,d}	0.6 (±0.6)	0.8 (±1)	0.002
C1q	0 (±0.1) ^{c,d}	1.7 (±0.7) ^{a,c,d}	0.2 (±0.5) ^d	0.6 (±0.9)	<0.001
Fibrinogen	0.4 (±0.9)	0.5 (±0.8)	0.3 (±0.7)	0.1 (±0.3) ^{a,b}	0.033
<i>Electron microscopy</i>					
Mesangial deposits	73% ^{c,d}	68%	48%	53%	0.051
Subepithelial deposits	48%	48%	10% ^{a,b,d}	42%	0.004
Subepithelial hump-like deposits	23%	15%	12%	23%	0.480
Subendothelial deposits	78%	85%	10% ^{a,b,d}	69%	<0.001
Intramembranous granular deposits	61% ^d	53%	0% ^{a,b,d}	41%	<0.001
Intramembranous highly electron-dense ribbon-like deposits	0%	0%	100% ^{a,b,d}	0%	<0.001

Table 11. Clinical features, complement assessment, genetic screening and histologic features in patients classified according to cluster groups calculated on the basis of three-step algorithm.

Continuous variables are reported as mean (\pm SD) unless otherwise specified.

Serum C3: reference 90-180 mg/dl; serum C4: reference 10-40 mg/dl; plasma SC5b-9: reference \leq 303 ng/ml.

^a Significant different from cluster 1.

^b Significant different from cluster 2.

^c Significant different from cluster 3.

^d Significant different from cluster 4.

^e Degree of mesangial proliferation, endocapillary proliferation, interstitial inflammation, interstitial fibrosis, and arteriolar sclerosis, as well as IF findings were graded using a scale of 0 to 3, including 0, trace (0.5+), 1+, 2+ and 3+.

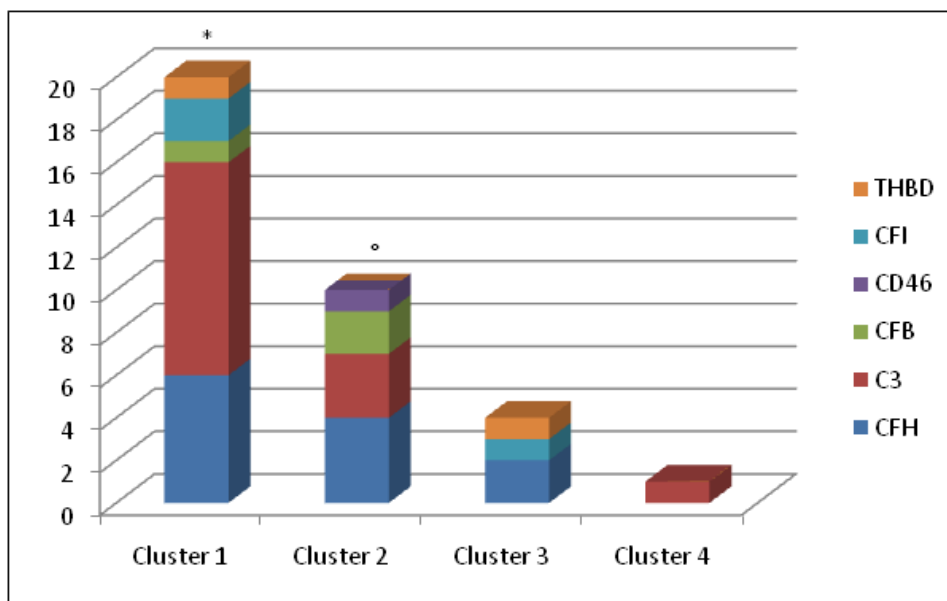


Figure 34. Complement likely pathogenic distribution in the four clusters.

* Significant different from cluster 4 ($p= 2.8 \text{ E-}04$);

° Significant different from cluster 4 ($p= 0.002$).

2.5.2.3 Renal survival

Fifteen patients developed end stage renal disease (cluster 1: $n=3$; cluster 2: $n=3$; cluster 3: $n=1$; cluster 4: $n=8$; $p=0.187$). Kaplan-Meier analysis showed that patients in cluster 4 had an higher risk to develop ESRD in comparison to the other patients ($p=0.0134$; cluster 1-3 vs cluster 4, Fig.35-36).

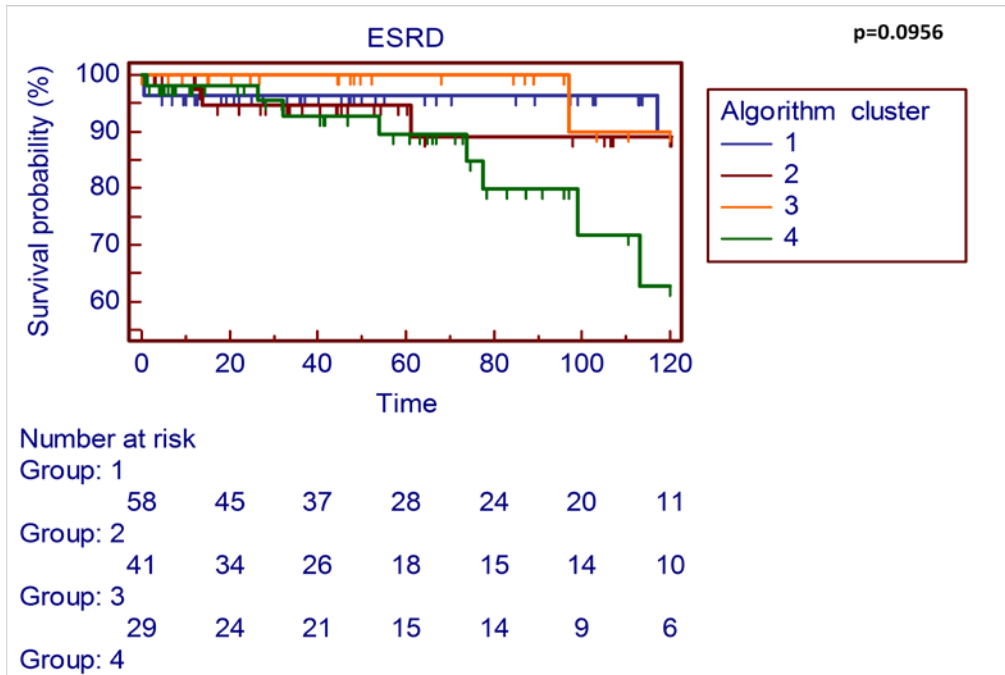


Figure 35. Kaplan-Meier representing the risk to develop ESRD in different groups of patients classified by the three-step algorithm.

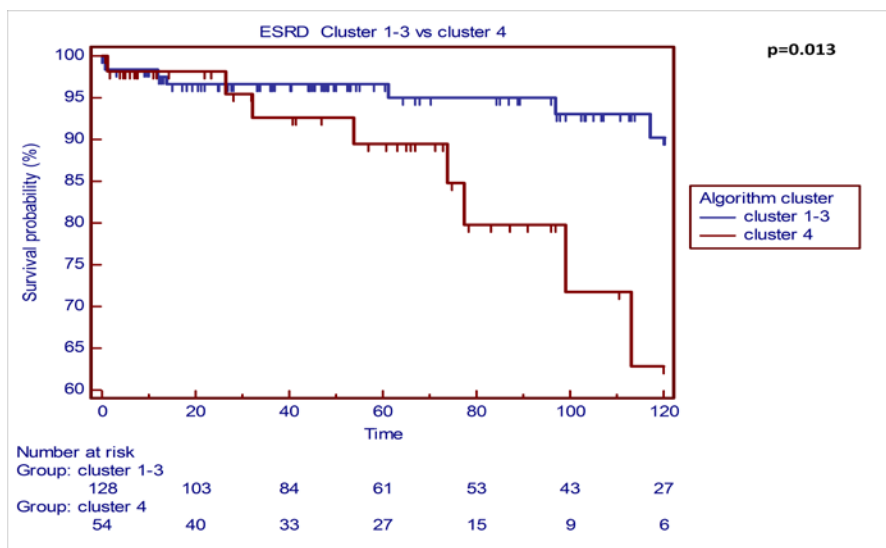


Figure 36. Kaplan-Meier representing the risk to develop ESRD in cluster 1-3 versus cluster 4.

2.5.2.4 Susceptibility genetic variants

Single nucleotide polymorphisms analyzed in the three histology groups (IC-MPGN, DDD and C3GN; section 2.5.1.6) were also studied in the four algorithm clusters (Table 12). The *CFH*, p.936D allele was over represented in cluster 2 (allele frequencies: cluster 2 = 0.31; ctrs = 0.18; $p = 0.008$), while the *THBD* p.A473 was in association with cluster 1 (allele frequencies: cluster 1 = 0.92; ctrs = 0.82; $p = 0.008$) and showed a trend of association with cluster 2 (allele frequency: 0.91; $p=0.098$). These results fitted with a recessive inheritance model (Table 14).

Genotype frequency analyses showed a trend of association for the *CFH*, c.-331T in cluster 2 (recessive model: $p=0.06$ vs. ctrs) and for *CD46* c.-366A in cluster 3 (recessive model: $p=0.068$ vs. ctrs, Table 14).

SNP	Cluster group	n	Genotype frequencies				Allele frequencies		
			A/A	A/a	a/a	p value vs ctrs	Allele frequency allele A	Allele frequency allele a	p value vs ctrs
<i>CFH</i> c.-331C>T rs3753394	Cluster 1	63	31	26	6	0.73	0.70	0.30	0.83
	Cluster 2	44	17	20	7	0.07	0.61	0.39	0.07
	Cluster 3	29	17	10	2	0.60	0.76	0.24	0.54
	Cluster 4	53	20	27	6	0.21	0.63	0.37	0.11
	Ctrs	452	223	198	31		0.71	0.29	
<i>CFH</i> p.V62I rs800292	Cluster 1	63	41	20	2	0.37	0.81	0.19	0.23
	Cluster 2	44	24	16	4	0.38	0.73	0.27	0.63
	Cluster 3	29	19	9	1	0.59	0.81	0.19	0.44
	Cluster 4	53	34	18	1	0.42	0.81	0.19	0.26
	Ctrs	452	252	180	20		0.76	0.24	

Table 12. Association study between common polymorphisms and patients included in different clusters. It continues in next pages.

SNP	Cluster group	n	Genotype frequencies			p value vs ctrs	Allele frequencies		p value vs ctrs
			A/A	A/a	a/a		Allele frequency allele A	Allele frequency allele a	
CFH p.H402Y rs1061170	Cluster 1	63	10	29	24	0.80	0.39	0.61	0.60
	Cluster 2	44	6	13	25	0.16	0.28	0.72	0.19
	Cluster 3	29	9	9	11	0.056	0.47	0.53	0.14
	Cluster 4	53	10	23	20	0.66	0.41	0.59	0.42
	Ctrs	452	66	194	192		0.36	0.64	
CFH p.E936D rs1065489	Cluster 1	63	40	21	2	0.87	0.80	0.20	0.78
	Cluster 2	44	23	15	6	0.003	0.69	0.31	0.008
	Cluster 3	29	21	8	0	0.56	0.86	0.14	0.48
	Cluster 4	53	36	13	4	0.25	0.80	0.20	0.82
	Ctrs	452	301	136	15		0.82	0.18	
CD46 c.-652G>A rs2796267	Cluster 1	58	9	25	24	0.96	0.37	0.63	0.95
	Cluster 2	43	7	13	23	0.34	0.31	0.69	0.44
	Cluster 3	25	4	9	12	0.86	0.34	0.66	0.86
	Cluster 4	51	4	23	24	0.34	0.30	0.70	0.29
	Ctrs	404	63	167	174		0.36	0.64	
CD46 c.-366A>G rs2796268	Cluster 1	62	12	27	23	0.56	0.41	0.59	0.47
	Cluster 2	44	5	18	21	0.57	0.32	0.68	0.37
	Cluster 3	29	5	7	17	0.06	0.29	0.71	0.28
	Cluster 4	53	6	22	25	0.55	0.32	0.68	0.34
	Ctrs	452	64	209	179		0.37	0.63	

Table 12. Association study between common polymorphisms and patients included in different clusters. It continues in next pages.

SNP	Cluster group	n	Genotype frequencies				Allele frequencies		
			A/A	A/a	a/a	p value vs ctrs	Allele frequency allele A	Allele frequency allele a	p value vs ctrs
CD46 p.A309V rs35366573	Cluster 1	48	48	0	0	0.61	1	0.00	0.62
	Cluster 2	39	37	2	0	0.35	0.97	0.03	0.56
	Cluster 3	24	24	0	0	0.78	1.00	0.00	1.00
	Cluster 4	40	40	0	0	0.67	1.00	0.00	0.72
	Ctrs	452	443	8	1		0.99	0.01	
CD46 c*783T>C rs7144	Cluster 1	62	28	25	9	0.67	0.65	0.35	0.56
	Cluster 2	44	22	18	4	0.32	0.70	0.30	0.16
	Cluster 3	29	16	8	5	0.16	0.69	0.31	0.37
	Cluster 4	53	26	23	4	0.22	0.71	0.29	0.10
	Ctrs	404	159	184	61		0.62	0.38	
CFB p.L9H rs4151667	Cluster 1	60	54	6	0	0.73	0.95	0.05	0.91
	Cluster 2	44	39	5	0	0.64	0.94	0.06	0.75
	Cluster 3	29	28	1	0	0.65	0.98	0.02	0.54
	Cluster 4	52	49	3	0	0.78	0.97	0.03	0.67
	Ctrs	452	415	35	2		0.96	0.04	
CFB p.K565E rs4151659	Cluster 1	52	51	1	0	0.97	0.99	0.01	0.97
	Cluster 2	42	40	2	0	0.90	0.98	0.02	0.90
	Cluster 3	26	26	0	0	0.75	1.00	0.00	0.76
	Cluster 4	46	45	1	0	0.92	0.99	0.01	0.92
	Ctrs	452	438	14	0		0.98	0.02	

Table 12. Association study between common polymorphisms and patients included in different clusters. It continues in next page.

SNP	Cluster group	n	Genotype frequencies				Allele frequencies		
			A/A	A/a	a/a	p value vs ctrs	Allele frequency allele A	Allele frequency allele a	p value vs ctrs
CFB p.E566A rs45484591	Cluster 1	55	54	1	0	0.99	0.99	0.01	0.99
	Cluster 2	42	41	1	0	0.76	0.99	0.01	0.77
	Cluster 3	26	25	1	0	0.75	0.98	0.02	0.76
	Cluster 4	47	44	3	0	0.39	0.97	0.03	0.39
	Ctrs	452	439	13	0		0.99	0.01	
C3 p.R102G rs2230199	Cluster 1	62	40	20	2	0.59	0.81	0.19	0.41
	Cluster 2	44	30	10	4	0.29	0.80	0.20	0.66
	Cluster 3	29	20	6	3	0.28	0.79	0.21	0.79
	Cluster 4	53	30	19	4	0.87	0.75	0.25	0.67
	Ctrs	452	271	153	28		0.77	0.23	
C3 p.P314L rs1047286	Cluster 1	62	42	18	2	0.67	0.82	0.18	0.43
	Cluster 2	44	29	13	2	0.91	0.81	0.19	0.78
	Cluster 3	29	21	6	2	0.42	0.83	0.17	0.58
	Cluster 4	53	35	16	2	0.85	0.81	0.19	0.66
	Ctrs	452	283	146	23		0.79	0.21	
THBD p.A473V rs1042579	Cluster 1	63	53	10	0	0.02	0.92	0.079	0.008
	Cluster 2	44	36	7	1	0.15	0.90	0.10	0.098
	Cluster 3	29	24	5	0	0.20	0.91	0.09	0.11
	Cluster 4	53	34	17	2	0.87	0.80	0.20	0.71
	Ctrs	452	306	131	15		0.82	0.18	

Table 12. Association study between common polymorphisms and patients included in different clusters.

<i>CFB</i> p.R32Q/W		Genotypes						<i>p</i> value vs ctrs
Histology group	<i>n</i>	RR	RQ	QQ	RW	WW	QW	
Cluster 1	62	41	5	1	15	0	0	0.44
Cluster 2	44	28	8	0	6	1	1	0.80
Cluster 3	29	18	6	0	2	0	3	0.13
Cluster 4	53	30	10	1	10	1	1	0.91
Ctrs	452	274	64	5	91	5	13	

<i>CFB</i> p.R32Q/W		Allelic frequencies				
Histology group	R	<i>p</i> value vs ctrs	Q	<i>p</i> value vs ctrs	W	<i>p</i> value vs ctrs
Cluster 1	0.82	0.31	0.06	0.20	0.12	0.99
Cluster 2	0.80	0.80	0.10	1.00	0.10	0.63
Cluster 3	0.76	0.86	0.16	0.22	0.09	0.49
Cluster 4	0.75	0.68	0.12	0.49	0.12	0.96
Ctrs	0.78		0.10		0.13	

Table 13. Frequency of the *CFB* polymorphism p.R32Q/W in different clusters.

snp	Risk allele	Cluster group	n	Genotype frequencies				Dominant model (homozygous or heterozygous for risk allele)			Recessive model (homozygous for risk allele)			
				A/A	A/a	a/a	p value vs ctrs	Risk allele	Frequency	p value vs ctrs	Risk allele	Frequency	p value vs ctrs	
<i>CFH</i>	c.-331C>T rs3753394	T	Cluster 1	63	31	26	6	0.73	32	0.51	0.91	6	0.10	0.61
			Cluster 2	44	17	20	7	0.07	27	0.61	0.23	7	0.16	0.06
			Cluster 3	29	17	10	2	0.60	12	0.41	0.44	2	0.07	0.71
			Cluster 4	53	20	27	6	0.21	33	0.62	0.15	6	0.11	0.37
			Ctrs	452	223	198	31		229	0.51		31	0.07	
<i>CFH</i>	p.E936D rs1065489	D	Cluster 1	63	40	21	2	0.87	23	0.37	0.73	2	0.03	0.75
			Cluster 2	44	23	15	6	0.0031	21	0.48	0.08	6	0.14	0.004
			Cluster 3	29	21	8	0	0.56	8	0.28	0.66	0	0.00	0.66
			Cluster 4	53	36	13	4	0.25	17	0.32	0.97	4	0.08	0.25
			Ctrs	452	301	136	15		151	0.33		15	0.03	
<i>CD46</i>	c.-366A>G rs2796268	G	Cluster 1	62	12	27	23	0.56	50	0.81	0.37	23	0.37	0.81
			Cluster 2	44	5	18	21	0.57	39	0.89	0.78	21	0.48	0.37
			Cluster 3	29	5	7	17	0.06	24	0.83	0.85	17	0.59	0.068
			Cluster 4	53	6	22	25	0.55	47	0.89	0.72	25	0.47	0.36
			Ctrs	452	64	209	179		388	0.86		179	0.40	
<i>THBD</i>	p.A473V rs1042579	A	Cluster 1	63	53	10	0	0.0213	63	1.00	0.29	53	0.84	0.01
			Cluster 2	44	36	7	1	0.15	43	0.98	0.94	36	0.82	0.08
			Cluster 3	29	24	5	0	0.20	29	1.00	0.66	24	0.83	0.14
			Cluster 4	53	34	17	2	0.87	51	0.96	0.82	34	0.64	0.71
			Ctrs	452	306	131	15		437	0.97		306	0.68	

Table 14. Genotype and allele frequencies and models of inheritance of complement gene polymorphisms showing a trend of association to different clusters in Table 13.

2.5.3 Discussion

In this study, 199 patients recruited by the Italian Registry of MPGN, were histologically classified in IC-MPGN, DDD and C3GN according to the current classification^{89, 185}.

Since hypocomplementemia (represented by low C3 levels) was present in all histology groups, genetic and biochemical analyses were performed to investigate the presence of likely pathogenic variants in complement genes and C3NeF, an autoantibody that stabilizes the C3 convertase. These results were then correlated with different ultrastructural lesions, complement profile and clinical outcome to understand the mechanism underlying IC-MPGN, DDD and C3GN and to contribute to identify new molecular targets for complement inhibitory therapies.

Onset of patients with IC-MPGN, that occurred at a mean age of 19.6 years, was mainly characterized by microhematuria and proteinuria that in 39% of cases was in the nephrotic range. Electron microscopy revealed predominant subendothelial deposits but also mesangial and intramembranous granular deposits whilst immunofluorescence showed a strong C3, IgG, IgM and C1q deposition. The presence of C3NeF was associated with low C3 levels and high SC5b-9 levels, while patients with LPVs showed high SC5b-9 levels and near normal C3 levels. These data suggest that in IC-MPGN patients C3NeF affected both C3 and C5 convertase activation while genetic abnormalities mainly influenced the terminal pathway of complement. LPVs identified in IC-MPGN patients were mainly localized in *CFH* and *C3* genes. Notably, a few IC-MPGN patients carried LPVs in *CFB* gene, while no *CFB* LPVs were identified in the other histology groups. A *CFB* mutation was already described in a familial case of C3GN, indicating that such abnormalities may not be restricted to IC-MPGN¹¹³. Although functional effects of *CFB* LPVs associated with IC-MPGN and C3GN are still

unknown, it is important to consider that FB, together with C3, generate the C3 convertase (C3bBb) and C5 convertase (C3bBbC3b) of the complement alternative pathway. I hypothesize that *C3* and *CFB* LPVs identified in these patients, may generate C3 and C5 convertases more resistant to inactivation by complement regulators causing complement activation until the terminal pathway.

Furthermore, association analysis showed that the presence of the *CFH* 936D polymorphism increased the risk to develop IC-MPGN.

These data suggest that, although the strong glomerular presence of immune-complexes indicates that IC-MPGN is initiated by activation of the classical complement pathway, genetic risk factors predisposes to a switch from classical pathway driven disease to a chronic alternative pathway-driven process.

Patients with C3GN showed a clinical onset (characterized by microhematuria, proteinuria, nephrotic syndrome, renal impairment and mean age of onset of 17.9 years) similar to IC-MPGN patients. Electron microscopy was characterized by mesangial, subepithelial and subendothelial deposits with predominant C3 deposition at IF. Low C3 levels and high SC5b-9 levels were associated with both LPVs and C3NeF although patients with only C3NeF had higher plasma SC5b-9 levels in comparison to patients with only LPVs. Compared to IC-MPGN and DDD patients, C3GN patients showed a higher frequency of LPVs, involving *CFH*, *CFI*, *C3* and *THBD* genes. The most abundant LPVs, involved the *C3* gene followed by the *CFH* gene, like in IC-MPGN. However, at variance with IC-MPGN patients in whom the *CFH* LPVs were broadly distributed, *CFH* LPVs in C3GN mainly affected the N-terminal domains that are responsible for the regulatory activity of FH.

Notably, about 46% of patients with IC-MPGN or C3GN did not carry either LPVs and/or C3NeF and showed normal complement profile in the face of strong C3

glomerular deposition, suggesting that in these patients other complement abnormalities not affecting circulating C3 and SC5b-9 levels may be present.

Patients with DDD had a slightly earlier onset in comparison to patients in the other two histology groups (mean age of onset: 15.1 years), characterized by the microhematuria, proteinuria but also by a more frequent gross hematuria. Differently from the other patient groups, DDD patients rarely showed renal impairment at onset. The frequency of genetic and/or acquired abnormalities was statistically higher than in the other patient groups mainly due to the significantly higher prevalence of C3NeF (79%). DDD patients had lower C3 levels than IC-MPGN patients while SC5b-9 levels were lower in DDD than in the other histology groups. Interestingly, DDD patients without genetic or acquired abnormalities showed low C3 levels but normal SC5b-9 levels suggesting the presence of an unknown factor underlying hypocomplementemia. In DDD patients, LPVs were localized in the *CFH*, *CFI* and *THBD* genes. Among them, the FH p.R1210C, carried by a DDD patient, is the most frequent LPV in aHUS and has been described to complex with albumin impairing accessibility to all FH functional domains^{166, 167}. The DDD-associated LPV in *THBD*, as well as the one identified in C3GN, were already described in aHUS and functional studies demonstrated that mutant THBD proteins affected the complement regulation through CFI-mediated C3b inactivation²². Thrombomodulin is a cell membrane protein but it also exists in a soluble plasma form that increases in diseases characterized by vascular damage and regulates complement and inflammation. Reported studies showed that high plasma thrombomodulin levels may be vasculoprotective^{195, 196}. An increased expression of thrombomodulin in glomerular endothelial cells was described in membranoproliferative glomerulonephritis and lupus glomerulonephritis and may represent a protective response following the glomerular complement activation occurring in MPGN^{120, 121}.

Altogether these data suggest that the presence of C3NeF is the main cause of low C3 levels in all histology groups. In DDD patients C3NeF seems to mainly affect the C3 convertase than the terminal pathway whilst in IC-MPGN and C3GN it showed greater effects on terminal pathway than on C3 convertase. These findings are in accordance with published data. Zhang et al¹⁹⁷ compared the complement profile between patients with DDD and C3GN, showing that C3 convertase dysregulation was higher in patients with DDD while C5 convertase dysregulation was predominant in C3GN.

C3NeFs represent a heterogeneous group of autoantibodies^{198, 199} with different effects on complement activation. Regarding the functional assays used to detect C3NeFs, different subtypes of these autoantibodies could be identified according to their capacity to selectively stabilize the C3 or the C5 convertases, or whether their stabilizing activity occurs in the absence or in the presence of properdin, the only known positive regulator of the AP complement system²⁰⁰⁻²⁰². Recently, the Fremaux-Bacchi's group described the presence of circulating autoantibodies that stabilize C5 convertase (C5 Nephritic Factors, C5NeFs). C5NeFs correlated with consumption of C3 and with SC5b-9 levels and were more frequent in patients with C3GN than in patients with DDD¹⁸⁴. The presence of C5NeF in C3GN and in IC-MPGN could explain the very high SC5b-9 levels in patients of these two histologic groups from our cohort. In addition, patients with IC-MPGN without C3NeF, may have high SC5b-9 levels because LPVs in two components of convertases result in hyperactivation of the AP C3 and C5 convertases.

Complement genetic abnormalities were identified in only 18% of IC-MPGN and C3G patients. However, the frequency of LPVs identified in our cohort may be underestimated. Indeed, we considered as likely pathogenetic variants those rare variants (MAF <0.001) with a pathogenicity score >10 calculated by an *in silico* predictive algorithm (CADD). Recently, Merinero et al²⁰³ showed that 73% of *CFH*

LPVs, predicted *in silico* to be benign or of uncertain significance were functionally pathogenic. These data indicate that *in silico* prediction may fail to assign a correct pathogenicity and that we may have lost rare genetic variants considered benign by *CADD*. Thus, functional studies on genetic variants are strongly required to better study their causal relationship with the pathology.

The finding of genetic complement abnormalities in IC-MPGN is not in accordance with the current classification that considers C3 glomerulopathy caused by a abnormal complement alternative pathway activation and IC-MPGN mediated by classic pathway because of the immune-complex deposition in the biopsy.

To address the above discrepancy, we recently proposed a new approach based on unsupervised hierarchical cluster analysis using histologic, biochemical, genetic and clinical data. The analysis separated patients in four homogeneous groups characterized by specific pathophysiologic mechanisms². We also provided a simple three-step algorithm (that had a 75% of concordance with the original cluster analysis) to assign patients to different groups.

In the updated cohort described in this chapter ($n=193$), patients with complete clinical, histological and laboratory data were classified using the three-step algorithm.² As already published, patients were included in four groups called clusters. Cluster 1, 2 and 3 were characterized by low C3 and high SCb-9 levels and high frequency of LPVs and or C3NeF . Cluster 4 had normal complement profile and low frequency of complement abnormalities and later age of onset.

Cluster 1 and 2 differentiated from cluster 3 for the very high levels of plasma SC5b-9. Indeed, in these clusters are included IC-MPGN and C3GN patients who, as discussed above, carried LPVs in the two convertase components (C3 and FB) and may have C5NeFs that stabilize the C5 convertase. The frequency of nephrotic syndrome at onset

was significantly higher in cluster 2 than in the other clusters. In addition, cluster 2 was represented by patients with low C4 levels and a significantly higher glomerular deposition of IgG, IgM and C1q in comparison to other patients suggesting an important role of classical pathway of complement in initiating the disease.

Cluster 3, composed by all DDD patients and few patients with IC-MPGN, was characterized by low C3 levels and only slightly elevated SC5b-9 levels, suggesting a prevalent C3 convertase dysregulation in fluid-phase. SC5b-9 levels in cluster 3 were significantly lower than in clusters 1 and 2, indicating the presence of different pathogenetic mechanisms leading to complement dysregulation. This hypothesis is confirmed by the difference in LPV localization that in cluster 3 mainly involved genes encoding complement regulator proteins (*CFH*, *CFI* and *THBD*), while no LPV localized on *C3* and *CFB* genes, at variance with clusters 1 and 2.

Finally, identification of cluster 4 including patients with IC-MPGN or C3GN and with a normal complement profile, rare C3NeF and LPVs in the face of intense C3 glomerular staining, indicates the existence of still unknown genetic or acquired factors determining local glomerular complement deposition in subgroups of IC-MPGN and C3GN patients.

This may result in accumulation of complement effector molecules causing slow chronic progression of injury that explain a late onset and an higher risk to develop end stage renal disease that characterize this cluster.

Altogether these findings confirmed our published data on cluster analysis identifying distinct pathogenetic patterns underlying IC-MPGN, DDD and C3GN². In summary, the histology, clinical, genetic and biochemical data in a large cohort of patients with kidney injury showed complement alternative pathway abnormalities both in C3 glomerulopathy and in IC-MPGN. Among the three histology groups, the DDD group showed a clinical and complement profile different from IC-MPGN and C3GN and

C3NeF or LPVs till now identified do not seem to be the only risk factors responsible for hypocomplementemia. Cluster analysis allowed the identification of distinct pathogenetic patterns separating patients with an intense C5 convertase activity from patients with a predominant C3 convertase activity (including DDD patients). Of interest, it also identified a group of patients without known complement abnormalities despite intense glomerular complement deposition.

These results may contribute to better discover target therapies and indicate that the identification of new biochemical and genetic factors is required to refine the classification of these glomerular diseases.

3. COMPLEMENT AND COAGULATION GENETIC SCREENING IN PATIENTS WITH DENSE DEPOSIT DISEASE

3.1 Introduction

Dense Deposit Disease (DDD) is a glomerular lesion with a prevalence of 2 to 3 individuals per million population and traditionally is diagnosed either in childhood or adulthood^{137,204,205}.

Due to the presence of intense glomerular C3 staining with scanty or no immunoglobulin at immunofluorescence, DDD is considered a C3 glomerulopathy (C3G). DDD is characterized at electron microscopy by electron-dense, sausage-shape deposits in the central layer (lamina densa) of GBM and often in the mesangium and Bowman's capsule¹³⁷. The dense deposits characteristic of DDD are composed both by components of the AP of complement (C3b and its breakdown products iC3b, C3dg, C3c) and also by component of the terminal pathway²⁰⁶.

The clinical onset of DDD is mainly characterized by microhematuria, proteinuria (with or without nephrotic syndrome) and hypertension¹³⁷. Among non renal manifestations of DDD, acquired partial lipodystrophy (APL) and ocular lesions similar to drusen have been reported⁹¹⁻⁹³.

Although the pathogenesis of DDD has not been fully clarified, hyperactivation of the complement alternative pathway (AP) is found in more than 80% of patients, as documented by low C3 levels with normal C4 levels in serum. The reported causes of the AP dysregulation include both acquired and genetic factors. Indeed, the C3 nephritic factor (C3NeF), an autoantibody that stabilizes the C3 convertase, is present in around 80% of DDD patients^{95,103} (Chapter 2, section 2.5.1.) and anti-factor B and anti-factor H autoantibodies have been also reported in a few cases^{96,97,100}. Mutations and rare

functional variants in genes coding the AP complement regulators Factor H (*CFH*) and Factor I (*CFI*) and more rarely, gain of function mutations in the gene coding the component of the AP C3 convertase, complement C3 (*C3*) have been reported^{95,101,103} (Chapter 2, section 2.5.1.3).

Genomic rearrangements in the complement factor H-related genes, that include a *CFHR2-CFHR5* hybrid gene and an internal duplication in *CFHR1*, have also been described in a few patients with DDD^{130,132}.

However, the genetic determinants of DDD are still unknown for the majority (>80%) of patients. The high rate of incomplete penetrance indicates that likely pathogenic variants (LPVs) and genomic rearrangements predispose individuals to diverse pathologies and that additional genetic risk factors are necessary to cause the disease and determine the final phenotype.

Indeed, besides LPVs and genomic rearrangements, there are also common variants in the *CFH*, *C3* and *CD46* genes that increase the risk of DDD^{95,116}. A trend of association of a common *THBD* allele (A473) was also observed in DDD patients from the Italian cohort¹⁰³ (see section 2.5.1.7).

Thanks to a collaboration with the University of Iowa, I spent 6 months at the laboratory of Dr Richard Smith where I used a wide NGS panel (called CasCADE) to search rare variants in complement and coagulation genes in patients with DDD. Eighty five genes were sequenced in 17 patients with DDD. All variants were filtered by quality parameters, frequency and functional effects. Final variants were classified by a pathogenicity score.

The majority of variants involved complement regulator genes. Besides abnormalities in the *CFH-CFHR* gene family, I also found likely deleterious variants in complement genes not previously associated with DDD, although always in combination with other

deleterious complement variants. Few variants were found in genes of classical and coagulation pathways.

Results from this study suggest the existence of new genetic risk factors that require further investigation to confirm their involvement in the pathogenesis of DDD.

This chapter was designed with the following objective:

- 1) To search new likely deleterious variants in candidate complement and coagulation genes in patients with Dense Deposit Disease.

3.2 Patients

Patients are included in the Italian cohort described in Chapter 2.

3.3 Methods

3.3.1 DNA samples

DNA samples were extracted and quantified as reported as reported in section 2.4.2

3.3.2 CasCADE panel

Target genomic enrichment was performed on DDD samples using a wide panel called CasCADE (called CasCADE: Capture and Sequencing of Complement- Associated Disease Exons), developed at the University of Iowa. CasCADE is a RNA-bait panel that, based on Agilent SureSelect Target Enrichment System, targets coding regions of 85 complement and coagulation genes. Following the manufacturer's protocol, 2 μ g genomic DNA was sheared to 100-300 bp fragments by Covaris sonification system. DNA fragments followed end-repair, 3' end adenylation, adapter ligation and pre-hybridization PCR steps. Prepped adaptor-ligated DNA libraries were combined with the biotinylated RNA-baits via a 24-hours hybridization at 65°C.

Then in the bead capture step, streptavidin-coated beads were used to selectively capture the biotinylated RNA-bait-DNA complexes. During the following post-hybridization PCR, targeted regions were enriched and each library barcoded with a unique index. Final libraries quality and concentration were verified by Agilent High Sensitivity DNA Kit on a Bioanalyzer 2100 (Agilent Technologies). After pooling, libraries were sequenced on a HiSeq 2000 (Illumina) at the DNA Core Facility of the University of Iowa's Institute of Human Genetics or on an in-house MiSeq (Illumina).

Sequence data analysis was performed using a bioinformatic pipeline on Galaxy, a web-based platform. All genetic variants were annotated by ANNOVAR software.

All annotated variants with QD <5, Depth <10 and phred-scaled quality score <30 were excluded. Among variants with a minor allele frequency (MAF) in 1000 genome, ESP6500 and Exac (European Non Finnish population) databases less than 0.001, I focused on nonsynonymous, frame shift, splicing e nonsense variants. A pathogenicity Score (PS) was calculated by combining prediction results deriving from PhyloP, Sift, Polyphen2_HDiv, Polyphen2_HVar, LRT, Mutation Taster and Gerp++ computational prediction methods. Variants with a PS ≥ 4 were considered "likely deleterious".

3.4 Results

Targeted genomic enrichment and next generation sequencing (TGE+NGS) were used to analyze 17 patients with DDD. The CasCADE panel covered 1071 exons of 85 complement and coagulation genes (Fig. 37).

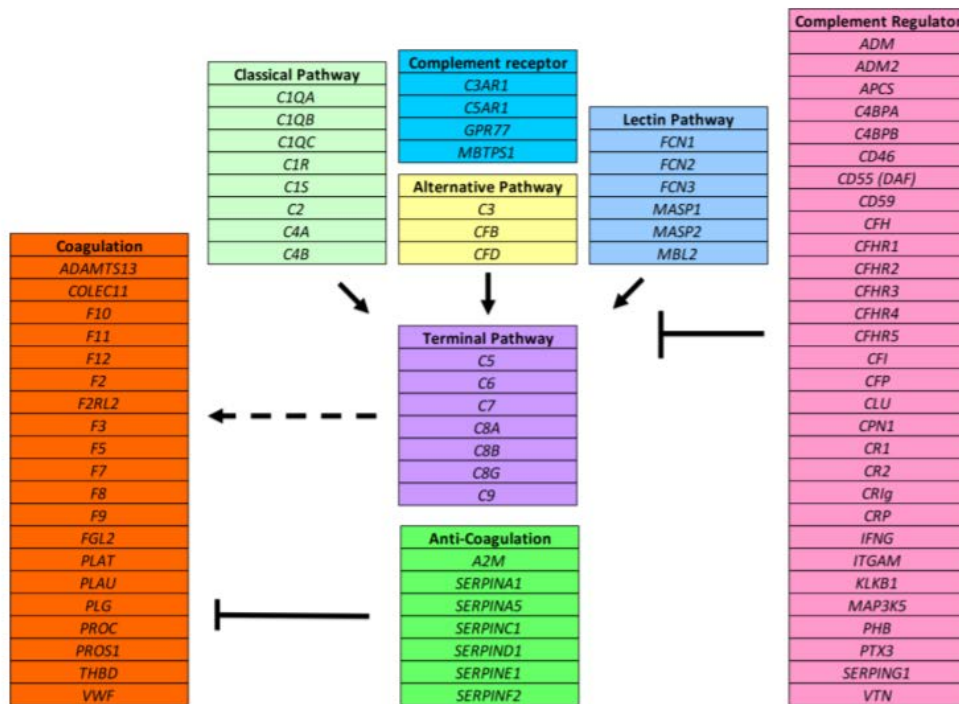


Figure 37. Complement and coagulation genes included in the CasCADE panel. Image taken from Fengxiao et al. (2014)⁴.

Among 9096 variants identified, 8231 passed the quality control step. Variants ($n=716$) with a minor allele frequency (MAF) in 1000 genome, ESP6500 and Exac (European Non Finnish population) databases less than 0.001 were retained and filtered by functional effect as described in methods. Filtering steps provided 25 heterozygous rare functional variants (including missense and nonsense variants) in 12 patients (Table 15). Eight patients (47%) carried two or more rare variants while four patients showed a single rare variant, two of them in *CFH* and *CFI* and already identified by the NGS minipanel (see section 2.5.1.3). In five patients no rare variants were detected in

complement and coagulation genes. Among rare variants, 17 were predicted likely deleterious by the presence of a premature stop codon or by a pathogenicity score (PS) ≥ 4 (Table 15).

The most frequent abnormalities (60%) involved complement regulator genes, followed by complement receptor (12%) and coagulation genes (12%) (Fig.38). Not surprisingly, 6 variants (24%) were found in the genes of the *CFH* family (*CFH*, *CFHR2*, *CFHR4* and *CFHR5*) suggesting their important role in the DDD phenotype.

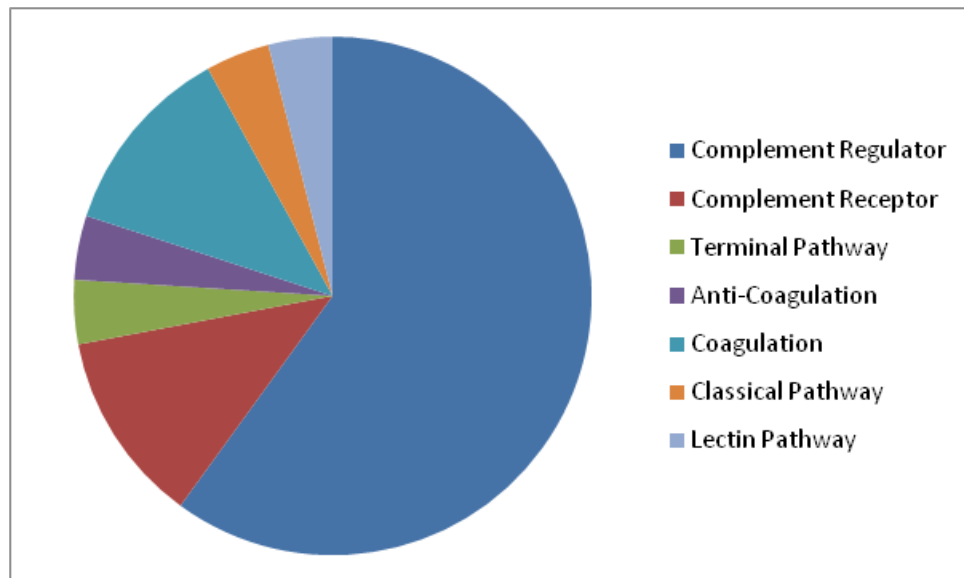


Figure 38. Distribution of variants identified in patients with DDD.

Sample ID	Gene	Nucleotide	AA Change	Exac European (Non Finnish) MAF	PS	dbSNP
633	<i>MASP2</i>	c.A1616G	p.N539S	1,50E-05	1/7	rs776770754
633	<i>PTX3</i>	c.A574G	p.I192V	1,05E-04	7/7	rs762560584
1101	<i>CFH</i>	c.C3628T	p.R1210C	2,85E-04	1/6	rs121913059
1124	<i>C4BPA</i>	c.G676A	p.V226I	1,50E-04	5/7	rs117760512
1124	<i>ITGAM</i>	c.G2486A	p.R829Q	1,05E-04	5/7	rs201299141
1149	<i>CR1</i>	c.A4594G	p.S1532G	2,85E-04	4/6	rs189863730
1149	<i>KLKB1</i>	c.G1694A	p.G565D	6,00E-05	7/7	rs150832692
1149	<i>C5AR1</i>	c.C185T	p.T62M	1,49E-05	4/7	rs200003809
1218	<i>C6</i>	c.G143A	p.R48K	3,75E-04	6/7	rs145422926
1218	<i>SERPINA1</i>	c.G1093T	p.D365Y	NA	5/7	NA
1218	<i>ITGAM</i>	c.C1226T	p.A409V	NA	2/6	NA
1332	<i>F11</i>	c.A731G	p.Q244R	5,10E-04	2/7	rs5969
1332	<i>MBTPS1</i>	c.A2873G	p.D958G	NA	4/7	NA
1409	<i>CFI</i>	c.G170A	p.G57D	0	6/7	rs776080713
1549	<i>CFH</i>	c.G5T	p.R2I	4,54E-05	3/6	rs142266551
1549	<i>VTN</i>	c.A831C	p.K277N	3,01E-05	1/7	rs201356175
1678	<i>CIQB</i>	c.C562T	p.R188W	4,50E-05	5/7	rs772220643
1678	<i>CFHR2</i>	c.C631T	p.Q211X	8,55E-05	-	rs41299605
1678	<i>CFHR2</i>	c.C760T	p.R254X	9,23E-04	-	rs41313888
1678	<i>CPN1</i>	c.C73T	p.H25Y	0	5/7	rs373785594
1742	<i>FGL2</i>	c.T16G	p.W6G	NA	3/7	NA
1773	<i>CFHR4</i>	c.G847A	p.E283K	0	1/6	rs780015139
1773	<i>CFHR5</i>	c.C865G	p.H289D	0	4/6	rs777469135
1773	<i>C3AR1</i>	c.C1346T	p.S449F	7,34E-04	7/7	rs147364129
1837	<i>COLEC11</i>	c.G92A	p.R31H	1,05E-04	6/7	rs139694918

Table 15. List of variants obtained after filtering steps.

The likely deleterious *SERPINA1* (PS=5/7) variant, found in the patient #1218 in combination with two additional variants, is reported in Human Gene Mutation Database (HGMD) in association with antitrypsin alpha-1-deficiency disease. A rare variant in *F11* gene (PS=2/7) was found in the patient #1332, in combination with a likely deleterious variant in *MBTPS1* (encoding the Membrane-bound transcription factor site-1 protease. MAF: NA and PS = 4/7). The *F11* variant is common in the African population and has been previously reported in combined heterozygosity with additional *F11* variants in patients with Factor XI deficiency disease²⁰⁷.

Missense variants were found in the genes of *C3aR1* and *C5aR1*, encoding receptors of the pro-inflammatory anaphylatoxins C3a and C5a, respectively. Although an insertion

in *C3aRI* was also reported in aHUS⁴, the effect of these abnormalities in complement-mediated diseases requires further investigation. The patient with the *C5aRI* rare variant (#1149), also carries two additional missense variants in *CRI* and *KLKBI* genes, respectively. *CRI* gene encodes a complement receptor, highly expressed on podocytes, that acts as surface complement regulator. Plasma kallikrein (encoded by *KLKBI* gene) has been reported to be able to cleave the C3 and also Factor B contributing to complement activation²⁰⁸.

Rare functional variants in the *ITGAM* gene were found in two DDD patients. This gene encodes an integrin, physiologically expressed on endothelial glomerular cells and peritubular capillaries of Bowman's capsule. It acts as a surface receptor protein implicated in monocytes, macrophage, and granulocyte interactions²⁰⁹. It has been suggested that genetic variants in *ITGAM* may determine an increased expression of a defective molecule, causing a loss of clearance of glomerular deposits, with inflammatory process development²¹⁰. Genetic variants in *ITGAM* were reported in Systemic Lupus Erythematosus²⁰⁹. In one of the two DDD patients with *ITGAM* variants, I also found a likely deleterious rare variant in *C4BPA* gene (PS=5/7). Human C4b-binding protein (C4BP) is the main fluid phase regulator of classical pathway²¹¹ but it has also been reported to regulate the complement alternative pathway acting as a co-factor of factor I in the proteolytic inactivation of C3b²⁶. However until now rare genetic variants in C4BP were not reported in association with DDD.

Relatives of #633 and #1678 patients were available for genetic screening.

Patient #633, an 11-year-old girl, presented with hematuria and nephrotic syndrome¹⁷⁷. She had low C3 levels (7 mg/dl; normal range: 90-180 mg/dl), normal C4 and high SC5b-9 levels (1364 mg/dl; normal range < 303 mg/dl). She received a bioptic diagnosis of DDD. After 5 years of ineffective treatment with glucocorticoids, patient

was referred to our center and she was treated with ramipril and losartan but nephrotic syndrome persisted.

Since laboratory studies showed the presence of C3NeF, patient was infused with rituximab without any reduction of proteinuria. Her serum creatinine increased.

Low C5 (30%; normal range, 70 to 130) and high SC5b-9 levels (>1000 ng/ml; normal range < 303 ng/ml) and C5b-9 glomerular deposition suggested an activation of the terminal complement pathway. On the basis of these findings, the patient was treated with Eculizumab. After 48 weeks of treatment, serum creatinine decreased, proteinuria decreased below the nephrotic range and SC5b-9 normalized¹⁷⁷.

Genetic screening of *CFH*, *CFI* and *MCP* disclosed the homozygous *CFH* V62 and H402 common variants, previously reported to affect FH functions on AP regulation^{117, 118,212}.

Next generation sequencing using the CasCADE panel, revealed the presence of a rare variant in the *MASP2* gene (p.N539S; PS=1/7), encoding a protease involved in the lectin pathway activation, and a likely deleterious rare variant in *PTX3* (p.I192V; PS=7/7). Both variants were inherited from the unaffected mother who carried the homozygous *CFH* V62 but the H402 in heterozygosity, while the patient was homozygous for the latter variant (Fig.39). In 2008, Deban et al,²¹³ showed that long pentraxin (PTX3) interacts with Factor H, modulating the activation of the AP and suppressing injury-induced inflammation.

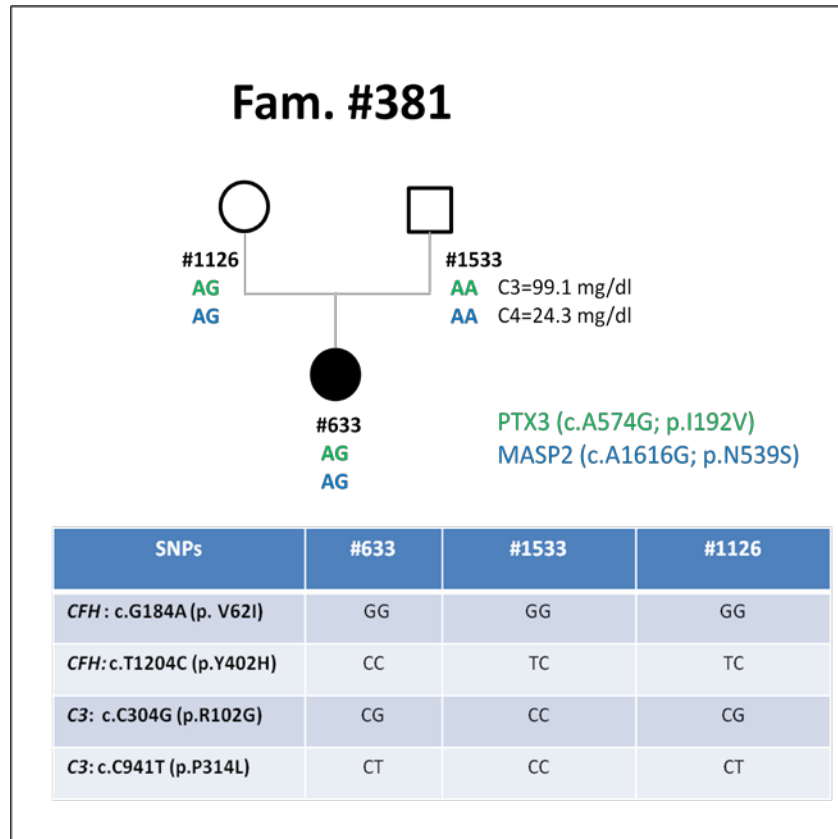


Figure 39. Pedigree #381. The proband (#633) inherited both rare variants from her mother (#1126). The only genetic difference between the proband and her mother is represented by the homozygous *CFH* SNP p.Y402H.

The patient #1678, a Caucasian female (Fig.40), presented at the age of 26 years with proteinuria (2g/day) and low C3 levels (C3=45 mg/dl; normal range: 90-180 mg/dl). Kidney biopsy showed DDD. She received 3 kidney grafts. The first and second grafts were lost due to disease recurrence. While on dialysis before the third transplant she had slight C3 reduction (72.5 mg/dl), normal C4 (23mg/dl; normal range: 10-40 mg/dl) and SC5b9 (269 ng/ml; normal range: normal levels \leq 303 ng/ml). C3NeF and anti-factor H (FH) autoantibodies were absent. Genetic screening using NGS diagnostic panel set up in our laboratory including 6 genes (*CFH*, *C3*, *MCP*, *CFI*, *CFB* and *THBD*) did not show any LPV. Targeted Sequencing using CasCADE identified two heterozygous stop codons in the *CFHR2* gene (p.Q211X and p.R254X), a likely deleterious variant in *CIQB* (PS=5/7), one of the genes that encodes for component C1q, and another

abnormality in the *CPNI* gene (PS= 5/7), encoding the catalytic subunit of carboxypeptidase N which is involved in the degradation of the anaphylatoxins C3a and C5a²¹⁴. The unaffected patient's sons, #2589 and #2171, inherited *CIQB* and *CPNI* variants, respectively, but not the two *CFHR2* nonsense variants (Fig.40).

In 2013 Eberhardt et al, showed that two molecules of FHR2 form homodimers through their N-term domains (SCR1 and SCR2) while the FHR2 C-term domains (SCR3-SCR4) can bind C3b although with a lower affinity than Factor H¹²⁷. In addition, SCR3 and SCR4 domains of FHR2 showed to have an inhibitory activity on C3 convertase while SCR1 and SCR2 inhibited the terminal complement pathway. They also reported that C3b and C3 convertases bound by FHR2 homodimers, were still accessible to complement regulation by FH (and FI in the case of C3 convertase). These data suggested that the combined FH and FHR2 binding to C3 convertase may ensure a fast and efficient control of complement hyperactivation. The p.R211X variant is located in the first portion of SCR4 and causes a premature protein truncation thus affecting cystein residues located in this domain (p.C241, C257, C267) and, consequently, protein folding.

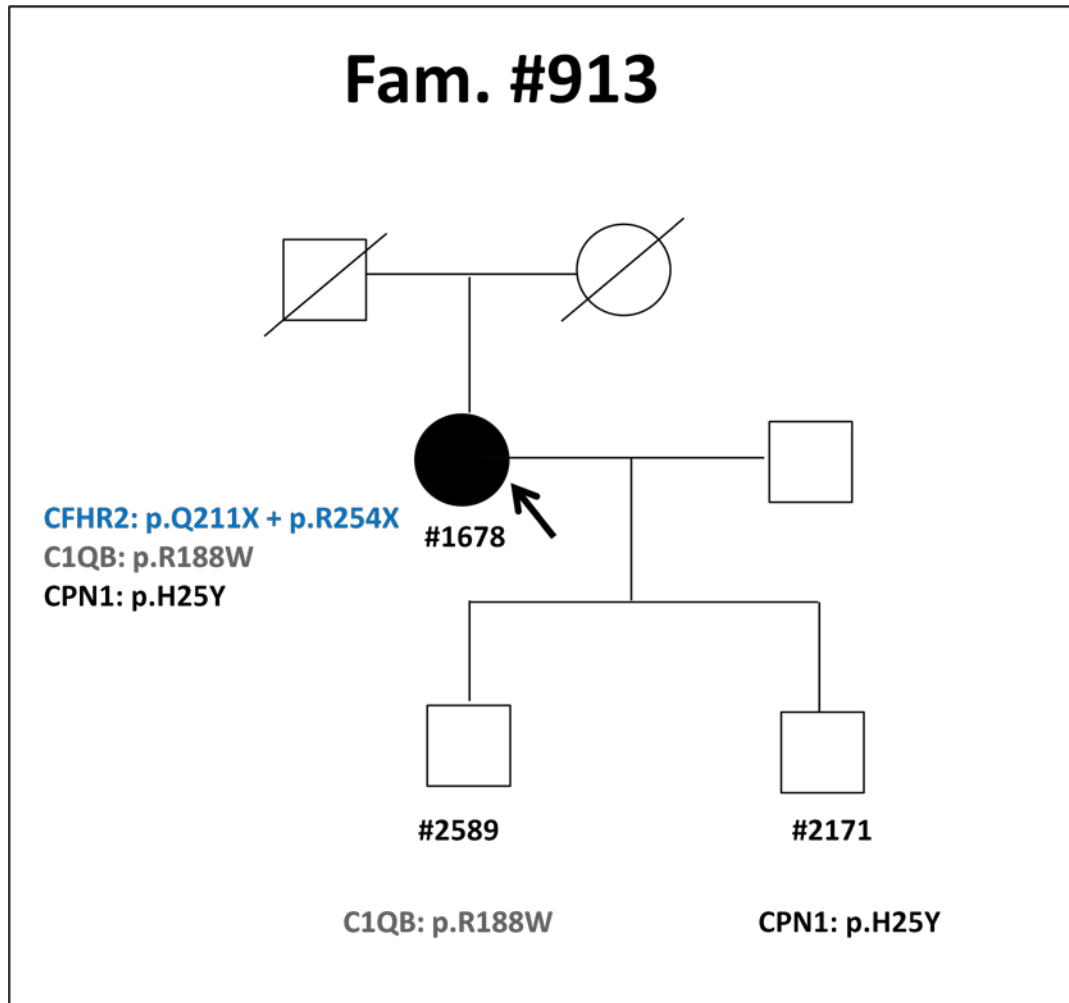


Figure 40. The proband carries two nonsense variants in *CFHR2* and two likely deleterious variants in *C1QB* and *CPN1*. Her sons did not inherit nonsense variants in *CFHR2*.

3.5 Discussion

A wide NGS panel (CasCADE) including 85 genes involved in complement and coagulation pathways, was used to study 17 DDD patients.

All variants were filtered by quality parameters, minor allele frequency and functional effects. The resulting variants ($n=25$) were analyzed by multiple predictor softwares to assign them a pathogenicity score (PS). Seventeen variants were considered likely deleterious because of a $PS \geq 4$ or nonsense variants.

Rare genetic variants in complement and coagulations genes were found in 70 % of patients ($n=12$) and all were heterozygous.

Sixty percent of variants ($n=15$) were found in complement regulator genes, including the already reported *CFH* variants (patient ID #1101 and #1549; see section 2.5.1.3) and those in *CFHR2* (patient ID #1678), *CFHR4* and *CFHR5* (both are present in patient #1773) genes.

Factor H-related proteins belong to the FH family composed by glycoproteins characterized by short consensus repeat (SCR) domains. FHR1, FHR2 and FHR5 are present in the plasma exclusively as dimers. Although their function is not completely clear, their involvement in the complement pathway has been reported.

FHR2 protein is a complement regulator that, through its C terminal domains (SCR3 and SCR4) binds C3b and inhibits the C3 convertase activity¹²⁷. The FHR2 nonsense variant (p.Q211X in SCR4) that I found in the patient #1678 by CasCADE and in another DDD patient by direct sequencing (see Chapter 4), creates a premature stop codon that leads to a early truncated protein. The resulting protein lacks 57 aminoacids, including three of the four cysteine residues involved in two disulfide bonds that are crucial for the proper folding of SCRs. On these basis, I hypothesize that the p.Q211X

variant may substantially alter the folding of the FHR2 protein resulting either in impaired protein secretion or complement regulatory activity.

FHR4 protein is reported to bind C3b and to form an active C3 convertase (FHR4-C3bBb) that is less sensitive to the decay mediated by Factor H compared to the normal C3Bb convertase. However, variant found in patient #1773 (PS=1/6), is located in the SCR5 domain, not involved in the C3b binding and its effect remains unknown.

FHR5 has been reported to co-localize with complexes derived from complement activation in human kidney diseases²¹⁵ and to bind the complement fragment C3b²¹⁶.

FHR5 has been reported to have a cofactor activity for factor I-mediated C3b cleavage and to inhibit the C3 convertase activity in fluid phase. However, non physiological concentrations were required for these activities¹²⁶. In addition, McRae et al reported that FHR5 binds C-reactive protein (CRP; belonging to the pentraxin family) and they hypothesized that CRP can recruit FHR5 to sites of tissue damage resulting in local complement inhibition¹²⁶. However the authors did not clarify the possible mechanisms by which CRP-FHR5 complexes could regulate complement.

More recent literature rather supports a complement activating function for FHR5. In 2010, Gale et al, described a mutation in *CFHR5* in Cypriot patients with glomerulonephritis, leading to the duplication of dimerization domains (SCR1 and SCR2). Functional studies on mutant FHR5₁₂₁₂ protein showed the generation of large multimeric complexes that strongly compete with FH to bind C3b, reducing cell surface protection from complement attack^{94,129}.

Furthermore, in 2015, Csinci et al, showed that physiological concentrations of FHR5 compete with FH to bind pentraxins CRP and PTX3 (long pentraxin), causing an enhanced complement activation²¹⁷.

Since the interaction site of FHR5 with PTX3 (as well as those with CRP) have been localized in SCR3-7 of the protein²¹⁷, I hypothesize that the p.H289D variant in SCR5

of FHR5 identified in the patient #1773, may act as a gain of function variant and increase the capability of FHR5 to compete with FH for CRP and PTX3 binding.

Due the complexity of FHR activities on the complement system, functional studies are needed to verify the effect of the above *CFHR* genetic variants on complement activation and disease pathogenesis.

A likely deleterious missense variant in *PTX3* gene, which causes the p.I192V amino acid change in the C terminal domain of the protein, was found in patient #633, combined with the common FH variant p.Y402H (located in SCR7 of the protein), previously associated with DDD. PTX3 is an acute phase protein involved in inflammation, innate immunity and female fertility²¹⁸. It also participates in complement classical pathway activation through its interaction with C1q²¹⁹⁻²²¹. It has been reported that glomerular cells produce PTX3²²². In addition, Deban et al²¹³ showed that the C-terminal pentraxin domain of PTX3 interacts with FH and can act as a nonactivating surface that anchors FH. They hypothesized that PTX3-bound FH at the site of tissue injury and inflammation regulates the activation of the complement AP, preventing the excessive inflammatory response following tissue injury. Since the p.I192V is located in the C terminal of PTX3, it is tempting to speculate that this variant may affect the interaction between PTX3 and FH. In addition, the FH H402 variant that is carried in homozygosity by patient #633, is known to reduce FH capability to bind glycosaminoglycans on cell surfaces and extracellular matrix¹¹⁷. I hypothesize that in this DDD patient, the PTX3 abnormality combined with the homozygous FH H402 variant concur to reduce the capability of FH to localize at glomerular level and exert complement regulation.

Besides abnormalities in known disease-associated complement genes and in PTX3, sequencing by CasCADE disclosed likely deleterious variants in complement genes not previously associated with C3G, like *ITGAM*, *C4BPA*, *C5aR1*, *C5aR2* and other genes.

These variants were all found in heterozygosity, and were always combined with one or two additional likely deleterious complement variants, thus it is difficult to establish their relative role in the pathogenesis of the disease.

I found only a rare variant (patient #1678) in genes of the classical pathway (p.R188W in C1QB), which is in accordance with normal serum C4 levels and the absence of immunoglobulins in the biopsy of patients with DDD.

Finally, only three variants were found in coagulation genes. This finding is consistent with clinical and histology data from patients with DDD from our cohort (see chapter 2) who did not show hematologic signs of thrombotic microangiopathy and their biopsies were negative for fibrinogen.

Altogether these data confirm an involvement of *CFH-CFHR* gene abnormalities in the predisposition to DDD and suggest the existence of variants in new complement genes that may represent potential risk factors. Genetic studies in other DDD cohorts and functional studies are required to clarify the role of the identified variants in disease pathogenesis.

4. ABNORMALITIES IN FH-FHR FAMILY

4.1 Introduction

The FH/FHR family is composed by a group of highly related proteins: factor H (FH), factor H-like (FHL-1), both deriving from different alternative splicing of *CFH*, and five complement factor H-related proteins (FHR1, FHR2, FHR3, FHR4 and FHR5). Factor H is abundant in the plasma and represents the main regulator of the complement alternative pathway, both in fluid and on cellular surfaces. Since FHRs are evolutionarily and structurally related to FH, it was expected that FHRs have similar complement inhibiting activities. Contrariwise, the FHR appear to promote the complement activation. However, the biological role of FHR proteins is not completely clear¹²⁹.

As described in Chapter 1, FHR proteins, each one composed by short consensus repeats (SCRs) of about 60 amino acids, have high sequence identity in their two N-terminal domains. In FHR1, FHR2 and FHR5 this identity constitutes a dimerization domain leading to generation of homodimers or heterodimers. This dimerization increases the FHR avidity for complement surface ligands and enables these proteins to efficiently compete with FH for ligand binding^{129,130}. The N-terminal domains of FHR3 and FHR4 (SCR1-3 of both) share high sequence similarity with FH SCR6 to SCR8 and FH SCR6-8-9, respectively, region involved in the binding to heparin, C-reactive protein and microbial surface ligands. Finally, the two C-terminal SCR domains of FHRs, are homologous to each other and also share an high sequence homology with the C-terminal SCR domains (SCR19-20) of FH (36-100%)¹²⁴. These similarities indicate that FHR proteins may bind similar surface ligands as FH. At variance, FHRs

do not show homology with complement regulatory domains of FH (SCR1-4), suggesting the absence of direct complement regulatory activity.

The chromosomal segment (1q32) including the six *CFH*, *CFHR1-5* genes is characterized by several large genomic repeat regions with high sequence similarity that predispose to genomic rearrangements, including deletions and duplications. The most frequent is the deletion of about 84kb resulting in the deficiency of *CFHR3* and *CFHR1* ($\Delta CFHR3-CFHR1$), which is found in normal population in heterozygosity with a frequency ranging from 2% to 51 %, depending on ethnicity, and is considered a polymorphism²²³. The homozygous $\Delta CFHR3-CFHR1$ has been associated with a lower risk of age-related macular degeneration (AMD)²²⁴ and IgA Nephropathy²²⁵ and a higher risk of aHUS²²⁶ and Systemic lupus erythematosus (SLE)²²⁷. A less common polymorphism is the deletion of *CFHR1* and *CFHR4* ($\Delta CFHR1-CFHR4$), also reported in aHUS patients²²⁶.

Genomic rearrangements in *CFHRs* have been reported in patients with C3 glomerulopathy^{94,130,132-135,136} (see Section 1.4.2). The majority of them result in duplication of the dimerization domains of FHRs leading to the generation of complexes that show a high avidity for surface ligands, thus reducing the FH capability to regulate complement activation.

The aims of this chapter are:

- to study *CFHR* copy number variations in an Italian cohort of patients with DDD, C3GN and also with IC-MPGN;
- to evaluate circulating levels and genetic and molecular patterns of FH/FHR proteins in a cohort of patients with DDD.

4.2 Methods

4.2.1 Patients

Patients with primary forms of IC-MPGN or C3G were recruited by the Italian Registry of MPGN and histologically classified as reported in Chapter 2. Patient #2026, with a secondary form of DDD (monoclonal gammopathy) was also included in the study of circulating levels and molecular pattern of FH/FHR proteins.

Biological samples from 54 healthy individuals were collected at Mario Negri Institute.

The study was approved by Ethics Committee of The Azienda Sanitaria Locale of Bergamo (Italy). All participants received detailed information on the purpose and design of the study, according to the guidelines of the Declaration of Helsinki.

4.2.2 Complement Minipanel and Genetic data analysis

CFH-CFHR genes were sequenced in 17 DDD patients using a wide NGS panel including 85 genes of complement and coagulation pathways (CasCADE; results reported in Chapter 3). To analyze 9 additional DDD patients, I used a new diagnostic NGS panel, recently developed in our laboratory, for the simultaneous sequencing of 15 complement genes (including six genes already included in the NGS minipanel described in chapter 2, and *CFHR1 to 5*, *C5*, *DGKE*, *ADAMTS13*, *MMACHC* genes). Library preparation, sequencing and data analysis were performed as reported in Chapter 2.

CFHR2 exons not fully covered by CasCADE and by the new NGS complement panel were analyzed by direct sequencing using primers reported in Table 16.

Exon	Left Primer (5'→3')	Right Primer (5'→3')
Exon 1	GTAGAGATGGGGTTTCACCAG	TGCAACTTAGAGGATGGAGAT
Exon 2	TGCTAGTCTTACACTCTGC	CTCCTCTGGTCACTGCT
Exon 3	AGTGCAGGGATTACCAGC	CTTAGACACAATTGGAAGTGAAG
Exon 4	GAATCATTTTCATTCAGCAC	AGCAGAATGCTTGTGTTGT
Exon 5	CATCCATTAAACATAGTACCTCAT	GGTTGTTACTTAGATTTGGTGAAGA

Table 16. Sequence primers used to analyze *CFHR2* gene.

4.2.3 Anti-FH Autoantibodies Assessment

The presence of autoantibodies anti-FH was evaluated by an Enzyme-Linked ImmunoSorbent Assay (ELISA). The original method is described by Dragon-Durey et al.²²⁸ but here a modified method was used. Nunc MaxiSorp ELISA plates (Nunc, Roskilde, Denmark) were coated with 0.1 µg of purified human FH (Calbiochem, Meudon, France) overnight at 4°C, washed with PBS, 0.2M NaCl and 0.1% Tween20, and blocked with PBS, 0.1% Tween20 and 0.3% milk for 1h at room temperature (RT). Diluted (1:100) patient plasma/serum samples were added and incubated for 40 minutes at RT, washed and incubated for 1 hour with goat anti-human IgG labelled with horseradish peroxidase (Sigma-Aldrich). After washing tetramethylbenzidine (TMB, Bethyl) substrate was used to reveal enzymatic activity. Two positive controls with 2000 and 1000 AU/ml titers at 1:100 dilution, kindly gifted by Dr. Dragon-Durey, were used as references. A standard curve was obtained by serial dilutions of reference positive plasma. All samples were tested in duplicate. The sample concentrations were determined by extrapolation of sigmoidal curve.

4.2.4 FH quantification

A homemade sandwich ELISA was developed in order to measure plasma or serum FH. Nunc MaxiSorp ELISA plates (Nunc, Roskilde, Denmark) were coated with 100 μ L of diluted sheep polyclonal anti-factor H antibody (dilution 1:6333; Abcam) and were incubated overnight at 4°C. The day after the plate was washed with PBS and 0.05% Tween20, and was blocked with PBS and 1% BSA for 1 hour at RT. After washing, 100 μ L of each diluted test and control samples and standard curve were added. Plasma/serum samples from patients and controls were diluted 1:10000 in PBS-BSA 1%. A standard curve was obtained by serial dilutions of purified human FH (Calbiochem, Meudon, France). The plate was incubated for 2 hours at RT and then was washed with PBS and 0.05% Tween20. 100 μ L of the mouse monoclonal anti human FH antibody (diluted 1:10000 in PBS-BSA 1%; LSBio), which specifically detects FH and FHL-1, was added to each well. After 2 hours of incubation at RT, wells were washed and 100 μ L of diluted goat anti-mouse IgG HRP conjugated (dilution 1:2000; Thermo Fischer Scientific) were added (1 hour of incubation at RT). After washing, tetramethylbenzidine (TMB, Bethyl) was used as substrate to reveal enzymatic activity. Enzymatic reaction was terminated using 100 μ L of sulphuric acid and the absorbance was read at 450 nm. All samples were tested in duplicate. The sample concentrations were determined by extrapolation of sigmoidal curve.

4.2.5 Copy Number Variations (CNVs)

Multiplex-ligation dependent probe amplification (SALSA MLPA; kit P236-A3) was used to search for rearrangements/deletions/duplications in the *CFH*, *CFHR3*, *CFHR1*, *CFHR2*, *CFHR5* genes. A subgroup of patients ($n=25$) were also analyzed for *CFHR4* CNVs.

CFHR4 copy number was measured by the use of a multiplex polymerase chain reaction (mPCR) that amplified the intron 1, the exon 2 of *CFHR4* and intron 3 of *CFHR1*, as reported by Moore et al²²⁶. This approach was also used to analyze 224 healthy controls. To analyze the uncovered regions of *CFHR4* and *CFHR5*, I designed new homemade probes (Table 17) that I set up using SALSA MLPA kit P300-B1.

The procedure of MLPA is the following:

After DNA denaturation, a mixture of MLPA probes was added to each sample, following the manufacturer's instructions. Each probe, consisting of two oligonucleotides that hybridize to immediately adjacent target sequences in order to be ligated into a single probe, has a unique amplicon length, ranging from 64 to 454 nucleotides. During the subsequent PCR reaction, all ligated probes were amplified simultaneously using the same PCR fluorescent prime pair. Fragment separation was done on the 48-capillary 3730 DNA Analyzer (Life Technologies), yielding a specific electropherogram. The height of each probe peak was subjected to an intrasample normalisation (comparison of each probe peak with peaks from reference probes) and intersample normalisation (comparison of previously normalized probe peaks with normalized probe from reference samples.)

Gene	Exon/Intron	Left Primer (5'→3')	Right Primer (5'→3')
<i>CFHR4</i>	Intron1	TACAACCATTTACAAGGCAA AGGAAGAGGCCTCAGAAGA ATGCAG	CCCTGTTGACAGCCACATCTCA AAGTATTAGCCTCCAGAA
<i>CFHR4</i>	Intron5	AACAGGAATGTTTCAGAGAC CTCAATTTGTTAATG	GACACAATGAGTCTTCAAGAAT GATATCCATTTATTG
<i>CFHR4</i>	Exon10	TTCGCATCTGGGGTATTCCA CTATGCCTTCCCT	ACACACTGCTTGAAATGATAGA ACTGATGTATTTCGATTATAT
<i>CFHR5</i>	Exon5	CACCTCCTCAACTCTCCAAT GGTGAAGTTAAG	GAGATAAGAAAAGAGGAATAT GGACACAATGAAGTAGTGG
<i>CFHR5</i>	Exon6*	GGATACATACCTGAACTCGA GTACGGTTATGTTTCAGCCGT CTGTC	CCTCCCTATCAACATGGAGTTT CAGTCGAGGTGAATTGC
<i>CFHR5</i>	Exon7	CGTTACAGATGTTTCAGACAT CTTCAGATACAG	GCACTCAGTCTGTATAAACGGG AAATGGA
<i>CFHR5</i>	Exon8*	GGGAACAATTCTGCCACCG CCACCTCAGATACCTAATG	CTCAGAATATGACAACCACAGT GAATTATCAGGATGG
<i>CFHR5</i>	Exon9*	CCCATTATCAGTATATCCTC CAGGGTCAACAGTGACGTA CCGTTGC	CAGTCCTTCTATAAACTCCAGG GCTCTGTAAGTGAACATGC
<i>CFHR5</i>	Exon10	GGATGCTGTTGAATTCCAGT GTAAATTCC	CACATAAAGCGATGATATCATC ACCACC

Table 17. Homemade MLPA probes hybridization sequences for *CFHR4* and *CFHR5*. * Sequence probes taken from Challis R. et al (2015)⁶.

4.2.6 Breakpoint Analyses

To identify the breakpoint region in a patient showing abnormal CNV in *CFHR3*-*CFHR4* genes, a long polymerase chain reaction was performed using a forward primer located in the intron 3 of *CFHR3* (5'GGAGAGTCTCCTAGATCTGCAC3') and a reverse primer designed in the exon 10 of *CFHR4* (5'CAGTTAAAAGGAAAAAGTGACAT3'). PCR was carried out in 25 ul of reaction volume using 125 ng of genomic DNA and the Accuprime Taq DNA Polymerase (Thermo Fisher Scientific; 35 cycles of amplification : 94°C for 30 seconds, 59°C for 30 seconds, 68°C for 10 minutes) according to the manufacture's protocol. The breakpoint region was identified by bidirectional sequencing of the long-range PCR product, using primers reported in Table 18 and BigDye® Terminator v3.1 Cycle Sequencing Kit

(Thermo Fisher Scientific) following the manufacturer's instructions. The BigDye XTerminator® Purification Kit (Thermo Fisher Scientific) was used to purify DNA sequencing reactions removing non-incorporated BigDye® terminators and salts. Sequencing analyses were carried out on the 48-capillary 3730 DNA Analyzer (Life Technologies).

The localization of the Alu-like repeat region was verified by PCR using 50 ng of genomic DNA, a forward primer within intron 5 of *CFHR3* (5'GAAGTATTTAGAGTTCAAAC-3') and a reverse primer within the Alu-like region (5'CTGCAGTCCGCAGTCCGGCCTG3') and Ampli Taq Gold DNA polymerase (Thermo Fisher Scientific; 35 cycles of amplification: 95°C for 45 seconds, 55°C for 30 seconds, 72°C for 35 seconds) according to the manufacture's protocol. Purified PCR products were sequenced and analyzed as reported above.

Gene	Exon/Intron	Primer sequences (5'→3')
<i>CFHR3</i>	Intron 3	GGAGAGTCTCCTAGATCTGCAC
<i>CFHR3</i>	Exon 4	GAAATTGAAAATGGATTCATTTC
<i>CFHR3</i>	Intron4	GCATGAGAGTATCAGCAAAATA
<i>CFHR3</i>	Intron 4	AGCTGCTTGTATTGCATTCCG
<i>CFHR3</i>	Intron 4	TTGAAAATGCAGATGTCTTCC
<i>CFHR3</i>	Intron 5	AGGCCGAGGCAGGCAGACCAT
<i>CFHR3</i>	Intron 5	CAAACCTATTAACCCTACTTGAAC
<i>CFHR3</i>	Intron 5	AGTCTTAAATTTGATTGACTGA
<i>CFHR3</i>	Intron 5	GAAGTATTTAGAGTTCAAAC
<i>CFHR4</i>	Intron 9	AGTCTCAAATTTGATTGAATGG
<i>CFHR4</i>	Intron 9	TAGGTATTAAGCCTAATT
<i>CFHR4</i>	Intron 9	CATACACCTCAATATCTGTCAA
<i>CFHR4</i>	Exon 10	ATGTCACCTTTTCCTTTTAACTG

Table 18. Sequence primers used to identify the breakpoint of the *CFHR3*₁₋₅-*CFHR4*₁₀.

4.2.7 Western-Blot

The molecular pattern of FH-FHRs was studied by Western Blot using serum/plasma (diluted 1:40 for FHRs and 1:80 for FH). Proteins were separated by 10-12% SDS-PAGE (Mini-Protean TGX Precast Gels, BioRad), under non reducing conditions, and transferred by electroblotting to a PVDF membrane (Trans-Blot[®] Turbo[™] Midi PVDF Transfer; Bio-Rad). The membranes were blocked in 4% skim milk and developed using FH/FHR antibodies (reported in Table 19) followed by horseradish peroxidase (HRP) conjugated secondary antibodies (Table 19) and ECL chemiluminescence detection system (Amersham).

Target protein	Primary antibody	Dilution	Secondary antibody
N-Term FHR1*	α FHR1 mAb (JHD)	1:1000	HRP goat anti-mouse IgG (dil 1:5000; Thermo Fisher, Ref 62-6520)
C-Term FHR2*	α FHR2 mAb (A72)	1:1000	HRP goat anti-mouse IgG (dil 1:5000; Thermo Fisher, Ref 62-6520)
FHR2 [°]	α FHR2 mAb(6F7)	1:300	HRP goat anti-mouse IgG (dil 1:5000; Thermo Fisher, Ref 62-6520)
FHR1-2-5 [°]	FHR1-2-5 mAb (2C6)	1:1000	HRP goat anti-mouse IgG (dil 1:5000; Thermo Fisher, Ref 62-6520)
FHR3*	α FHR3 pAs	1:2000	HRP Goat Anti-Rabbit IgG (dil 1:30000; Vector Laboratories)
FHR4*	α FHR4 pAs	1:3000	HRP Goat Anti-Rabbit IgG (dil 1:30000; Vector Laboratories)
FH	α FH mAb (OX-23; LS-C58560;LSBio)	1:3000	HRP goat anti-mouse IgG (dil 1:5000; Thermo Fisher, Ref 62-6520)

Table 19. List of antibodies used in Western Blot experiments.

*kindly given from Prof. Zipfel;

[°]kindly given from Prof. DeCordoba.

4.2.8 FHR quantitative Western Blot analysis

Quantitative variations in FHR molecular pattern were confirmed by a quantitative WB analysis of FHRs bands using FH band as reference standard. Each membrane was cut

in two parts; the upper part was incubated with the anti-FH Ab that detects a FH band at 155 kDa; the lower part was incubated either with an anti-FHR3 Ab (that detects bands at 35-56 kDa) or an anti-FHR4A revealing a 86 kDa band. Each protein band intensity was calculated by densitometry using ImageJ (NIH). For patients we calculated the FHR3/FH and/or the FHR4/FH band intensity Ratios and compared them with the median FHR3/FH or FHR4/FH Ratios in a set of 5 plasma control samples (with normal CNVs and normal FH levels) analyzed in the same experiment, taken as 100%.

4.2.9 AP convertase formation and C3 convertase decay.

Microtiter wells were coated with purified C3b (5µg/ml; Complement Technology) in PBS by overnight incubation at 4°C, blocked with 1% bovine serum albumin (BSA), 0.1% Tween20 in PBS for 1h at 37°C, and washed with a wash buffer (8.1 mM Na₂HPO₄, 1.8mM NaH₂PO₄, 0.1% Tween 20, 25mM NaCl) supplemented with 5mM MgCl₂. C3 [C3bBb(Mg²⁺)] and C5 [C3bBbC3b(Mg²⁺)] convertase complexes were assembled by incubating C3b-coated wells at 37°C for 30 minutes with 20% normal human serum (NHS; a pool obtained from 15 healthy volunteers) or serum from a patient with DDD and the *CFHR3*₁₋₅-*CFHR4*₁₀ hybrid or serum from her unaffected sons, diluted in PBS containing 5mM MgCl₂. After washes, the remaining C3 and C5 convertase complexes were detached from wells by incubation with 10 mM EDTA and 1% SDS for 1h at room temperature and analyzed by WB under reducing conditions (baseline). Convertase complexes were detected by Bb band (60kDa) with a goat anti-FB antibody (Quidel; dilution 1:10000; incubation over night at 4°C), followed by HRP-conjugated anti-goat antibody (Vector Laboratories; dilution 1:10000; 1h at room temperature) and ECL chemiluminescence detection system (Amersham). In additional wells, formed C3 and C5 convertase complexes were then allowed to dissociate for a

further 60 min at 25°C in the absence (spontaneous decay) or in the presence of FH (FH-mediated decay; 60 µg/ml; Calbiochem, Meudon, France). After washing, convertase complexes were detached and analyzed as described above.

4.2.10 Statistics

Analyses to calculate odds ratios (OR) and 95% CI were performed with the MedCalc software.

The control population used to calculate OR was represented by the 54 healthy Italian subjects recruited by the Italian Registry of MPGN and published data on healthy Italian population²²³ ($n=103$ total healthy controls).

4.3 Results

4.3.1 Copy number variations (CNVs)

4.3.1.1 Common CNVs

Among 185 patients (IC-MPGN=86; DDD=26; C3GN=73) analyzed by MLPA (kit P236-A3), copy number variations (CNVs) of *CFHR* genes were found in 32% of them. As shown in Fig. 41, the common heterozygous deletion of *CFHR3-CFHR1* (Het *CFHR3-CFHR1*Δ; frequency in Italian healthy population: 33%²²³) was found in all histology groups whilst the same deletion in homozygosity (Hom *CFHR3-CFHR1*Δ; frequency in Italian healthy population: 6%²²³) was found in patients with IC-MPGN ($n=3$) and in DDD ($n=3$) but not in patients with C3GN. No significant difference in the prevalence of the deletion was found between patients and controls (Table 20).

In one C3GN patient the heterozygous *CFHR3-CFHR1*Δ was found in combination with the known deletion of *CFHR1-CFHR4* (frequency in UK healthy population: 1.8%²²⁶).

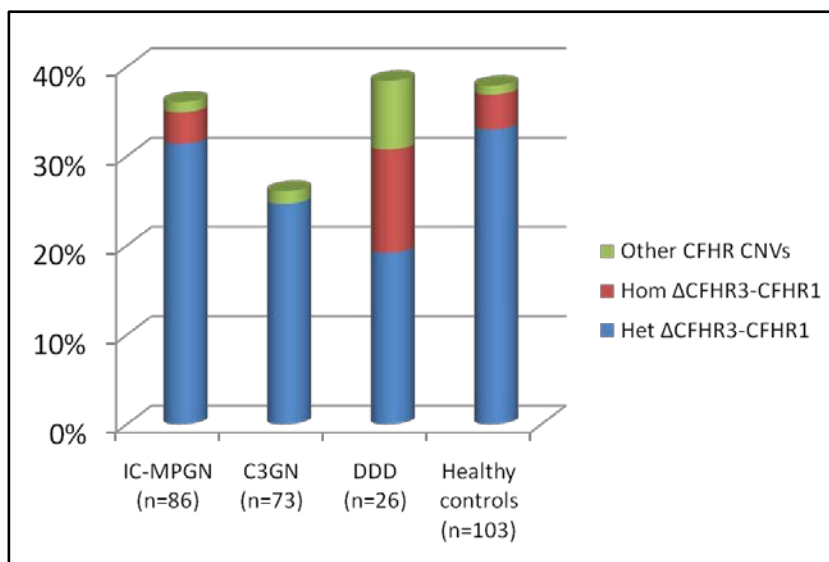


Figure 41. Histogram representing CNVs in the three histology groups.

	Δ Het <i>CFHR3-CFHR1</i>	OR	95% CI	<i>p</i> value
IC-MPGN <i>n</i> =86	27	0.93	0.50 - 1.71	0.81
DDD <i>n</i> =26	5	0.48	0.17 - 1.40	0.18
C3GN <i>n</i> =73	18	0.66	0.34 - 1.30	0.23
Ctrs <i>n</i> =103	34			
	Δ Hom <i>CFHR3-CFHR1</i>	OR	95% CI	<i>p</i> value
IC-MPGN <i>n</i> =86	3	0.89	0.19 - 4.11	0.89
DDD <i>n</i> =26	3	3.23	0.68 - 15.43	0.14
C3GN <i>n</i> =73	0	0.15	0.008 - 2.84	0.21
Ctrs <i>n</i> =103	4			
	Other <i>CFHR CNVs</i>	OR	95% CI	<i>p</i> value
IC-MPGN <i>n</i> =86	1	1.20	0.074 - 19.5	0.90
DDD <i>n</i> =26	2	8.50	0.74 - 97.66	0.09
C3GN <i>n</i> =73	1	1.41	0.09 - 23.02	0.81
Ctrs <i>n</i> =103	1			

Table 20. OR to carry common and uncommon copy number abnormalities in patients with IC-MPGN, DDD and C3GN vs. controls.

4.3.1.2 Uncommon CNVs in IC-MPGN and DDD

In one IC-MPGN patient (#1726; also carrying the homozygous *CFB* LPV p.R649W, section 2.5.1.3) and in one DDD patient (#1549; also carrying the heterozygous *CFH* LPV, p.R2I, section 2.5.1.3), MLPA analysis showed one copy of *CFHR3* while the other *CFHRs* showed normal copies. By a further analysis using homemade probes covering *CFHR4* and *CFHR5*, I found three copies of *CFHR4* in both patients (Fig.42). In detail, homemade probes on *CFHR4* located in the intron 1, the intron 5 and the exon 10 of *CFHR4* allowing to conclude that the duplication involved the entire *CFHR4* gene.

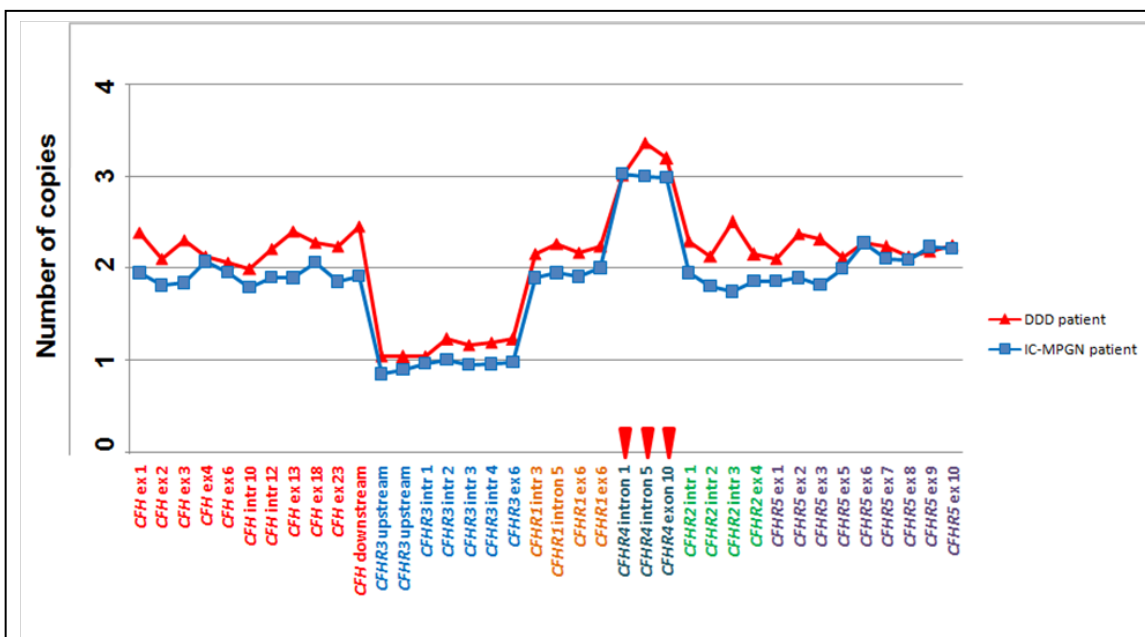


Figure 42. Results of MLPA showing in the DDD patient #1549 and in IC-MPGN patient #1726, the presence of one copy of *CFHR3*, two normal copies of *CFHR1* and three copies of *CFHR4* in both patients.

In Fig.43 is reported the pedigree (Family code #950) of the IC-MPGN patient (#1726) carrying the *CFB* variant and the *CFHR4* duplication. Copy number variations studies in healthy subjects of the family indicated that the IC-MPGN patient carries 0 copy of

CFHR3, a copy of *CFHR1* and two copies of *CFHR4* on the same allele (*CFHR4-R1-R4-R2-R5* allele). I speculate that this allele may derive from a double rearrangement implying *CFHR1-CFHR4* duplication and *CFHR3-CFHR1* deletion.

This allele is also present in other family members (Fig.43, III-5 and V-2) who also carry the *CFB* *lpv p.R679W* in heterozygosity.

I hypothesize that the DDD patient (#1549) with one copy of *CFHR3* and three copies of *CFHR4*, whose family members were not available, may have the same *CFHR4-R1-R4-R2-R5* allele.

Besides the patients #1549 and #2026, I did not find additional patients with a MLPA pattern that might suggest the presence of the *CFHR1-CFHR4* duplication. Two hundred twenty four healthy subjects were analyzed by mPCR (that amplifies the intron 1 and exon 2 of *CFHR4* and intron 3 of *CFHR1* genes), and nobody resulted with more than 2 copies of *CFHR4*.

However, the presence of *CFHR4-R1-R4-R2-R5* allele may be hidden in individuals who, by MLPA analysis, showed one copy of both *CFHR3* and *CFHR1* and normal *CFHR4* (compatible with the heterozygous *CFHR3-CFHR1Δ*). Indeed, this MLPA pattern may also theoretically apply to individuals who carry the *CFHR4-R1-R4-R2-R5* allele and the *CFHR1-CFHR4Δ* rare deletion (Fig.44) on the other allele, although the effect in term of gene copy number will appear be the same as in subjects with the heterozygous *CFHR3-CFHR1Δ*.

Identification of the *CFHR1-CFHR4dupl* breakpoint and further studies to easily recognize the *CFHR1-CFHR4dupl* and to estimate its frequency in healthy population and in patients are required.

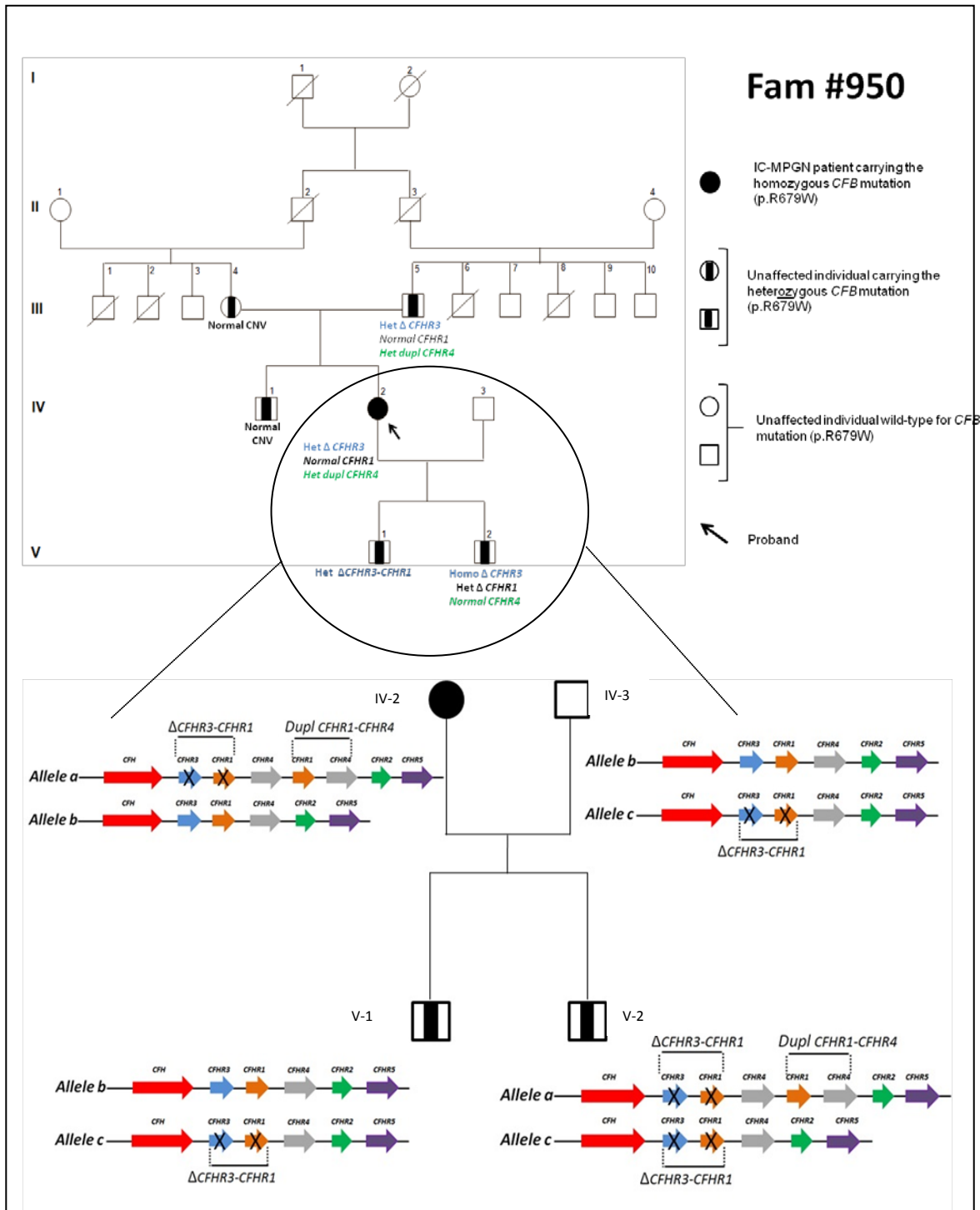


Figure 43. CNVs in the members of the family #950. The proband (IV-2; #1726) who also carries a homozygous *CFB* LPV (p.R679W), has the same MLPA pattern of her father (III-5) characterized by 1 copy of *CFHR3*, 2 copies of *CFHR1* and 3 copies of *CFHR4*. The patient's son (V-2) carries the heterozygous *CFHR4* duplication and also the homozygous deletion of *CFHR3* and the heterozygous deletion of *CFHR1*. Altogether these data suggest that the duplication involves both *CFHR1* and *CFHR4* and that a double rearrangement implying the *CFHR1*-*CFHR4* duplication and the *CFHR3*-*CFHR1* Δ may be occurred.

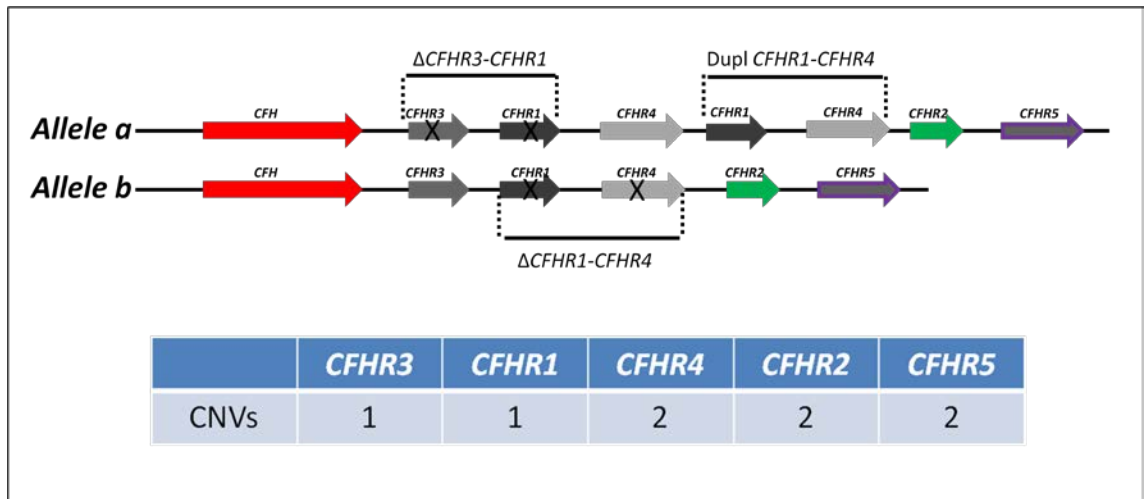


Figure 44. Schematic representation of the hypothesized condition with a *CFHR4-R1-R4-R2-R5* allele (allele a) and the allele with *CFHR1-CFHR4* Δ (allele b). The MLPA pattern is the same observed in individuals with the heterozygous *CFHR3-CFHR1* Δ .

4.3.1.3 CFHR abnormalities in a DDD patient

In one DDD patient (#1678) I found an uncommon deletion involving *CFHR3* and *CFHR1*.

Clinical history of the patient #1678 has been reported in section 3.4. Briefly, she received 3 kidney grafts. While on dialysis, before the third transplant, she had slight C3 reduction (72.5 mg/dl; normal range: 90-180 mg/dl) and normal C4 and SC5-b9 levels. C3NeF and anti-factor H (FH) autoantibodies were absent.

MLPA analysis was consistent with the absence of the *CFHR1* genes. There was also evidence of only one copy of the *CFHR3* gene. Notably, this single *CFHR3* gene lacked exon 6 (Fig.45). MLPA analysis of the unaffected patient's son (III-2; Fig.46) were consistent with one copy of *CFHR1*, one normal copy of *CFHR3* and one *CFHR3* gene missing exon 6 (Fig.45).

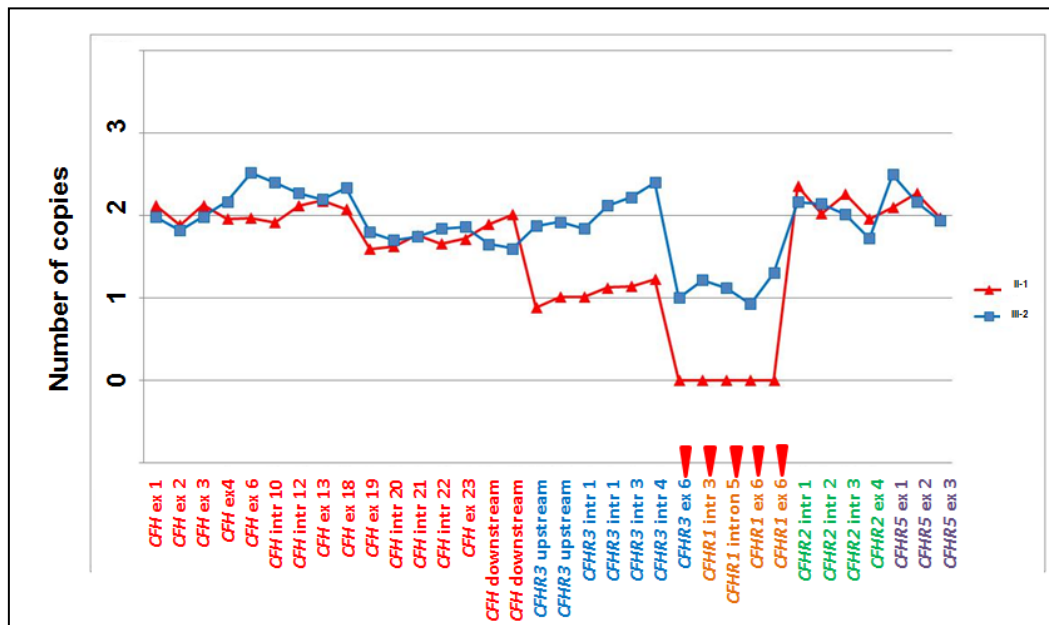


Figure 45. Results of MLPA showing the genomic deletion including *CFHR3*-exon 6 and the intron 3, intron 5 and exon 6 of *CFHR1*, found in patient #1678 (in red) and in her healthy son (in blue).

Genetic screening using the NGS diagnostic panel including 6 genes (*CFH*, *C3*, *MCP*, *CFI*, *CFB* and *THBD*) did not show any LPV. As previously reported (section 3.4), Targeted Sequencing using the wide CasCADE panel identified two heterozygous stop codons in the *CFHR2* gene (p.Q211X, Exac European MAF: 8,55E-05; p.R254X, Exac European MAF: 9,23E-04). The two *CFHR2* variants were not present in the unaffected patient's son (III-2; Fig. 46) suggesting that the two stop codons in the *CFHR2* gene were not on the allele carrying the exon 6-deleted *CFHR3* gene.

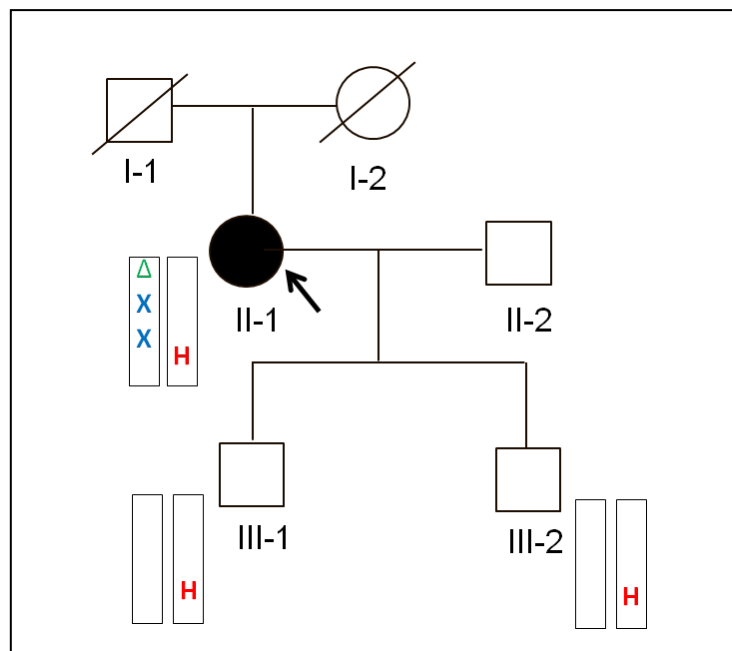


Figure 46 . Pedigree of family #913 with genetic abnormalities. The proband (II-1; #1678) is indicated by the arrow.
H = Hybrid gene *CFHR3-CFHR4*; **Δ** = Deletion *CFHR3-CFHR1*; **X** = *CFHR2* p.Q211X; *CFHR2* p.R254X.

To establish whether the exon 6 deletion in the *CFHR3* gene, also included the *CFHR4* gene, I performed a quantitative mPCR using primers located within intron 1 and exon 2 of *CFHR4* gene and intron 3 of the *CFHR1* gene²²⁶. Results showed that both patient (II-1) and the unaffected son (III-2) have only one copy of intron 1 and exon 2 of

CFHR4, indicating that the deletion also involves exon 1 and 2 of the *CFHR4* gene (Fig. 47).

Sequencing reads obtained by NGS with the CasCADE panel in the DNA from the patient (II-1; #1678) were aligned and quantified on the Integrative Genomics Viewer (IGV). There were no reads within exon 6 of the *CFHR3* gene and within the *CFHR1* gene. In comparison to controls carrying two copies of *CFHR3* and *CFHR4* genes, reads in the patient (II-1; #1678) were 50% of normal from exon 1 to exon 8 of *CFHR4* and normal (100 %) in exon 9 and exon 10 of the *CFHR4* gene.

Data obtained by MLPA, NGS and quantitative mPCR suggested that the patient (II-1; #1678) and her unaffected son (III-2; DNA code #2171), have an allele that contains a deletion of exon 6 of the *CFHR3* gene, deletion of the whole *CFHR1* gene and deletion of exons 1 to 8 of the *CFHR4* gene. This data would predict the presence of a hybrid gene consisting of *CFHR3* exons 1-5 and *CFHR4* exons 9/10 (Fig.48).

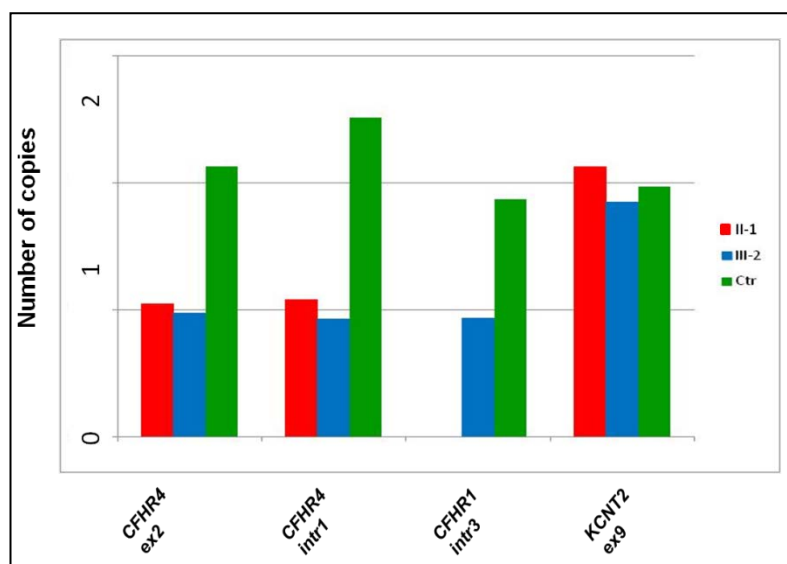


Figure 47. Results of the quantitative multiplex PCR.

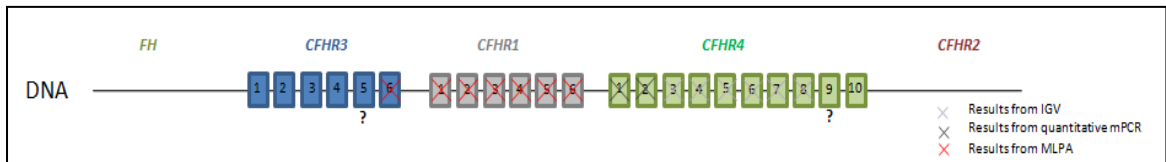


Figure 48. Graphic representation summarizing data obtained by MLPA, NGS and quantitative mPCR.

Since the sequence of exon 5 of the *CFHR3* and the sequence of exon 9 of *CFHR4* gene differ by only a single nucleotide (Fig.49a), I had to exclude that reads containing the sequence of exon 5 of the *CFHR3* gene had been mistakenly aligned to exon 9 of the *CFHR4* gene or *viceversa*. Sanger sequencing of exon 5 of the *CFHR3* gene in the patient identified three homozygous variants: c.721C>T; c.786A>T; c.796+22T>A. Among them, the variant c.721C>T (p.P241S) converts exon 5 of the *CFHR3* gene into exon 9 of the *CFHR4* gene (Fig.49a). However I excluded amplification of exon 9 of the *CFHR4* gene since primers used to amplify exon 5 of the *CFHR3* gene were specific for this exon since no amplification was obtained using DNA from individuals lacking *CFHR3* (samples homozygous for the $\Delta CFHR3$ -*CFHR1* alleles, Fig.49b).

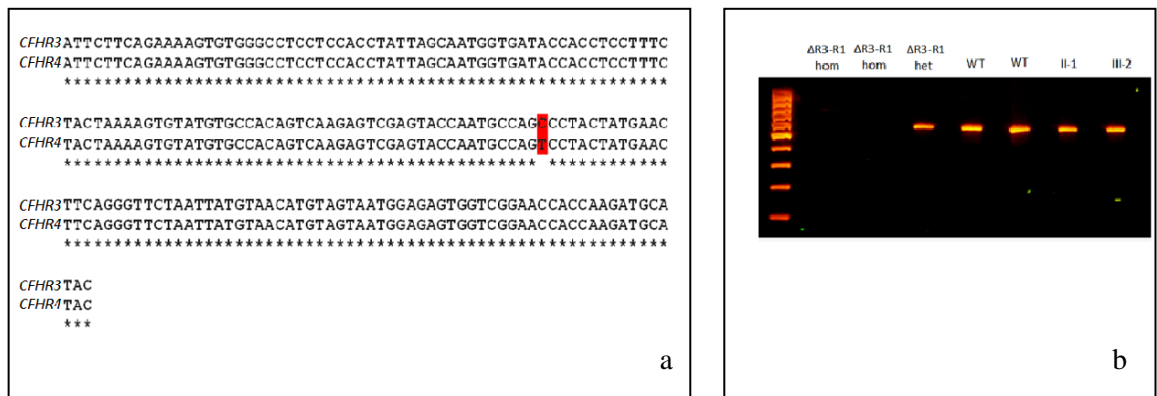


Figure 49. Panel a: DNA sequence alignment between exon5-*CFHR3* and exon 9-*CFHR4* that shows the high homology between the two exons. In red is indicated the only nucleotide that is different in the two sequences. Panel b: Agarose gel image that shows no amplification for DNA with the homozygous $\Delta CFHR3$ -*CFHR1* confirming the primer specificity .

Combined data from the above approaches revealed in the proband (II-1) the following: 1) *CFHR1*: zero copies; 2) *CFHR3*: one copy which lacks exon 6; 3) *CFHR4*: one normal copy and one copy lacking exons 1 to 8 or 9 (Fig.50). These results indicate the formation of a *CFHR3-CFHR4* hybrid gene that consisted of exon 1 to 5 of *CFHR3* and most likely exon 9 or 10 of *CFHR4*.

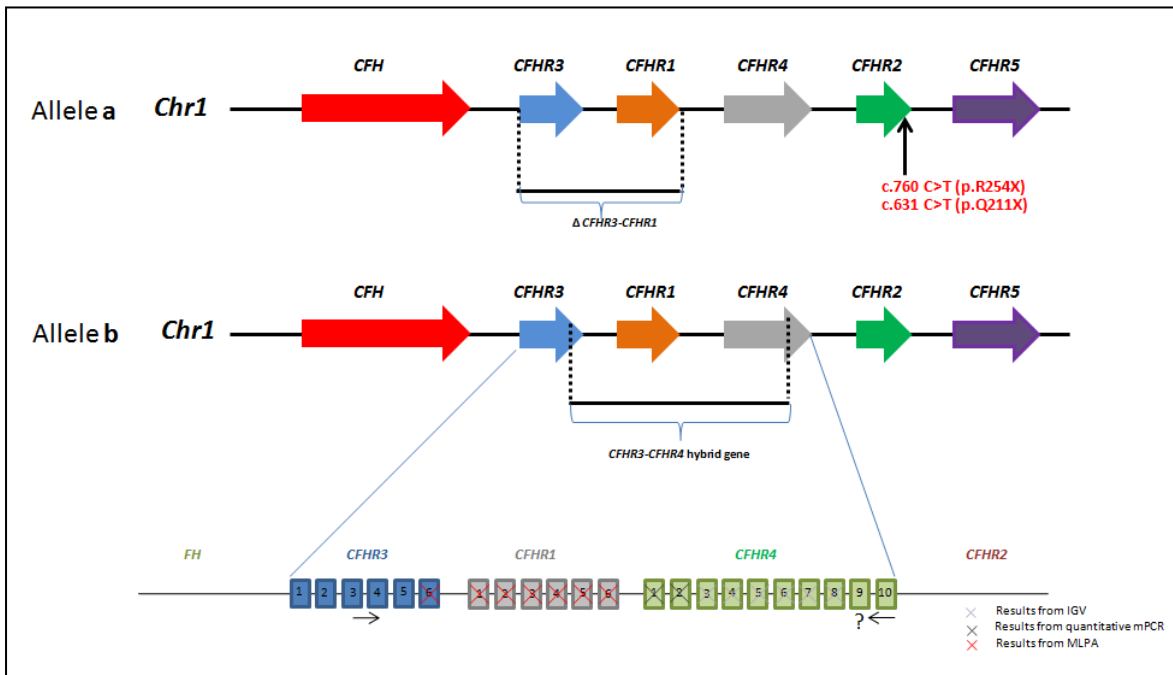


Figure 50. Graphic representation of the 2 alleles in the DDD patient. On one allele the patient carries the deletion of *CFHR3-CFHR1* ($\Delta CFHR3-CFHR1$) and the two *CFHR2* nonsense variants. On the other allele she carries the *CFHR3-CFHR4* hybrid gene.

To define the extent of the deletion and the breakpoint, genomic DNA was amplified using a forward primer specific for the intron 3 of the *CFHR3* gene together with a reverse primer located at the end of intron 9 of the *CFHR4* gene (Fig.51a). Sanger sequencing showed a deletion extending from exon 6 of the *CFHR3* gene to exon 9 of the *CFHR4* gene. The breakpoint region was located between chr1:196,760,556 in intron 5 of *CFHR3* and chr1: 196,886,396 in intron 9 of *CFHR4*. Unexpectedly, within the breakpoint area I also found an insertion of 305 bp (Fig. 51b). This sequence is not

present in the reference sequence of either intron 5 of *CFHR3* or intron 9 of *CFHR4*. However it is common in the genome. In particular, this sequence has a 100% of homology with two BAC clones (CH17-370K15 and CH17-86J21 on chromosome 1) and about 98-99 % of homology with several sequences scattered within the genome.

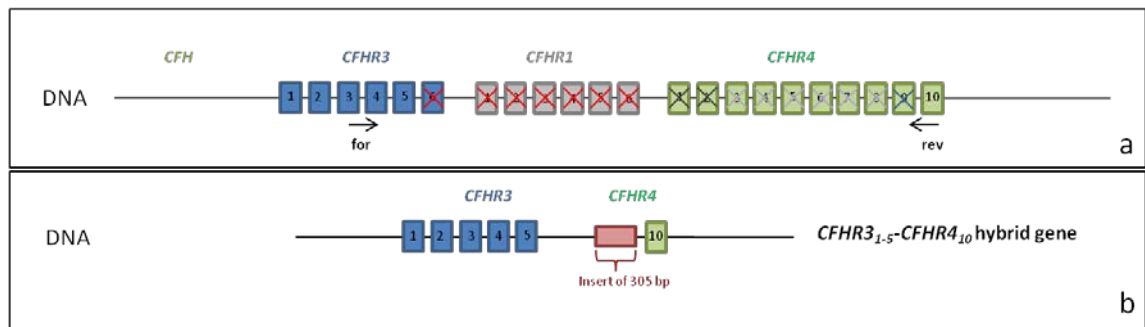


Figure 51. (a) Representation indicating the deleted exons in the *CFHR3*_{1.5}-*CFHR4*₁₀ hybrid gene. The arrows indicate primers used to amplify the *CFHR3*_{1.5}-*CFHR4*₁₀ hybrid gene. (b) The *CFHR3*_{1.5}-*CFHR4*₁₀ hybrid gene with the breakpoint region including the insertion of a 305bp sequence.

Analysis of the sequence of CH17-370K15, indicated that it included the sequence of *CFH*, *CFHR3* and *CFHR1* with only minimal differences from the reference sequence. The BAC clone sequence of intron 5 of the *CFHR3* gene showed minimal mismatches with the *CFHR3* gene reference sequence. The BAC sequence matched the first part of the *CFHR3* intron 5 sequence of *CFHR3*_{1.5}-*CFHR4*₁₀ hybrid gene. This included the insertion of 305 bp, which is not present in the *CFHR3* reference sequence. After the 305bp insertion, the sequence of the CH17-370K15- BAC clone continues with the last part of intron 5 of *CFHR3* gene and with exon 6 of *CFHR3* (Fig.52a). In contrast, after the 305bp insertion, the sequence of the *CFHR3*_{1.5}-*CFHR4*₁₀ hybrid gene continues with the intron 9 of the *CFHR4* gene.

The sequence of the 305 bp insertion looks similar (but with several mismatches) to the ones of two Alu repeats located in the first part of intron 5 of *CFHR3* and of intron 9 of *CFHR4* and in other introns of *CFHR* genes (Fig.52b). My hypothesis is that the 305

bp insertion may be present in intron 5 of normal controls and might predispose to rearrangements, similarly to previously reported effect of Alu repeats in other diseases²²⁹. By sequencing with specific primers, I detected the 305 bp insertion in 2 healthy controls who have normal copies of the genes across the *CFHR* region. Therefore, the Alu-like insertion is not restricted to individuals with the *CFHR3*₁₋₅-*CFHR4*₁₀ hybrid gene. The same PCR done in a subject homozygous for the Δ *CFHR3*-*CFHR1* did not give any product confirming that the Alu-like insertion is located in intron 5 of *CFHR3*.

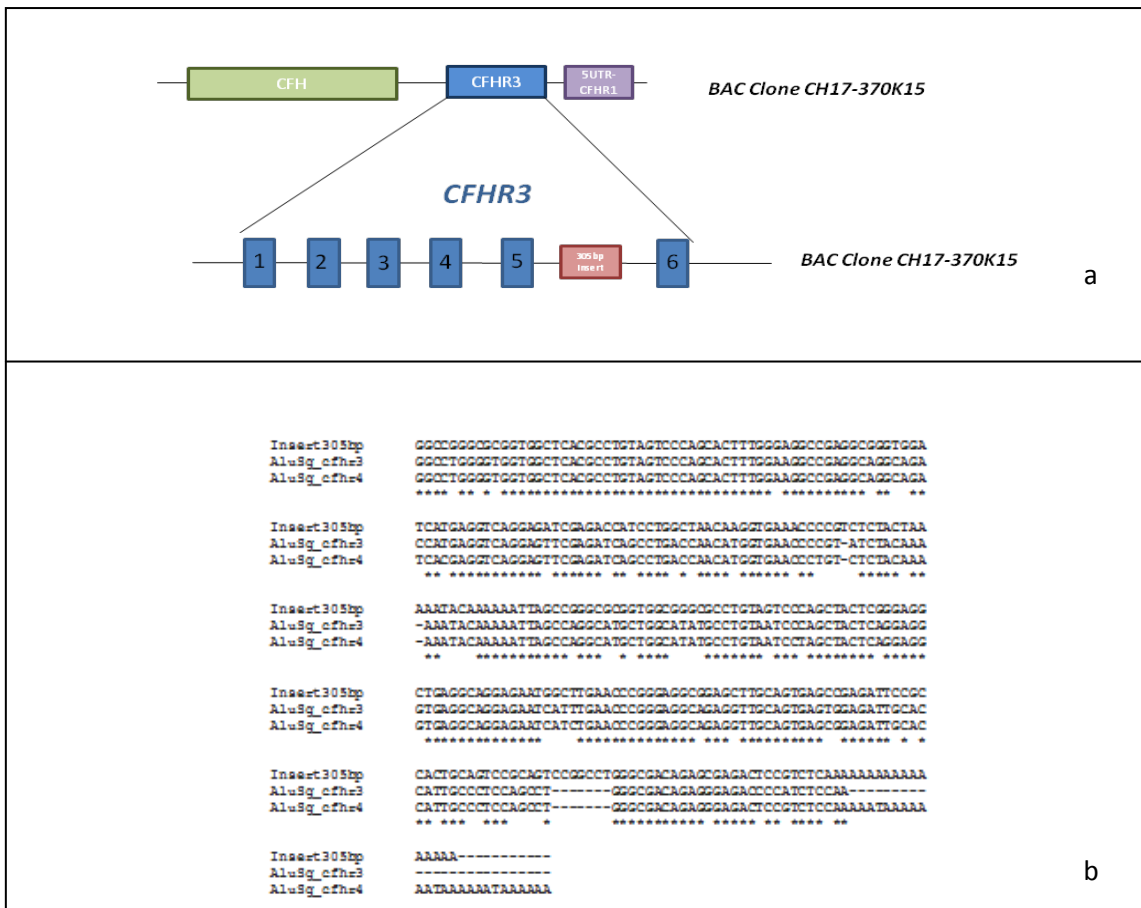


Figure 52. Representation of CH17-370K15- BAC clone (panel a) and its sequence alignment with Alu sequences located in intron5 of *CFHR3* and intron 9 of *CFHR4* (panel b).

Genetic studies in the other unaffected son of #1678 (Fig.46, III-1; DNA code #2589) subsequently recruited, revealed the presence of the *CFHR3*₁₋₅-*CFHR4*₁₀ hybrid gene

but no missense variant in *CFHR2*.

Among 290 patients with aHUS analyzed for CNVs by MLPA we identified four with the *CFHR3*₁₋₅-*CFHR4*₁₀ hybrid gene; three of them carries other complement abnormalities (Table 21) . The hybrid and breakpoint were confirmed by PCR and Sequencing.

In all the four aHUS patients and the control with the *CFHR3*₁₋₅-*CFHR4*₁₀ hybrid gene we found the presence of the 305bp insertion.

We genotyped all the carriers of the *CFHR3*₁₋₅-*CFHR4*₁₀ hybrid gene for a number of SNPs in *CFH*, *CFHR1* and *CFHR3* to establish the haplotype associated with the hybrid.

As shown in Table 21, in all carriers the *CFHR3*₁₋₅-*CFHR4*₁₀ hybrid gene was associated with the H3 haplotype.

Patient ID	CNVs	Haplotype	<i>CFH</i>	<i>CFH</i>	<i>CFH</i>	<i>CFH</i>	<i>CFH</i>	<i>CFH</i>	<i>CFHR3</i>	<i>CFHR3</i>	<i>CFHR3</i>	<i>CFHR1</i>	<i>CFHR1</i>	305bp Insertion	Notes
			c1-331C>T rs3753394	c.184G>A Val62Ile rs800292	c.1204T>C Tyr402His rs1061170	c.2016A>G Gln672Gln rs3753396	c.2237-543G>A rs1410996	c.2808G>T Glu936Asp rs1065489	c1-90A>C rs385390	c1-53C>A rs446868	<i>CFHR3</i> c.721C>T Pro241Ser rs13867543 3	c.906G>T Arg302Arg rs4230	c.942A>T Arg314Arg rs414628		
DDD patient (II-1)	hybrid <i>CFHR3</i> ₁₋₅ - <i>CFHR4</i> ₁₀ + <i>ΔCFHR3-CFHR1</i>	H4b	T	G	T	A	A	G	del	del	del	del	del	no	<i>CFHR2</i> : p.Q211X + p.R254X
		H3	T	G	T	G	G	T	C	A	T	del	del	yes	
Healthy DDD patient's son (III-2)	hybrid <i>CFHR3</i> ₁₋₅ - <i>CFHR4</i> ₁₀	H2	C	A	T	A	A	G	A	C	C	T	T	no	
		H3	T	G	T	G	G	T	C	A	T	del	del	yes	
UP003 (healthy subject)	hybrid <i>CFHR3</i> ₁₋₅ - <i>CFHR4</i> ₁₀	H3	T	G	T	G	G	T	C	A	T	del	del	yes	
		H3	T	G	T	G	G	T	C	A	T	T	T	no	
aHUS patient_1	hybrid <i>CFHR3</i> ₁₋₅ - <i>CFHR4</i> ₁₀	H3	T	G	T	G	G	T	C	A	T	del	del	yes	C3 : p.D1115H
		H7	T	G	T	A	G	G	A	C	C	G	A	no	
aHUS patient_2	hybrid <i>CFHR3</i> ₁₋₅ - <i>CFHR4</i> ₁₀	H3	T	G	T	G	G	T	C	A	T	del	del	yes	
		H1	C	G	C	A	G	G	A	C	C	G	A	no	
aHUS patient_3	hybrid <i>CFHR3</i> - <i>CFHR4</i> + <i>ΔCFHR3-CFHR1</i>	H3	T	G	T	G	G	T	C	A	T	del	del	yes	FH autoantibodies
		H4a	C	G	T	A	A	G	del	del	del	del	del	no	
aHUS patient_4	hybrid <i>CFHR3</i> ₁₋₅ - <i>CFHR4</i> ₁₀	H3	T	G	T	G	G	T	C	A	T	del	del	yes	C3 : p.I167F + p.L1434M
		H1	C	G	C	A	G	G	A	C	C	G	A	no	

Table 21. List of subjects carrying the *CFHR3*₁₋₅-*CFHR4*₁₀ hybrid gene and the corresponding haplotype in the region of *CFH*-*CFHR3*. Some of them also carry additional complement abnormalities (see Notes).

We also analyzed 224 healthy controls and found one carrier of the *CFHR3*₁₋₅-*CFHR4*₁₀ hybrid gene. This was rather unexpected since in the published description of the rare *CFHR1*-*CFHR4* deletion (detected in 9/503 controls), the *CFHR3* gene was intact in all subjects that carried this deletion, which would exclude the presence of carriers of the *CFHR3*₁₋₅-*CFHR4*₁₀ hybrid gene in this large control cohort²²⁶.

4.3.2 The FHR3₁₋₄-FHR4₉ hybrid protein

4.3.2.1 Protein studies on a DDD patient with multiple FHR abnormalities.

To understand the effect of *CFHR3*₁₋₅-*CFHR4*₁₀ hybrid gene and the nonsense *CFHR2* likely deleterious variants at protein level, we performed Western blot (WB) experiments by using a panel of antibodies against FHR proteins with the serum of the patient (Fig.46; II-1; #1678), her unaffected son (III-2; Fig.46) carrying the *CFHR3*₁₋₅-*CFHR4*₁₀ hybrid gene but not the two nonsense *CFHR2* variants, an healthy subject with two copies of *CFHR3*-*CFHR1* (CTR038) and a DDD patient (#1135) with the homozygous *CFHR3*-*CFHR1* deletion.

WB experiments by using a monoclonal anti-human Factor H-Related 1 (FHR1) antibody, in non reducing conditions, confirmed that the DDD_{*CFHR3*₁₋₅-*CFHR4*₁₀} patient has a total deficiency of FHR1 (Fig.53).

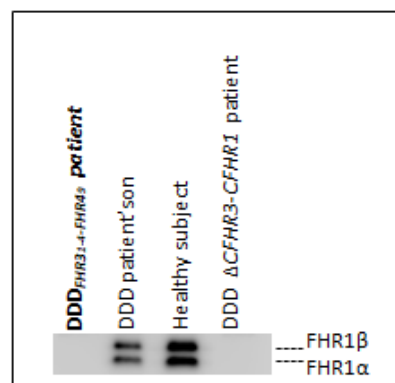


Figure 53. Western blot analysis of FHR1 confirmed the total FHR1 deficiency in the DDD_{*CFHR3*₁₋₅-*CFHR4*₁₀} patient. In the DDD patient's son the FHR1 bands appeared slightly weaker than in the healthy subject with normal CNVs. DDDΔ_{*CFHR3*-*CFHR1*} patient carries the homozygous Δ_{*CFHR3*-*CFHR1*} and represents the negative control.

Since the $DDD_{CFHR31-5-CFHR410}$ patient carries two stop codons (p.Q211X and p.R254X) in one copy of *CFHR2* gene, we expected to find a different FHR2 pattern on WB in comparison to the healthy control. However, using a monoclonal anti-human C-terminal FHR2 antibody (A72), the WB membrane showed similar FHR2 bands and intensity between the patient and the control (Fig.54a). WB using a different monoclonal FHR2 antibody (6F7; Fig.54b) and an anti-human FHR1-FHR2-FHR5 antibody (2C6; Fig.54c), displayed FHR2 bands that appeared slightly weaker in the $DDD_{CFHR31-5-CFHR410}$ patient than in the healthy subject.

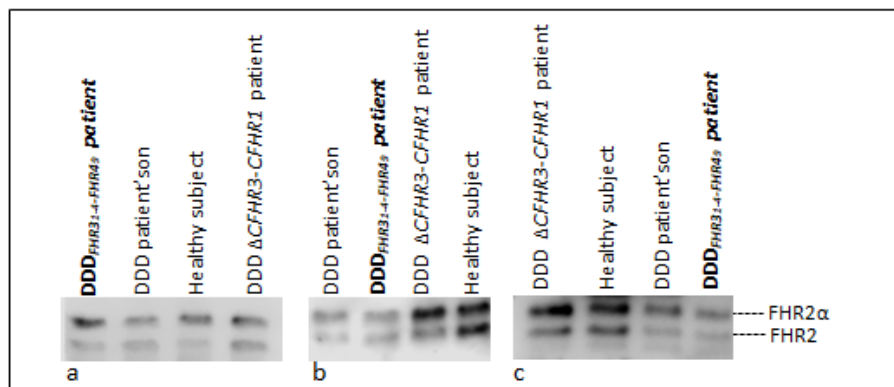


Figure 54. Western blot analysis of FHR2 using anti-human C-terminal FHR2 antibody (panel a), monoclonal FHR2 antibody (6F7; panel b) and an anti-human FHR1-FHR2-FHR5 antibody (2C6; panel c).

WB by using a polyclonal anti-human FHR3 antibody (Fig.55) showed 3 bands in the $DDD_{CFHR31-5-CFHR410}$ patient, corresponding to the different glycosylated variants of FHR3. These bands were absent in the negative control homozygous for the *CFHR3-CFHR1* deletion and notably were more intense in the $DDD_{CFHR31-5-CFHR410}$ patient than in the healthy subject. Since the $DDD_{CFHR31-5-CFHR410}$ patient carries the deletion of *CFHR3-CFHR1* on one allele and the *CFHR3₁₋₅-CFHR4₁₀* hybrid gene on the other allele, the only *CFHR3* copy is the one involved in the hybrid gene. Thus the finding of specific FHR3 bands on WB indicates that the FHR3₁₋₄-FHR4₉ hybrid protein, which is

predicted to have a molecular weight and migration pattern almost identical to FHR3, is well secreted in the serum of the $DDD_{CFHR31-5-CFHR410}$ patient.

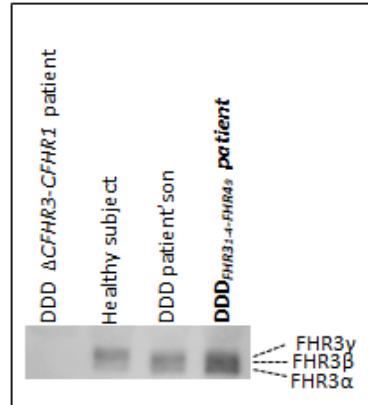


Figure 55. Western blot analysis of FHR3 showing that FHR3₁₋₄-FHR4₉ hybrid protein is secreted in the serum of the $DDD_{CFHR31-5-CFHR410}$ patient.

WB by using the polyclonal anti-human FHR4 antibody (Fig.56) showed a FHR4A band of similar molecular weight and intensity in the $DDD_{CFHR31-5-CFHR410}$ patient as compared to the healthy subject. Instead, in the unaffected patient's son the FHR4A band is weaker compared to the other samples, even though he has the same *CFHR4* copy number as the $DDD_{CFHR31-5-CFHR410}$ mother.

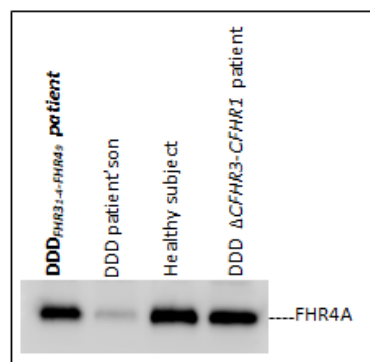


Figure 56. Western blot analysis of FHR4.

4.3.2.2 *Effect of DDD_{CFHR31-5-CFHR410} patient serum on C3 and C5 convertase formation and C3 convertase decay.*

To understand whether the FHR3₁₋₄-FHR4₉ hybrid protein alone (present in the plasma of the DDD_{CFHR31-5-CFHR410} patient as well as in her unaffected sons) or its combination with the *FHR2* abnormalities (present only in the DDD_{CFHR31-5-CFHR410} patient) could affect the formation and decay of the alternative pathway C3 and C5 convertase complexes, C3b- coated wells were incubated with NHS or DDD_{CFHR31-5-CFHR410} patient serum or serum from her unaffected sons. C3 [C3bBb(Mg²⁺)] and C5 [C3bBbC3b(Mg²⁺)] convertase complexes, remaining on the wells after decay with buffer alone or added with FH (60 µg/ml), were analyzed by WB and the Bb was detected. As reported in Fig.57, Bb bands corresponding to the spontaneous decay were slightly more intense in the wells added with serum from DDD_{CFHR31-5-CFHR410} patient (Fig.57a, lane 5; Fig.57b, lane 5) and from her healthy sons (III-1: Fig.57a, lane 8; III-2: Fig.57b, lane 8) in comparison wells incubated with NHS (Fig.57a, lane 2; Fig.57b, lane 2). A weak C3/C5 convertase stabilization was also detected in the condition of FH-mediated decay in the well with serum from the DDD_{CFHR31-5-CFHR410} patient (Fig.57a, lane 6; Fig.57b, lane 6) and from her sons (III-1: Fig.57a, lane 9; III-2: Fig.57b, lane 9) compared to NHS (Fig.57a, lane 3; Fig.57b, lane 3).

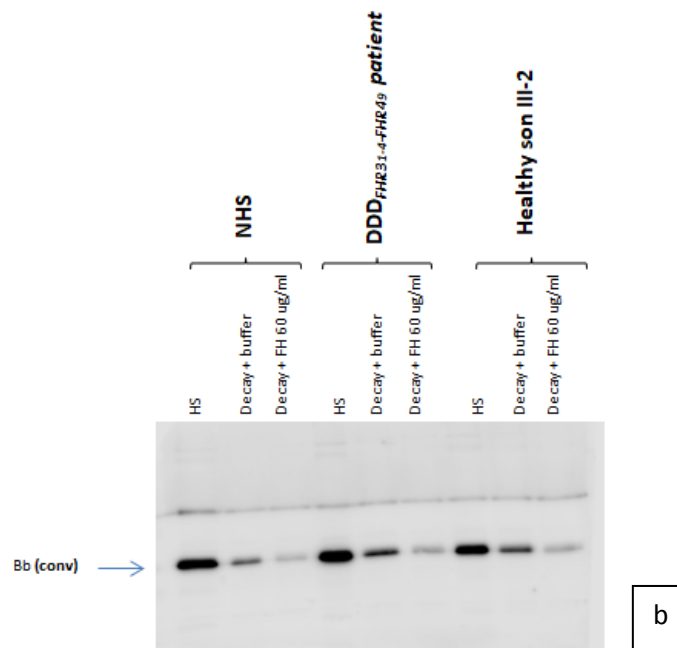
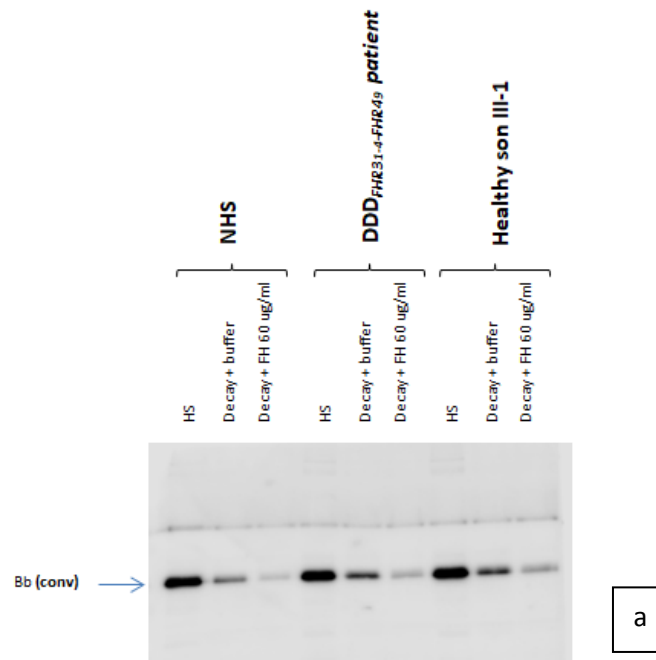


Figure 57. Microtiter wells coated with C3b, were incubated with NHS or DDD_{CFHR31-5-CFHR410} patient serum or serum from her unaffected sons (III-1, panel a; III-2, panel b). Spontaneous (decay +buffer; panel a: lanes 2, 5, 8) and FH-mediated decay (Decay+FH 60ug/ml; lanes 3, 6, 9) were tested. C3/C5 convertase formation was detected as Bb band (60 kDa).

4.3.2.3 Future studies

- Mass spectrometry studies have been planned to verify the exact FHR₃₁₋₄-FHR₄₉ hybrid protein sequence in the DDD patient.
- To confirm the convertase stabilizing properties of the serum from carriers of the FHR₃₁₋₄-FHR₄₉ hybrid protein and establish whether the convertase stabilization described above includes C3 convertase or C5 convertase or both, the assay with 20% of serum on C3b-coated wells, will be repeated to analyze: 1) C3 convertase formation and decay by detection of C3b β -chain (75 kDa) and Bb (60 kDa) bands on WB at baseline and after different times of spontaneous and FH-mediated decay; 2) C5 convertase activity by detection of C5b α' -chain (104 kDa) band on WB; 3) the terminal complement C5b-9 complex formation by detection of C6 (105 kDa) and C9 (66 kDa) bands on WB; 4) Binding of FHRs proteins to C3b by detection of corresponding bands on WB.
- Serum samples from the DDD patient with the *CFHR3*₁₋₅-*CFHR4*₁₀ hybrid on one allele and the *CFHR3*-*CFHR1* deletion on the other allele will be used for FHR₃₁₋₄-FHR₄₉ hybrid protein purification and functional studies since this patient lacks normal FHR3 and is predicted to carry only the hybrid copy of FHR₃₁₋₄-FHR₄₉.

4.3.3 Likely pathogenic variants across CFH-CFHR gene cluster in DDD patients.

In 17 DDD patients we sequenced *CFHR* genes using a wide NGS panel including 85 genes of complement and coagulation pathways (CasCADE; results reported in Chapter 3). In addition, we used a new diagnostic NGS panel for the simultaneous sequencing of 15 complement genes, recently developed in our laboratory, to analyze 9 additional DDD patients. Sequencing data showed the presence of two likely pathogenetic variants in *CFHR4* (p.E283K) and *CFHR5* (p.H289D) in the patient #1773 (See section 3.4). A rare variant in *CFHR5*, tolerated by prediction softwares and with PHRED CADD score of 0.001 (p.I222T; ExAC MAF All: 4.9×10^{-5} ; Polyphen/Sift: benign/Tolerated), has been found in the patient #2162. Less rare variants, but with a deleterious software prediction, are the heterozygous variants identified in the patient #1742 (*CFHR2*: p.Y264C; ExAC MAF All: 0.014; Polyphen/Sift: probably damaging/deleterious; PHRED CADD score: 23.2) and in the patient #2507 (*CFHR4*: p.Q142L; ExAC MAF All: 0.002; Polyphen/Sift: probably damaging/tolerated; PHRED CADD score: 10.19). Since *CFHR2* is not fully covered by the CasCADE and the new NGS complement panel, I also performed direct sequencing of the *CFHR2* gene in 25 patients with DDD and found another patient (#1286) with the same p.Q211X and p.R254X nonsense variants as the index patient #1678 previously described (Section 3.4 and 4.3.1.3). The newly identified patient carries the *CFHR3/CFHR1* deletion in homozygosity and, at variance with the index case, does not carry the *CFHR3/R4* hybrid gene. Plasma/serum samples from this patient were not available to analyze FHR pattern on WB.

4.3.4 Circulating levels and molecular pattern of FH/FHR proteins in a cohort of DDD patients.

Factor H levels were measured in 22 DDD patients (whose plasma or serum was available). Only one patient (DNA code #1149; negative for *CFH* likely pathogenic variants) showed a slightly decreased level of FH (160 mg/L; normal range: 173-507 mg/L). All remaining patients showed normal FH levels ranging from 179 mg/L to 357 mg/L.

ELISA to detect circulating anti-FH autoantibodies in 23 DDD patients showed a high titer (451 AU/ml) in a patient (DNA code#1837) who carries the homozygous *CFHR3-CFHR1* deletion. This patient was also positive for C3NeF.

The molecular pattern of circulating FH/FHR proteins in our cohort of DDD patients was studied by WB experiments.

FHR1

FHR1 circulates in plasma in two glycosylated forms: FHR1 α at 37kDa and FHR1 β at 43 kDa. Results of WB analysis in 24 DDD patients (each identified by the specific DNA code) are reported in Fig. 58.

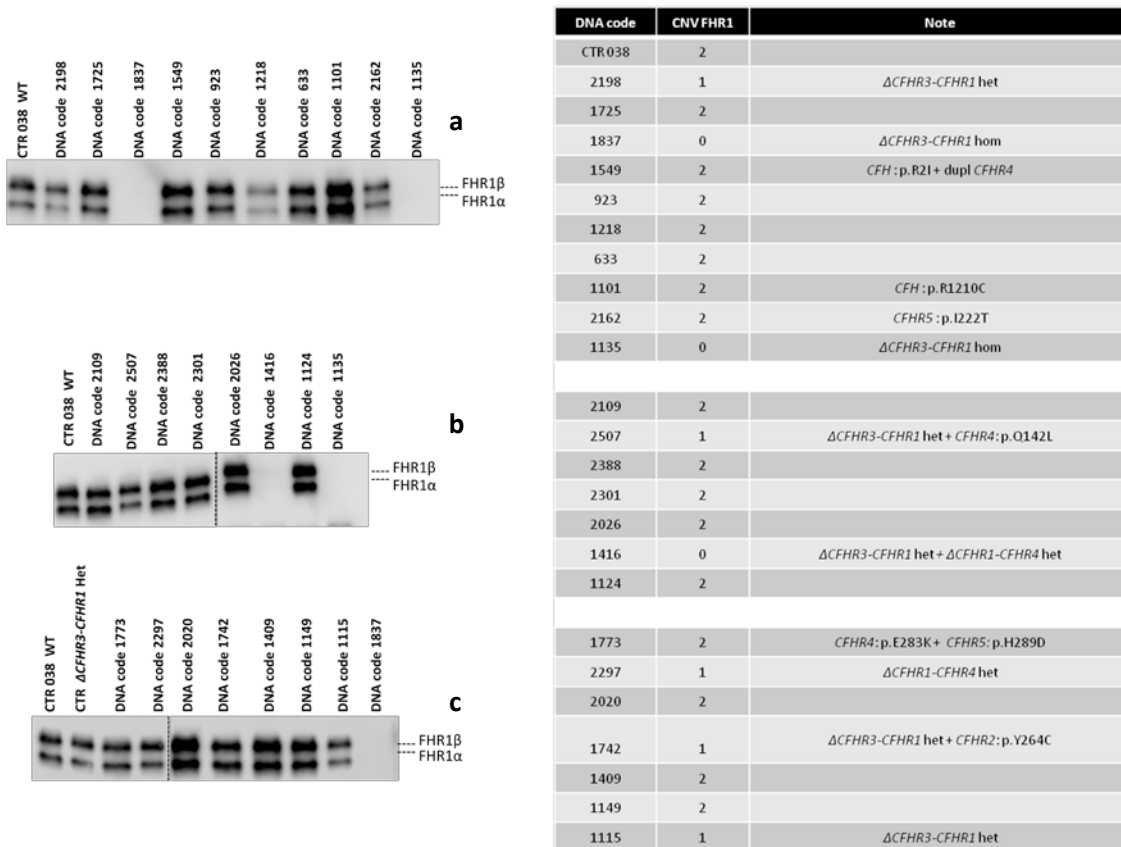


Figure 58. Western blot analysis of FHR1 and table resuming *CFHR1* copy number.

WB results confirmed the total absence of FHR1 in all patients with the homozygous deletion of *CFHR1* (Fig.58; #1837, panel a, lane 4; #1135, panel a, lane 11; #1416, panel b, lane 7). Bands weaker than in the wt CTR 038 (with 2 copies of *CFHR1*), were evident in those patients with the heterozygous deletion of *CFHR1* but notably also in samples from patients with DNA codes #1218 (Fig.58, panel a, lane 7) and #2162 (Fig.58, panel a, lane 10) who have normal *CFHR1* copies. In samples from patients

with DNA codes #1101 and #2020 (with 2 copies of *CFHRI*) FHR1 bands were stronger than in the control and in the other DDD patients with normal *CFHRI* copies. An abnormal band with an apparent molecular weight around 45kDa was evident in the patient #1742 (Fig.59, lane 7). The band was not present in healthy controls (Fig.59).

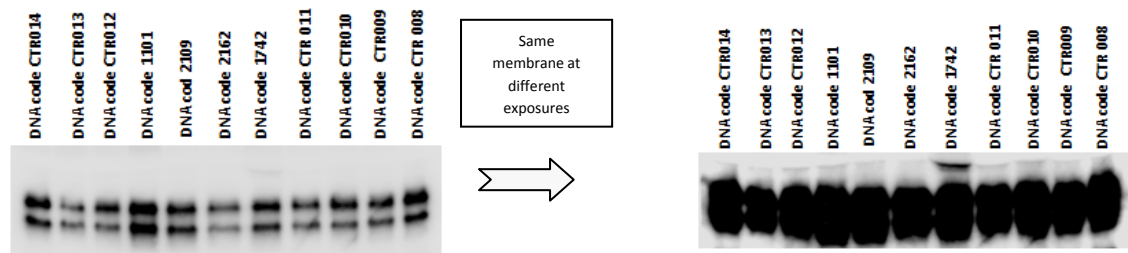


Figure 59. The same membrane exposed for two different times to underline the abnormal band detected in patient #1742. All samples indicated with “DNA code CTR” are healthy controls with normal CNVs.

FHR2

FHR2 has two glycosylated forms, FHR2 (at 24KDa) and FHR2 α (at 28KDa). Results of WB analysis in 24 DDD patients are reported in Fig.60. Although the intensity of the two FHR2 bands on WB was very variable among plasma's patients, we did not observe any abnormal band.

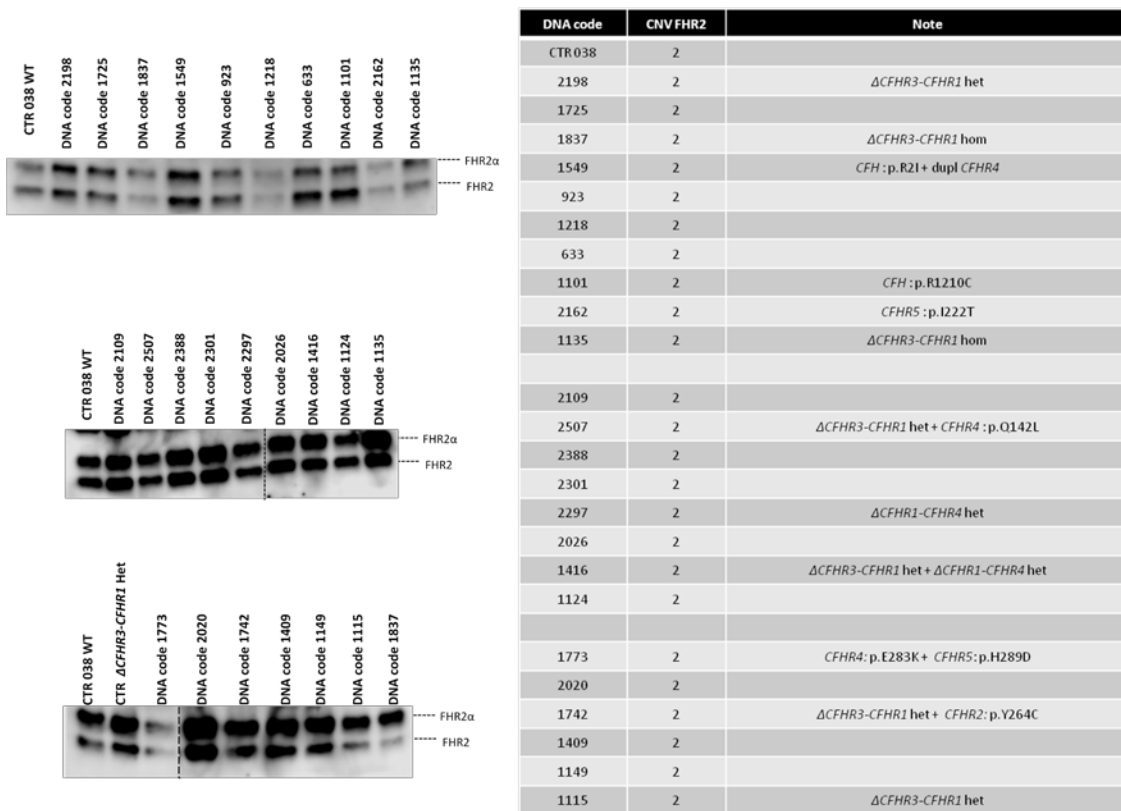
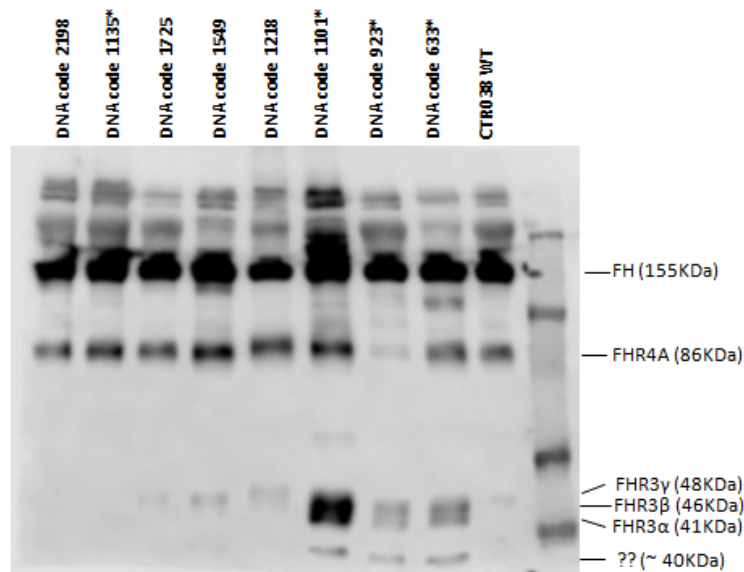


Figure 60. Western blot analysis of FHR2 and table resuming *CFHR2* copy number.

FHR3

In plasma, multiple variants of FHR3 (ranging from 35 to 56 kDa) are detected (Fig.61-62). The polyclonal antibody we used to detect FHR3 (Ab α FHR3) in 25 DDD patients also recognizes FHR4A (at 86 kDa), FH (at 155 kDa) and a band at low molecular mass, previously associated to FHR4B (about 40kDa)²³⁰.



Same membrane at different exposures

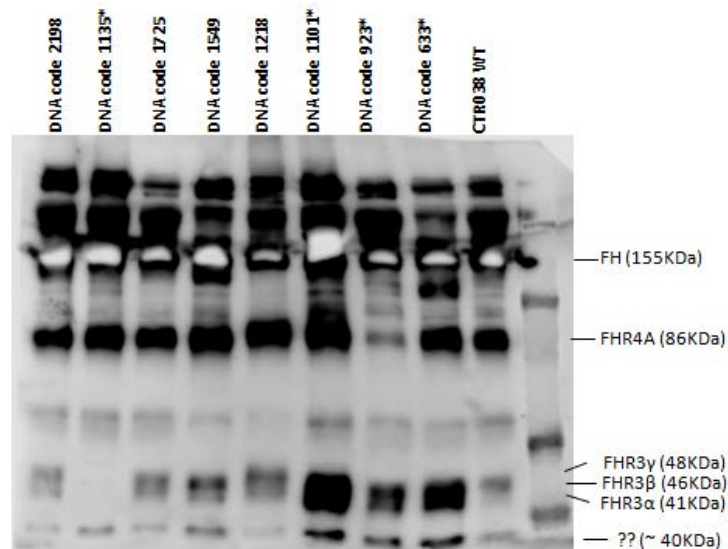


Figure 61. Western blot analysis of FHR3.

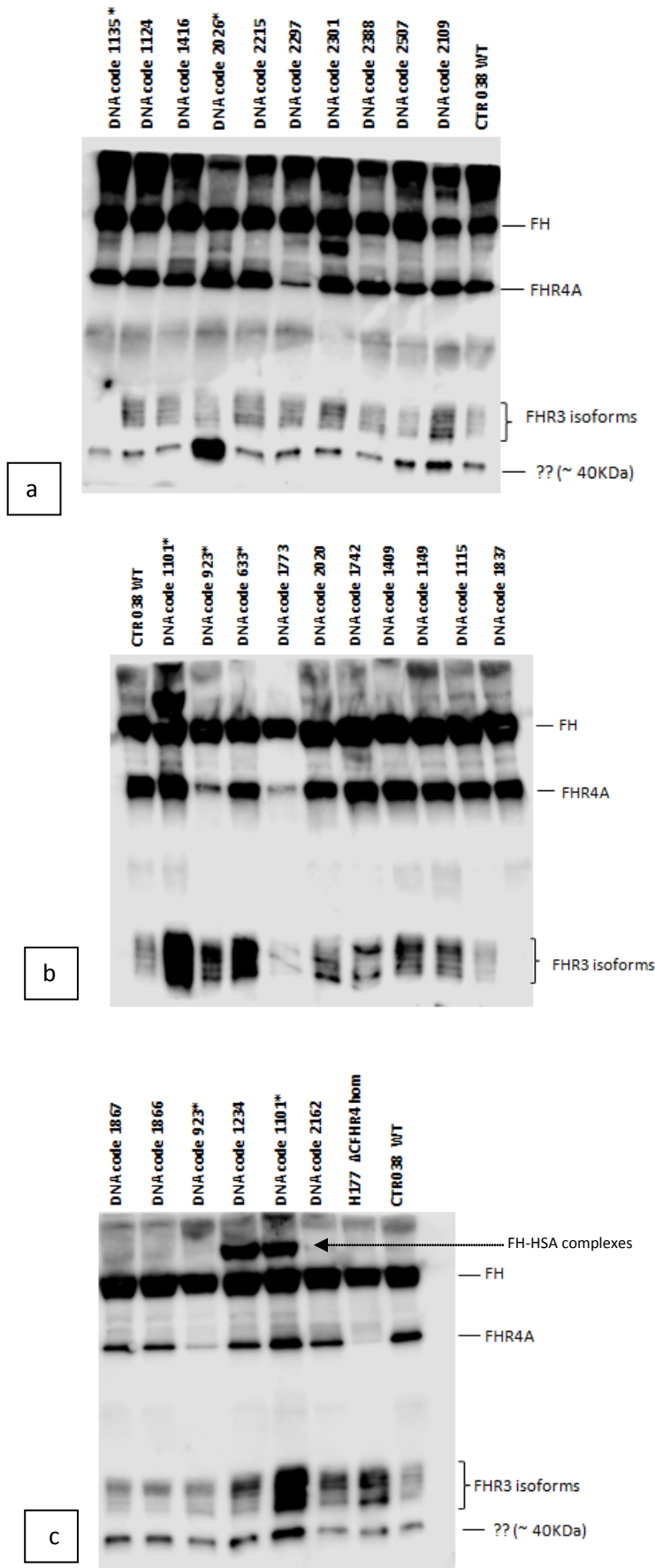


Figure 62. Western blot analysis of FHR3.

DNA code	CNV CFHR3	Note
CTR 038	2	
2198	1	Δ CFHR3-CFHR1 het
1135	0	Δ CFHR3-CFHR1 hom
1725	2	
1549	1	CFH : p.R2I + dupl CFHR4
1218	2	
1101 *	2	CFH : p.R1210C
923*	2	CFHR4 snp in homozygosity: p.G306E (rs10494745)
633*	2	
1124	2	
1416	1	Δ CFHR3-CFHR1 het + Δ CFHR1-CFHR4 het
2026	2	
2215	2	
2297	2	Δ CFHR1-CFHR4 het
2301	2	
2388	2	
2507	1	Δ CFHR3-CFHR1 het + CFHR4: p.Q142L
2109	2	
1773	2	CFHR4: p.E283K + CFHR5: p.H289D
2020	2	
1742	1	Δ CFHR3-CFHR1 het + CFHR2: p.Y264C
1409	2	
1149	2	
1115	1	Δ CFHR3-CFHR1 het
1837	0	Δ CFHR3-CFHR1 hom
2162	2	CFHR5: p.I222T

Table 22. Table resumming *CFHR3* copy number.

WB confirmed the total FHR3 deficiency for patients with DNA code #1135 (Fig.61, lane 2; Fig.62, panel a, lane 1) and #1837 (Fig.62, panel b, lane11) who have zero copy of *CFHR3* (Table 22).

Patient with DNA code #1773 (Fig. 62, panel b, lane 5) with 2 copies of *CFHR3* showed weaker FHR3 bands than the wt control (CTR 038), while for patients #633 (Fig.61, lane 8; Fig.62, panel b, lane 4) and #1101 (Fig.61, lane 6; Fig.62, panel b, lane 2 and panel c, lane 5) stronger than normal FHR3 bands were evident.

In patient #1101, I observed an extra FH band at higher molecular weight, with an apparent molecular weight of 210 kDa, in the WB lane, and FHR3 bands more intense than the control. This patient, who has a healthy identical unaffected twin (DNA code #1234), was analyzed by our in house NGS complement minipanel, by CasCADE and by MLPA for CNVs: both the patient and the identical twin carry a heterozygous pathogenetic variant in *CFH* (p.R1210C), previously reported in aHUS patients and shown in functional studies to affect protein function²³¹. The FH 1210C variant forms high-molecular-weight complexes with human serum albumin (HSA)²³², which explains the extra FH band at higher molecular weight observed in patient #1101 and of his identical twin #1234 (Fig. 62, panel c, lanes 4 and 5, see arrow).

At variance with patient #1101, his unaffected twin #1234 showed FHR3 bands of normal intensity (Fig.62 panel c, lane 4). To exclude that the high intensity observed for FHR3 bands in patient #1101 was related to the severe renal impairment (serum creatinine : 1.77 mg/dl) that the patient had developed at the time of blood sampling, we analyzed additional samples collected on previous dates, including the one of July 2009, when the patient had normal renal function (serum creatinine levels lower than 1.1 mg/dl). All samples from patient #1101 showed stronger than normal FHR3 bands (Fig. 63), indicating that the high levels of FHR3 were not associated to kidney failure. Consistently, plasma from a patient with glomerulopathy with fibronectin deposits

(GFND) and renal impairment (creatinine levels of 2.52 mg/dl) showed normal intensity of FHR3 bands on WB (#720, Fig. 63, lane 8).

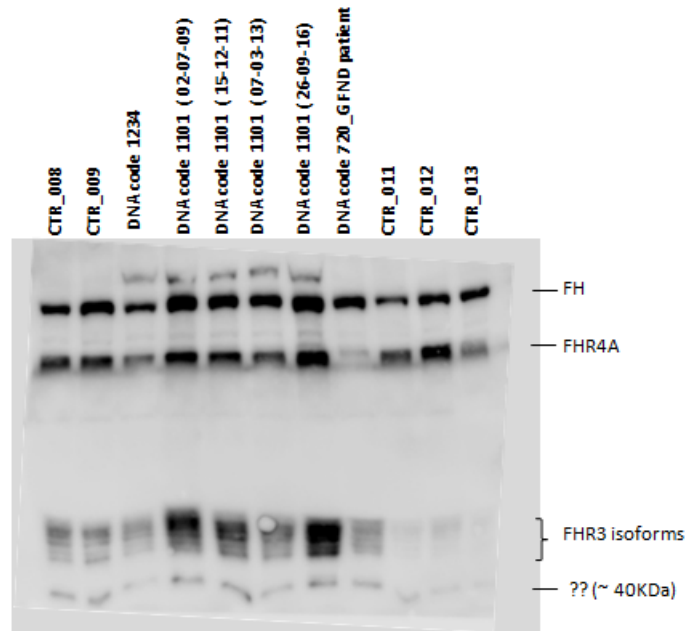


Figure 63. Plasma of #1101 from different data collections were analyzed on Western Blot in comparison to that from his identical healthy twin (#1234) and from a GFND patient with creatinine levels of 2.52 mg/dl (#720) and from healthy controls.

We observed interesting WB abnormalities in other patients. As reported in Fig.61 (lane 7) and Fig. 62 (panel b and c, lane 3), patient #923 showed normal FHR3 bands but a weaker than normal band corresponding to the MW of FHR4A. He carries normal copies for *CFHR4* but *CFHR* sequencing revealed that he has a homozygous Single Nucleotide Polymorphism in *CFHR4* (SNP; rs10494745; p.G306E; MAF_All_Frequency from ExAC: 0.08), inherited from his heterozygous parents. The variant is predicted to be damaging by some computational prediction softwares (Sift: deleterious; polyphen2: possibly damaging; Mutation Taster: polymorphism; Gerp++: highly conserved; CADD: 22.7). Among 27 patients sequenced on *CFHR4*, we found that #923 is the only one carrying this SNP in homozygosity. WB analysis showed

normal FHR4A band in the parents (Fig.62, panel c; #1866: father of 923; #1867: mother of 923) and confirmed a reduction of FHR4A in the patient, which was specific for FHR4A since it was not associated to a global reduction of FHRs.

Abnormal bands at high molecular weight (above 100 kDa) appeared on WB of patients with DNA codes #1742 (Fig.62, panel b, lane 7), #2026 (Fig.62, panel a, lane 4; Fig.64, lane 6) and #2301 (Fig.62, panel a, lane 7; Fig. 64, lane 7). Although some healthy controls showed bands above 100 KDa of similar apparent molecular weight (MW) to that identified in #2301 and #1742, the molecular patterns of patient #2026 was very peculiar (Fig.64).

Finally, in patient #2026 the band appearing at around 40KDa was very intense as compared with the ones in other patients and the controls (Fig.64, lane 6).

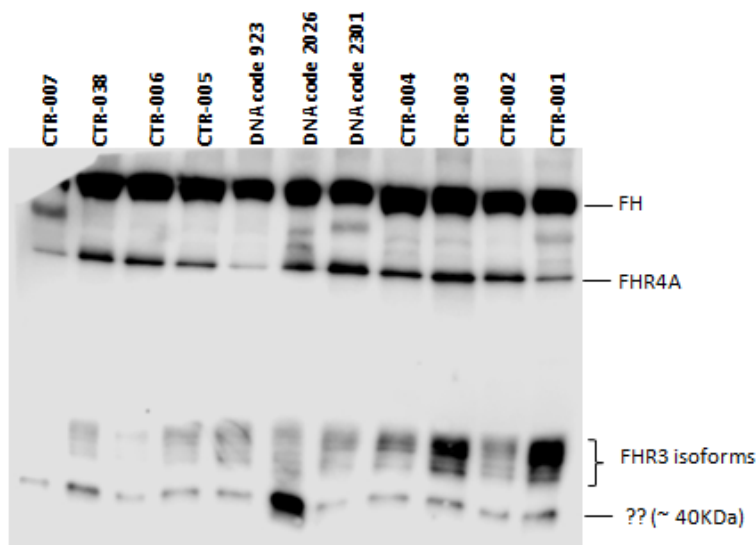


Figure 64. Western blot analysis of FHR3 showing the weaker FHR4A band in patient #923 in comparison to healthy controls and the peculiar molecular pattern in patient #2026.

FHR4

FHR4 has been described to circulate in plasma in two spliced variants, FHR4A (86kDa) and FHR4B (42kDa).

Results of WB analysis in 24 DDD patients are shown in Fig.65 and Fig.66.

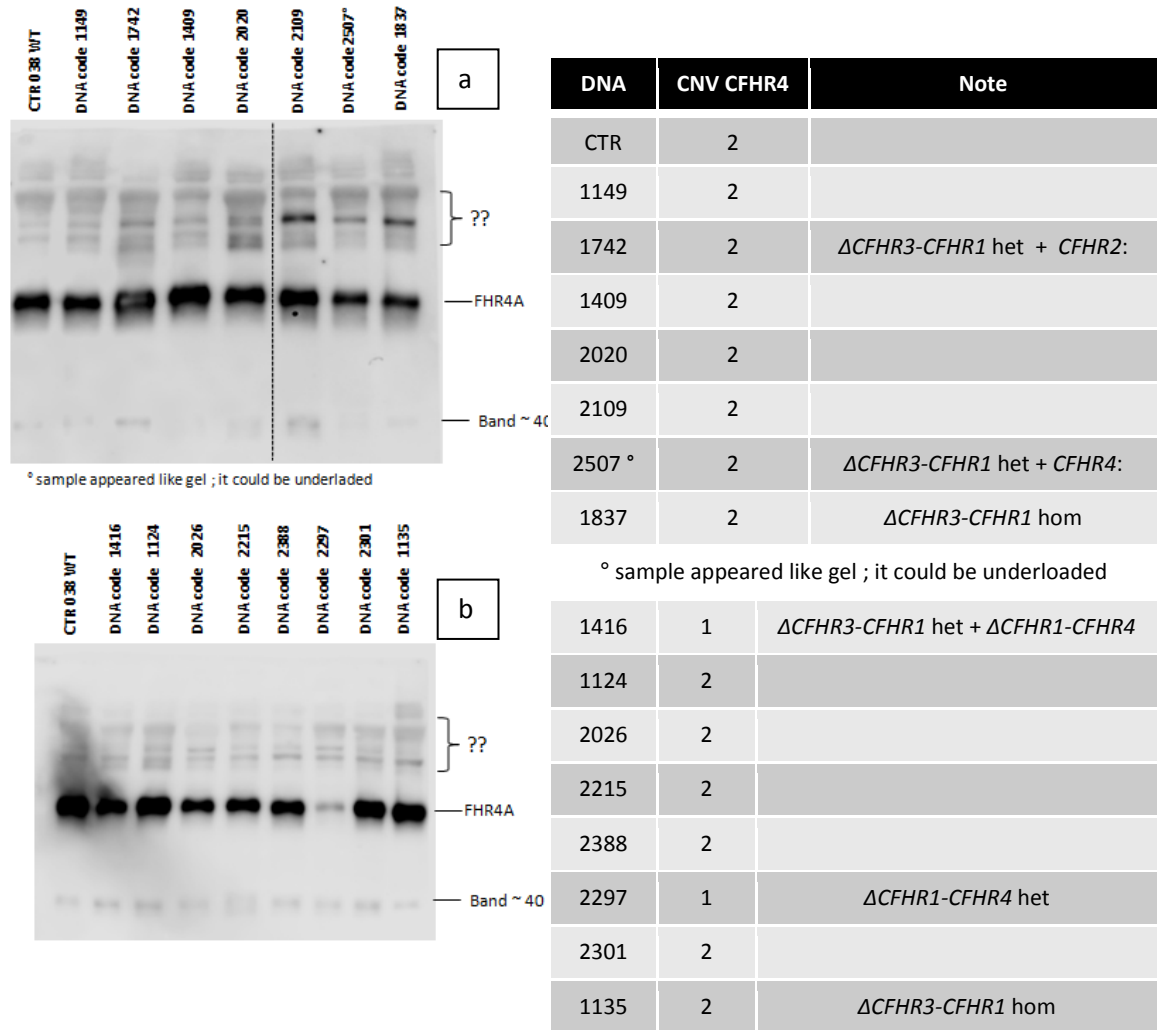


Figure 65. Western blot analysis of FHR4 and table resuming *CFHR4* copy number.

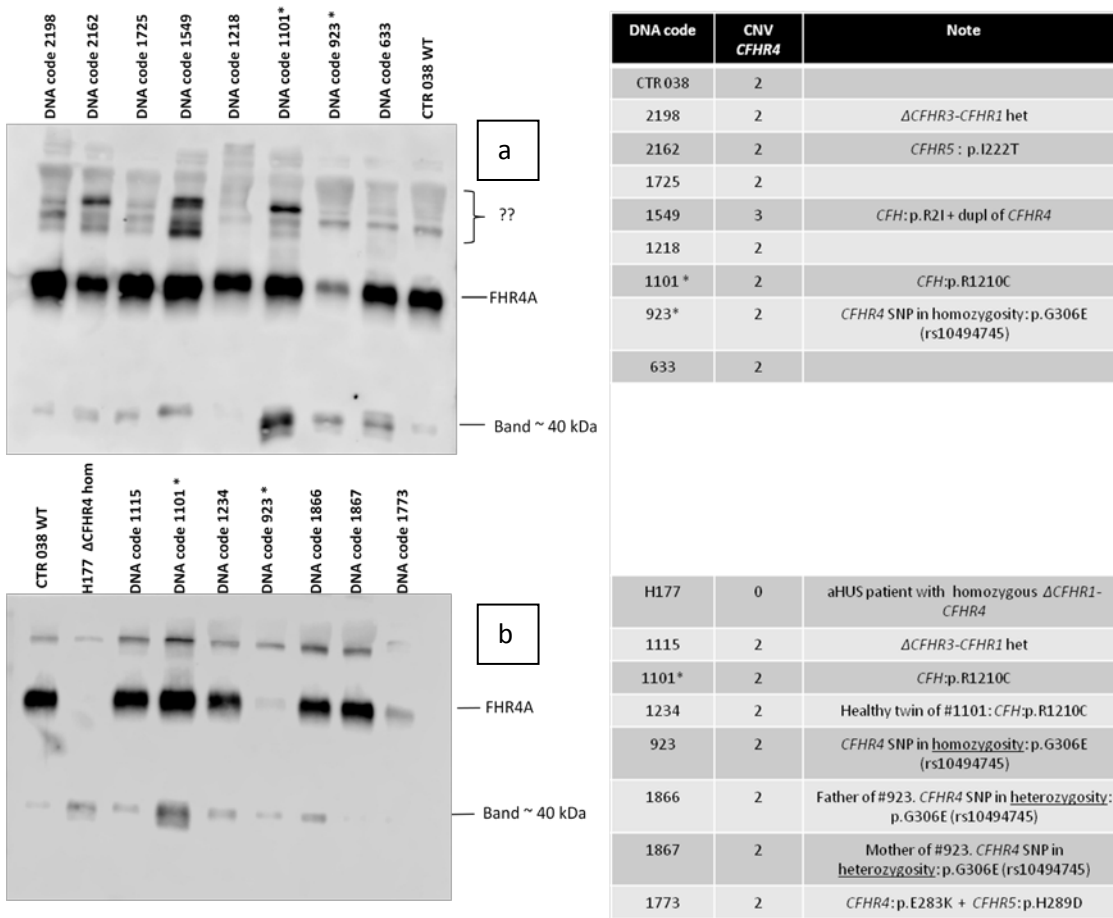


Figure 66. Western blot analysis of FHR4 and table resuming *CFHR4* copy number. *samples loaded in different western blot experiments. #1866 and #1867 are the parents of patient #923.

WB analysis using a polyclonal antibody α FHR4 ($Ab\alpha$ FHR4) confirmed in patient #923 the FHR4A partial deficiency observed with the $Ab\alpha$ FHR3 antibody, and the normal FHR4 molecular pattern in his parents (Fig.66, panel b, lanes 6,7,8).

Although multiple abnormal bands at high molecular mass were visible in the majority of patients, the molecular pattern of #1742 (Fig.65, upper panel, lane 3) , #2020 (Fig. 65, upper panel, lane 5) and #1549 (Fig 66, panel a, lane 4) were peculiar and not comparable to those identified in the other DDD patients and in healthy controls (Fig.65, 66, 67). Genetic studies on patient #1549 showed a heterozygous likely

pathogenic variant in *CFH* (p.R2I; see chapter 2.5.1.3) and a duplication of *CFHR4* that needs further investigation (see chapter 4.3.1.2).

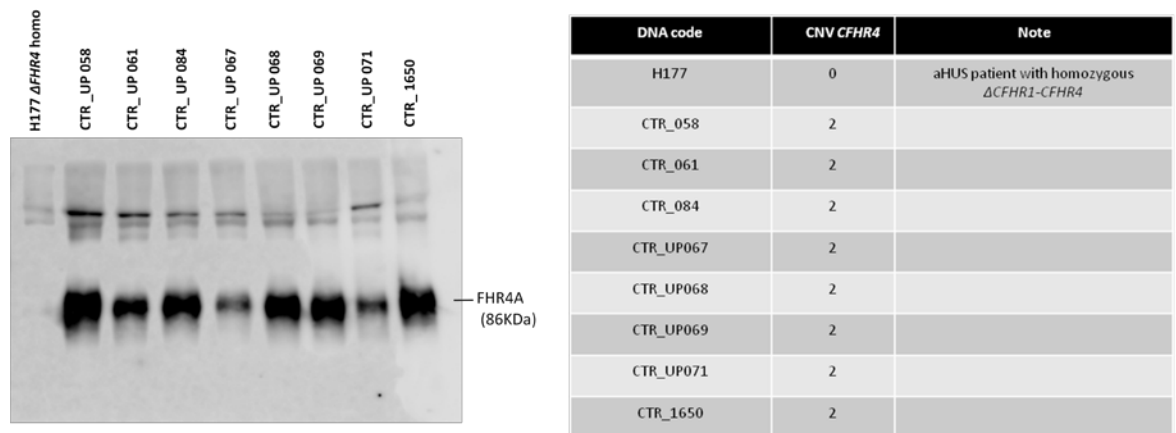


Figure 67. Western blot analysis of FHR4 in healthy subjects and table resuming *CFHR4* copy number.

Jozsi et al. in 2005²³⁰ reported two transcript products of *CFHR4*: FHR4A with a mobility of 86 kDa on WB and FHR4B with a mobility of about 42kDa. As shown in figure 66, in the aHUS patient #H177, carrying the homozygous *CFHR1-CFHR4* deletion, the band at around 40kDa was detected on the WB with the Ab α FHR4 antibody, excluding that this band corresponds to FHR4B. These results suggest that the Ab α FHR4 antibody recognizes another protein at low molecular weight that is not FHR4B and is likely the same recognized also by the Ab α FHR3 antibody. This band was very strong in the patient #1101 (Fig. 66, panel a, lane 6; panel b, lane 4) and #2026 (Fig.64, lane 6).

FHR5

In the FHR family, FHR5 is the longest protein with nine short consensus repeats (SCRs) and is present in plasma as a glycosylated protein of 62kDa. Results of WB analysis in 24 DDD patients are shown in Fig.68.

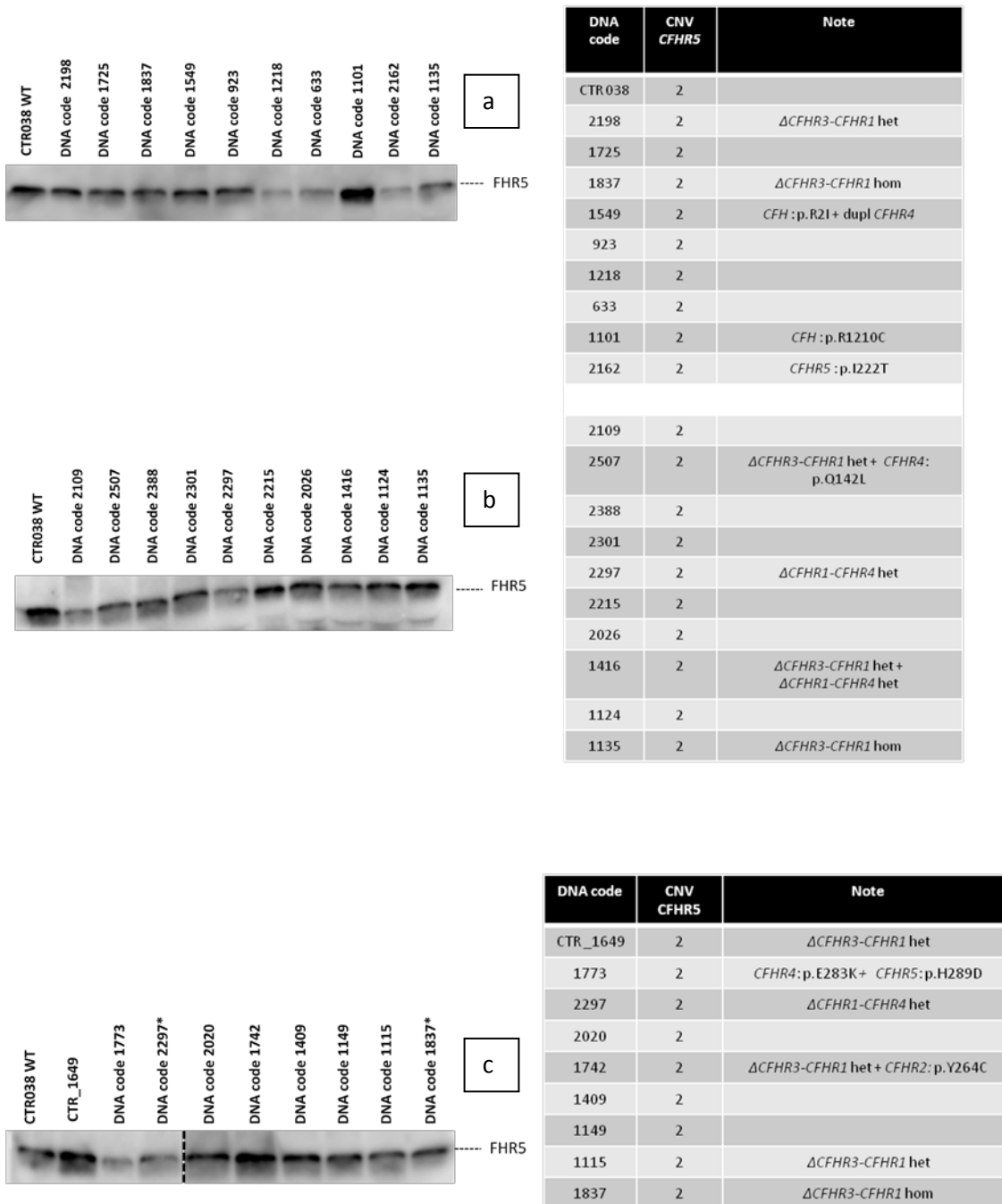


Figure 68. Western blot analysis of FHR5 and table resuming *CFHR5* copy number.

*samples loaded in different western blot experiments.

The intensity of bands of FHR5 was very variable among plasma's patients. In detail, patients #1218, #633, #2162, #2297 and #1773 showed a weaker than normal FHR5 band. The most clear-cut abnormality was the strongest FHR5 band in the WB of patient #1101 (Fig.68 panel a, lane 9).

FH

Factor H (FH) is a plasma glycoprotein with a molecular weight of 155kDa. In Fig.69 are reported results of WB analysis in 25 DDD patients.

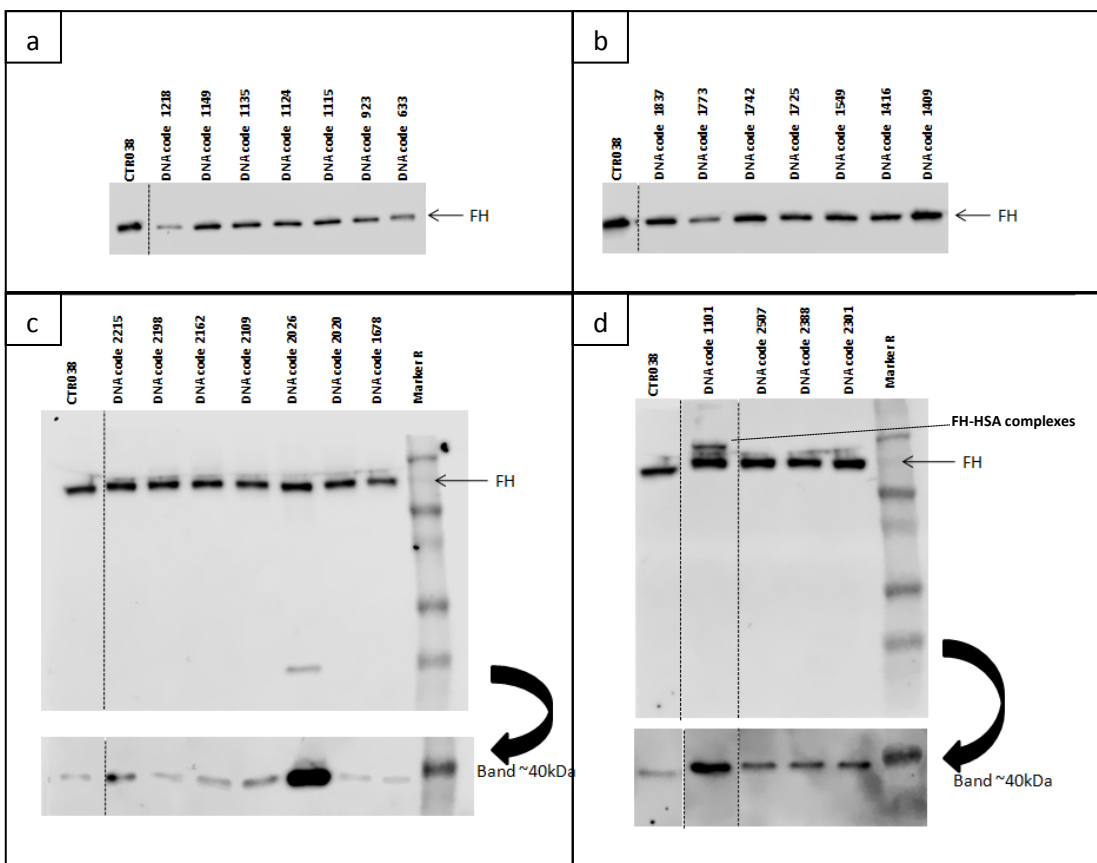


Figure 69. Western blot analysis of FH.

WB with a specific anti-FH antibody did not reveal any abnormal band with the exception of patient #1101 that showed two bands corresponding to the wild-type and mutant proteins (p.R1210C) (Fig.69, panel d, lane 2; Table 23). This data, already observed in WB with the anti-FHR3 antibody, was confirmed using plasma samples of #1101 from different data collection (Fig.70)

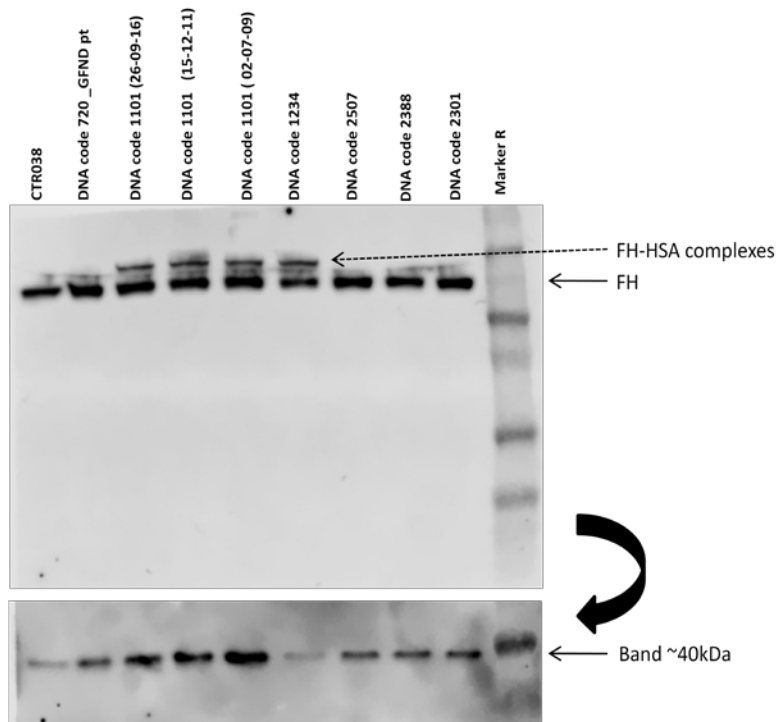


Figure 70. Plasmas from #1101 taken on different data were analyzed in comparison to plasma from his identical healthy twin (#1234) and from a GFND patient with creatinine levels of 2.52 mg/dl (#720).

A strong band around 40kDa already observed in #1101 and #2026 using Ab α FHR3 (Fig.62), was evident in the same patients also using the antibody that recognizes FH and the FH-like (FHL1) (Fig.69 , panels c and d) and represented the product of the alternative transcript derived from the *CFH* gene.

These data indicate that the band with a mobility around 40kDa appearing on WB using Ab α FH, Ab α FHR3 and Ab α FHR4 corresponded to FHL1 and not to FHR4B, as reported in literature²³⁰.

DNA code	CNV CFH	Note	FH levels (n.r.:173-507 mg/L)	DNA code	CNV CFH	Note	FH levels (n.r.:173-507 mg/L)
CTR 038	2		NA	1416	2	Δ CFHR3-CFHR1 het + Δ CFHR1-CFHR4 het	244
1218	2		280	1409	2		246
1149	2		160	2198	2	Δ CFHR3-CFHR1 het	357
1135	2	Δ CFHR3-CFHR1 hom	287	2162	2	CFHR5: p.I222T	179
1124	2		209	2109	2		276
1115	2	Δ CFHR3-CFHR1 het	NA	2026	2		355
923	2		201	2020	2		311
633	2		252	1678	2	CFHR2:p.Q211X +p.R254X + CFHR3 ₂₋₅ -CFHR4 ₂₀ hybrid gene	239
1837	2	Δ CFHR3-CFHR1 hom	264	1101	2	CFH: p.R1210C	351
1773	2	CFHR4: p.E283K + CFHR5: p.H289D	NA	2507	2	Δ CFHR3-CFHR1 het + CFHR4: p.Q142L	309
1742	2	Δ CFHR3-CFHR1 het + CFHR2: p.Y264C	315	2388	2		324
1725	2		213	2301	2		301
1549	2	CFH: p.R21 + dupl CFHR4	192				

Table 23. Tables resuming *CFH* copy number and FH circulating levels.

4.3.4.1 Quantitative WB analysis.

Among 25 DDD patients analyzed, 8 showed either FHR quantitative abnormalities or FHR abnormal bands (Table 24). To confirm quantitative variations (patients #633, #1101, #1218 and #1773; for #923 plasma/serum samples were no more available) we performed a quantitative WB analysis of FHRs bands using FH band as reference standard. Results showed 27% and 97% reduction of FHR4A/FH ratio in patients #1218 and #1773, respectively (Fig.71). FHR3/FH reduction was 80% in patient #1218 and 99% in patient #1773. In patients #633 and #1101 we observed 260% and 370% FHR3/FH intensity ratios in respect to control medians, respectively (Fig.72).

Patient	Interpretation of WB results	Genetic results
#633	High FHR3 levels	No LPVs; normal copy number.
#923*	Decreased FHR4A levels	No LPVs; normal copy number.
#1101	All FHR proteins and FHL1 are overexpressed; presence of FH wild-type and p.1210C mutant in plasma	LPV: <i>CFHp.R1210C</i> ; normal copy number.
#1218	Global reduction of FHRs	No LPVs; normal copy number.
#1549*	Multiple abnormal bands above 100KDa detectable by Ab α FHR4	- LPV: <i>CFHp.R2I</i> . - Duplication of <i>CFHR4</i> .
#1742	Abnormal band around 40kDa detected by Ab α FHR1; Multiple abnormal bands above 100kDa detectable by Ab α FHR3 and Ab α FHR4	- Variant: <i>CFHR2</i> : p.Y264C; - Δ <i>CFHR3-CFHR1</i> het.
#1773	Global reduction of FHRs	- LPVs: <i>CFHR4</i> :p.E283K; <i>CFHR5</i> : p.H289D; - normal copy number.
#2026*	Multiple abnormal bands above 100kDa detectable by Ab α FHR3; Peculiar intense expression of FHL1	No LPVs; normal copy number.

Table 24. DDD samples with an abnormal molecular pattern identified by WB.

*Samples included in the pilot study of SMRT (see next section)

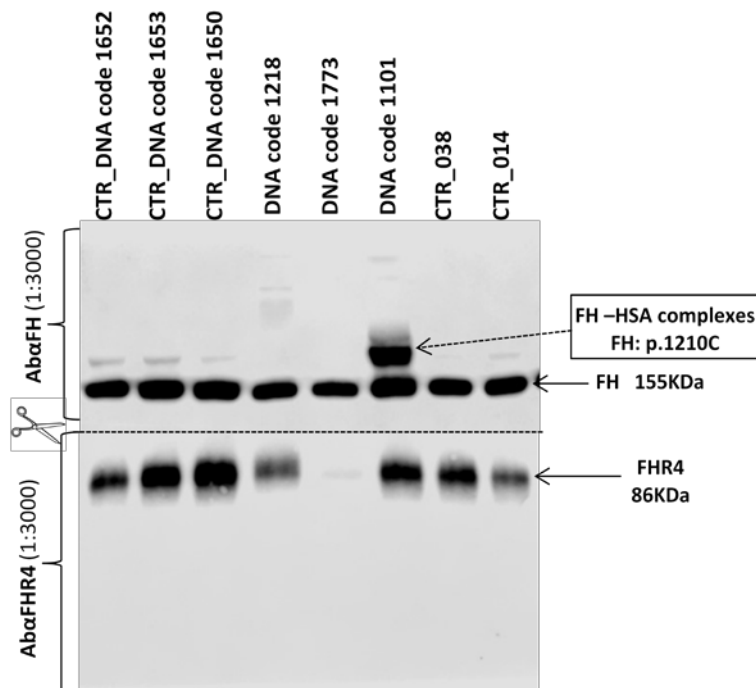


Figure 71. Western blot to quantify FHR4 variations. The membrane was cut in two parts: the upper part was incubated with the anti-FH Ab to detects the FH (155 kDa) while the lower part was incubated with an anti-FHR4A to reveal the FHR4 (86 kDa). In patient #1101 is evident the band corresponding to FH 1210C, already described in section 4.6.

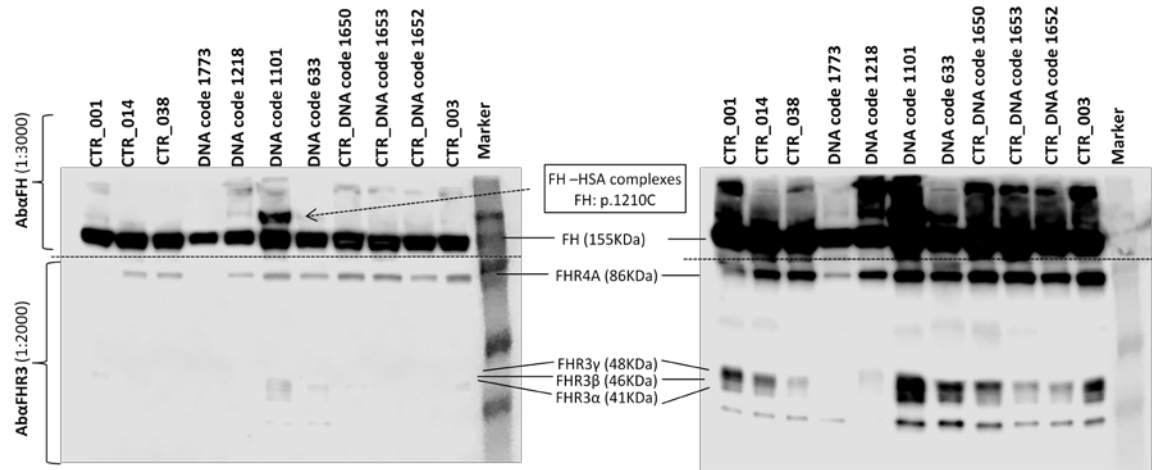


Figure 72. Western blot to quantify FHR3 variations. The membrane was exposed twice to clearly reveal the FH (at first exposure) and FHR3 (at the second exposure).

4.3.5 Prospective Studies

To identify genetic basis of the above reported abnormalities, we chose the emerging technique of Single Molecule Real Time sequencing (SMRT) sequencing. This new technique uses long-read sequencing and can be coupled with target enrichment capture methods to study genomic regions of interest to discover variants, gene isoforms and structural variations²³³. On this basis, we decided to use this strategy to study the complex genomic region of chromosome 1 spanning *CFH* and the 5 *CFHR* genes. To test the quality and depth of PacBio sequencing, we designed a pilot study selecting 5 samples to be sequenced on Sequel system, the most powerful platform for SMRT sequencing (output 4-7 Gb per run). The 5 selected samples include 3 patients (#923, #1549 and #2026, Table 24) with an abnormal molecular pattern on WB, a healthy subject with no CNVs in *CFH/CFHRs* (CTR038; negative control in the pilot study) and a DDD patient with the hybrid gene *CFHR3₁₋₅-CFHR4₁₀* (#1678; positive control). We designed probes targeting *CFH-CFHRs* on the human genome reference hg19 using the online Nimble Design Software. 2 μ g of genomic DNA, fragmented at 7-8 Kb and

processed following standard manufacturer's procedures, will be sequenced using the Sequel system (output 4-7 Gb).

SMRT Library preparation and Sequencing are ongoing at a Certified Service Provider (Norwegian Sequencing Centre, Oslo University).

We expect that the pilot study will document that SMRT with PacBio sequencing is capable to correctly detect the *CFHR3₁₋₅-CFHR4₁₀* hybrid and the corresponding breakpoint in the positive control, and will be successful in disclosing the genomic abnormalities in test DDD patients #923, #1549 and #2026. The pilot study will also allow determining the maximum number of patients that can be successfully sequenced in each run.

Results of the pilot study will be the basis to sequence by SMRT with PacBio the other DDD patients with the abnormal molecular pattern reported in Table 24, namely patients #633, #1101, #1218, #1742 and #1773.

4.3.6 Discussion

In this study I analyzed *CFH-CFHR* copy number variations in an Italian cohort of patients with IC-MPGN, DDD and C3GN diagnosis. I found that the frequency of *CFHR3-CFHR1* deletion (*CFHR3-CFHR1* Δ) was similar in IC-MPGN, DDD and C3GN and was not different from that observed in Italian healthy controls.

However, I found two new rearrangements in the *CFH-CFHR* genomic region both in patients with DDD and IC-MPGN. Both rearrangements involve the *CFHR4* gene.

The first one is an uncommon duplication of the *CFHR4* gene that was identified in a DDD patient (#1549) and in an IC-MPGN patient (#1726), carrying a *CFH* and a *CFB* likely pathogenic variants (LPVs), respectively. Copy number analysis in the family members of the IC-MPGN patient supported the presence of the *CFHR4* duplicated gene in the allele carrying zero copy of *CFHR3*, and a copy of *CFHR1* suggesting that a double rearrangement involving *CFHR1-CFHR4* duplication and *CFHR3-CFHR1* deletion may be occurred.

Although the *CFHR1-CFHR4* duplication (*CFHR1-CFHR4dupl*) was not previously described in literature, data regarding the duplication of *CFHR1* in patients with aHUS and in healthy controls were reported^{226, 234} suggesting that further studies involving also *CFHR4* (not commonly analyzed) and the breakpoint localization of *CFHR1-CFHR4dupl* are required to establish its frequency in aHUS and in healthy controls. The patient #1726 also carries a homozygous LPV in *CFB* (p.R679W). Although I hypothesize that the abnormal FB generates strong AP C3 convertases hardly inactivated by complement regulators, functional studies are necessary to understand the effect of the *CFB* LPV and *CFHR1-CFHR4dupl* and whether these abnormalities may synergize in inducing to AP complement hyperactivation.

The other rearrangement was represented by the *CFHR3*₁₋₅-*CFHR4*₁₀ hybrid gene, identified in a DDD patient (#1678), with slightly reduced C3 levels. The same hybrid gene was found in her healthy sons and also in four patients with aHUS, three of them with other complement abnormalities.

An insertion of 305 bp located in intron 5 of *CFHR3* was found in linkage with the *CFHR3*₁₋₅-*CFHR4*₁₀ hybrid gene. However, the insertion (here called Alu-like region because of its sequence similarity with Alu repeat sequences located in *CFHR3* and *CFHR4*) was also found in some individuals without the *CFHR3*₁₋₅-*CFHR4*₁₀ hybrid gene suggesting that the insertion fixed in a peculiar genome haplotype ancestrally before the formation of the hybrid. I hypothesize that the Alu-like region might predispose to genomic rearrangements, similarly to previously reported data for Alu repeats in other genetic diseases²²⁹.

Western Blot (WB) experiments document that the FHR3₁₋₄-FHR4₉ hybrid protein is produced and secreted in the serum of the DDD_{*CFHR31-5-CFHR410*} patient and her unaffected son. Hebecker and Jozsi showed that FHR4 protein serves as platform to assemble the AP C3 convertase through its C-terminal region which contains the C3b binding sites²³⁵. In addition, SCR1-3 of FHR3 show a high sequence similarity with the FH domains (SCR6-8) involved in the binding to heparin and other surface ligands⁹. On these basis, the hypothesis is that FHR3₁₋₄-FHR4₉ hybrid protein through its N-terminal domains (deriving from SCR1-3 of FHR3) binds to heparin, glycosaminoglycans, sialic acid molecules on cell surfaces and the glomerular basement membrane (GBM) while through its C-terminal domain (deriving from SCR9 of FHR4) binds C3b fragments and favors the activation of the AP C3 convertase.

However, the *CFHR3*₁₋₅-*CFHR4*₁₀ hybrid gene may not be the main responsible of DDD in the patient #1678. Indeed, the DDD patient with the FHR3₁₋₄-FHR4₉ hybrid protein has a general deficiency of FHR proteins: 1) a reduced FHR2 protein (caused by

p.Q211X variant) 2) total deficiency of FHR1; 3) a FHR3 involved in a novel hybrid protein with FHR4. Since FHRs are circulating proteins, the abnormalities in this patient could not be corrected by kidney transplant, which is consistent with the clinical history of the patient who manifested relapsing disease in two kidney grafts. Although further studies are necessary to understand the effect of the FHR abnormalities identified in the DDD patient #1678, the data obtained from this study suggest that the *CFHR3*₁₋₅-*CFHR4*₁₀ hybrid gene may be present in patients with other genetic or acquired factors and that the specific combination of the hybrid gene with other complement abnormalities may determine the disease phenotype resulting in aHUS or DDD.

The study of the FH/FHRs molecular pattern in DDD patients allowed identifying FHR abnormalities in 30% of them. Among them, only the patient #1549 showed abnormal copy numbers (represented by *CFHR1-CFHR4dupl* described above) identified by MLPA, which may explain the abnormal bands observed in the WB analysis. DDD patients with a unexplained abnormal FHR molecular pattern on WB have been selected for deep sequencing of the entire *CFH-CFHR* genomic region by a new technique (Single Molecule Real-time sequencing, SMRT) that uses a DNA sequencing long-read approach thus overcoming the problem of read-mapping ambiguity of this genomic region. Bioinformatic analyses are still ongoing. I expect to identify new rearrangements and or new intronic and intergenic variants accounting for expression of the altered proteins. The combined molecular and genetic approach may represent a valuable tool to discover and characterize at genetic and protein levels new abnormalities in the FH-FHR proteins. Results will deepen the knowledge on the pathogenetic mechanisms underlying DDD and may contribute to identify new molecular targets for complement inhibitory therapies.

5. CONCLUSIONS

In the past decade new insights in the pathogenic mechanisms have changed our understanding and the classification of membranoproliferative glomerulonephritis (MPGN). The current classification distinguishes C3 Glomerulopathy (C3G), including Dense Deposit Disease (DDD) and C3 glomerulonephritis (C3GN), characterized by strong glomerular C3 deposition, from immune-complex-mediated MPGN (IC-MPGN), characterized by a predominant deposition of immune-complexes.

In this thesis, a well characterized Italian cohort of patients with IC-MPGN, DDD and C3GN was studied (Chapter 2). Genetic and biochemical data obtained from this study were correlated with histological features, complement profile, clinical phenotype and outcome to examine the pathogenic mechanisms underlying these glomerular diseases. About 75% of patients showed low C3 and normal C4, indicating an activation of the alternative pathway (AP) of complement. Likely pathogenic variants (LPVs) in *C3*, *CFB*, *CFH*, *CFI* and *CD46* genes were present both in IC-MPGN and C3G patients. In patients with C3G we also identified two LPVs in the *THBD* gene. These variants were previously described in patients with atypical haemolytic uremic syndrome (aHUS) and *in vitro* functional studies showed that the mutant THBD proteins impaired complement regulation through FI-mediated C3b inactivation²² supporting their involvement in the pathogenesis of C3G. However, complement LPVs carriers ranged only from 15 to 24% across the three histological groups. Biochemical studies revealed that C3NeF, identified in 40% of IC-MPGN and C3GN patients and in 79% of patients with DDD, is associated with low C3 levels in all three histology groups. Our study on complement profiles suggested two different mechanisms. C3NeF mainly affected the C3 convertase in patients with DDD, whereas it appeared to act predominantly on terminal pathway in patients with IC-MPGN and C3GN.

However, this study did not disclose genetic or acquired abnormalities in 17% of DDD patients although they showed low circulating C3 levels, suggesting that other abnormalities in unknown factors are involved in AP complement regulation in patients with DDD.

Another important finding from this study is the evident involvement of AP dysregulation in patients with IC-MPGN, as documented by low C3 and normal C4 (in 70% of patients) and the presence of complement LPVs and/or C3NeF (in 49% of patients). These data are not consistent with the current MPGN classification that considers the IC-MPGN mediated by the activation of the complement classical pathway and indicate that further studies were needed to better classify patients on the basis of the underlying pathogenetic mechanisms¹⁸⁵.

The risk to develop end stage renal disease (ESRD) was similar among the three histology groups. However, patients without genetic and or acquired abnormalities showed a higher risk to develop ESRD in comparison to those patients carrying LPVs and or C3NeF indicating that another mechanism is also involved in the progression of renal disease in IC-MPGN/C3G patients.

To make a step forward into the classification of IC-MPGN and C3G patients based on pathophysiologic mechanisms, five parameters (presence of LPVs, presence of C3NeF, serum C3 \leq 50mg/dl, serum C3 $>$ 50 & $<$ 90 mg/dl, presence of intramembranous highly electron-dense deposits) were used to create a three-step algorithm² that was used to classify patients from our Italian cohort of IC-MPGN/C3G patients. The analysis divided patients with abnormal AP complement profile and carrying genetic and/or acquired abnormalities (cluster 1-3) from patients with normal complement profile and low frequency of LPVs and or C3NeF (cluster 4). Cluster 1 and 2 were characterized

by very high SC5b-9 levels suggesting a strong complement activation until the terminal pathway. Notably, cluster 2, mainly composed by IC-MPGN patients and few C3GN patients, was also characterized by strong deposition of IgG, IgM and C1q and abnormal C4 levels (24%) suggesting also an involvement of the classical pathway.

Cluster 3 included all DDD patients and few IC-MPGN patients, showing low serum C3 and normal or mildly increased plasma SC5b-9 levels indicating a prevalent activation of the C3 convertase in fluid-phase.

Cluster 4 is different from the others 3 groups because of the normal complement profile and the low prevalence of genetic and acquired complement abnormalities. The strong glomerular C3 deposition, the normal complement profile and the development of thrombotic microangiopathy in 11% of them suggest the presence of unknown factors that cause local glomerular activation in subgroups of IC-MPGN and C3GN patients.

Cluster analysis confirmed our published data and separated patients with fluid-phase complement activation from patients with solid-phase complement activation. Among patients with AP activation in fluid phase, cluster analysis allowing us to identify distinct pathogenetic patterns separating patients with terminal complement activation from patients with a predominant C3 convertase activity.

The above mentioned study evidenced that:

- The majority of C3GN patients and some IC-MPGN patients are characterized by fluid phase complement activation of the terminal pathway (complement LPVs and/or C3NeFs are often present).
- The majority of IC-MPGN and few C3GN patients are characterized by the activation of both alternative and classical pathways (complement LPVs and/or C3NeFs are often present)

- A consistent number of patients with IC-MPGN and C3GN are characterized by a local glomerular activation (in absence of known complement LPVs and/or C3NeFs);
- Few IC-MPGN patients are characterized by fluid phase complement activation predominantly at C3 convertase level;
- The majority of DDD patients are characterized by fluid phase complement activation predominantly at C3 convertase level, usually in association with the presence of C3NeFs;
- Some DDD patients are characterized by fluid phase complement activation predominantly at C3 convertase level because of the presence of unknown genetic and or acquired factors.

In order to identify new genetic abnormalities, 17 of 26 DDD patients included in this study were analyzed by a wide NGS panel including 85 complement and coagulation genes (Chapter 3). Although likely deleterious variants in new complement genes (like *PTX3*, *ITGAM*, *C4BPA*, *C5aR1*, *C5aR2* and others) were identified in combination with one or two additional complement variants, the most interesting finding was represented by the 60% of variants in complement regulators/activators genes, including *CFH* and *CFHR* genes, that require further investigation.

The study of *CFH-CFHR* family in patients from our cohort (Chapter 4) revealed the presence of unknown copy number abnormalities involving the *CFHR4* gene both in C3G and IC-MPGN patients. Although functional studies are necessary to understand their functional effects, these data suggest that analysis of copy number variations (CNVs) in *CFH-CFHR* genes should also be extended to patients with IC-MPGN. Furthermore, the *CFHR4* gene, not commonly analyzed, should be included in the study of *CFH-CFHR* CNVs.

In addition Western Blot study in DDD patients disclosed abnormal molecular patterns of FHRs in patients with normal CNVs. Since the homologies within *CFH-CFHRs* represent a strong limitation for both the read alignment step in NGS techniques that produce reads of few hundred base pairs, and for designing probes for CNV techniques, we planned a combined genetic and molecular approach to disclose new abnormalities in the FH-FHR family. Indeed, patients with abnormal molecular pattern and normal CNV were selected to be analyzed by Single Molecule Real Time (SMRT), a new sequencing technique based on long-read sequencing. We expect that this new technique, coupled with target enrichment capture method, will enable us to avoid the problem of read-mapping ambiguity of the *CFH-CFHR* region, and will disclose new genomic rearrangements or intronic/intergenic variants accounting the abnormal molecular pattern observed in patients with DDD.

Altogether the above reported data indicate that:

- functional studies are required to understand the effect of *C3*, *CFB*, *CFH*, *CFI* LPVs identified in our cohort on complement activation;
- we have to verify whether autoantibodies here identified as C3NeFs, also include other nephritic factors (C4NeF or C5NeF);
- the presence of other acquired factors (anti-factor H, anti-factor B autoantibodies) in all patients should be verified;
- genetic studies in other cohorts of DDD patients are required to confirm the involvement of new identified complement genes (*PTX3*, *ITGAM*, *C4BPA*, *C5aR1*, *C5aR2* and others);
- functional studies on *CFHR* variants identified in patients with DDD are required to understand their role in the pathogenesis of disease;
- genetic abnormalities in new complement genes (Exome Sequencing) should be searched.

In summary, in this study the correlation of genetic and biochemical abnormalities with clinical and histological parameters allowed us to deepen the knowledge on the pathogenetic mechanisms underlying IC-MPGN, DDD and C3G that may contribute to identify new molecular targets for complement inhibitory therapies.

BIBLIOGRAPHY

1. Appel GB, Cook HT, Hageman G, et al. Membranoproliferative glomerulonephritis type II (dense deposit disease): an update. *J Am Soc Nephrol* 2005;16:1392-403.
2. Iatropoulos P, Daina E, Curreri M, et al. Cluster Analysis Identifies Distinct Pathogenetic Patterns in C3 Glomerulopathies/Immune Complex-Mediated Membranoproliferative GN. *J Am Soc Nephrol* 2017.
3. Noris M, Remuzzi G. Glomerular Diseases Dependent on Complement Activation, Including Atypical Hemolytic Uremic Syndrome, Membranoproliferative Glomerulonephritis, and C3 Glomerulopathy: Core Curriculum 2015. *Am J Kidney Dis* 2015;66:359-75.
4. Bu F, Maga T, Meyer NC, et al. Comprehensive genetic analysis of complement and coagulation genes in atypical hemolytic uremic syndrome. *J Am Soc Nephrol* 2014;25:55-64.
5. Hou J, Markowitz GS, Bomback AS, et al. Toward a working definition of C3 glomerulopathy by immunofluorescence. *Kidney Int* 2014;85:450-6.
6. Challis RC, Araujo GS, Wong EK, et al. A De Novo Deletion in the Regulators of Complement Activation Cluster Producing a Hybrid Complement Factor H/Complement Factor H-Related 3 Gene in Atypical Hemolytic Uremic Syndrome. *J Am Soc Nephrol* 2016;27:1617-24.
7. Ricklin D, Barratt-Due A, Mollnes TE. Complement in clinical medicine: Clinical trials, case reports and therapy monitoring. *Mol Immunol* 2017;89:10-21.
8. de Cordoba SR, Tortajada A, Harris CL, Morgan BP. Complement dysregulation and disease: from genes and proteins to diagnostics and drugs. *Immunobiology* 2012;217:1034-46.
9. Jozsi M, Tortajada A, Uzonyi B, Goicoechea de Jorge E, Rodriguez de Cordoba S. Factor H-related proteins determine complement-activating surfaces. *Trends Immunol* 2015;36:374-84.
10. Bomback AS, Smith RJ, Barile GR, et al. Eculizumab for dense deposit disease and C3 glomerulonephritis. *Clin J Am Soc Nephrol* 2012;7:748-56.
11. Reidy K, Kang HM, Hostetter T, Susztak K. Molecular mechanisms of diabetic kidney disease. *J Clin Invest* 2014;124:2333-40.
12. Jefferson JA, Shankland SJ, Pichler RH. Proteinuria in diabetic kidney disease: a mechanistic viewpoint. *Kidney Int* 2008;74:22-36.
13. Sethi S, Fervenza FC. Membranoproliferative glomerulonephritis--a new look at an old entity. *N Engl J Med* 2012;366:1119-31.
14. de Cordoba SR, de Jorge EG. Translational mini-review series on complement factor H: genetics and disease associations of human complement factor H. *Clin Exp Immunol* 2008;151:1-13.
15. Mathern DR, Heeger PS. Molecules Great and Small: The Complement System. *Clin J Am Soc Nephrol* 2015;10:1636-50.
16. Thurman JM, Nester CM. All Things Complement. *Clin J Am Soc Nephrol* 2016;11:1856-66.
17. Pangburn MK, Muller-Eberhard HJ. The alternative pathway of complement. *Springer Semin Immunopathol* 1984;7:163-92.
18. Law SKAr, K.B.M. Complement, 2nd edit. IRL Press, Oxford, UK 1995.
19. Fujita T. Evolution of the lectin-complement pathway and its role in innate immunity. *Nat Rev Immunol* 2002;2:346-53.
20. Degn SE, Thiel S, Jensenius JC. New perspectives on mannan-binding lectin-mediated complement activation. *Immunobiology* 2007;212:301-11.

21. Farrar CA, Tran D, Li K, et al. Collectin-11 detects stress-induced L-fucose pattern to trigger renal epithelial injury. *J Clin Invest* 2016;126:1911-25.
22. Delvaeye M, Noris M, De Vriese A, et al. Thrombomodulin mutations in atypical hemolytic-uremic syndrome. *N Engl J Med* 2009;361:345-57.
23. Morgan BP. Regulation of the complement membrane attack pathway. *Crit Rev Immunol* 1999;19:173-98.
24. Bhakdi S, Trantum-Jensen J. Damage to cell membranes by pore-forming bacterial cytolysins. *Prog Allergy* 1988;40:1-43.
25. Muller-Eberhard HJ. The membrane attack complex of complement. *Annu Rev Immunol* 1986;4:503-28.
26. Schmidt CQ, Lambris JD, Ricklin D. Protection of host cells by complement regulators. *Immunol Rev* 2016;274:152-71.
27. Wiggins RC, Giclas PC, Henson PM. Chemotactic activity generated from the fifth component of complement by plasma kallikrein of the rabbit. *J Exp Med* 1981;153:1391-404.
28. Davis AE, 3rd. Biological effects of C1 inhibitor. *Drug News Perspect* 2004;17:439-46.
29. Amara U RD, Flierl M, Bruckner U, Klos A, Gebhard F, Lambris JD, Huber-Lang M. Interaction between the coagulation and complement system. *Adv Exp Med Biol* 2008;632:71-9.
30. Haviland RAWKL. Complement Anaphylatoxins (C3a, C4a, C5a) and Their Receptors (C3aR, C5aR/CD88) as Therapeutic Targets in Inflammation: Humana Press, Totowa, NJ.
31. Nesargikar PN, Spiller B, Chavez R. The complement system: history, pathways, cascade and inhibitors. *Eur J Microbiol Immunol (Bp)* 2012;2:103-11.
32. Myles T, Nishimura T, Yun TH, et al. Thrombin activatable fibrinolysis inhibitor, a potential regulator of vascular inflammation. *J Biol Chem* 2003;278:51059-67.
33. Weiler H, Lindner V, Kerlin B, et al. Characterization of a mouse model for thrombomodulin deficiency. *Arterioscler Thromb Vasc Biol* 2001;21:1531-7.
34. Puelles VG, Hoy WE, Hughson MD, Diouf B, Douglas-Denton RN, Bertram JF. Glomerular number and size variability and risk for kidney disease. *Curr Opin Nephrol Hypertens* 2011;20:7-15.
35. Levick JR, Smaje LH. An analysis of the permeability of a fenestra. *Microvasc Res* 1987;33:233-56.
36. Haraldsson B, Nystrom J, Deen WM. Properties of the glomerular barrier and mechanisms of proteinuria. *Physiol Rev* 2008;88:451-87.
37. Rostgaard J, Qvortrup K. Sieve plugs in fenestrae of glomerular capillaries--site of the filtration barrier? *Cells Tissues Organs* 2002;170:132-8.
38. Curry FE, Adamson RH. Endothelial glycocalyx: permeability barrier and mechanosensor. *Ann Biomed Eng* 2012;40:828-39.
39. Hjalmarsson C, Johansson BR, Haraldsson B. Electron microscopic evaluation of the endothelial surface layer of glomerular capillaries. *Microvasc Res* 2004;67:9-17.
40. Gelberg H, Healy L, Whiteley H, Miller LA, Vimr E. In vivo enzymatic removal of alpha 2-->6-linked sialic acid from the glomerular filtration barrier results in podocyte charge alteration and glomerular injury. *Lab Invest* 1996;74:907-20.
41. Dane MJ, van den Berg BM, Avramut MC, et al. Glomerular endothelial surface layer acts as a barrier against albumin filtration. *Am J Pathol* 2013;182:1532-40.
42. Jeansson M, Bjorck K, Tenstad O, Haraldsson B. Adriamycin alters glomerular endothelium to induce proteinuria. *J Am Soc Nephrol* 2009;20:114-22.

43. Scott RP, Quaggin SE. Review series: The cell biology of renal filtration. *J Cell Biol* 2015;209:199-210.
44. Byron A, Randles MJ, Humphries JD, et al. Glomerular cell cross-talk influences composition and assembly of extracellular matrix. *J Am Soc Nephrol* 2014;25:953-66.
45. Lennon R, Byron A, Humphries JD, et al. Global analysis reveals the complexity of the human glomerular extracellular matrix. *J Am Soc Nephrol* 2014;25:939-51.
46. Gunwar S, Ballester F, Noelken ME, Sado Y, Ninomiya Y, Hudson BG. Glomerular basement membrane. Identification of a novel disulfide-cross-linked network of alpha3, alpha4, and alpha5 chains of type IV collagen and its implications for the pathogenesis of Alport syndrome. *J Biol Chem* 1998;273:8767-75.
47. Miner JH, Sanes JR. Collagen IV alpha 3, alpha 4, and alpha 5 chains in rodent basal laminae: sequence, distribution, association with laminins, and developmental switches. *J Cell Biol* 1994;127:879-91.
48. Naito I, Kawai S, Nomura S, Sado Y, Osawa G. Relationship between COL4A5 gene mutation and distribution of type IV collagen in male X-linked Alport syndrome. Japanese Alport Network. *Kidney Int* 1996;50:304-11.
49. Cui Z, Zhao MH. Advances in human antglomerular basement membrane disease. *Nat Rev Nephrol* 2011;7:697-705.
50. Zenker M, Aigner T, Wendler O, et al. Human laminin beta2 deficiency causes congenital nephrosis with mesangial sclerosis and distinct eye abnormalities. *Hum Mol Genet* 2004;13:2625-32.
51. Pena-Gonzalez L, Guerra-Garcia P, Sanchez-Calvin MT, Delgado-Ledesma F, de Alba-Romero C. [New genetic mutation associated with Pierson syndrome]. *An Pediatr (Barc)* 2016;85:321-2.
52. Murshed M, Smyth N, Miosge N, et al. The absence of nidogen 1 does not affect murine basement membrane formation. *Mol Cell Biol* 2000;20:7007-12.
53. Schymeinsky J, Nedbal S, Miosge N, et al. Gene structure and functional analysis of the mouse nidogen-2 gene: nidogen-2 is not essential for basement membrane formation in mice. *Mol Cell Biol* 2002;22:6820-30.
54. Bader BL, Smyth N, Nedbal S, et al. Compound genetic ablation of nidogen 1 and 2 causes basement membrane defects and perinatal lethality in mice. *Mol Cell Biol* 2005;25:6846-56.
55. Suh JH, Miner JH. The glomerular basement membrane as a barrier to albumin. *Nat Rev Nephrol* 2013;9:470-7.
56. Groffen AJ, Ruegg MA, Dijkman H, et al. Agrin is a major heparan sulfate proteoglycan in the human glomerular basement membrane. *J Histochem Cytochem* 1998;46:19-27.
57. van den Hoven MJ, Wijnhoven TJ, Li JP, et al. Reduction of anionic sites in the glomerular basement membrane by heparanase does not lead to proteinuria. *Kidney Int* 2008;73:278-87.
58. Harvey SJ, Jarad G, Cunningham J, et al. Disruption of glomerular basement membrane charge through podocyte-specific mutation of agrin does not alter glomerular permselectivity. *Am J Pathol* 2007;171:139-52.
59. Mundel P, Kriz W. Structure and function of podocytes: an update. *Anat Embryol (Berl)* 1995;192:385-97.
60. Neal CR, Muston PR, Njegovan D, et al. Glomerular filtration into the subpodocyte space is highly restricted under physiological perfusion conditions. *Am J Physiol Renal Physiol* 2007;293:F1787-98.
61. Asanuma K, Mundel P. The role of podocytes in glomerular pathobiology. *Clin Exp Nephrol* 2003;7:255-9.

62. Wartiovaara J, Ofverstedt LG, Khoshnoodi J, et al. Nephrin strands contribute to a porous slit diaphragm scaffold as revealed by electron tomography. *J Clin Invest* 2004;114:1475-83.
63. Liu G, Kaw B, Kurfis J, Rahmanuddin S, Kanwar YS, Chugh SS. Nephrin and nephrin interaction in the slit diaphragm is an important determinant of glomerular permeability. *J Clin Invest* 2003;112:209-21.
64. Menon MC, Chuang PY, He CJ. The glomerular filtration barrier: components and crosstalk. *Int J Nephrol* 2012;2012:749010.
65. Kestila M, Lenkkeri U, Mannikko M, et al. Positionally cloned gene for a novel glomerular protein--nephrin--is mutated in congenital nephrotic syndrome. *Mol Cell* 1998;1:575-82.
66. Boute N, Gribouval O, Roselli S, et al. NPHS2, encoding the glomerular protein podocin, is mutated in autosomal recessive steroid-resistant nephrotic syndrome. *Nat Genet* 2000;24:349-54.
67. Tryggvason K, Wartiovaara J. How does the kidney filter plasma? *Physiology (Bethesda)* 2005;20:96-101.
68. Simon M, Rockl W, Hornig C, et al. Receptors of vascular endothelial growth factor/vascular permeability factor (VEGF/VPF) in fetal and adult human kidney: localization and [¹²⁵I]VEGF binding sites. *J Am Soc Nephrol* 1998;9:1032-44.
69. Saleem MA, Ni L, Witherden I, et al. Co-localization of nephrin, podocin, and the actin cytoskeleton: evidence for a role in podocyte foot process formation. *Am J Pathol* 2002;161:1459-66.
70. Kaplan JM, Kim SH, North KN, et al. Mutations in ACTN4, encoding alpha-actinin-4, cause familial focal segmental glomerulosclerosis. *Nat Genet* 2000;24:251-6.
71. Smoyer WE, Mundel P, Gupta A, Welsh MJ. Podocyte alpha-actinin induction precedes foot process effacement in experimental nephrotic syndrome. *Am J Physiol* 1997;273:F150-7.
72. Kretzler M. Regulation of adhesive interaction between podocytes and glomerular basement membrane. *Microsc Res Tech* 2002;57:247-53.
73. Regele HM, Fillipovic E, Langer B, et al. Glomerular expression of dystroglycans is reduced in minimal change nephrosis but not in focal segmental glomerulosclerosis. *J Am Soc Nephrol* 2000;11:403-12.
74. Johnson RJ, Couser WG, Chi EY, Adler S, Klebanoff SJ. New mechanism for glomerular injury. Myeloperoxidase-hydrogen peroxide-halide system. *J Clin Invest* 1987;79:1379-87.
75. Macconi D, Ghilardi M, Bonassi ME, et al. Effect of angiotensin-converting enzyme inhibition on glomerular basement membrane permeability and distribution of zonula occludens-1 in MWF rats. *J Am Soc Nephrol* 2000;11:477-89.
76. Orikasa M, Matsui K, Oite T, Shimizu F. Massive proteinuria induced in rats by a single intravenous injection of a monoclonal antibody. *J Immunol* 1988;141:807-14.
77. Yoshioka T, Ichikawa I, Fogo A. Reactive oxygen metabolites cause massive, reversible proteinuria and glomerular sieving defect without apparent ultrastructural abnormality. *J Am Soc Nephrol* 1991;2:902-12.
78. Lahdenkari AT, Lounatmaa K, Patrakka J, et al. Podocytes are firmly attached to glomerular basement membrane in kidneys with heavy proteinuria. *J Am Soc Nephrol* 2004;15:2611-8.
79. Kreisberg JI, Venkatachalam M, Troyer D. Contractile properties of cultured glomerular mesangial cells. *Am J Physiol* 1985;249:F457-63.
80. Schlondorff D. The glomerular mesangial cell: an expanding role for a specialized pericyte. *FASEB J* 1987;1:272-81.

81. Leveen P, Pekny M, Gebre-Medhin S, Swolin B, Larsson E, Betsholtz C. Mice deficient for PDGF B show renal, cardiovascular, and hematological abnormalities. *Genes Dev* 1994;8:1875-87.
82. Soriano P. Abnormal kidney development and hematological disorders in PDGF beta-receptor mutant mice. *Genes Dev* 1994;8:1888-96.
83. Ziyadeh FN, Sharma K, Ericksen M, Wolf G. Stimulation of collagen gene expression and protein synthesis in murine mesangial cells by high glucose is mediated by autocrine activation of transforming growth factor-beta. *J Clin Invest* 1994;93:536-42.
84. Lai KN, Tang SC, Guh JY, et al. Polymeric IgA1 from patients with IgA nephropathy upregulates transforming growth factor-beta synthesis and signal transduction in human mesangial cells via the renin-angiotensin system. *J Am Soc Nephrol* 2003;14:3127-37.
85. Julian BA, Novak J. IgA nephropathy: an update. *Curr Opin Nephrol Hypertens* 2004;13:171-9.
86. Noris M, Remuzzi G. Genetics of Immune-Mediated Glomerular Diseases: Focus on Complement. *Semin Nephrol* 2017;37:447-63.
87. Cook HT, Pickering MC. Histopathology of MPGN and C3 glomerulopathies. *Nat Rev Nephrol* 2015;11:14-22.
88. Anders D, Thoenes W. Basement membrane-changes in membranoproliferative glomerulonephritis: a light and electron microscopic study. *Virchows Arch A Pathol Anat Histol* 1975;369:87-109.
89. Pickering MC, D'Agati VD, Nester CM, et al. C3 glomerulopathy: consensus report. *Kidney Int* 2013;84:1079-89.
90. Goodship TH, Cook HT, Fakhouri F, et al. Atypical hemolytic uremic syndrome and C3 glomerulopathy: conclusions from a "Kidney Disease: Improving Global Outcomes" (KDIGO) Controversies Conference. *Kidney Int* 2017;91:539-51.
91. Misra A, Peethambaram A, Garg A. Clinical features and metabolic and autoimmune derangements in acquired partial lipodystrophy: report of 35 cases and review of the literature. *Medicine (Baltimore)* 2004;83:18-34.
92. Dalvin LA, Fervenza FC, Sethi S, Pulido JS. Shedding Light on Fundus Drusen Associated with Membranoproliferative Glomerulonephritis: Breaking Stereotypes of Types I, II, and III. *Retin Cases Brief Rep* 2016;10:72-8.
93. Duvall-Young J, MacDonald MK, McKechnie NM. Fundus changes in (type II) mesangiocapillary glomerulonephritis simulating drusen: a histopathological report. *Br J Ophthalmol* 1989;73:297-302.
94. Gale DP, de Jorge EG, Cook HT, et al. Identification of a mutation in complement factor H-related protein 5 in patients of Cypriot origin with glomerulonephritis. *Lancet* 2010;376:794-801.
95. Servais A, Noel LH, Roumenina LT, et al. Acquired and genetic complement abnormalities play a critical role in dense deposit disease and other C3 glomerulopathies. *Kidney Int* 2012;82:454-64.
96. Strobel S, Zimmering M, Papp K, Prechl J, Jozsi M. Anti-factor B autoantibody in dense deposit disease. *Mol Immunol* 2010;47:1476-83.
97. Sethi S, Sukow WR, Zhang Y, et al. Dense deposit disease associated with monoclonal gammopathy of undetermined significance. *Am J Kidney Dis* 2010;56:977-82.
98. Jokiranta TS, Solomon A, Pangburn MK, Zipfel PF, Meri S. Nephritogenic lambda light chain dimer: a unique human miniautoantibody against complement factor H. *J Immunol* 1999;163:4590-6.

99. Chen Q, Muller D, Rudolph B, et al. Combined C3b and factor B autoantibodies and MPGN type II. *N Engl J Med* 2011;365:2340-2.
100. Blanc C, Togarsimalemath SK, Chauvet S, et al. Anti-factor H autoantibodies in C3 glomerulopathies and in atypical hemolytic uremic syndrome: one target, two diseases. *J Immunol* 2015;194:5129-38.
101. Martinez-Barricarte R, Heurich M, Valdes-Canedo F, et al. Human C3 mutation reveals a mechanism of dense deposit disease pathogenesis and provides insights into complement activation and regulation. *J Clin Invest* 2010;120:3702-12.
102. Valoti E, Alberti M, Tortajada A, et al. A novel atypical hemolytic uremic syndrome-associated hybrid CFHR1/CFH gene encoding a fusion protein that antagonizes factor H-dependent complement regulation. *J Am Soc Nephrol* 2015;26:209-19.
103. Iatropoulos P, Noris M, Mele C, et al. Complement gene variants determine the risk of immunoglobulin-associated MPGN and C3 glomerulopathy and predict long-term renal outcome. *Mol Immunol* 2016;71:131-42.
104. Alfandary H, Davidovits M. Novel factor H mutation associated with familial membranoproliferative glomerulonephritis type I. *Pediatr Nephrol* 2015;30:2129-34.
105. Ault BH, Schmidt BZ, Fowler NL, et al. Human factor H deficiency. Mutations in framework cysteine residues and block in H protein secretion and intracellular catabolism. *J Biol Chem* 1997;272:25168-75.
106. Dragon-Durey MA, Fremeaux-Bacchi V, Loirat C, et al. Heterozygous and homozygous factor h deficiencies associated with hemolytic uremic syndrome or membranoproliferative glomerulonephritis: report and genetic analysis of 16 cases. *J Am Soc Nephrol* 2004;15:787-95.
107. Levy M, Halbwachs-Mecarelli L, Gubler MC, et al. H deficiency in two brothers with atypical dense intramembranous deposit disease. *Kidney Int* 1986;30:949-56.
108. Licht C, Heinen S, Jozsi M, et al. Deletion of Lys224 in regulatory domain 4 of Factor H reveals a novel pathomechanism for dense deposit disease (MPGN II). *Kidney Int* 2006;70:42-50.
109. Servais A, Noel LH, Dragon-Durey MA, et al. Heterogeneous pattern of renal disease associated with homozygous factor H deficiency. *Hum Pathol* 2011;42:1305-11.
110. Hegasy GA, Manuelian T, Hogasen K, Jansen JH, Zipfel PF. The molecular basis for hereditary porcine membranoproliferative glomerulonephritis type II: point mutations in the factor H coding sequence block protein secretion. *Am J Pathol* 2002;161:2027-34.
111. Pickering MC, Cook HT, Warren J, et al. Uncontrolled C3 activation causes membranoproliferative glomerulonephritis in mice deficient in complement factor H. *Nat Genet* 2002;31:424-8.
112. Chauvet S, Roumenina LT, Bruneau S, et al. A Familial C3GN Secondary to Defective C3 Regulation by Complement Receptor 1 and Complement Factor H. *J Am Soc Nephrol* 2016;27:1665-77.
113. Imamura H, Konomoto T, Tanaka E, et al. Familial C3 glomerulonephritis associated with mutations in the gene for complement factor B. *Nephrol Dial Transplant* 2015;30:862-4.
114. Holz FG, Pauleikhoff D, Klein R, Bird AC. Pathogenesis of lesions in late age-related macular disease. *Am J Ophthalmol* 2004;137:504-10.
115. Abrera-Abeleda MA, Nishimura C, Smith JL, et al. Variations in the complement regulatory genes factor H (CFH) and factor H related 5 (CFHR5) are associated with membranoproliferative glomerulonephritis type II (dense deposit disease). *J Med Genet* 2006;43:582-9.

116. Abrera-Abeleda MA, Nishimura C, Frees K, et al. Allelic variants of complement genes associated with dense deposit disease. *J Am Soc Nephrol* 2011;22:1551-9.
117. Laine M, Jarva H, Seitsonen S, et al. Y402H polymorphism of complement factor H affects binding affinity to C-reactive protein. *J Immunol* 2007;178:3831-6.
118. Skerka C, Lauer N, Weinberger AA, et al. Defective complement control of factor H (Y402H) and FHL-1 in age-related macular degeneration. *Mol Immunol* 2007;44:3398-406.
119. Pickering MC, de Jorge EG, Martinez-Barricarte R, et al. Spontaneous hemolytic uremic syndrome triggered by complement factor H lacking surface recognition domains. *J Exp Med* 2007;204:1249-56.
120. Mizutani M, Yuzawa Y, Maruyama I, Sakamoto N, Matsuo S. Glomerular localization of thrombomodulin in human glomerulonephritis. *Lab Invest* 1993;69:193-202.
121. Niemir ZI, Kubiak A, Olejniczak P, Nowak A, Czekalski S. Can von Willebrand factor, platelet-endothelial cell adhesion molecule-1 and thrombomodulin be used as alternative markers of endothelial cell injury in human glomerulonephritis? *Rocz Akad Med Bialymst* 2004;49:213-8.
122. Heurich M, Martinez-Barricarte R, Francis NJ, et al. Common polymorphisms in C3, factor B, and factor H collaborate to determine systemic complement activity and disease risk. *Proc Natl Acad Sci U S A* 2011;108:8761-6.
123. Perez-Caballero D, Gonzalez-Rubio C, Gallardo ME, et al. Clustering of missense mutations in the C-terminal region of factor H in atypical hemolytic uremic syndrome. *Am J Hum Genet* 2001;68:478-84.
124. Skerka C, Chen Q, Fremeaux-Bacchi V, Roumenina LT. Complement factor H related proteins (CFHRs). *Mol Immunol* 2013;56:170-80.
125. Hellwage J, Jokiranta TS, Koistinen V, Vaarala O, Meri S, Zipfel PF. Functional properties of complement factor H-related proteins FHR-3 and FHR-4: binding to the C3d region of C3b and differential regulation by heparin. *FEBS Lett* 1999;462:345-52.
126. McRae JL, Duthy TG, Griggs KM, et al. Human factor H-related protein 5 has cofactor activity, inhibits C3 convertase activity, binds heparin and C-reactive protein, and associates with lipoprotein. *J Immunol* 2005;174:6250-6.
127. Eberhardt HU, Buhlmann D, Hortschansky P, et al. Human factor H-related protein 2 (CFHR2) regulates complement activation. *PLoS One* 2013;8:e78617.
128. Heinen S, Hartmann A, Lauer N, et al. Factor H-related protein 1 (CFHR-1) inhibits complement C5 convertase activity and terminal complex formation. *Blood* 2009;114:2439-47.
129. Goicoechea de Jorge E, Caesar JJ, Malik TH, et al. Dimerization of complement factor H-related proteins modulates complement activation in vivo. *Proc Natl Acad Sci U S A* 2013;110:4685-90.
130. Tortajada A, Yebenes H, Abarregui-Garrido C, et al. C3 glomerulopathy-associated CFHR1 mutation alters FHR oligomerization and complement regulation. *J Clin Invest* 2013;123:2434-46.
131. Lupski JR, Stankiewicz P. Genomic disorders: molecular mechanisms for rearrangements and conveyed phenotypes. *PLoS Genet* 2005;1:e49.
132. Chen Q, Wiesener M, Eberhardt HU, et al. Complement factor H-related hybrid protein deregulates complement in dense deposit disease. *J Clin Invest* 2014;124:145-55.
133. Malik TH, Lavin PJ, Goicoechea de Jorge E, et al. A hybrid CFHR3-1 gene causes familial C3 glomerulopathy. *J Am Soc Nephrol* 2012;23:1155-60.

134. Medjeral-Thomas N, Malik TH, Patel MP, et al. A novel CFHR5 fusion protein causes C3 glomerulopathy in a family without Cypriot ancestry. *Kidney Int* 2014;85:933-7.
135. Xiao X, Ghossein C, Tortajada A, et al. Familial C3 glomerulonephritis caused by a novel CFHR5-CFHR2 fusion gene. *Mol Immunol* 2016;77:89-96.
136. Togarsimalemath SK, Sethi SK, Duggal R, et al. A novel CFHR1-CFHR5 hybrid leads to a familial dominant C3 glomerulopathy. *Kidney Int* 2017;92:876-87.
137. Barbour TD, Pickering MC, Terence Cook H. Dense deposit disease and C3 glomerulopathy. *Semin Nephrol* 2013;33:493-507.
138. Zipfel PF, Skerka C, Chen Q, et al. The role of complement in C3 glomerulopathy. *Mol Immunol* 2015;67:21-30.
139. Dragon-Durey MA, Blanc C, Marinozzi MC, van Schaarenburg RA, Trouw LA. Autoantibodies against complement components and functional consequences. *Mol Immunol* 2013;56:213-21.
140. Sissons JG, West RJ, Fallows J, et al. The complement abnormalities of lipodystrophy. *N Engl J Med* 1976;294:461-5.
141. Gewurz AT, Imherr SM, Strauss S, Gewurz H, Mold C. C3 nephritic factor and hypocomplementaemia in a clinically healthy individual. *Clin Exp Immunol* 1983;54:253-8.
142. Zhang Y, Meyer NC, Fervenza FC, et al. C4 Nephritic Factors in C3 Glomerulopathy: A Case Series. *Am J Kidney Dis* 2017.
143. Blom AM, Corvillo F, Magda M, et al. Testing the Activity of Complement Convertases in Serum/Plasma for Diagnosis of C4NeF-Mediated C3 Glomerulonephritis. *J Clin Immunol* 2016;36:517-27.
144. Halbwachs L, Leveille M, Lesavre P, Wattel S, Leibowitch J. Nephritic factor of the classical pathway of complement: immunoglobulin G autoantibody directed against the classical pathway C3 convertase enzyme. *J Clin Invest* 1980;65:1249-56.
145. Daha MR, Van Es LA. Modulation of complement by autoimmune antibodies isolated from sera of patients with membranoproliferative glomerulonephritis and systemic lupus erythematosus. *Neth J Med* 1982;25:202-7.
146. Miller EC, Chase NM, Densen P, Hintermeyer MK, Casper JT, Atkinson JP. Autoantibody stabilization of the classical pathway C3 convertase leading to C3 deficiency and Neisserial sepsis: C4 nephritic factor revisited. *Clin Immunol* 2012;145:241-50.
147. Marinozzi MC, Chauvet S, Le Quintrec M, et al. C5 nephritic factors drive the biological phenotype of C3 glomerulopathies. *Kidney Int* 2017;92:1232-41.
148. López-Trascasa PNSSMIDLPS-CSRdCMJM. Anti-factor H antibody affecting factor H cofactor activity in a patient with dense deposit disease. *Clinical Kidney Journal* 2012;5:133-6.
149. Goodship TH, Pappworth IY, Toth T, et al. Factor H autoantibodies in membranoproliferative glomerulonephritis. *Mol Immunol* 2012;52:200-6.
150. Meri S, Koistinen V, Miettinen A, Tornroth T, Seppala IJ. Activation of the alternative pathway of complement by monoclonal lambda light chains in membranoproliferative glomerulonephritis. *J Exp Med* 1992;175:939-50.
151. Zhang Y, Meyer NC, Wang K, et al. Causes of alternative pathway dysregulation in dense deposit disease. *Clin J Am Soc Nephrol* 2012;7:265-74.
152. Mathieson PW, Peters DK. Lipodystrophy in MCGN type II: the clue to links between the adipocyte and the complement system. *Nephrol Dial Transplant* 1997;12:1804-6.

153. Mullins RF, Aptsiauri N, Hageman GS. Structure and composition of drusen associated with glomerulonephritis: implications for the role of complement activation in drusen biogenesis. *Eye (Lond)* 2001;15:390-5.
154. Han DP, Sievers S. Extensive drusen in type I membranoproliferative glomerulonephritis. *Arch Ophthalmol* 2009;127:577-9.
155. Smith KD, Alpers CE. Pathogenic mechanisms in membranoproliferative glomerulonephritis. *Curr Opin Nephrol Hypertens* 2005;14:396-403.
156. Rennke HG. Secondary membranoproliferative glomerulonephritis. *Kidney Int* 1995;47:643-56.
157. Alpers CE, Smith KD. Cryoglobulinemia and renal disease. *Curr Opin Nephrol Hypertens* 2008;17:243-9.
158. Roccatello D, Fornasieri A, Giachino O, et al. Multicenter study on hepatitis C virus-related cryoglobulinemic glomerulonephritis. *Am J Kidney Dis* 2007;49:69-82.
159. Sethi S, Zand L, Leung N, et al. Membranoproliferative glomerulonephritis secondary to monoclonal gammopathy. *Clin J Am Soc Nephrol* 2010;5:770-82.
160. Sethi S, Fervenza FC, Zhang Y, et al. Proliferative glomerulonephritis secondary to dysfunction of the alternative pathway of complement. *Clin J Am Soc Nephrol* 2011;6:1009-17.
161. Noris M, Remuzzi G. Atypical hemolytic-uremic syndrome. *N Engl J Med* 2009;361:1676-87.
162. Carreras L, Romero R, Requesens C, et al. Familial hypocomplementemic hemolytic uremic syndrome with HLA-A3,B7 haplotype. *JAMA* 1981;245:602-4.
163. Stuhlinger W, Kourilsky O, Kanfer A, Sraer JD. Letter: Haemolytic-uraemic syndrome: evidence for intravascular C3 activation. *Lancet* 1974;2:788-9.
164. Noris M, Ruggenenti P, Perna A, et al. Hypocomplementemia discloses genetic predisposition to hemolytic uremic syndrome and thrombotic thrombocytopenic purpura: role of factor H abnormalities. Italian Registry of Familial and Recurrent Hemolytic Uremic Syndrome/Thrombotic Thrombocytopenic Purpura. *J Am Soc Nephrol* 1999;10:281-93.
165. Noris M, Galbusera M, Gastoldi S, et al. Dynamics of complement activation in aHUS and how to monitor eculizumab therapy. *Blood* 2014;124:1715-26.
166. Noris M, Caprioli J, Bresin E, et al. Relative role of genetic complement abnormalities in sporadic and familial aHUS and their impact on clinical phenotype. *Clin J Am Soc Nephrol* 2010;5:1844-59.
167. Recalde S, Tortajada A, Subias M, et al. Molecular Basis of Factor H R1210C Association with Ocular and Renal Diseases. *J Am Soc Nephrol* 2016;27:1305-11.
168. Esparza-Gordillo J, Goicoechea de Jorge E, Buil A, et al. Predisposition to atypical hemolytic uremic syndrome involves the concurrence of different susceptibility alleles in the regulators of complement activation gene cluster in 1q32. *Hum Mol Genet* 2005;14:703-12.
169. Maga TK, Meyer NC, Belsha C, Nishimura CJ, Zhang Y, Smith RJ. A novel deletion in the RCA gene cluster causes atypical hemolytic uremic syndrome. *Nephrol Dial Transplant* 2011;26:739-41.
170. Venables JP, Strain L, Routledge D, et al. Atypical haemolytic uraemic syndrome associated with a hybrid complement gene. *PLoS Med* 2006;3:e431.
171. Francis NJ, McNicholas B, Awan A, et al. A novel hybrid CFH/CFHR3 gene generated by a microhomology-mediated deletion in familial atypical hemolytic uremic syndrome. *Blood* 2012;119:591-601.
172. Eyler SJ, Meyer NC, Zhang Y, Xiao X, Nester CM, Smith RJ. A novel hybrid CFHR1/CFH gene causes atypical hemolytic uremic syndrome. *Pediatr Nephrol* 2013;28:2221-5.

173. Rabasco C, Cavero T, Roman E, et al. Effectiveness of mycophenolate mofetil in C3 glomerulonephritis. *Kidney Int* 2015;88:1153-60.
174. Habbig S, Mihatsch MJ, Heinen S, et al. C3 deposition glomerulopathy due to a functional factor H defect. *Kidney Int* 2009;75:1230-4.
175. Zhang Y, Nester CM, Holanda DG, et al. Soluble CR1 therapy improves complement regulation in C3 glomerulopathy. *J Am Soc Nephrol* 2013;24:1820-9.
176. Zhang Y, Shao D, Ricklin D, et al. Compstatin analog Cp40 inhibits complement dysregulation in vitro in C3 glomerulopathy. *Immunobiology* 2015;220:993-8.
177. Daina E, Noris M, Remuzzi G. Eculizumab in a patient with dense-deposit disease. *N Engl J Med* 2012;366:1161-3.
178. Marques ID, Ramalho J, David DR, Nahas WC, David-Neto E. Rituximab in a B cell-driven regimen for the treatment of recurrent membranoproliferative glomerulonephritis after kidney transplantation. *Int Urol Nephrol* 2014;46:2053-4.
179. Farooqui M, Alsaad K, Aloudah N, Alhamdan H. Treatment-resistant recurrent membranoproliferative glomerulonephritis in renal allograft responding to rituximab: case report. *Transplant Proc* 2015;47:823-6.
180. Giaime P, Daniel L, Burtsey S. Remission of C3 glomerulopathy with rituximab as only immunosuppressive therapy. *Clin Nephrol* 2015;83:57-60.
181. Radhakrishnan S, Lunn A, Kirschfink M, et al. Eculizumab and refractory membranoproliferative glomerulonephritis. *N Engl J Med* 2012;366:1165-6.
182. Evaluating the morphofunctional effects of eculizumab therapy in primary membranoproliferative glomerulonephritis: a pilot, single arm study in ten patients with persistent heavy proteinuria., 2014. (Accessed at
183. Thurman JM, Le Quintrec M. Targeting the complement cascade: novel treatments coming down the pike. *Kidney Int* 2016;90:746-52.
184. Marinozzi MC, Chauvet S, Le Quintrec M, et al. C5 nephritic factors drive the biological phenotype of C3 glomerulopathies. *Kidney Int* 2017.
185. Sethi S, Fervenza FC. Membranoproliferative glomerulonephritis: pathogenetic heterogeneity and proposal for a new classification. *Semin Nephrol* 2011;31:341-8.
186. Fremeaux-Bacchi V, Weiss L, Brun P, Kazatchkine MD. Selective disappearance of C3NeF IgG autoantibody in the plasma of a patient with membranoproliferative glomerulonephritis following renal transplantation. *Nephrol Dial Transplant* 1994;9:811-4.
187. Kircher M, Witten DM, Jain P, O'Roak BJ, Cooper GM, Shendure J. A general framework for estimating the relative pathogenicity of human genetic variants. *Nat Genet* 2014;46:310-5.
188. Rooijackers SH, Wu J, Ruyken M, et al. Structural and functional implications of the alternative complement pathway C3 convertase stabilized by a staphylococcal inhibitor. *Nat Immunol* 2009;10:721-7.
189. Wu J, Wu YQ, Ricklin D, Janssen BJ, Lambris JD, Gros P. Structure of complement fragment C3b-factor H and implications for host protection by complement regulators. *Nat Immunol* 2009;10:728-33.
190. Schramm EC, Roumenina LT, Rybkine T, et al. Mapping interactions between complement C3 and regulators using mutations in atypical hemolytic uremic syndrome. *Blood* 2015;125:2359-69.
191. Forneris F, Ricklin D, Wu J, et al. Structures of C3b in complex with factors B and D give insight into complement convertase formation. *Science* 2010;330:1816-20.
192. Maga TK, Nishimura CJ, Weaver AE, Frees KL, Smith RJ. Mutations in alternative pathway complement proteins in American patients with atypical hemolytic uremic syndrome. *Hum Mutat* 2010;31:E1445-60.

193. van de Ven JP, Nilsson SC, Tan PL, et al. A functional variant in the CFI gene confers a high risk of age-related macular degeneration. *Nat Genet* 2013;45:813-7.
194. Nilsson SC, Nita I, Mansson L, et al. Analysis of binding sites on complement factor I that are required for its activity. *J Biol Chem* 2010;285:6235-45.
195. Salomaa V, Matei C, Aleksic N, et al. Soluble thrombomodulin as a predictor of incident coronary heart disease and symptomless carotid artery atherosclerosis in the Atherosclerosis Risk in Communities (ARIC) Study: a case-cohort study. *Lancet* 1999;353:1729-34.
196. Van de Wouwer M, Collen D, Conway EM. Thrombomodulin-protein C-EPCR system: integrated to regulate coagulation and inflammation. *Arterioscler Thromb Vasc Biol* 2004;24:1374-83.
197. Zhang Y, Nester CM, Martin B, et al. Defining the complement biomarker profile of C3 glomerulopathy. *Clin J Am Soc Nephrol* 2014;9:1876-82.
198. Davis AE, 3rd, Ziegler JB, Gelfand EW, Rosen FS, Alper CA. Heterogeneity of nephritic factor and its identification as an immunoglobulin. *Proc Natl Acad Sci U S A* 1977;74:3980-3.
199. Daha MR, Austen KF, Fearon DT. Heterogeneity, polypeptide chain composition and antigenic reactivity of C3 nephritic factor. *J Immunol* 1978;120:1389-94.
200. Józsi MI . Anti-Complement Autoantibodies in Membranoproliferative Glomerulonephritis and Dense Deposit Disease, An update on glomerulopathies-Etiology and pathogenesis. Prof.Sharma Prabhakar Available from: <https://www.intechopen.com/books/an-update-on-glomerulopathies-etiology-and-pathogenesis/anti-complement-autoantibodies-in-membranoproliferative-glomerulonephritis-and-dense-deposit-disease>
In: (Ed) PSP, ed. September 2011 ed; 2011.
201. Clardy CW, Forristal J, Strife CF, West CD. A properdin dependent nephritic factor slowly activating C3, C5, and C9 in membranoproliferative glomerulonephritis, types I and III. *Clin Immunol Immunopathol* 1989;50:333-47.
202. Mollnes TE, Ng YC, Peters DK, Lea T, Tschopp J, Harboe M. Effect of nephritic factor on C3 and on the terminal pathway of complement in vivo and in vitro. *Clin Exp Immunol* 1986;65:73-9.
203. Merinero HM, Garcia SP, Garcia-Fernandez J, Arjona E, Tortajada A, Rodriguez de Cordoba S. Complete functional characterization of disease-associated genetic variants in the complement factor H gene. *Kidney Int* 2018;93:470-81.
204. Smith RJ, Harris CL, Pickering MC. Dense deposit disease. *Mol Immunol* 2011;48:1604-10.
205. Galle P, Mahieu P. Electron dense alteration of kidney basement membranes. A renal lesion specific of a systemic disease. *Am J Med* 1975;58:749-64.
206. Sethi S, Gamez JD, Vrana JA, et al. Glomeruli of Dense Deposit Disease contain components of the alternative and terminal complement pathway. *Kidney Int* 2009;75:952-60.
207. Martincic D, Zimmerman SA, Ware RE, Sun MF, Whitlock JA, Gailani D. Identification of mutations and polymorphisms in the factor XI genes of an African American family by dideoxyfingerprinting. *Blood* 1998;92:3309-17.
208. Irmscher S, Doring N, Halder LD, et al. Kallikrein Cleaves C3 and Activates Complement. *J Innate Immun* 2017.
209. Ceccarelli F, Perricone C, Borgiani P, et al. Genetic Factors in Systemic Lupus Erythematosus: Contribution to Disease Phenotype. *J Immunol Res* 2015;2015:745647.
210. Kim-Howard X, Maiti AK, Anaya JM, et al. ITGAM coding variant (rs1143679) influences the risk of renal disease, discoid rash and immunological manifestations in

- patients with systemic lupus erythematosus with European ancestry. *Ann Rheum Dis* 2010;69:1329-32.
211. Gigli I, Fujita T, Nussenzweig V. Modulation of the classical pathway C3 convertase by plasma proteins C4 binding protein and C3b inactivator. *Proc Natl Acad Sci U S A* 1979;76:6596-600.
212. Tortajada A, Montes T, Martinez-Barricarte R, Morgan BP, Harris CL, de Cordoba SR. The disease-protective complement factor H allotypic variant Ile62 shows increased binding affinity for C3b and enhanced cofactor activity. *Hum Mol Genet* 2009;18:3452-61.
213. Deban L, Jarva H, Lehtinen MJ, et al. Binding of the long pentraxin PTX3 to factor H: interacting domains and function in the regulation of complement activation. *J Immunol* 2008;181:8433-40.
214. Bokisch VA, Muller-Eberhard HJ. Anaphylatoxin inactivator of human plasma: its isolation and characterization as a carboxypeptidase. *J Clin Invest* 1970;49:2427-36.
215. Murphy B, Georgiou T, Machet D, Hill P, McRae J. Factor H-related protein-5: a novel component of human glomerular immune deposits. *Am J Kidney Dis* 2002;39:24-7.
216. McRae JL, Cowan PJ, Power DA, et al. Human factor H-related protein 5 (FHR-5). A new complement-associated protein. *J Biol Chem* 2001;276:6747-54.
217. Csicsi AI, Kopp A, Zoldi M, et al. Factor H-related protein 5 interacts with pentraxin 3 and the extracellular matrix and modulates complement activation. *J Immunol* 2015;194:4963-73.
218. Garlanda C, Bottazzi B, Bastone A, Mantovani A. Pentraxins at the crossroads between innate immunity, inflammation, matrix deposition, and female fertility. *Annu Rev Immunol* 2005;23:337-66.
219. Nauta AJ, Bottazzi B, Mantovani A, et al. Biochemical and functional characterization of the interaction between pentraxin 3 and C1q. *Eur J Immunol* 2003;33:465-73.
220. Baruah P, Dumitriu IE, Peri G, et al. The tissue pentraxin PTX3 limits C1q-mediated complement activation and phagocytosis of apoptotic cells by dendritic cells. *J Leukoc Biol* 2006;80:87-95.
221. Inforzato A, Peri G, Doni A, et al. Structure and function of the long pentraxin PTX3 glycosidic moiety: fine-tuning of the interaction with C1q and complement activation. *Biochemistry* 2006;45:11540-51.
222. Bussolati B, Peri G, Salvidio G, Verzola D, Mantovani A, Camussi G. The long pentraxin PTX3 is synthesized in IgA glomerulonephritis and activates mesangial cells. *J Immunol* 2003;170:1466-72.
223. Holmes LV, Strain L, Staniforth SJ, et al. Determining the population frequency of the CFHR3/CFHR1 deletion at 1q32. *PLoS One* 2013;8:e60352.
224. Hughes AE, Orr N, Esfandiary H, Diaz-Torres M, Goodship T, Chakravarthy U. A common CFH haplotype, with deletion of CFHR1 and CFHR3, is associated with lower risk of age-related macular degeneration. *Nat Genet* 2006;38:1173-7.
225. Gharavi AG, Kiryluk K, Choi M, et al. Genome-wide association study identifies susceptibility loci for IgA nephropathy. *Nat Genet* 2011;43:321-7.
226. Moore I, Strain L, Pappworth I, et al. Association of factor H autoantibodies with deletions of CFHR1, CFHR3, CFHR4, and with mutations in CFH, CFI, CD46, and C3 in patients with atypical hemolytic uremic syndrome. *Blood* 2010;115:379-87.
227. Zhao J, Wu H, Khosravi M, et al. Association of genetic variants in complement factor H and factor H-related genes with systemic lupus erythematosus susceptibility. *PLoS Genet* 2011;7:e1002079.

228. Dragon-Durey MA, Loirat C, Cloarec S, et al. Anti-Factor H autoantibodies associated with atypical hemolytic uremic syndrome. *J Am Soc Nephrol* 2005;16:555-63.
229. Lopez E, Casasnovas C, Gimenez J, Matilla-Duenas A, Sanchez I, Volpini V. Characterization of Alu and recombination-associated motifs mediating a large homozygous SPG7 gene rearrangement causing hereditary spastic paraplegia. *Neurogenetics* 2015;16:97-105.
230. Jozsi M, Richter H, Loschmann I, et al. FHR-4A: a new factor H-related protein is encoded by the human FHR-4 gene. *Eur J Hum Genet* 2005;13:321-9.
231. Manuelian T, Hellwage J, Meri S, et al. Mutations in factor H reduce binding affinity to C3b and heparin and surface attachment to endothelial cells in hemolytic uremic syndrome. *J Clin Invest* 2003;111:1181-90.
232. Sanchez-Corral P, Perez-Caballero D, Huarte O, et al. Structural and functional characterization of factor H mutations associated with atypical hemolytic uremic syndrome. *Am J Hum Genet* 2002;71:1285-95.
233. Wang M, Beck CR, English AC, et al. PacBio-LITS: a large-insert targeted sequencing method for characterization of human disease-associated chromosomal structural variations. *BMC Genomics* 2015;16:214.
234. Pouw RB, Brouwer MC, Geissler J, et al. Complement Factor H-Related Protein 3 Serum Levels Are Low Compared to Factor H and Mainly Determined by Gene Copy Number Variation in CFHR3. *PLoS One* 2016;11:e0152164.
235. Hebecker M, Jozsi M. Factor H-related protein 4 activates complement by serving as a platform for the assembly of alternative pathway C3 convertase via its interaction with C3b protein. *J Biol Chem* 2012;287:19528-36.